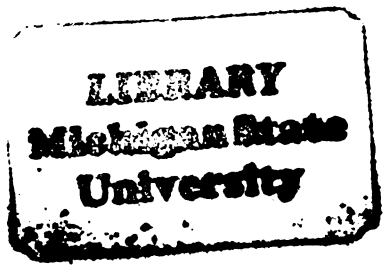

This is to certify that the

thesis entitled

ELECTROCHEMICAL AND OTHER ANALYTICAL STUDIES

ON PLATINUM BLUES AND RELATED COMPOUNDS

presented by

Tore Ramstad

has been accepted towards fulfillment
of the requirements for

M.S. degree in Chemistry

John Allen

Major professor

Date 20 Feb 1984

O-7639

MSU is an Affirmative Action/Equal Opportunity Institution

RETURNING MATERIALS:
Place in book drop to remove this checkout from your record. FINES will be charged if book is returned after the date stamped below.

ELECTROCHEMICAL AND OTHER ANALYTICAL STUDIES ON PLATINUM BLUES AND RELATED COMPOUNDS

By

Tore Ramstad

A DISSERTATION

Submitted to

Michigan State University

in partial fulfillment of the requirements

for the degree of

MASTER OF SCIENCE

Department of Chemistry

1984

ABSTRACT

ELECTROCHEMICAL AND OTHER ANALYTICAL STUDIES
ON PLATINUM BLUES AND RELATED COMPOUNDS

By

Tore Ramstad

The platinum blue platinum 1-methyluracil blue and its parent or precursor complex, platinum 1-methyluracil, were extensively characterized as to their electrochemical and spectroscopic properties, and as to their chromatographic behavior. Several related blues and precursor compounds were less intensely studied. These are compounds which exhibit multiple valence states for platinum and which possess unusually intense color, color explainable in terms of intervalent electron transfer. Platinum blues are amorphous and consist of complex distributions of oligomeric chains.

Techniques used in the characterization of these compounds included various electrochemical probes, most notably cyclic voltammetry, rotating disk voltammetry, and controlled potential coulometry. Application of redox titrimetry allowed a comparison of chemical and electrochemical oxidation modes. Visible and near infrared spectral measurements combined with the Hush theoretical treatment of intervalence electron transfer afforded a fundamental study of color. Paramagnetic states were identified by ESR directly

and NMR indirectly. Liquid chromatography was used to study time behavior (stability) and was also used to expose the complexity of the polymeric blue.

ACKNOWLEDGEMENTS

The author expresses his thanks to his major professor, Dr. M. Weaver, for a meaningful introduction to electrochemical research; to his second reader, Dr. J. Allison, for a careful reading of the thesis; and to Drs. S. Crouch and C. Brubaker, the remaining members of the examining committee. Dr. D. Woollins of the laboratory of Dr. B. Rosenberg, formerly of the Department of Biophysics, is singled out for special acknowledgement; he introduced the author to the subject matter of this dissertation, he jointly performed several of the experiments with him, and he proved an invaluable resource throughout this work. The generosity of Dr. Rosenberg in making available to the author certain equipment, particularly liquid chromatographs, was greatly appreciated. Postdoctoral researcher Dr. T. Li is greatfully acknowledged for having assisted in the acquisition of several types of spectroscopic data. Several others who also provided data are acknowledged where appropriate in the text. The thesis was typed by Gail Shively of the Department of Chemistry, Purdue University.

Og endelig takker forfatteren sin mor, som i så mange veier, for tallrike a nevne her, har gjort det mulig å fullføre dette arbeidet.

TABLE OF CONTENTS

	Page
LIST OF TABLES	vii
LIST OF FIGURES	viii
INTRODUCTION	1
Introduction to Platinum Blues	1
General Background	1
Purpose of Study	5
Primer on Platinum Chemistry	8
Review of Published Literature	10
Overview of Platinum Blues and Related Compounds	10
Mixed-Valence Compounds	15
Introduction	15
Classification Scheme	15
Properties	17
Mixed-Valency in the Current Study	18
Origin of Color in Platinum Blues. Hush Model Interpretation of Spectra	19
Properties of Blues	20
Techniques Used	20
Platinblau	21
Platinum α-Pyridone Blue	26
Approximate Structures of Blues by X-Ray Diffraction and EXAFS	29
Properties of α-Pyridone Blue	31
Magnetic Susceptibility	32
Single Crystal ESR Measurements	32
Comparison of Properties of Platinum Blues	32
Variability of Preparations	34
Optical Spectra	34
ESR Spectra	35
Oxidative Titrations	36
Reductive Titrations	38
Size Determination by Gel Electrophoresis	40
Molecular Weight by Sedimentation	41
Electrochemistry of Blues	41
Paramagnetism of Platinum Blues	44
Nature of NMR Signals	45
Chemical Evidence for Paramagnetism	45
ESR of Platinum Blues	46

Page

Type O and R Spectra..... 47
Paramagnetism of Nonpyrimidine Blues..... 49
Photoelectron Spectroscopy of Platinum Blues..... 52
Background..... 52
Application to Mixed-Valent Compounds..... 53
Pertinent Literature Reports..... 55
Binuclear Platinum(III) Complexes..... 57

EXPERIMENTAL..... 59

Introduction..... 59
Rationale for Interest in Pl-MeU..... 60
Synthesis..... 66
Analysis..... 67
Electrochemistry..... 68
Cyclic Voltammetry (CV)..... 69
Fast Cyclic Voltammetry (FCV)..... 69
Rotating Disk Voltammetry (RDV)..... 70
Differential Pulse Voltammetry (DPV)..... 71
Controlled-Potential Coulometry (CPC)..... 71
Electrosynthesis..... 72
Work-ups..... 73
Physical and Chemical Characterization..... 74
Elemental Analysis..... 74
Visible Spectrophotometry..... 74
Infrared Spectroscopy..... 75
Mass Spectrometry..... 76
Solubility..... 77
Redox Titrimetry..... 78
Redox Titrimetry/EPR..... 79
Controlled-Potential Coulometry in Conjunction with Vis/NIR Spectroscopy..... 79
Controlled-Potential Coulometry in Conjunction with Electron Paramagnetic Resonance Spectroscopy..... 80
Controlled-Potential Coulometry in Conjunction with Paramagnetic Nuclear Magnetic Resonance Spectroscopy... 81
X-ray Photoelectron Spectroscopy..... 82
Liquid Chromatography (LC)..... 82
Isotachophoresis..... 83

RESULTS AND DISCUSSION..... 85

Electrochemistry..... 85
Cyclic Voltammetry (CV)..... 85
Initial Surveys..... 86
Fast Cyclic Voltammetry (FCV)..... 98
CV's of Aged Pl-MeU..... 115
FCV Applied to Pl-MeUB..... 118
Comparison with CV's of Related Complexes..... 120
Determination of n for Pl-MeU..... 123

Page

Rotating Disk Voltammetry (RDV)..... 126
Determination of n by RDV..... 128
A Calculation of the Mol. Wt. of P1-MeUB from RDV Data..... 134
Adsorptive Behavior by RDV..... 138
Controlled-Potential Coulometry (CPC)..... 141
CPC of P1-MeU..... 142
Determination of K_{sp} for [P(II,III)1-MeU]-$(ClO_4)_3$..... 148
Chemical Reversibility of Precipitation of $[P(II,III)1\text{-}MeU]^{3+}$ with ClO_4^-..... 148
Electrolysis of P1-MeU Coupled with CV..... 150
CPC of P1-MeUB..... 156
Adsorption of P1-MeUB on Pt..... 157
Further Interpretations of CPC Behavior of P1-MeUB..... 163
Mechanistic Treatment of CPC of P1-MeUB..... 165
Calculation of Valence of Pt in P1-MeUB..... 172
Electrolysis of P1-MeUB Coupled with CV..... 174
Summary of Electrochemical Findings..... 180
Redox Titrimetry - Oxidative Titrations Using Ce(IV)... 182
Titration of P1-MeU..... 188
Calculation of $E^{o'}$..... 197
Ce(IV) Titration of Related Compounds..... 199
Titration of P1-MeUB with Ce(IV)..... 200
Calculation of the Extent of Mixed-Valency of P1-MeUB by Titrimetry..... 202
Ce(IV) Titration of Other Blues..... 209
Summary of Titrimetry Findings..... 212
CPC/Vis-NIR Spectroscopy..... 214
P1-MeU..... 214
Hush Model Treatment of P1-MeU..... 217
P1-MeUB..... 224
Hush Model Treatment of P1-MeUB..... 228
Controlled-Potential Coulometry Coupled with Electron Spin Resonance Spectroscopy..... 229
ESR of P1-MeU..... 231
Interpretation of Spectra..... 235
Improved g Values..... 243
Hyperfine Splitting in P(II,III)1-MeU..... 244
Hyperfine vs No Hyperfine..... 247
EPR of P1-MeUB..... 250
Splitting Pattern of P1-MeUB..... 253
Summary of ESR Results..... 255
P1-MeU..... 255
P1-MeUB..... 257
Controlled-Potential Coulometry in Conjunction with Paramagnetic Nuclear Resonance Spectroscopy..... 258
CPC/PNMR of P1-MeU..... 259
CPC/PNMR of P1-MeUB..... 262
X-ray Photoelectron Spectroscopy..... 264

Page

Liquid Chromatography..... 264
Goal..... 264
Introduction..... 265
Pertinent Literature on LC..... 271
Detection..... 272
Method Development..... 273
Electrolysis/LC of Pl-MeU..... 276
Survey of Pl-MeU by LC..... 280
LC of Pl-MeUB..... 284
Method Development..... 284
Characterization of Pl-MeUB..... 285
A Method for the Estimation of the Molecular Weight Range of Platinum 1-Methyluracil Blue..... 291
Size-Exclusion Chromatography..... 296
Isotachophoresis..... 298
Goals..... 298
Introduction..... 299
Isotachophoretic Apparatus..... 302
Applications..... 303
Applicability to Pl-MeU and Pl-MeUB..... 303
Results..... 305

CONCLUSIONS AND RECOMMENDATIONS..... 307

REFERENCES..... 315

APPENDIX A - Applicable Equations for Single-Sweep and Cyclic Voltammetry at a Planar Electrode..... 326

APPENDIX B - The Levich Equation in Rotating Disk Voltammetry..... 329

APPENDIX C..... 330

LIST OF TABLES

Tables		Page
1.	FCV Data for Pl-MeU	104
2.	CV Data for the Calculation of n in Pl-MeU	124
3.	RDV Data for the Calculation of n for Pl-MeU	133
4.	Precision Study on cis-Pt	187
5.	Average Formal Oxidation State for Platinum in Pl-MeUB Based on Assumed Structure	205
6.	Average Formal Oxidation State for Platinum in Pl-MeUB Based on Percent Platinum. I	206
7.	Average Formal Oxidation State for Platinum in Pl-MeUB Based on Percent Platinum. II	207
8.	Average Formal Oxidation State of Platinum in Platinum Benzoate Blue Based on Percent Platinum	210
9.	Molar Absorptivity, ε_{742}, of Pl-MeU as a Function of the Extent of Electrolysis	216
10.	Peak-to-Peak Amplitude of Differential Signal vs Percent Electrolysis for Pl-MeU	234
11.	Comparison of N and $\xi/\Delta E$ Values	244
12.	Comparison of Splitting Constants for P(II,III)-1-MeU and PPB	246
13.	Comparison of $g_{\perp}$, $g_{\parallel}$, N, and $\xi/\Delta E$ Values for Platinum Blues	253

LIST OF FIGURES

Figures		Page
1.	Arrangement for fast cyclic voltammetry.....	70
2.	Initial cyclic voltammogram of platinum(II) 1-methyluracil (Pl-MeU, 9.7 mg/10 ml, 1.2 mM) obtained at Pt; scan rate (v) of 100 mV/s.....	86
3.	A more usual CV of Pl-MeU (2.4 mg/5.0 ml, 0.58 mM) over the same approximate potential range; v = 100 mV/s.....	87
4.	A representative CV of Pl-MeUB (10.0 mg/5.0 ml) at Pt over approximately the same limited potential range used in Figures 2 and 3; v = 100 mV/s.....	88
5.	CV's of Pl-MeU (8.3 mg/5.0 ml, 2.0 mM) at a) vitreous carbon and at b) Pt as a function of v....	90
6.	CV's of Pl-MeUB (39 mg/5.0 ml) at Pt as a function of v.....	92
7.	Double-sweep voltammogram of Pl-MeU (8.3 mg/5.0 ml, 2.0 mM) at a hanging mercury electrode (HME); v = 100 mV/s.....	93
8.	Single-sweep voltammogram of Pl-MeUB (39 mg/5.0 ml) at a HME; v = 100 mV/s. No peak was obtained in the reverse sweep.....	93
9.	Single-sweep voltammograms of a) platinum phthalate blue (40 mg/5.0 ml) and b) platinum benzoate blue (40 mg/5.0 ml) at a HME; v = 100 mV/s. PPhB gave no peak on reversal.....	95
10.	CV of platinum phthalate blue containing Cl ligands (PPhB-Cl_2) (35 mg/5.0 ml); v = 100 mV/s....	96
11.	CV's of a) platinum benzoate blue containing Cl ligands (PBzB-Cl_2) (30 mg/5.0 ml) and b) platinum phthalate blue containing Cl ligands (PPhB-Cl_2) (35 mg/5.0 ml), both at Pt; v = 100 mV/s.....	96

Page

12. CV's of Pl-MeU (8.2 mg/5.0 ml, 2.0 mM) at Pt over the sweep range v = 20 mV/s to 10 V/s..... 99

13. Correspondence of cathodic and anodic peaks in the CV's of Pl-MeU; v = 500 mV/s..... 101

14. Possible cyclic voltammograms for two-step reversible process (taken from ref. 87)..... 107

15. CV's from 20 mV/s - 2 V/s of aged Pl-MeU (8.2 mg/5.0 ml, 2.0 mM), to be contrasted with Figure 12.... 116

16. CV's of Pl-MeUB (24.4 mg/5.0 ml) over the sweep range 10 mV/s - 2 V/s..... 118

17. CV of cis-$Pt(NH_3)_2(1\text{-MeU})_2$ (3.0 mg/5.0 ml, 1.2 mM) at Pt; $v \cong 100$ mV/s..... 121

18. CV's of model compound $[Ru(NH_3)_6]Cl_3$ (4.7 mg/5.0 ml, 3.0 mM) and of Pl-MeU (8.2 mg/5.0 ml, 2.0 mM) taken at v = 10 mV/s, 20 mV/s, and 2 V/s for the purpose of calculating n, the number of electrons transferred per molecule of Pl-MeU. The noisy CV's at v = 10 and 20 mV/s stem from the high magnification used..... 124

19. Rotating disk voltammograms of Pl-MeU (5.6 mg/10 ml, 0.67 mM) and Pl-MeUB (22.3 mg/10 ml) taken at 500 rpm (ω = 52 rad/s)..... 127

20. Concentration profile of electroactive species in RDV in terms of dimensionless coordinates (taken from ref. 88)..... 129

21. RDV's of a) model compound $[Ru(NH_3)_6]Cl_3$ (2.4 mg/10 ml, 0.78 mM) and b) Pl-MeU (4.2 mg/10 ml, 0.50 mM) as a function of ω for the purpose of calculating n. In b) the runs are offset for the sake of clarity; each scan was from 0.4 - 1.2 V vs ssce. The circled numbers correspond to the order in which the runs were made (see text)..... 131

22. Consecutive RDV's of Pl-MeUB (27.0 mg/10 ml) in perchlorate medium generated at $\omega = 42\ s^{-1}$ 139

23. Limiting current by RDV for successive runs of Pl-MeUB as a function of ω..... 140

Page

24. Comparative adsorptive behavior in perchlorate medium by RDV of a) Pl-MeU at a concentration of 5.1 mg/10 ml (0.6$\underline{1}_1$mM) and b) Pl-MeUB, also at 5.1 mg/10 ml; ω = 42 s^{-1}. Successive runs were made as per Figure 22..... 141

25. Controlled-potential electrolysis curves for Pl-MeU (5.9 mg/5.0 ml, 1.4 mM) conducted in 0.1 F $NaNO_3$: a) current-time curve (1) and charge-time curve (2); b) the corresponding ln i-vs-t plot. The electrolysis potential was maintained at +1.1 V vs ssce throughout the electrolysis..... 142

26. Electrolysis curves of Pl-MeU (as ln i-vs-t plots) at a concentration of 1.4 mM at +1.1, 0.80, 0.75, and 0.70 V vs ssce. The arrow denotes the point at which the electrolysis is judged to be complete (by the color); the electrolysis at 0.70 V was not carried to completion..... 146

27. Cyclic voltammograms of Pl-MeU (5.7 mg/6.0 ml, 1.14 mM) recorded throughout an oxidative electrolysis conducted at + 1.1 V vs ssce; v = 100 mV/s. Cyclics 2 - 9 were recorded at app. 1/8 increments throughout the electrolysis; 1 was taken prior to the electrolysis..... 151

28. CV's of Pl-MeU (5.7 mg/6.0 ml, 1.14 mM) obtained during reductive electrolysis at -0.1 V conducted subsequent to the oxidative electrolysis of Figure 27; v = 100 mV/s. 10 is the CV prior to reductive electrolysis, 17 the CV at the completion of electrolysis..... 152

29. CV's before (1), between (2), and after (3) oxidative and reductive electrolysis of Pl-MeU (5.8 mg/6.0 ml, 1.16 mM); v = 100 mV/s..... 155

30. Electrolysis (oxidative) curves for Pl-MeUB (13.25 mg/6.0 ml): a) over ~4 hrs, b) over 14 hrs..... 157

31. Relative adsorption of a) Pl-MeU and b)Pl-MeUB at Pt. The relative adsorption is gauged by noting the change in slope of the electrolysis curve when an electrode is lowered an additional length d. If there were no adsorptive effect, the instantaneous slope would double.. 158

32. Electrolysis curves of Pl-MeUB generated over the concentration range 0.048 mg/ml to 5.79 mg/ml..... 160

33. Slopes (dQ/dt) of electrolysis curves of Pl-MeUB and of the blank plotted out to ~4 hrs..... 161

Page

34. Electrolysis curves of Pl-MeUB plotted as ln i-vs-t: a) 5.33 mg/6.0 ml, b) 13.25 mg/6.0 ml, c) 40.54 mg/7.0 ml..... 168

35. Reductive electrolysis curve for Pl-MeUB conducted at -0.1 V vs ssce..... 173

36. Cyclic voltammograms of Pl-MeUB (5.4 mg/6.0 ml) recorded throughout an oxidative electrolysis conducted at +1.1 V vs ssce. Cyclics 2 - 9 were recorded at ~1/8 increments throughout the electrolysis; 1 is the CV prior to electrolysis..... 175

37. CV's of Pl-MeUB (5.4 mg/6.0 ml) obtained during reductive electrolysis conducted at -0.1 V subsequent to the oxidative electrolysis of Figure 36. 10 was taken prior to reductive electrolysis, 17 is the CV at the conclusion of the electrolysis, and 18 is the CV after standing overnight..... 176

38. CV's of Pl-MeUB (5.4 mg/6.0 ml) as a function of v after sequential oxidative and reductive electrolysis. These may be compared with the CV's in Figure 16..... 179

39. A titration curve for the Ce(IV) titration of cis-$Pt(NH_3)_2Cl_2$..... 186

40. Titration curves for the titration of platinum(II) 1-methyluracil (Pl-MeU) with Ce(IV) taken nearly six months apart. Plot a) was drawn from readings made on the mV scale of a pH meter, while b), generated six months after a), was obtained using a high input impedance digital voltmeter..... 189

41. Titration curve for $Pt(NH_3)_2(1\text{-MeU})_2$. The break corresponds to 2 equivalents of electrons, thereby implicating a Pt(II) $\xrightarrow{-2e}$ Pt(IV) transition..... 190

42. A titration curve for the Ce(IV) titration of Pl-MeUB. The end point was taken at the point marked by the arrow..... 200

43. A titration curve for the Ce(IV) titration of PBzB. The end point was taken at the point marked by the arrow..... 210

44. NIR/Vis spectra of Pl-MeU (2.4 mM) taken at 1/8 intervals throughout an oxidative electrolysis; sensitivity, 1.0 AUFS..... 215

Page

45. NIR/Vis spectra of Pl-MeUB (conc. of 1 mg/ml) taken at 1/8 intervals throughout an oxidative electrolysis; sensitivity, 0.2 AUFS..... 225

46. ESR frozen-solution (~ -140°C) spectra of a) native (unelectrolyzed), b) 1/4-, c) 1/2-, d) 3/4-, and e) fully-electrolyzed Pl-MeU (2.4 mM) in nitrate (0.01F) medium. X band, freq. ≅ 9.14×10^9 Hz, field set at ~3270 G, mod. freq. = 100 kHz, mod. amp. = 25 G, microwave power = 30 mW..... 232

47. ESR frozen-solution (~-150°C) spectra of a) native (unelectrolyzed), b) 1/4-, c) 1/2-, d) 3/4-, and e) fully-electrolyzed Pl-MeU (2.4 mM) in perchlorate (0.02F) medium. X band, freq. = 9.52×10^9 Hz, field set at ~3400 G, mod. freq. = 100 kHz, mod. amp. = 32 G, microwave power = 15.8 mW. The differential presentation shown here is the usual one; that in Figure 46 is inverted..... 233

48. Ordering of the five d orbitals in an octahedral field with increasing axially-elongated tetragonal distortion from left to right (taken from ref. 59)..... 238

49. Possible molecular orbital energy level scheme for tetragonally-distorted octahedral field (taken from ref. 59)..... 239

50. ESR spectra of a) [P(II,III)1-MeU]$(ClO_4)_3$ as the solid and of b) the solid in aqueous frozen solution (~-140°C). Measured g values are shown. Instrumental settings were as in Figure 46..... 245

51. ESR frozen-solution (~-150°C) spectra of a) native (unelectrolyzed), b) 1/4-, c) 1/2-, d) 3/4-, and e) fully-electrolyzed Pl-MeUB (2.0 mg/ml) in perchlorate (0.02F) medium. Instrumental settings were as in Figure 47..... 251

52. NMR spectra of a) native, b) half-electrolyzed, and c) fully-electrolyzed Pl-MeU (6.0 mg/6.0 ml, 1.2 mM) in 0.02F $NaNO_3$ in D_2O; 2000 scans accumulated..... 260

53. NMR spectrum of native Pl-MeUB (12.0 mg/6.0 ml) in 0.1F $NaNO_3$; 2000 scans..... 264

54. Three chromatograms illustrating the operability of the ion-pair reversed phase mode in the analysis of [P(II,II)1-MeU]$(NO_3)_2$: a) 50% MeOH/0.01 M $HepSO_3Na$/0.005 M TBA^+, b) 50% MeOH/0.01 M $OctSO_3Na$/0.005 M TBA^+, c) 45% MeOH/0.01 M $OctSO_3Na$/0.005 M TBA^+..... 275

Page

55. Chromatograms of a) $[P(II,II)1\text{-MeU}]^{2+}$ as the ethanesulfonate ion-pair and of b) the solvent front.... 277

56. Chromatograms obtained a) prior to, and at the b) 1/4, c) 1/2, d) 3/4, and e) 4/4 points in the oxidative electrolysis of Pl-MeU (λ = 280 nm). The reduced peak intensity with extent of electrolysis is real, not artifactual..... 278

57. Chromatograms illustrating the time-behavior of Pl-MeU.. 281

58. Chromatograms of platinum 1-methyluracil blue (Pl-MeUB). 286

59. Plots of $\ln(t_R - L/\ )$ vs $\ln[C_{aq}]$ for $[C^-]$ over the range a) 4-14 mM and b) 1-5 mM..... 295

Appendix
Figure

C1. a) Transmission spectrum of $[P(II,III)1\text{-MeU}](ClO_4)_3$ as the KBr pellet; b) absorbance spectrum of $[P(II,III)\text{-}1\text{-MeU}](NO_3)_3$ in solution..... 330

INTRODUCTION

Introduction to Platinum Blues

General Background -

The story of the discovery of platinum coordination complexes as compounds which eventually proved to be potent antitumor agents is an example of the oft serendipitious nature of science. Largely by chance, cis-dichlorodiammineplatinum(II) was discovered to possess antibacterial activity. When subsequently tested for antitumor activity, it proved effective against a broad spectrum of tumors. Today cis-platinum (as cis-dichlorodiammineplatinum(II) is often called) is widely used, often in a synergistic fashion in conjunction with other drugs, to combat a wide range of cancers. While the cis isomer of dichlorodiammineplatinum(II) is active, the trans isomer is not.

Since the initial discoveries made in the 1960's, many additional platinum-family complexes have been synthesized, some of which also exhibit anticancer activity. Structure-activity studies with these compounds led to the rules of thumb that 1) a complex (as administered) should be electrically neutral (that is, not be a salt), 2) either a square planar (as in Pt(II)) or an octahedral (as in Pt(IV)) configuration about the metal is required, 3) two cis monodentate (as, e.g., Cl^-) or one bidentate leaving group is

required. Despite the efficacy of cis-platinum, various toxic side effects, particularly renal toxicity, tend to hamper wider usage of this important drug (1).

In the course of an investigation into the mechanism of action of cis-platinum on DNA, researchers noted that reaction of cis-platinum with polyuracil, and later with uracil, produced a dark blue complex. Thus began the chemistry of platinum pyrimidine blues and of platinum blues in general (2). Like cis-platinum, many platinum blues exhibit potent antitumor activity, but without the dose-limiting kidney toxicity of the former.

Although the report by Rosenberg et al. (2) marks the birth of the modern era of the chemistry of platinum blues, the first compound that may be classified as a blue was synthesized in the late 19^{th} century (3), although the credit for its synthesis is usually given to Hofmann and Bugge (4).

The platinum blue complexes reported by Rosenberg et al. (2) were prepared by reacting cis-diaquodiammineplatinum, $[cis\text{-}Pt(NH_3)_2(H_2O)_2]^{2+}$, formed by hydrolyzing $cis\text{-}Pt(NH_3)_2Cl_2$ in the presence of $AgNO_3$, with uracil (a pyrimidine base), its substituted derivatives, or various amides. The rationale behind the synthetic pathway lay in the discovery that $cis\text{-}Pt(NH_3)_2Cl_2$ loses its two chlorines to form various diaquo intermediates preliminary to attack on DNA (2,5). More generally, the platinum pyrimidine blues are formed from the reaction of cis-dichlorodiammineplatinum(II) with various pyrimidine bases of DNA and RNA or other substituted 2,4-dihydroxypyrimidines. Trans complexes do not yield blues.

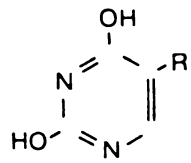

2,4-Dihydroxypyrimidine

Substitution at the 1, 5, and 6 positions of pyrimidines resulted in blue complexes exhibiting high antitumor activity. In general, the blues exhibit activity toward a broad spectrum of tumors, as does cis-platinum. It has been proposed that they act by slow release of the monomer which can penetrate the cell membrane (6), and then by attachment to DNA, as for cis-platinum (7). In contrast to cis-platinum, impairment of kidney function is relatively low; hence the active interest in the pyrimidine blues. Several reviews deal with the use of platinum compounds in cancer therapy (2,8-11).

Platinum blues are polymeric compounds on the order of a few thousand molecular weight in which the platinums are believed to be coordinated to the ligands through amidate linkages.

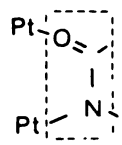

Amidate linkage

A characteristic feature of platinum blues is their mixed-valency, with platinum variously assuming oxidation states of 2, 3, or 4, depending on the compound. As will be discussed, the +3 state has important consequences in terms of color, extent of paramagnetism,

and also, perhaps, in terms of mode of action and potency as an antitumor drug (5). A striking feature of the blues is their intense color, quite uncharacteristic of most platinum compounds, which it is believed, results from intervalence electron transfer between platinum atoms. This has implications concerning direct Pt-Pt bonding as well. The platinum blues are cationic polymers, with nitrate being the most common counter ion. A common trait of the blues is their noncrystallinity; consequently, structural information has been difficult to obtain directly. Nevertheless, structural features have been inferred, primarily by allusion to a crystalline analog known as platinum α-pyridone blue, from powder X-ray data, and from the use of the relatively new technique known as EXAFS - extended X-ray absorption fine structure. Structural data will be presented subsequently. A structure proposed for a platinum uracil blue over a 3-Pt length (12) is given:

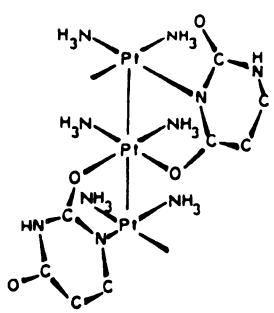

A proposed structure for platinum uracil blue

Three classes of blues were defined by Rosenberg according to the method of preparation, with the uracil blues (of primary interest in this dissertation) being classified as type I.

Purpose of Study -

While it is the blues' efficacy as antitumor agents that gave rise to and continues to attract interest in these platinum compounds, for the chemist, it is not so much their value as a drug that makes them interesting, but rather it is their intriguing chemical properties which hold high interest. The purpose of this work was to shed further light on their properties through the application of a variety of techniques. Compounds examined consisted of several blues of local interest[1] - cis-diammineplatinum 1-methyluracil blue (Pl-MeUB), cis-diammineplatinum benzoate blue, and cis-diammineplatinum phthalate blue - and of what may be termed the parent complex (or precursor compound) of the first of these blues (Pl-MeUB): bis(μ-(1-methyl-uracilato-N^3,O^2))-bis(cis-diammine-platinum(II)), $[(NH_3)_2Pt(C_5H_5N_2O_2)_2Pt(NH_3)_2](NO_3)_2$. This latter compound will be referred to as platinum(II) 1-methyluracil or Pl-MeU.

---

1. In the laboratory of Dr. Barnett Rosenberg, formerly of the Department of Biophysics, Michigan State University, E. Lansing, MI.

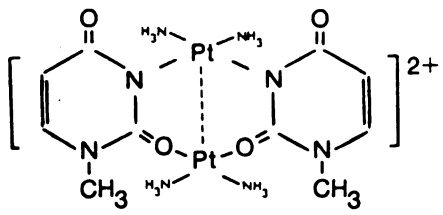

Pl-MeU

In carrying out this investigation, little effort was directed toward the benzoate and phthalate blues. Several additional compounds related to Pl-MeU were less intensely studied; they will be mentioned where appropriate.

The principal investigative tool used in this study was electrochemisty, although several ancillary techniques were employed in order to provide a fuller characterization of these systems. The primary electrochemical techniques used consisted of cyclic voltammetry and rotating disk voltammetry for overall electrochemical characterization, controlled-potential coulometry to determine n, the number of electrons transferred, and controlled-potential electrosynthesis. Electrosynthesized products were studied by visible/near infrared spectroscopy (Vis/NIR), electron spin resonance (ESR) and nuclear magnetic resonance spectroscopy (NMR). Electrolysis in conjunction with Vis/NIR measurements permitted an estimate of the intervalence charge transfer rate via application of the Hush model treatment. Both ESR and NMR were used to ascertain the extent of paramagnetism, the former directly and the latter indirectly. Cerium oxidative titrimetry served as a useful complement to electrochemical studies in characterizing the redox behavior of these systems. Application of X-ray photoelectron spectroscopy (ESCA, Electron Spectroscopy for Chemical Analysis) to elucidate Pt oxidation states

in the solid state was intended to complement solution studies. Liquid chromatography and to a lesser extent, isotachophoresis, were used for fundamental characterization and to follow the progress of electrolytic oxidations. Through the combination of these various techniques, new information was obtained on the blues and related compounds.

There is little literature on the properties of the so-called parent complexes other than structural information obtained by X-ray crystallography (references will be cited later). These are compounds which initially were isolated during the preparation of the pyrimidine blues, but later were made deliberately. The reason that these parent compounds have received scant attention is that they display little or no antitumor activity. However, quite apart from the question of antitumor potency - since they may be viewed as the repeating units of polymeric blues, they can serve as model compounds whose chemical properties may be compared with those of the blues. Such is the case for Pl-MeU. A fuller rationale for interest in this simpler, model system is given later. In contrast to the limited literature on these compounds, the literature on the blues themselves is quite extensive. A review of that literature is pertinent to this study and is presented in the sections to follow. However, before doing this, it is appropriate to first present a brief primer on platinum chemistry, particularly since much of this thesis deals with Pt^{III} chemistry, a relatively recent addition to the recognized oxidation states of platinum.

Primer on Platinum Chemistry (13, 14)

Platinum, a Group VIII transition metal, is the heaviest member of the group comprising the platinum metals. The electronic configuration of the free metal is $[Xe]4f^{14}5d^{9}6s^{1}$. The principal oxidation states of platinum are II ($5d^{8}$) and IV ($5d^{6}$), with square planar being the normal coordination for the former and octahedral for the latter. Less common oxidation states include 0, I, V, VI and the recently recognized III state. In addition, negative oxidation states are known in cluster-type carbonyl anions.

Pt^{0} (d^{10}) is found with tertiary phosphine, CO, or other π-acid ligands and also in Pt_3 and Pt_4 clusters. An example is given by $Pt(CO)(PPh_3)_3$. The I state always involves M-M bonds. The binuclear anion $[Cl_2(CO)Pt\text{-}Pt(CO)Cl_2]^{2-}$ serves as an example. At present the V and VI states are restricted to a few fluorine compounds: $[PtF_5]_4$ and PtF_6^- for the +5 state and PtF_6 for the +6 state. In $[Pt_3(CO)_3(\mu\text{-}CO)_3]_n^{2-}$ platinum assumes a negative valence, where n values ranging from 1 to 10 are known.

The II and IV states are best known in platinum chemistry, with many different kinds of complexes, both neutral and charged, having been prepared. They may be monomeric, oligomeric, and/or bridged binuclear species; none displays paramagnetism. In addition, mixed-valence, chainlike compounds containing both Pt^{II} and Pt^{IV} separated by briding halides are known to exist.

Until recently the III state has been virtually unknown. A compound originally thought to contain Pt^{III} is described by the empirical formula $PtCl_3$, but was later shown to contain both Pt^{II} and

Pt^{IV} with units of $[Pt_6Cl_{12}]$. Apparently, the only example of a mononuclear Pt^{III} complex is the ion [bis-(diphenylglyoximato)Pt]$^-$ (15). In contrast, several binuclear Pt^{III} complexes have been reported in the last few years; these will be treated in a later section. With the growing recognition that the Pt(III) state plays a role in the chemistry of at least some of the compounds generically termed platinum blues - for example, in terms of color, paramagnetism, and biological activity - Pt(III) chemistry is beginning to stand on firmer ground. In the current investigation, the III state was invoked to explain the redox behavior of the parent compound platinum 1-methyluracil (Pl-MeU) as well as the platinum blue, Pl-MeUB.

Since the electrochemical behavior of the blues and precursor compounds was of interest in this work, it is appropriate to examine tabulated values of $E^{o'}$s for platinum compounds and to compare these with those obtained (estimated) in this study. A fairly comprehensive tabulation is given by Goldberg and Hepler (14). They list $E^{o'}$s for the $Pt^{IV} \rightarrow Pt^{II}$ and $Pt^{II} \rightarrow Pt^{0}$ transitions; also, $E^{o'}$s for several $Pt^{IV} \rightarrow Pt^{0}$ transitions were calculated. For some 35 half reactions of monomeric platinum complexes, some exclusively inorganic and some containing organic ligands, $E^{o'}$s vs nhe range from 0.89 to 0.09 V. It will become apparent in the Results section of this dissertation that the binuclear and higher order platinum blues investigated as a part of this work are not so readily reduced.

Review of Published Literature

Overview of Platinum Blues and Related Compounds -

The platinum blues are polymeric, paramagnetic complexes deep blue in color. The color is distinctive in that nearly all platinum complexes exhibiting the principal valence states of +2 and +4 are either a pale yellow or are colorless. The blues are further believed to be characterized by amidate linkages between the metal and bridging groups. As mentioned, compounds which today are recognized as members of the platinum blues family, were prepared as early as 1895 (3) and again in 1908 (4). In more recent times, Gillard and Wilkinson repeated the earlier work on "platinblau" and also prepared several related complexes (16). These earlier contributions aside, the current surge of interest in platinum blues has its origin in the publication of Rosenberg et al. in 1975 in which they reported the preparation and properties of a host of platinum blues (2). In these blues, cis-diamminated platinum was coordinated to the pyrimidines thymine and uracil, to substituted uracils, and to acetamide and higher primary amides, including cyclic amides.

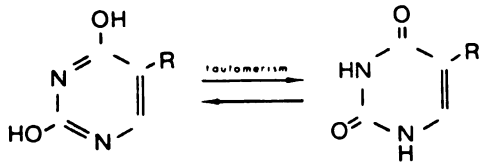

2,4-Dihydroxypyrimidine Pyrimidine-2,4-dione

Uracil (R=H)

Thymine ($R=CH_3$)

Other nucleic acid bases, and replacement of ammonia with substituted amines in the starting complex failed to yield products (17).

The term platinum blues is a generic one, more a descriptor of chemical behavior than color. While platinum complexes which are blue are best known, other products are green or purple (17); the color is dependent on reaction conditions. For example, with cis-$[(NH_3)_2Pt(H_2O)_2]^{2+}$, either as sulfate or nitrate, purple, blue, or green products were obtained using the same molar ratio with uracil, 1-methyluracil, dihydrouracil, uridine, and the three corresponding thymine (5-methyluracil) compounds. Orange to red colors were obtained for certain amides (17). Barton et al. reported the formation of a green purine complex, cis-diammineplatinum hypoxanthine green (PHG) (18). Reaction of cis-dichloro-bis(cyclopropylamine)platinum(II) with 1-methylthymine led to the formation of a purple platinum complex (19). Similarly, cis-dichloro-bis(cyclopropylamine)platinum(II), when reacted with uridine (a nucleoside), also yielded a purple product (20). Some workers have reported the formation of a tan product in the synthesis of platinum blues (5,18,21). However, regardless of the color, all these compounds come under the generic heading platinum blues because of certain features they all share (vide infra).

Newly-synthesized platinum blues expand the list of workable bridging ligands. An example is platinum cytidine blue (22); cytidine is a constituent of nucleic acids. Another example is given by the purple complex formed by reacting cis-$Pt(NH_3)_2Cl_2$ and cytosine (23). Platinum phthalimide blue, which may be made by reacting

cis-dichlorodiammineplatinum(II) and potassium phthalimide (24), may also be cited.

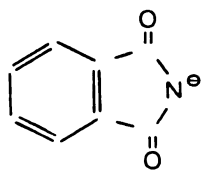

Phthalimide

The phthalimide blue is one of only a few blues whose optical absorption spectra have been subjected to rigorous theoretical treatment (by the Hush model) to ascertain the origin of the distinctive color (this is covered in a later section). By way of contrast to these newer blues, an older and particularly well-studied blue is trimethylacetamide platinum blue, originally reported by Brown et al. (25,26). Its properties will be dealt with at some length because it serves as a model system.

All platinum blues exhibiting antitumor activity appear to be amorphous. As far as can be ascertained, they consist of complex mixtures of oligomers containing up to 20 units. The complexity may arise not only from varying chain lengths, but also from attachment of platinum at different sites on the bridging ligands along the length of a chain. It is not surprising then that material suitable for X-ray crystallographic structural determination has not been obtained.

However, by reacting an analog of a pyrimidine - α-pyridone -

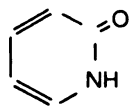

α-Pyridone

a crystalline platinum blue known as platinum α-pyridone blue was obtained whose structure has been delineated by X-ray crystallography (27).

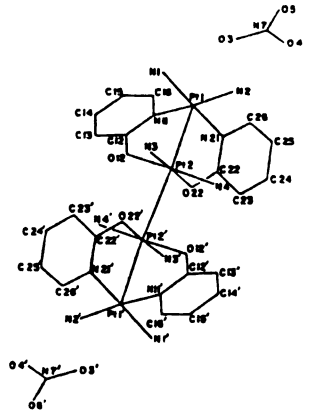

Skeletal structure of platinum α-pyridone blue (includes capping nitrates)

Study of this crystalline blue has proven invaluable in providing clues to the properties and behavior of platinum blues in general. It should be mentioned here, though, that platinum α-pyridone blue itself is not a true platinum blue for the reasons that 1) it is not amorphous and 2) it has no therapeutic value; 2) may be related to 1). (A more extensive discussion of platinum α-pyridone blue is to follow.) A second complex, an analog of the blue, has also yielded

to crystallographic structural determination: cis-diammineplatinum α-Pyrrolidone tan (21).

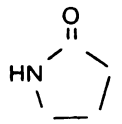

α-Pyrrolidone

The preparation of new platinum blues continues to be reported as part of an effort to discover compounds combining anticancer activity with low toxicity. Because the mechanism of action of platinum blues is thought to involve binding at the bases of cellular DNA (2,28), pyrimidine, and to a lesser extent, purine blues (18,29), of which one containing guanosine (a purine) and 1-methylnicotinamide is an example (30), dominate activity in the field. However, other potential target sites have been postulated as well - e.g., amino acids and proteins (31,32). This has led to the synthesis of compounds utilizing ligands other than the pyrimidine and purine bases.

Reaction of K_2PtCl_4 with L-asparagine, an amino acid, yielded a complex, which, by the criteria of intense blue color and apparent mixed-valency (paramagnetism), may be classified as a platinum blue (33). A second blue, paramagnetic complex was obtained from the reaction of K_2PtCl_4 with L-glutamine (34). A dark brown product, also

paramagnetic, was formed on reaction of cis-$Pt(NH_3)_2Cl_2$ with tryptophan (31).

Mixed-Valence Compounds (35) -

At this point we need to briefly digress to introduce more fully the concept of mixed-valency, to describe a classification scheme, and to point out methods of studying this property. The concept of mixed valency is integral to the study of platinum blues and related compounds.

Introduction. Much of the current investigation is concerned with compounds of presumed mixed valency. Evidence will be presented for a Pt(II)-Pt(III) mixed-valency in the partially-electrolyzed platinum 1-methyluracil (Pl-MeU, average oxidation state of +2.5 at the halfway point in an electrolysis), and for an average oxidation state slightly in excess of 2 in platinum 1-methyluracil blue (Pl-MeUB). The binuclear Pl-MeU is a model system for the study of mixed valency in that only two metal centers are present. In contrast, Pl-MeUB is a very complex system exhibiting a distribution of oligomers with unknown numbers of platinum atoms. Examples of mixed-valence compounds which may be recognized include Fe_3O_4, Prussian Blue ($Fe_4[FeCN)_6]_3 \cdot xH_2O$), the Creutz-Taube ion - $[(NH_3)_5Ru$-(pyrazine)$Ru(NH_3)_5]^{5+}$, the ferredoxins, which are electron transfer enzymes containing Fe_4S_4 units, and the platinum blues.

Classification Scheme. In some mixed-valence compounds, atoms A and B on which the oxidation states might be localized are crystallographically distinguishable. If the environments are

sufficiently different that, say, an A(II)B(III) valence configuration is of markedly different energy than the corresponding A(III)B(II) configuration, then the interconversion rate will be immeasurably slow. This is a class I compound in the scheme first proposed by Robin and Day (36). An example is given by $GaCl_2$, which contains Ga(I) and Ga(III) in a 1:1 stoichiometry. The other extreme fits a class III classification, which applies to compounds in which atoms A and B are crystallographically indistinguishable. Intervalence transfer is so rapid that no localized oxidation states exist. An example is Gd_2Cl_3.

In the middle are those mixed-valence compounds in which sites A and B are distinguishable but similar, compounds in which the internuclear electron transfer rate is readily measurable; these are classified as class II types. A caveat exists, though, in that if the time scale of the measurement technique is too long in order to be able to distinguish between two oxidation states, then a class II type could be classified as type III. Hence, the time scale of the measuring technique is critical to the resultant classification. Techniques which may be used to study intervalence charge transfer include ultraviolet-visible/near IR spectrophotometry, photoelectron spectroscopy, and Mössbauer spectroscopy. In later sections the application of the first two of these to the current investigation is discussed. Mössbauer spectroscopy, which was not used in this work, is a nuclear technique in which the position (wavelength) of γ-ray absorption is affected by the electron density about the nucleus. Hence, this "chemical shift" often allows a distinction between

oxidation states (37). Mössbauer spectroscopy has been applied to mixed-valence compounds (38).

Properties. One of the common features of mixed-valence compounds is their color - they are very often dark. As mentioned previously, the platinum blues are so named because of their intense (usually) blue color. P(II,III)1-MeU studied in this work is dark green. The intensity of the color in mixed-valence compounds is not attributable merely to a summation of the spectra of their component parts, nor is it (in solids) regarded as solely the result of intervalence electron transfer (although this may be the case in solution). One author writes that the intense color is attributable to "a high effective concentration of the chromophore through pairwise interactions in the solid" (39). Solid and solution spectra of these compounds often are not the same.

It is known that bridging ligands can profoundly affect the properties of a mixed-valence compound. That this must be so is apparent from the fact that despite a separation of up to 5-6 Å between metal centers, mixed-valence compounds displaying intervalence transfer bands are known that exhibit class II behavior; 5-6 Å is well beyond the distance at which direct bonding can exist. Ligand bridges have the effect of shortening the metal-metal distance which in turn affects intervalence transfer rates. In Pl-MeU there are two ligands bridging two platinum atoms. For Pl-MeUB this almost certainly is not the case for the length of the oligomeric chains,

simply out of steric considerations. A chain with single bridging is more likely (18).

Mixed-Valency in the Current Study. Much attention is devoted in this thesis to the subject of mixed valency. Unperturbed Pl-MeU (signified by P(II,II)l-MeU or $[P(II,II)l\text{-}MeU](NO_3)_2$) is, obviously, not a mixed-valence compound, but the partially-oxidized, intensely green complex - $[P(II,III)l\text{-}MeU]^{3+}$ - is. The corresponding polymeric blue - Pl-MeUB - is weakly paramagnetic (meaning that there is an occasional Pt^{III} among mostly Pt^{II}) and intensely blue in color. The color in both of these systems is appropriately treated in terms of charge-transfer spectroscopic principles. The color intensity is related to the number of free or unpaired electrons which can participate in intervalence transfer between Pt centers. The extent of direct Pt-Pt bonding and the degree of delocalization is also important. The presence of a Pt(III) atom with its unpaired electron in either of these compounds was readily detectable by electron paramagnetic resonance spectroscopy.

Having alluded several times to the existence of the Pt(III) state both in the few compounds reported in the literature (either binuclear save for one monomeric compound or polymeric) and in compounds to be discussed in the Results section of this thesis, the question as to why the Pt(III) state is so unstable naturally arises. As is discussed on p. 58, in the binuclear Pt(III)-Pt(III) compounds, the absence of antibonding electrons may provide a driving force for the formation of these compounds. Other experimental observations which bear on this question appear from time-to-time in

the body of the thesis. While Ni, the lightest of the three Group VIII metals, may adopt the III state in a few mononuclear compounds (it is somewhat uncertain whether or not it does), Pd and Pt are alike in their disinclination to adopt the +3 state; each ion is d^7 in the III state.

Origin of Color in Platinum Blues. Hush Model Interpretation of Optical Spectra. Over the short recent history of the platinum blues, there has been much speculation about the origin of the intense color, mostly having to do with a mixed-valence or intervalence electronic transition. As indicated, in simplest terms, an intervalence transition is one which arises from an electronic transition between metal centers of differing oxidation state. The first rigorous study of the absorption behavior of platinum blues was reported by Chang et al. in 1981 (24). These authors applied Hush model formulae to platinum phthalimide blue, platinum α-pyridone blue, and platinblau. A fuller discussion of the Hush model treatment is postponed to the Results section. Suffice it here to say that the Hush model allows one to calculate the extent of electron delocalization in a mixed-valence compound, and then to classify the compound as class I, II, or III in accordance with the Robin and Day classification scheme (36) mentioned above. Chang and coworkers established that, contrary to the Hush model prediction, the half-bandwidth did not decrease at low temperatures (down to 80 K). Nevertheless, they used the Hush model equations to conclude generally, that the platinum blues are best decribed as class II -

class III borderline or class III mixed-valence compounds. (The distinction between classes is not sharp.)

Properties of Blues -

Fundamental characterization of the blues has proven elusive to investigators. Because of their amorphous nature, only the α-pyridone analog (not a true blue; it possesses no chemotherapeutic value) has yielded to complete structural elucidation (12,27). Many techniques have been used to study the blues' properties; these are outlined in the next paragraph. The results of these studies are given in the next few sections.

Techniques Used. In order to ascertain the oligomeric distribution of the blues, sedimentation studies and electrophoresis experiments have been conducted. While only the α-pyridone has yielded to crystallographic determination, powder X-ray diffraction has been applied in several instances and extended X-ray absorption fine structure (EXAFS) measurements have been made in at least three cases. Because the blues are cationic polymers of relatively high molecular weight (several thousand), they are not amenable to mass spectrometric analysis employing conventional hard ionization techniques. However, californium-252 plasma desorption mass spectrometry, used with nonvolatile compounds, has been successfully applied to elucidate the molecular weight range of a platinum blue (40).

Mixed-valency in solution has been studied indirectly by redox titrimetry, by controlled-potential coulometry, and most extensively

by electron spin resonance spectroscopy (ESR). Both ^{1}H and ^{195}Pt NMR studies have been made, as NMR often lends evidence to the presence or absence of paramagnetic species (explained later). The paramagnetism of blues has also been studied by invoking magnetic susceptibility measurements. In the solid state, X-ray photoelectron spectroscopy (XPS or ESCA, Electron Spectroscopy for Chemical Analysis, as it is most commonly known) can often be used to assign oxidation states, and thereby the degree of mixed-valency. The intense color of the blues lends itself to visible spectroscopic examination, and through the application of the Hush model formulae the rate of intervalent electron transfer can be calculated. Surprising to the author, electrochemical studies of the platinum blues have been extremely sparse, with only a single paper having appeared, and that one dealing with the α-pyridone simulant (41).

Platinblau. The first example of a platinum blue - platinblau - is credited to Hofmann and Bugge (4) and was made by reacting dichlorobis(acetonitrile)platinum(II) with K_2PtCl_4. It was believed to be monomeric with the platinum in a square planar arrangement. It was assigned the formula $Pt^{II}(CH_3CONH)_2 \cdot H_2O$ with the structure shown.

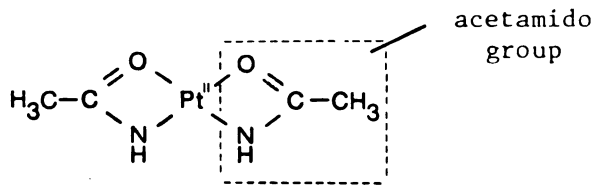

Postulated structure of platinblau

In view of the pale or colorless (or infrequent red) appearance of virtually all other Pt(II) (as well as Pt(IV)) compounds, and in view of the fact that all other known blue complexes of platinum (i.e., the platinum blues) are now believed to be polymeric, the original structural assignment for platinblau came into question. In 1969 Brown et al. reported that they were unable to obtain a crystalline platinblau suitable for X-ray crystallographic analysis (26); the difficulty lay, apparently, in cocontamination by silver from silver nitrate used in the synthetic procedure. In fact, in attempting to prepare various platinum complexes suitable for crystallographic determination, only a single complex, that formed from 2,2-dimethylpropanamide (trimethylacetamide, TMA) could be obtained in crystalline form. Surprisingly, chromatography on silica gel of the crystalline TMA yielded three components - two bands (I & II) composed of yellow needles, and a deep blue, amorphous powder (band III). All three fractions yielded an identical elemental analysis, and by X-ray powder diffractometry the yellow needles were shown to be isostructural with the original, unchromatographed material. Careful NMR and IR examination revealed amide tautomerism for I with bonding to platinum occurring through the nitrogen of an iminol ($-C(=NH)-OH$) group (25). Through the application of both direct and indirect methods involving X-ray diffraction, mass spectrometry, NMR, IR, and UV spectroscopic analysis, it was concluded that the structure of platinblau should be reassigned as $Pt^{IV}(CH_3CONH)_2(OH)_2$, a tetravalent complex containing two anionic ligands.

Laurent et al., in a 1980 report, further investigated platinblau and form III of the trimethylacetamide platinum blue, and compared their behavior to that of the structurally-characterized blue analog, platinum α-pyridone blue (42). The methods employed consisted of redox titrimetry using Ce(IV) and UV-Vis spectral measurements combined with extended Hückel molecular orbital calculations. The titrant was a 5 mM solution of Ce(IV) in 0.7 H_2SO_4 while the titrand was prepared in 4.5 N HCl. The high chloride ion content was required to obtain rapidly stabilized voltage readings (improved the kinetics). While sharp end points were obtained with the test compounds K_2PtCl_4 and cis-$Pt(NH_3)_2Cl_2$, this was not the case when the α-pyridone blue was titrated. As the present author observed in some titrations to be described later, the addition of Ce(IV) titrant to the α-pyridone complex led to a sharp initial rise in the voltage followed by a decay of many minutes. The procedure adopted was to take readings at an arbitrary time (e.g., 1 min) following each addition of titrant. While apparently a common practice, it may be a questionable one. The trimethylacetamide blue could not be titrated with Ce(IV) because of its water insolubility.

A sharp end point was obtained for platinblau; an average oxidation state of 3.0 was assigned to platinum. The fact that 1 (.99 actually) equivalent of oxidant was required per mole of platinum definitely ruled out Pt in the +4 oxidation state as had been proposed by Brown et al. X-ray photoelectron experiments conducted by Barton et al. (43) also ruled out platinum(IV). However, the potentiometric titration curves obtained by Laurent et

al. could also be explained, as the authors point out, by 1) postulating a +2.0 oxidation state for Pt, with half of it being unreactive toward Ce(IV), or by 2) assuming that the end product of the oxidation is a Pt(III) product which is unreactive toward further oxidation by Ce(IV). Concomitant measurements of paramagnetism by magnetic susceptibility or ESR could have removed the uncertainty. In any event, the intriguing and elusive platinblau has had the chronologically-ordered values II, IV, and III assigned for the average formal oxidation state of platinum.

Extended Hückel molecular orbital (EHMO) calculations confirm that platinblau and form III of the acetamide blue should not be formulated as monomeric Pt(IV) complexes (42). However, the authors seem to cloud the issue by reporting a molecular weight in water of 372, which requires a monomeric complex; yet, except possibly for a single example (15), monomeric Pt(III) is not known to exist. Perhaps molecular weight is intended to be synonomous with empirical weight. As mentioned, the break in the platinblau titration curve is quite sharp, although not quite as sharp as for the test compounds K_2PtCl_4 and cis-$Pt(NH_3)_2Cl_2$, but sharper than for other platinum blues which are presumed to be mixed-valent and which are also presumed to contain mixtures of oligomers. One is led to surmise that platinblau may be a short, ordered oligomer. In fact, Gillard and Wilkinson, in a 1964 publication, proposed the following structure involving three platinums and two acetamido bridges (16).

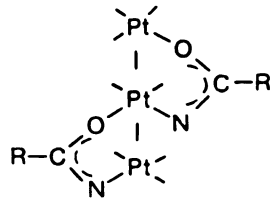

A proposed structure for platinblau

In a following publication (submitted approximately 1 year after ref. 42), Laurent et al. reported that, based on X-ray powder diffraction data, the Pt-Pt bond length in platinblau is 2.76 Å (44). By comparing this length with those in known platinum complexes, they formulated platinblau as a partial oxidation platinum chain complex composed of "entities" of at least four or five "rather linearly bound" platinum atoms. It may well be, though, that oligomers besides the tetra- and pentanuclear characterize the structure of platinblau. Since in this publication, as in their previous one (42), the molecular weight in water is also taken to be 372, the reader has to assume that either 1) the structure in solution and the structure in the solid state are not the same, or 2) the terms molecular weight and empirical weight are being used synonomously. As prepared by Laurent et al., platinblau exhibited magnetic susceptibility, although Gillard and Wilkinson reported their platinblau to be diamagnetic (16). This apparent discrepancy points out a general feature of platinum blues chemistry, and that is the potential variability in the chemistry. (This is not hard to understand if one examines the synthetic procedures.)

As regards form III of the trimethylacetamide blue, the use of various techniques led Laurent et al. to conclude that form III, an

amorphous blue complex, consists of a "nonequilibrium" mixture of oligomers of variable chain length. They further concluded that Pt-Pt interactions are significant and postulated an average formal oxidation state greater than 2, largely based on EHMO calculations. Broad signals in the proton NMR spectrum and in the KBr IR spectrum suggested a mixture of ligand environments suggestive of mixed products or polymerized species. Further, the X-ray powder diffraction pattern was one characteristic of an amorphous substance. By analogy to platinum α-pyridone blue (vide infra), an average formal oxidation state in excess of 2 was assigned to form III of platinum trimethylacetamide blue. Since neither magnetic susceptibility nor ESR measurements gave evidence for unpaired electrons, the nonintegral oxidation state has to be accounted for by assuming a mixture of Pt(II) and Pt(IV).

Platinum α-Pyridone Blue. Because of the lack of reproducibility in preparing the platinum blues, it was realized that unambiguous determination of the properties of blues demanded the preparation of a crystalline material that would yield to X-ray crystallographic analysis. Using synthetic insights provided by Lerner (45), a crystalline platinum blue was synthesized by reacting the diaquo derivative of cis-diamminedichloroplatinum(II) with α-pyridone, a pyrimidine analog (46) (redrawn here).

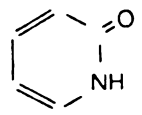

α-Pyridone

α-pyridone furnishes only a single N donor atom and only a single exocyclic oxygen, thereby precluding the formation of mixtures of compounds differing in the site of attachment of platinum to the ligand. Also, by eliminating a second nitrogen from the ring with its attached proton, hydrogen bonding between chains, which may lead to the formation of a mixture of oligomeric species, is avoided. It is probably the formation of oligomers of variable composition that is most limiting to the production of crystals.

The compound may be formulated as $[Pt_2(NH_3)_4(C_5H_4ON)_2]_2(NO_3)_5$ with the platinum atoms having an average formal oxidation state of 2.25. The structure of platinum α-pyridone blue, including the positions of the capping nitrates, is reproduced here (47).

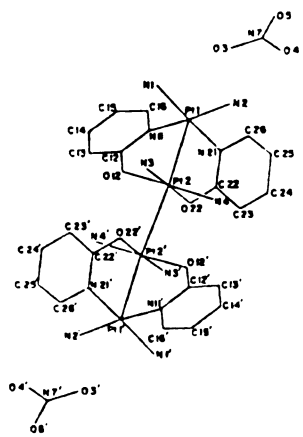

α-Pyridone Blue

Two planar cis-diammineplatinum units are bridged by two α-pyridonate ligands (deprotonated α-pyridone) with a Pt-Pt bond length of 2.774 Å, a length indicative of partial metal-metal bonding. Each of these α-pyridonate-bridged dimers is linked across a center of inversion with a Pt-Pt bond distance of 2.877 Å. From other studies a correlation has been shown to exist between metal-metal bond distance and formal oxidation state of the metal, both with and without bridging ligands (27). The Pt-Pt bond distances of 2.774 and 2.877 Å observed in platinum α-pyridone blue are intermediate between those found in bridged Pt(II) and Pt(III) complexes (47). This is consistent with the average formal platinum oxidation state of 2.25 deduced from the crystallographic data.

Stabilization in the α-pyridone structure is provided by hydrogen bonding between ammine hydrogens of one dimer and the α-pyridone keto oxygens on the neighboring dimer. The four platinum atoms take the form of a zig-zag chain. As is evident, the outer platinums are bonded to the two deprotonated ring nitrogens of the α-pyridonate ligand, while the inner platinum atoms are bonded to the two exocyclic oxygen atoms; this is a head-to-head arrangement. A full account of the crystallographic determination is given in ref. 47. The four-platinum chain length is in contrast to the oligomeric nature of the pyrimidine blues. The structural elucidation of the platinum blue analog α-pyridone blue is signifiant in that this structure may embody features common to all or most amido platinum blues, although it should be recognized that the pyrimidines uracil and thymine, when unsubstituted at N, can bind to platinum through

both keto oxygens and both nitrogens, leading to many more possible structures down the length of a chain.

Approximate Structures of Blues by X-ray Diffraction and EXAFS. As mentioned, cis-diammineplatinum α-pyridone blue is the only blue which has lent itself to complete structural determination by X-ray crystallography, although several nonblue crystalline products have been isolated both from the α-pyridone reaction mix (48) and from reaction mixtures that ultimately produced pyrimidine blues (49-51). One, a crystalline platinum tan, reported to appear in the synthesis of certain blues (5,18,21), was also deliberately prepared as the cis-diammineplatinum α-pyrrolidone tan, $[Pt_4(NH_3)_8(C_4H_6ON)_4]^{6+}$.

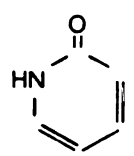

α-Pyridone

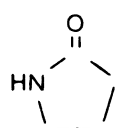

α-Pyrrolidone

Its structure has been determined by X-ray crystallography (21). The structure is striking in that it proved to be nearly identical to that of the α-pyridone blue; that is, a head-to-head amidate-bridged tetranuclear complex. However, in contrast to the 2.25 average platinum oxidation state for α-pyridone blue, an average oxidation state of 2.5 was deduced for the α-pyrrolidone tan (21).

Equally as striking as the structure of the tan is the structure of a crystalline greenish-yellow tetranuclear platinum α-pyridone compound, also head-to-head - $[Pt_2(NH_3)_4(C_5H_4ON)_2](NO_3)_4$ - isolated

by Lippard and Hollis (48), whose structure is practically identical to that of both the α-pyridone blue and the α-pyrrolidone tan. Its platinum oxidation state, however, was shown to be 2.0 (48). These are all compounds that, strictly speaking, are analogs of the true platinum blues; nevertheless, they may be loosely categorized under the generic heading platinum blues. Here are three compounds of virtually identical structure, with only the inter-platinum distances varying somewhat (becoming shorter for higher oxidation states), and each differing from the others in the number of associated counter ions, as required to balance the average Pt oxidation states of 2.0 (48), 2.25 (43,46,47), and 2.5 (21) for the tetranuclear chains. These comparisons confer credibility to the tenet that the color of the platinum blues is clearly associated with the extent of Pt-Pt bonding (vide infra).

A less complete structural characterization was obtained for platinum trimethylacetamide blue, probably for the reason, as previously mentioned, that the crystals were a mixture of three components (bands I, II, & III by silica gel chromatography), one of which (band III), consisted of amorphous blues particles. X-ray powder diffractometry proved useful in elucidating Pt-Pt distances in the latter case. More recently, the newer technique of extended X-ray absorption fine structure (EXAFS) spectroscopy has been utilized for studying the structural variation in several of the amorphous blues. For example, Teo et al. used EXAFS to study a blue compound prepared from cis-$[Pt(NH_3)_2(H_2O)_2](NO_3)_2$ and uridine (a nucleoside), and a purple compound obtained by reacting

cis-[Pt(cyclopropylamine)$_2$]Cl$_2$ with uridine (20).

EXAFS is a technique that allows short-range order about an atom to be determined in cases where the long-range order of crystals, required for diffraction studies, does not exist (52). In EXAFS the X-ray absorption spectrum of a material is measured over an extended energy range in the vicinity of the absorption edge of one particular element. Interatomic distances for Pt-Pt of app. 2.90 Å were established by Teo et al. for both the purple and blue complexes (20). This distance suggests "partial but distinct" bonding between the platinum atoms, and tends to generally substantiate the existence of distinct metal-metal bonding in the family of blues. Pt-ligand separations were also estimated, although the identity of the bonded atoms was not always certain. Since the long-term spatial arrangement is not obtainable by EXAFS, postulating an overall structure is somewhat speculative. In considering several possible structures consistent with the EXAFS data, Teo et al. write, "We believe that the large number of plausible isomers or oligomers (and the numerous reaction pathways for their interconversion) with similar local structures in these platinum pyrimidine blue complexes accounts to a large extent for the difficulty in crystallizing these amorphous materials." In a related work, EXAFS has been used to study the Pt environment in the complex formed by the reaction of the hydroxo-bridged Pt dimer $[(NH_3)_2Pt(OH)_2Pt(NH_3)_2]^{2+}$ with calf thymus DNA (53).

Properties of α-Pyridone Blue. Although platinum α-pyridone blue is not a pyrimidine blue, and although it exhibits no activity toward

malignancies, nevertheless, as the only platinum blue structurally characterized, and because it is not unreasonable to expect α-pyridone blue to embody features common to all platinum blues, it is of interest to study the properties of α-pyridone blue and then to compare these properties with those of other blues. α-pyridone blue has been studied in both the solid state and in aqueous solution. Much of the work to be cited in this section and in the next is due to Barton et al. (18,47).

Magnetic Susceptibility - Magnetic susceptibility measurements revealed an effective magnetic moment of 1.81 μ_B (Bohr magnetons), a value consistent with the presence of one unpaired electron, which is, presumably, delocalized over the length of the tetranuclear chain since only a single set of 4f binding energies was obtained by X-ray photoelectron spectroscopy (43, vide infra). In the α-pyridone tetramer, the paramagnetism arises, formally, from the presence of three diamagnetic Pt(II)(d^8) atoms and one paramagnetic Pt(III)(d^7).

Single Crystal ESR Measurements - ESR measurements on the single crystal confirmed the paramagnetism of α-pyridone blue. Careful analysis indicated that the unpaired spin is delocalized, residing in a molecular orbital derived from d_{z2} orbitals directed along the platinum chain axis. No hyperfine interactions were observed in the single-crystal spectra; this is to be contrasted with the solution spectra (vide infra).

Comparison of Properties of Platinum Blues. Both chemical and spectroscopic properties of various platinum blues in aqueous

solution will be reviewed in this section, but with emphasis on the behavior of platinum α-pyridone blue (PPB). In the most complete comparison made to date, Lippard et al. (18) compare the structurally-characterized PPB, platinum acetamide blue (platinblau, PAB), cis-diammineplatinum uracil blue (PUB), and cis-diammineplatinum hypoxanthine green (PHG, a purine blue).

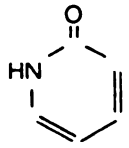

α-Pyridone

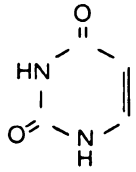

Uracil

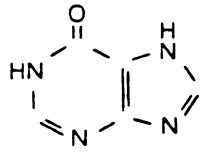

Hypoxanthine

Visible spectroscopy was used to study the stability with time, and ESR and visible spectroscopy were jointly used to show the correspondence between an unpaired electron and color. That is, as the color intensity of PPB faded during the course of a Ce(IV) titration, there was a concomitant decrease in the ESR signal. As the ESR signal is a measure of the unpaired spin intensity, the implication of the role an unbound and unpaired electron plays in conferring color is clear. Oxidation beyond the 2.25 state, the oxidation state indigenous to the tetranuclear PPB, allows for coupling of spins and leads to a more localized system. Formal oxidation states were guaged by both oxidative titration using Ce(IV) and reductive titration (reducing platinum to the metal) using ferrous sulfate. The latter is an indirect titration and was plagued by slow kinetics and a blank level, due to the ligands, corresponding

to 60% of the volume of titrant used. Finally, gel electrophoresis was used to compare relative lengths of the various blues.

Variability of Preparations - The appearance (including color) and nature of the blues obtained are dependent on reaction conditions, with many factors being under the experimenter's control. The difficulty in producing a reproducible platinblau (platinum acetamide blue) has been referred to earlier. Typically, incubation times of a day on up to a week are required at temperatures (usually) slightly above room temperature. Using an incubation period in excess of four days with α-pyridone leads only to the production of noncrystalline material. Indeed, the chemical and spectral characteristics of the noncrystalline PPB resemble more closely those of the pyrimidine blues than those of crystalline PPB.

Optical Spectra - The visible spectrum of PPB, characterized by a broad transition centered at 680 nm, is highly sensitive to conditions, including temperature, the presence of anions or acid, and time, the last demonstrating that aqueous solutions of PPB are unstable. The molar absorptivity at 25°C (0 time) was calculated to be ε_{680} (PPB) = 60 ± 15 M^{-1} cm^{-1} (18). Extraneous salts containing nitrate or perchlorate increase ε_{680} by a factor of 5-20 while chloride or acetate leads to complete discharge of the color.

The other platinum blues, particularly PUB, exhibit variations in their band maxima, and as such, provide a means for monitoring the reproducibility of a preparation. Ordinarily, the maximum shifts throughout the course of a synthesis, which, as stated, can take many

days. Flynn et al. report that, depending on conditions with 1-substituted uracils, peaks or shoulders appear from 450-480, 560-580, and 680-720 nm (17); these obviously correspond to solutions of different colors. These results are indicative of a multiplicity of species in solution.

As with the crystalline PPB, the molar absorptivities of the other platinum blues vary with the manner of preparation, but to a lesser extent. Molar absorptivities of several hundred are estimated for PUB and PHG, while the range is estimated to be 1100-1500 M^{-1} cm^{-1} for PAB (18). These other blues also appear to be more stable in aqueous solution than PPB, although Lippert reports on the instability of a platinum uridine blue in DMF solution (5). The electronic spectrum of a platinum acetamide blue (platinblau) was referred to earlier. The breadth of the absorption peak(s) in all blues is indicative of their complexity and suggests that they are variable mixtures of several components (17). The breadth may also be indicative of a valence-delocalized system (19).

ESR Spectra - In aqueous solution the ESR spectrum of PPB is characterized by a broad, approximately axial signal with $g_{\perp} \simeq 2.4$; the parallel component, $g_{\parallel}$, was found to be $\simeq 2.0$ (18). (A free electron has $g = 2.0023$.) The anisotropy (i.e., distinct g values perpendicular to and parallel to the field) stems from the fact that the ESR spectra were recorded on frozen solutions (77 K). Hyperfine coupling interactions, which are presumed to arise from the interaction of the unpaired spin with ^{195}Pt nuclei (33.7% naturally abundant), are apparent. However, incomplete resolution of the

hyperfine structure complicates interpretation. In any event, the hyperfine structure is suggestive of electron delocalization over several platinum atoms. Double integration of the derivative spectra yielded 0.8 $\pm$ 0.2 unpaired spins per tetramer, a value consistent with the average formal oxidation state of 2.25 assigned on the basis of crystallographic data.

The ESR spectrum of PUB is striking in its similarity to that of PPB (5), PUB also exhibiting extensive ^{195}Pt hyperfine interactions. The precise g values for PPB were determined to be $g_{\parallel}$ (PPB) = 1.976 and $g_{\perp}$ = 2.380. The corresponding values for PUB are $g_{\parallel}$ (PUB) = 1.97 and $g_{\perp}$ (PUB) = 2.38. The intensity of the perpendicular component obtained for PUB is substantially lower than that of PPB. Although the authors do not say so, this difference in intensity may well reflect the difference in formal oxidation state possessed by these two species, as was determined by redox titrimetry (vide infra, also determined by X-ray crystallography in the case of PPB). PAB exhibits an even weaker ESR signal, as does PHG (18). By monitoring either the ESR signal intensity or the intensity of the blue absorption band, the decomposition of PPB with time could be monitored. Their parallel dimunition demonstrates the correspondence of the blue chromophore with the unpaired spin density.

Oxidative Titrations - The oxidation of PPB by Ce(IV) was followed spectrophotometrically and by ESR, and later was followed potentiometrically as well (42). A parallel, linear reduction in the intensity of both signals was observed out to the end point, which corresponded to 3 equiv/tetramer. This result is consistent with the

previously-assigned average oxidation state of 2.25 when the product of the titration is postulated to be two diamagnetic platinum(III) dimers. This behavior further supports the conclusion that, at least initially, aqueous solutions of PPB contain the tetranuclear structure determined in the solid state.

PAB and PHG were not as well behaved as PPB in that a linear extrapolation in the spectrophotometric titration curves was required to define an end point. The difference in behavior may reflect both the greater structural complexity and variability of these blues relative to the crystalline PPB tetramer. Unlike PPB, where 0.75 equiv of cerium/platinum was required, 1.75 equiv Ce/Pt were required for PAB and 1.54 $\pm$ 0.20 equiv Ce/Pt for PAG. These results show that the metal oxidation state is nonintegral in all of these platinum complexes. These latter two numbers of equivalents require that platinum(IV) be the end product of the titration. For the more precise value 1.75 equiv Ce/Pt, obtained for PAB, an average initial oxidation state of 2.25 may be assigned to platinum (not in agreement with any of the values previously proposed for platinblau). Platinum uracil blue (PUB) could not be measured, because in the HNO_3-NH_4NO_3 medium used for the titration, precipitation occurred. (In the Experimental and Results sections, the Ce(IV) titration of platinum 1-methyluracil blue (Pl-MeUB), carried out in a different acid medium, is described.)

Spectrophotometric titrations of cyclopropylamineplatinum 1-methylthymine purple with Ce(IV) have, analogously, shown this purple platinum complex to be mixed valent, although in this instance

a formal platinum oxidation state of 3.72 ± 0.05 was assigned (19). This average state was postulated to arise from a combination of Pt(II) and Pt(IV) ions, hence requiring a minimum of six Pt atoms per polymeric unit. In another study, three related platinum phthalimide blues, obtained by varying slightly the reaction conditions, were titrated in 4.5 N HCl by Ce(IV) in sulfuric acid (24). Average oxidation states of 2.9, 3.0, and 3.3 were assigned. Armed with elemental analyses and the fact that all three species proved to be diamagnetic, the phthalimide blues were postulated to consist of Pt(II)- and Pt(IV)-containing polymer units.

Reductive Titrations - Reductive titrations were performed using an excess of ferrous sulfate as the reductant; the excess was then titrated with permagnanate solution to the first stable appearance of a pink color. Because of the significant volume of titrant consumed by the reducible bridging ligands, the uncertainty in the indirect reductive titration of platinum to the metal was large. A value of 2.27 ± 0.10 was assigned to platinum in PPB, a result that encompasses the value of 2.25 deduced from X-ray crystallography and calculated from oxidative titrations. A value of 2.08 ± 0.15 was obtained for PUB, a value suggesting weak paramagnetism, consistent with the weak signal intensity observed in ESR. A value of 2.28 ± 0.17 was assigned to PHG. In the Gel Electrophoresis section to follow, evidence is presented that indicates that of these three complexes, PUB has the longest chain length. It may be that paramagnetism in long platinum chains is diminished due to a delocalized molecular orbital over many centers.

Recall that in order to explain the oxidative titration data, an end product containing Pt(III) was postulated for PPB while Pt(IV) was invoked to account for the PAB and PHG titration curves. It has been suggested by Lippard et al. (18) that bridging by two α-pyridonate ligands per dimer facilitates formation of the Pt(III) state. This can perhaps be understood by visualizing the Pt(III)-Pt(III) dimer as being formed by transfer of two Pt(II)-Pt(II) d_{σ^*} electrons to the unsaturated ligands provided by the dual bridges, thereby removing antibonding electrons and leaving $[Pt(III)]_2$ as $d_{\sigma 2}$ (54). The longer the platinum chain, the more unlikely it is, based simply on a consideration of steric factors, that double bridging will occur over the length of the chain. Rather, single amidate bridging, as shown, may be more reasonable for the longer-chain oligomers as typified by true platinum blues.

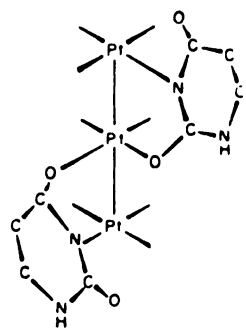

A likely structure for a platinum blue - one exhibiting alternate single bridging

An argument might be then that without the facilitation or stability accorded by double bridging, the more usual oxidation state of +4 may be a more reasonable value for the end product of these other titrations. However, since the III state will be invoked in the

Results section for the end product of an oxidative titration of Pl-MeUB, I would not adopt this argument as universally applicable.

Other possible structures for a platinum pyrimidine (uracil) blue are shown below (taken from ref. 12). Amidate linkages through both deprotonated N1 and N3 nitrogen atoms are shown on the left. PUB could also consist of a mixture of these various representations. In addition, uracil has provision for hydrogen bonding interactions between ammine hydrogens and the nonbonding keto oxygen of the neighboring uracil moiety.

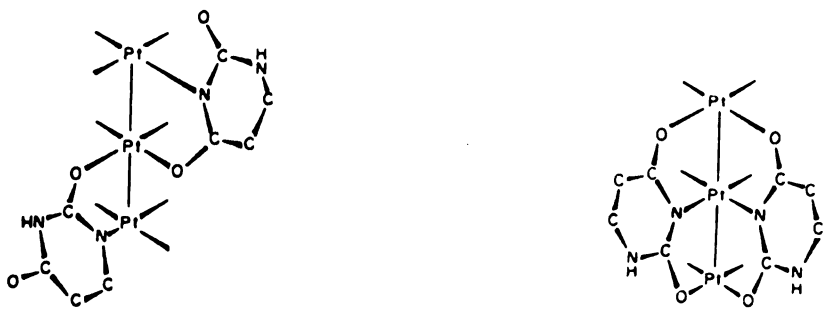

Alternate proposed structures for a platinum uracil blue

Size Determination by Gel Electrophoresis - Gel electrophoresis experiments in which band position was determined by first staining the gel and then measuring platinum by atomic absorption spectroscopy, showed the relative sizes of the three blues considered to fall in the order PPB < PHG < PUB. This series was deduced from their relative mobilities and assumes the same charge per repeating monomeric unit - $[(NH_3)_2Pt(amidate)]^{1.25+}$. (In electrophoresis, the mobility is inversely proportional to molecular weight or chain

length.) Based on the reductive titration results presented above, this assumption is not rigorously correct. Each of the bands had a breadth indicative of a large distribution in the linear (also assumed) platinum oligomers. In another study, also based on gel electrophoresis, platinum thymine blue was shown to possess a continuous distribution of molecular weights ranging from 3000 to 1000 or less with a maximum around 2000 amu (5).

Molecular Weight by Sedimentation - An alternate approach to molecular weight determination is sedimentation by ultracentrifugation. The polymeric nature of bis(cyclopropylamine)platinum 1-methylthymine blue was confirmed by sedimentation analysis (19). Although several assumptions were inherent to the authors' approach, an upper limit to the molecular weight was calculated to be about 5000 amu.

Electrochemistry of Blues. To the author's knowledge, no electrochemical studies of the true platinum blues have been published. A single study was concerned with the electrochemical characterization of a compound derived from platinum α-pyridone blue (PPB) and of another compound obtained in the preparation of PPB, both structurally characterized (41). Presumably, a study of compounds whose structures are known was undertaken to render interpretation more meaningful, much as was done for other kinds of measurements on PPB.

Oxidation by 3-5N HNO_3 of the crystalline α-pyridone blue, $[Pt_2(NH_3)_4(C_5H_4NO_2)]_2(NO_3)_5 \cdot H_2O$, a head-to-head tetramer, produced a

red-orange, head-to-head, metal-metal bonded Pt(III) dimer of composition $[(H_2O)(NH_3)_2Pt(C_5H_4NO)_2Pt(NH_3)_2(NO_3)](NO_3)_3 \cdot 2H_2O$, [A], also crystalline. A red, crystalline head-to-tail platinum(III) dimer, cis-$[(NO_3)(NH_3)_2Pt(C_5H_4NO)_2Pt(NH_3)_2(NO_3)](NO_3)_2 \cdot H_2O$, [B], was similarly produced from the corresponding Pt(II) dimer, $[Pt(NH_3)_2(C_5H_4NO)]_2(NO_3)_2 \cdot 2H_2O$, a compound isolated from the reaction mixture of α-pyridone blue (41). The +3 oxidation state in these compounds was established by a combination of elemental analysis, spectroscopic and electrochemical measurements. Combining the fact that each of these compounds proved to be diamagnetic with the results of controlled-potential coulometry for the determination of n, and knowing the oxidation states of platinum in the starting materials, allowed a deduction of the +3 state. The Pt-Pt bond in these compounds is taken to be a single bond as expected in a d^7-d^7 system with the electronic configuration $\sigma^2\pi^4\delta^2\delta^*2\pi^*4$. Electrochemical techniques employed included cyclic voltammetry, controlled-potential coulometry, and differential pulse voltammetry (differential pulse polarography).

Electrochemical oxidation of the head-to-tail Pt(II) dimer (precursor of [B]) was shown to be reversible only at slow scan rates (<50 mV/s). This observation, coupled with changes in the anodic-to-cathodic peak current ratio (i_{pa}/i_{pc}) and changes in the peak-to-peak potential difference (ΔE_{p-p}), led the authors to postulate a coupled chemical reaction, possibly involving the coordination of the axial ligands NO_3^- or H_2O (see chemical formulae above). As expected, exhaustive oxidative electrolysis produced a

net loss of one electron per platinum atom. Cyclic voltammograms recorded before and after electrolysis were identical. From the cyclics it was deduced that removal of a second electron ($Pt^{II}Pt^{III} \xrightarrow{-e^-} Pt^{III}Pt^{III}$) is easier (occurs at a less positive potential) than removal of the first ($Pt^{II}Pt^{II} \xrightarrow{-e^-} Pt^{II}Pt^{III}$). In such a case only a single wave is apparent in the voltammogram (41):

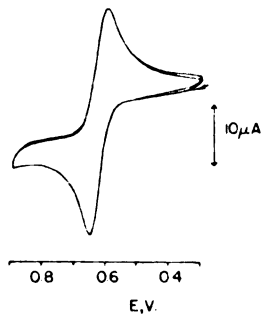

Cyclic voltammogram of head-to-tail platinum(II) dimer $[Pt(NH_3)_2(C_5H_4NO)]_2 \cdot 2H_2O$(v = 20 mV/s)

This precludes the isolation of an intermediate $Pt^{II}Pt^{III}$ species. This behavior is, according to the authors, unusual for an inorganic system.

The electrochemical behavior of the α-pyridone-derived head-to-head Pt(III) dimer, [A], was similar to that of [B] in that a single wave was observed in the cyclic voltammogram. In contrast to [B], reversible behavior was not observed at any scan rate, only quasi-reversible. In the case of [A], the redox process also appeared to involve a coupled chemical reaction following overall two-electron transfer, although the kinetics of the coupled reaction were not the same as for [B]. This is perhaps not surprising since

the dimer [A] was obtained from the α-pyridone tetramer, whereas the dimer [B] derives from another dimer.

Controlled-potential reductive electrolysis of [A] saw a change in color from the starting orange to green to blue, and finally to a colorless solution. The intermediate blue color is probably due to the formation of the mixed-valence α-pyridone blue, while the colorless solution has all platinums in the +2 state. Electrochemical formation of the platinum α-pyridone from [A] requires the transformation of a Pt_2 system to a Pt_4 system. Because of presumed steric effects which prevent the close approach of two dimeric units, a mixed-valence tetranuclear species cannot form in the reduction of [B] (41). The authors state that, if one assumes reversible behavior for [A] in the slow scan rate limit, then a value for the difference in half-wave potential ($\Delta E_{1/2}$) is obtained (30 $\pm$ 10 mV) that implies that the second electron is harder to remove than the first. They conclude from this that for the α-pyridone-derived head-to-head isomer [A], the mixed-valence $Pt^{II}Pt^{III}$ dimer is therefore a possible intermediate in the electrochemical conversion of PPB to [A]. The conclusion that the second electron is less easily removed than the first (which implies a second wave) is not consistent with their report of a single wave in the cyclic voltammogram.

Paramagnetism of Platinum Blues. Because of the central role paramagnetism plays in an understanding of platinum blues, a separate section is devoted to a review of this topic.

Nature of NMR Signals - Paramagnetism is most straightforwardly measured by ESR, but confirming evidence can often be obtained by NMR. NMR peaks become broader and smaller, and can even disappear into the baseline. The origin of the degraded NMR signal intensity lies in relaxation effects which depend on the extent of interaction between nuclear and electron spins; this will be explained more fully in the Results section under the NMR coverage. This degradative effect can be observed by monitoring the formation of a blue by NMR during its incubation, and noting the degradation and eventual disappearance of the absorptions arising from ligand protons. This is concurrent with the appearance and gradual rise of the EPR signals (5).

Illustrative of this effect, Flynn et al. found it difficult to acquire NMR spectra of the pyrimidine blues, which they attributed to the appearance of paramagnetic species (17). The proton peaks were either very broad or nonexistent. As part of a monumental study on the binding sites of unsubstituted uracils in platinum complexes, Lippert reported on the broad and asymmetric peaks obtained in the ^{1}H NMR spectra of a uracil blue (55). It should be mentioned that a broad absorption may also be indicative of a polymeric material (19), and, in fact, for the blues, the broad signals observed may be related to both effects (55).

Chemical Evidence for Paramagnetism - While most evidence for the partially-oxidized nature of platinum in the platinum blues stems from spectral measurements or titrations, chemical evidence has been advanced as well. Discharge of a uracil blue's color was achieved

with a fractional equivalent of V(II), suggestive of an average oxidation state slightly in excess of 2 (17). In addition, reaction with I^- to give a brown rather than a yellow product provided further support for an oxidation state in excess of 2 (17).

ESR of Platinum Blues - Lippert reported ESR studies of a number of platinum blues, including several preparations of uracil blue, a 5,6-dihydrouracil, 6-methyluracil, thymine, and uridine blue (5). A $g_\perp$ value of app. 2.4 was common to these compounds. The observed paramagnetism was attributed to a paramagnetic platinum ion, most likely Pt(III) (although the +3 oxidation state of platinum was assumed by Lippert to be only metastable). Further analysis of the spectra led to the conclusion that the hyperfine splitting present was indicative of only a single nuclear species, that being ^{195}Pt (I = 1/2), although the intensity pattern suggested that more than one Pt nucleus was involved, as in a chain.

Quantitative measurements obtained by double integration of the first derivative spectra revealed only a small percentage of paramagnetic Pt (attributed to Pt(III)) in these blues: uracil - 1.36 (8 preparations); 6-methyluracil - 1.66 (2); 5,6-dihydrouracil - 3.56 (2); thymine - 3.35 (3); and uridine - 0.60 (1). These percentages in turn translate to the following average formal oxidation states for Pt:

uracil - 2.014
6-methyluracil - 2.017
5,6-dihydrouracil - 2.036
thymine - 2.034
uridine - 2.006

Hence, these blues appear to be only very weakly paramagnetic. Lippert advanced the interesting thesis, based on animal studies, that the extent of antitumor activity is dependent on (proportional to) the intensity of the ESR signal (extent of mixed-valency) (5).

Type O and R Spectra - Seul et al. performed redox experiments on aqueous solutions of platinum 6-methyluracil blue (P6-MeUB), measuring the ESR spectra of oxidized and reduced forms (56). In contrast to the weakness of the ESR spectra of most "untreated" blues (as noted in the previous paragraph), a spectrum of considerable intensity and relatively high resolution was obtained for P6-MeUB. In fact, cis-diammineplatinum 6-methyluracil blue was reported to yield the highest spin concentration of all the blues tested (57). These authors reported generating type R (reduced), type O (oxidized), and type R/O ESR spectra, spectra they regarded as being fundamentally different, upon reduction and oxidation with ascorbic acid and hydrogen peroxide, respectively. They employed second derivative analysis to detect type R and type O contributions to a given spectrum. Untreated P6-MeU was regarded as O type. Interestingly, they demonstrated a corresponding difference in the optical spectra as well.

The reporting of R and O type spectra by Seul et al. contrasts with the observations of Lippard et al., who, in following the oxidative titration of PPB by ESR, noted a reduction in the $g_{\perp}$ and $g_{\parallel}$ signals and a concomitant emergence of a signal attributed to Ce(III), but reported no other changes (18). In light of the discussion to be presented in the Results section, this contrasting

behavior is understandable: While additional Pt(III) states are being generated during the oxidative titration of PPB, as soon as the average oxidation state exceeds the indigenous state of 2.25, the electron spins begin to pair up through orbital overlap; consequently the ESR signal due to platinum gradually vanishes. In the case of O and R spectra, the overall spin intensity is increased over the indigenously small spin intensity upon chemical oxidation or reduction with hydrogen peroxide or ascorbic acid, respectively. This is so because delocalization is (presumably) confined to more-or-less discrete lengths of the platinum chain (to a single Pt atom for an R type system, vide infra), which means that up to a certain point in the oxidative process, spin-pairing will be at a minimum.

To explain the R type system, the authors invoked the concept of electronic states localized to approximately a single Pt site, reflective of inequivalent Pt sites (different local pyrimidine ligand-to-Pt stoichiometries). A study of the temperature dependence of the O species' ESR signal revealed an abrupt change in the line pattern between -39 and -34°C. By comparing this behavior with that noted for Magnus' Green Salt, a linear Pt(II) chain containing Pt(IV) impurities, the authors concluded that for type O species the electron spin interacts over several Pt centers.

Neubacher et al. extended this study to other ligands, including uracil, 1-methyluracil, 5-methyluracil (thymine), and 1,5-dimethyluracil (58). It was mentioned that of the several species examined by Seul et al. (56), the platinum 6-methyluracil blue

solution turned out to contain the highest concentration of paramagnetic species. For these other ligands, the same O type spectra were obtained as for 6-methyluracil, whereas there were differences in their R type spectra. It is suggested that the paramagnetic species and corresponding O type spectra formed upon oxidation by H_2O_2 derive from Pt(II)-containing oligomers whereas Pt(IV) is the precursor to type R. There might be value in studying this redox behavior electrochemically, where the experimenter has precise control over redox potentials.

Paramagnetism of Nonpyrimidine Blues - A compound related to platinum blues, one containing both guanosine (a purine) and 1-methylnicotinamide as ligands, exhibited several features common to the platinum blues: 1) the UV and visible spectra displayed broad absorptions, 2) ^{1}H and ^{13}C NMR spectral signals were somewhat broadened, 3) ESR signals were detected in both the solid and in solution, and 4) the color could be discharged by either oxidizing or reducing agents (30). Oxidative titration by Ce(IV) revealed that 1.75 $\pm$ 0.08 equiv Ce/Pt were required for complete oxidation, which, when assuming Pt(IV) as the titration end product, leads to an average formal oxidation state of 2.2-2.3. ESR measurements in solution revealed relatively simple, well-resolved hyperfine interactions for both the perpendicular and parallel g components (3 absorptions for each). This stands in contrast to the extensive coupling observed in the aqueous solutions of α-pyridone blue, as discussed earlier. As the extensive hyperfine coupling was attributed to delocalization over several platinum centers in the

case of the α-pyridone blue, the simpler spectrum obtained in this case for the purine blue suggests the occurrence of a localized, unpaired spin. The authors accounted for the paramagnetism by postulating a mixed-valent species involving Pt(II) and Pt(III) in an oligomeric unit. As with other blues, a large $g_{\perp}$ (=2.41) was obtained, indicative of considerable spin-orbit coupling of the odd electron, a behavior typical of the heavier paramagnetic transition metal ions.

Another compound displaying the characteristics of the generic platinum blues - blue color, paramagnestism, antitumor activity - is formed from the reaction of K_2PtCl_4 and asparagine (33, mentioned earlier). Its ESR spectrum, like all the others considered, is typical for an axially-symmetrical complex, and has $g_{\perp} = 2.39$ and $g_{\parallel} = 1.97$. Unlike the preceding case for the purine, the hyperfine pattern in the perpendicular component is ill-resolved, and is assigned, as before, to the interaction of the unpaired spin with the ^{195}Pt nucleus. The authors suggest that the paramagnetic species is Pt(III) of d^7 configuration.

When cis-diamminedichloroplatinum(II) and tryptophan, an amino acid, are reacted, a paramagnetic reaction product is obtained (31); the product is dark brown. This compound may have relevance since amino acids and proteins have been shown to be molecular sites of action of platinum complexes (31,32). Again, the ESR spectrum is interpreted to be that of an axially-symmetrical complex with $g_{\perp} = 2.006 \pm 0.005$ and $g_{\parallel} = 1.905 \pm 0.005$. The paramagnetism is believed to be due to Pt(III) with a hole, most likely in a d_{z^2} orbital. The

reaction between cis-$Pt(NH_3)_2Cl_2$ and cytosine also yielded a paramagnetic species (23), but the authors offered no interpretation as to the probable orbital description.

When two platinum L-glutamine complexes, one blue and the other green, were examined by ESR, only the former proved to be paramagnetic. Again, the spectra were interpretable in terms of an axially-symmetrical ion with $g_{\perp} = 2.44$ and $g_{\parallel} = 1.99$. It is becoming clear at this point that the paramagnetic platinum blues are, in general, characterized by an upfield shift in $g_{\perp}$ of app. 0.4 from the position of the free electron. The interpretation usually given is one of a d_{z^2} hole state with an admixture of the degenerate $d_{xy,yz}$ state due to spin-orbit coupling. The ground states d_{xz} and $d_{x^2-y^2}$ are eliminated from consideration on the basis of ligand field arguments (59,60). (This will be expounded on in the Results section.)

The fact that the platinum L-glutamine blue is paramagnetic and the L-glutamine green diamagnetic is reminiscent of the correlation between the paramagnetism of platinum α-pyridone blue and its blue color and the diamagnetism (deduced from its valence of 2.0) of the isostructural greenish-yellow compound isolated from the PPB reaction mix (see p. 29). It was noted that the shorter the Pt-Pt distance, the more intense is the color and the greater the paramagnetism. It may be that the Pt-Pt proximity acts to stabilize the paramagnetism through delocalization of the unpaired spin over several platinum atoms. A discussion of the origin of the color is deferred to later.

In summary, the consensus seems to be that the ESR spectra of the platinum blues and related compounds imply axial symmetry. The observation made, without exception, is that the order $g_{\perp} > 2 > g_{\parallel}$ is consistent with the postulation that the unpaired spin of d^7 Pt(III) occupies a d_{z^2} orbital. The extent of hyperfine coupling varies, but in the true blues, the coupling pattern suggests interaction over several platinum centers. Interaction over several centers in turn suggests a polymeric nature to the blues.

Photoelectron Spectroscopy of Platinum Blues. X-ray photoelectron spectroscopy (XPS) can be used to elucidate oxidation states in the solid state, and as such could be expected to have utility for the mixed-valent platinum blues. This is indeed the case. Because XPS may not be as familiar to the reader as other techniques discussed here, it is presented more fully, with an introduction provided prior to reviewing the pertinent literature.

Background (61-63) - In photoelectron spectroscopy (PES, also known as Electron Spectroscopy for Chemical Analysis, ESCA), binding energies of electrons are determined. These binding energies are characteristic of atoms and allow, in most cases, atoms to be identified and their oxidation states to be specified. Either ultraviolet or X-ray excitation is used to eject electrons whose kinetic energy distributions are subsequently measured; a plot of electron counts vs. binding energy yields the PES spectrum. Application of UV-PES is generally restricted to gases and yields primarily binding energies of valence electrons. For the ejection of

core electrons (non-valence electrons) from solids, the higher-energy X-ray source is required; the technique is then known as XPS.

The resultant kinetic energy of an ejected electron obeys the relationship $E_k = E_{source} - I_k$ where I_k is the electron's ionization energy. The binding energy E_b is related to E_k through $E_b = E_{source} - E_k - \phi_{spec}$, where ϕ_{spec} is the spectrometer work function, the energy necessary to remove an electron from the surface of a spectrometer. While the X-radiation normally leads to the ejection of a single electron, any electron of binding energy less than E_{source} is a candidate for emission.

A change in the local environment of an atom alters the charge distribution at that atom and in turn reflects itself as a change in the binding energies, not only of the valence electrons, but of core electrons as well. This is the potential field model of XPS. Elaborating on this - a change in the formal charge of the atom, which results from a redistribution of valence electrons upon a change in the atomic environment, alters the effective nuclear charge felt in all orbitals; consequently the binding energies change. The higher the oxidation state, the more tightly held is an electron by the nucleus. This manifests itself as an increase in the binding energy. The shift in energy is known as a chemical shift and has its counterpart in the correlation tables of NMR and IR.

Application to Mixed-Valent Compounds - An obvious application of XPS is to compounds of mixed valency in which oxidation states may be distinguished. The time scale of XPS is on the order of $1x10^{-17}$ - $3x10^{-16}$ s, so that for all but the most rapid intervalence transfers

(includes class I and class II compounds), a distinct peak corresponding to each oxidation state should be obtained. For platinum 1-methyluracil (Pl-MeU) the pertinent interconversion is represented by

$$Pt_A(II)Pt_B(III) \xrightarrow{h\nu}_{IV} Pt_A(III)Pt_B(II)$$

Since the platinums are in different chemical environments in the head-to-head Pl-MeU dimer, a total of four peaks might be anticipated. Whether or not this expectation is realized depends upon the resolution of the system.

There are several seminal points that may limit the information obtained: 1) chemical shift differences are not large (generally within a few eV for a given element; since half-widths are on the order of 1 eV, resolution is limited; 2) small satellite peaks which result from coincident promotion of an electron (not the same one whose kinetic energy is measured) to an unoccupied orbital can make spectral interpretation difficult; 3) so-called exchange peaks sometimes appear in the spectra of paramagnetic species; 4) surface effects, which are legion in XPS, may lead to spectra not representative of the bulk sample. The useful penetration depth in XPS is ordinarily no more than about 2 nm.

XPS offers two potential benefits to the current investigation: 1) examination of the oxidation states of the partially-electrolyzed Pl-MeU can be made in the solid-state; 2) the extent of mixed valency of platinum in Pl-MeUB, also in the solid state, can be made, thereby

complementing the determinations made in solution using other techniques.

Pertinent Literature Reports - Although the oxidation state of a metal ion can often be determined through a measurement of binding energy, this is not necessarily the case, as was shown by Matienzo in a study of about 70 nickel compounds. A variation of 4.3 eV was obtained for a series of Ni(II) compounds when ligands of different electronegativity were situated around the metal ion (64). It follows that the correlation between oxidation number and binding energy for a closely-related series of compounds is valid only when the ligands are quite similar. In the absence, though, of environmental influences (ligand effects), it has been shown that binding energies for Pt(IV) are between 2 and 3 eV higher than those for Pt(II) compounds (65).

The first application of XPS to blues was made in 1975 on a class I platinum uracil blue (2). A binding energy of 73.6 eV was reported for 4f electrons in platinum. The authors stated that platinum(IV) complexes yield binding energies between 75.9 and 76.1 eV and platinum(II) complexes have binding energies between 72.3 and 74.0 eV (the energy level is, apparently, the $4f_{7/2}$). Therefore they concluded that the platinum was divalent. (The concept of platinum(III) did not exist at that time.) Later measurements by ESR on a variety of platinum methyluracil blues revealed that a paramagnetic species was present only to the extent of 0.1 to 6 mole-percent based on the amount of platinum (5).

An extensive XPS study of three platinum blues was published by Barton et al. in 1978 (43). They compared the spectra of platinum α-pyridone blue, the only blue whose structure has been crystallographically determined, platinum acetamide blue, and platinum uracil blue. Although the platinums have been shown to reside in two distinct environments in the α-pyridone blue, only the $4f_{5/2,7/2}$ doublet (fwhm ~1.3 eV) expected from the $4f_{5/2}$ and $4f_{7/2}$ levels of a single platinum was observed, hence suggesting extensive delocalization. Furthermore, the binding energies were similar to those exhibited by Pt(II) complexes such as cis-$Pt(NH_3)_2Cl_2$, a result which the authors claimed was "in accord" with the previously-postulated formal average oxidation state of 2.25 for platinum in the blue α-pyridone complex. The XPS spectra of the uracil and acetamide blues were strikingly similar to the α-pyridone spectrum, also suggesting an average oxidation state close to 2 in these two compounds. The only spectral difference of any consequence in the uracil and acetamide blues was a slightly greater peak width (fwhm ~1.5 eV). These results led to the conclusion that the electronic structures are similar in all three compounds. This is a significant conclusion in that the uracil and acetamide blues, unlike the α-pyridone complex, are amorphous materials.

An XPS study on a related compound - a platinum oxamate blue, a compound believed to consist of repeating polyanionic platinum-containing structural units - provides evidence for mixed-valency, according to the author (66). As in the previous study, a single doublet is observed in the XPS spectrum; however, the

breadth of the peak (up to 2.3 eV at fwhm), prompted the author to deconvolute the spectrum. The deconvolution revealed two pairs of doublets, a result which can be interpreted in either of two ways: 1) the existence of two different oxidation states on the platinums (mixed-valency) or 2) different ionic environments (that is, different bridging ligands, a distinct possibility for the oxamate). It is clear that interpretation is not always straightforward. As the previous study of the α-pyridone shows, mixed-valency is not always reflected in the photoelectron spectrum.

Binuclear Platinum(III) Complexes -

Part of this dissertation involves the production and characterization of a binuclear platinum(III) compound as well as an intermediate $Pt^{II}Pt^{III}$ compound. The possible intermediacy of a $Pt^{II}Pt^{III}$ complex was mentioned in the section on Electrochemistry of Blues in connection with the production of platinum α-pyridone blue by reductive electrolysis. However, no such compound was identified or isolated. As already indicated, platinum(III) appears to be a relatively recently recognized species in platinum chemistry. To date only a few binuclear Pt(III) compounds are known, and except for the two dimers [A] and [B] discussed in the Electrochemistry section, and a related compound, $[(NO_2)(NH_3)_2Pt(C_5H_4NO)_2Pt(NH_3)_2(NO_2)](NO_3)_2 \cdot H_2O$ (67), none relates to the chemistry of the platinum blues.

In addition to those Pt(III) compounds mentioned above, the known Pt(III) binuclear compounds include $K_2[Pt_2(SO_4)_4(H_2O)_2]$ (68), $Pt_2(O_2C_2F_3)_2(CH_3)_4(NC_6H_7)_2$ (69), $Na_2[Pt_2(HPO_4)_4(H_2O)_2]$ (70),

$[PtR_2(OAc)L]_2$ where R=Ph, L=Et_2S, Pr_2S or R=p-MeC_6H_4, L=Et_2S (71), and most recently, $K_4[Pt_2(P_2O_5H_2)_4X_2]$ where X = Cl^-, Br^-, or I^-, and $K_4[Pt_2(P_2O_5H_2)_4(CH_3)I]$ (54). In the last of these publications (54), NMR spectra (^{31}P, ^{195}Pt, ^{1}H) with sharp resonances characteristic of diamagnetic species were obtained, hence providing evidence for the pairing up of spins. This may be accounted for by the electron configuration $(d\sigma)^2$ in $Pt(III)_2$, in which the two Pt-Pt $d\sigma^*$ electrons of $[Pt(II)]_2((d\sigma)^2(d\sigma^*)^2)$ have transferred to X_2.

EXPERIMENTAL

Introduction

Most experiments were conducted on bis(μ-(1-methyluracilato-N^3,O^2))bis(cis-diammineplatinum(II)), $[(NH_3)_2Pt(C_5H_5N_2O_2)_2Pt(NH_3)_2](NO_3)_2$ (or $[(NH_3)_2Pt(1\text{-MeU})_2Pt(NH_3)_2](NO_3)_2$ where 1-MeU = the monoanion of 1-methyluracil),

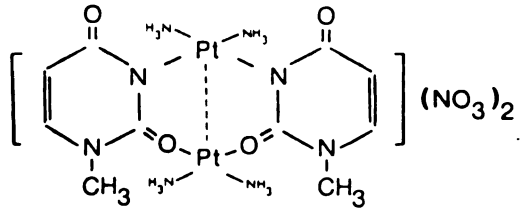

Pl-MeU

to be referred to as platinum (II) 1-methyluracil (Pl-MeU), and on platinum 1-methyluracil blue (Pl-MeUB).

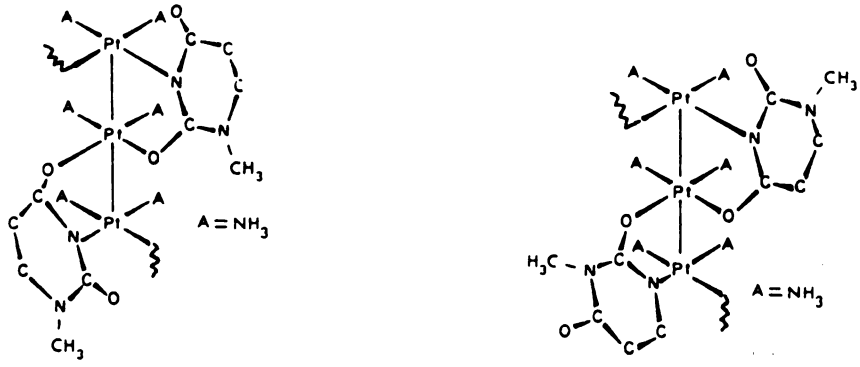

Possible structures for Pl-MeUB over a 3 Pt length (12)
(N-methyl groups added by present author)

Several other compounds related to these - including a platinum benzoate blue and a platinum phthalate blue - were briefly examined and will be mentioned where appropriate in the text.

cis-Diammineplatinum(II) 1-methyluracil (Pl-MeU) is related to the platinum blues in a manner as is described in the next section. It is one example of a number of compounds which have been isolated from reaction mixtures in the course of preparing various platinum blues, compounds which have become of interest in their own right, and as possible precursors to the blues. Several (including Pl-MeU) were later prepared deliberately in designed syntheses. As the reader is aware by now, platinum 1-methyluracil blue is an example of a pyrimidine blue, one of local interest which has been extensively studied in the laboratory of Dr. B. Rosenberg, formerly of the Department of Biophysics, Michigan State University.

Rationale for Interest in Pl-MeU

Compounds originally isolated during the preparation of platinum blues or analogous compounds, but later deliberately prepared in designed syntheses, have been mentioned previously - for example, the head-to-head isomer of cis-$[(H_2O)(NH_3)_2Pt(C_5H_4NO)_2Pt(NH_3)_2(NO_3)](NO_3)_3\cdot 2H_2O$ obtained by oxidizing platinum α-pyridone blue in 5M HNO_3 (41), the head-to-tail platinum(II) dimer $[Pt(NH_3)_2(C_5H_4NO)]_2(NO_3)_2\cdot 2H_2O$ (48) and the corresponding Pt(III) dimer (41), cis-$[Pt(NH_3)_2(C_5H_5NO)_2]Cl_2$ (48), and the tetramer $[Pt_2(NH_3)_4(C_5H_4ON)_2]_2(NO_3)_4$ (48), all related to platinum α-pyridone blue chemistry. A crystalline "diaquo" species, $[(NH_3)_2Pt(OH)_2Pt(NH_3)_2]^{2+}$, was shown to be a product of the

hydrolysis of cis-$(NH_3)_2PtCl_2$ using $AgNO_3$ (72) and has been conjectured as a possible intermediate in the interaction with DNA (53); the two hydroxyls serve as bridges between the platinums. Lippert and Neugebauer isolated a [Pt_4,Ag] complex, $Ag[Pt(NH_3)_2$-(1-MeU)$]_4(NO_3)_5 \cdot 4H_2O$, from a solution of the head-to-head dimer cis-$[Pt_2(NH_3)_4(C_5H_5N_2O_2)_2](NO_3)_2 \cdot H_2O$ (73), which in turn was prepared in analogous fashion to the head-to-head 1-methylthymine dimer $[(NH_3)_2Pt(C_6H_7N_2O_2)]_2(NO_3)_2$ (50).

The latter compound is named bis(μ-(1-methylthyminato-N^3,O^4))-bis(cis-diammineplatinum(II)) dinitrate, and relates to the current investigation in that the synthesis of Pl-MeU was patterned after the synthesis of this compound. Since the structure of Pl-MeU was shown above (p. 59) as containing an N3,O2 linkage rather than an N3,O4 as was obtained for the 1-methylthyminate, it is relevant to point out that in the X-ray analysis of the 1-methylthyminate, there was some uncertainity in the methylated N(1) and C(5) positions, and, in fact, the bridging may be N3,O2 rather than N3,O4.[1]

A similar compound, a yellow platinum dimer containing two bridging 1-methylthymine anions in a head-to-tail arrangement had been reported previously (49). Its formula is also represented as $[(NH_3)_2Pt(C_6H_7N_2O_2)_2Pt(NH_3)_2](NO_3)_2 \cdot 2H_2O$. For this head-to-tail arrangement as well, there was the possibility of ambiguity since N1

---

1. In IUPAC nomenclature the designations N3,O4 etc., do not refer to atoms in a specific ring whereas N(3),O(4A) etc. refer to specific atoms.

and C5 could be interchanged, in which case the bonding would be N3,O2 rather than N3,O4. The authors state that for a similar complex of uracil (not precisely specified), there is no such ambiguity, and, in fact, the bonding is through N3 and O4 (74).

In both the head-to-head and head-to-tail 1-methylthymine dimers, each platinum assumes a square planar configuration with the ammines cis, and each platinum lying roughly on top of the other. The Pt-Pt distance in the head-to-tail 1-methylthymine dimer is 2.974 Å, short enough to suggest a metal-metal bond. The Pt-Pt distance within the head-to-head dimer is 2.909 Å, shorter yet. Both distances are longer than the 2.7745 Å length obtained for the partially-oxidized α-pyridone dimer unit.

The head-to-head dimer is of particular interest because it bears a close resemblance to the head-to-head dimer units comprising one-half of platinum α-pyridone blue. Reaction of bis(1-methylthyminato-N^3)cis-diammineplatinum(II) with the cis-diaquodiammineplatinum(II) cation to form the head-to-head bis-(μ-1-methylthyminato-N^3,O^4)-bis(cis-diammineplatinum(II)), a reaction analogous to the reaction of bis(1-methyluracilato-N^3)cis-diammineplatinum(II) with cis-diaquodiammineplatinum(II) (vide infra) to form the corresponding head-to-head bis(μ-1-methyluracilato-N^3,O^2)-bis(cis-diammineplatinum(II)), may provide a clue as to how N1-substituted pyrimidine-2,4-diones could be arranged in blues, since a substantial amount of blue product is formed in the reaction. A dimer of dimers, as in α-pyridone blue, is one possibility, but attempts to isolate a blue crystalline product

have not been successful in this case (50).

If it is assumed that the 1-methylthymine ligands in bis(1-methylthyminato-N^3)cis-diammineplatinum(II) are free to rotate about the Pt-N(3) bond, then the two reaction products shown below are possible (50):

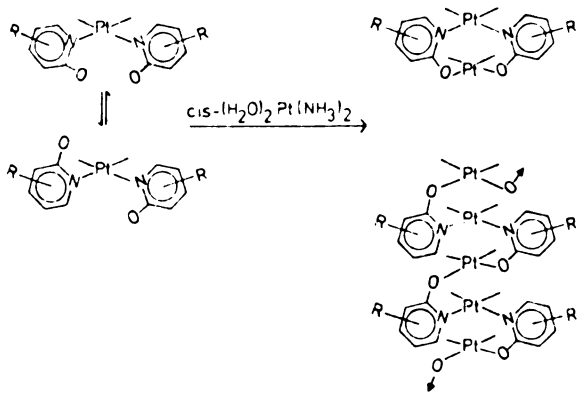

A scheme for the formation of a blue from precursors

The bridging is head-to-head in both products. This model is able to provide for those features believed to be characteristic of the platinum pyrimidine blues: variable chain length, leading to a mixture of oligomers; Pt-Pt distances sufficiently short to permit metal-metal interaction; and, upon oxidation, production of a stabilized Pt mixed-valence state (50). By analogy, the same arguments may be applied to the platinum 1-methyluracil dimer, bis(μ-1-methyluracilato-N^3,O^2)-bis(cis-diammineplatinum(II)). Hence the potential interest in these compounds, both as models and as possible precursors to the platinum pyrimidine blues.

Faggiani et al. deduced the structure of a platinum 1-methyluracilate whose structure was shown to be very similar to that of the head-to-tail isomer of the dimeric platinum

1-methylthymine complex discussed above (74): bis(μ-(1-methyluracilato-N^3,O^4))-bis(cis-diammineplatinum(II)) dinitrate trihydrate, $[(NH_3)_2Pt(C_5H_5N_2O_2)_2Pt(NH_3)_2](NO_3)_2 \cdot 3H_2O$. The synthesis was achieved by reacting 1-methyluracil with cis-$Pt(NH_3)_2(OH_2)_2$. (Production of a head-to-head dimer apparently requires an indirect procedure, as is given in the Synthesis section.) The semicrystalline compound obtained was striking in its blue color. However, since the corresponding 1-methylthymine complex was not a blue, it was deemed unlikely that the 1-methyluracil complex was a true blue. The fact that bond-for-bond and angle-for-angle the two structures proved to be nearly identical (e.g., a Pt-Pt distance of 2.954 Å in the 1-methyluracilate vs 2.974 Å in the 1-methylthyminate) served to reinforce the unlikelihood.

Indeed, it turned out that the blue color did not arise from the named compound, but, as was the case for trimethylacetamide blue (26, see p. 22), the blueness was contributed by an impurity. Also, just as with the trimethylacetamide blue, without the impurity, crystals could not be obtained. Although repeated preparations consistently yielded a yellow-green material, the authors concluded that the head-to-tail platinum 1-methyluracilate is a yellow compound as in the corresponding platinum 1-methylthyminate. While perhaps not of direct bearing to the current topic, a number of other platinum complexes, ones involving methylcytosine ligands, have also been prepared (75-79).

Beyond the structural relevance of Pl-MeU to Pl-MeUB and to platinum pyrimidine blues in general, it may have significance in its

own right as an antitumor agent. In tests against the Ascites S-180J tumor in mice, it proved, surprisingly, to have activity. At a dosage of 100 mg/kg of body weight, 3 cures were obtained in 6 test cases. By comparison, Pl-MeUB, whose antitumor activity had been previously established (2), registered 4 cures in 6 tries at its optimal dosage level of 125 mg/kg (80). The results for Pl-MeU may have significance since this compound does not fit the general empirical rules which have been proposed for antitumor activity in platinum compounds.

As will become amply clear, Pl-MeU proved to be an interesting compound for study from a chemical standpoint. Also, as should be abundantly clear to the reader by now, Pl-MeUB, an obvious relative of Pl-MeU, and a representative of the family of platinum pyrimidine blues, is an equally chemically-intriguing system. Experiments were designed to examine these two systems by electrochemistry (EC), EC/ESR, EC/NMR, EC/Vis, X-ray photoelectron spectroscopy (XPS), redox titrimetry, liquid chromatography, EC/LC, isotachophoresis (ITP) and EC/ITP.

Electrochemistry proved useful in studying redox behavior - in ascertaining extent of reversibility, in determining the number of electrons transferred, and, at least in a qualitative sense, in assessing kinetic behavior. The primary electrochemical techniques used were cyclic voltammetry, rotating disk voltammetry, and controlled-potential coulometry. As the question of oxidation state - i.e., Pt^{II}, Pt^{III}, or Pt^{IV}? - pervaded much of the activity in this work, ESR proved invaluable in addressing this point since Pt^{II} and

Pt^{IV} are diamagnetic whereas Pt^{III} is paramagnetic. In an indirect fashion, NMR can often indicate paramagnetism through deteriorated spectra. The colored species could be studied by visible (and near infrared) spectrophotometry; through application of the Hush treatment, the interatomic electron transfer (intervalence transfer), which is the predominant mechanism contributing color, could be put on a firm theoretical footing. XPS (also known as ESCA) serves to provide information in the solid state complementary to studies in solution involving both ESR and redox titrimetry. Application of Ce(IV) oxidative titrimetry allowed a chemical redox (less selective) study to be compared with electrochemical redox (more selective) behavior, and in particular addressed the question of platinum oxidation state, albeit indirectly. Liquid chromatography was used to characterize the polymeric blue and to study the time behavior of both chemical systems. Isotachophoresis was intended to complement the LC studies.

Synthesis

$[(NH_3)_2Pt(1\text{-MeU})_2Pt(NH_3)_2](NO_3)_2$ was prepared by Dr. J. D. Woollins of Dr. Rosenberg's laboratory using a procedure adapted from that used by Lippert et al. (50) for the corresponding 1-methylthymine compound (vide supra): cis-$Pt(NH_3)_2Cl_2$ was stirred overnight in the dark with $AgNO_3$ in water. After removal of AgCl by filtration, the diaquo product (believed to be a mixture of products, represented generically by $[Pt(NH_3)_2(H_2O)_2]^{2+}$) was treated with $Pt(NH_3)_2(1\text{-MeU})_2 \cdot 2H_2O$ (synthesis described in ref. 41) and its pH

adjusted to 3.0 with 1M HNO_3. The solution was stoppered and stored overnight at room temperature. The volume was then reduced to 5 ml in a rotary evaporator and the product filtered off, washed with ice cold water (3x5 ml) and dried in vacuo. The compound is yellow. The crystals were not of suitable size to readily lend themselves to X-ray crystallographic structural analysis (81).

Platinum 1-methyluracil blue (Pl-MeUB) was also prepared by Dr. J. D. Woollins according to the procedure of Rosenberg et al. (2): cis-Diamminedichloroplatinum(II) was hydrolyzed overnight in water using $AgNO_3$. The cis-diaquodiammineplatinum(II) nitrate product was subsequently reacted with 1-methyluracil at a pH of 7.8. The Pl-MeUB formed slowly over a several days' incubation period at 40°C. The reaction mix was then cooled to 0°C and the blue solid collected by filtration. Reprecipitation of the blue powder was accomplished with ethanol.

Analysis

Microanalysis of Pl-MeU, $[(NH_3)_2Pt(1\text{-}MeU)_2Pt(NH_3)_2](NO_3)_2$, yielded the following elemental composition (80): C, 14.40%; H, 2.42; N, 16.30; O, 19.84; Pt, 44.4 $\pm$ 1.1 (1s)[1] (calc'd: 14.42, 2.64, 16.83, 19.23, 46.9). ^1H and ^{195}Pt NMR along with IR analysis were further used to characterize the compound (80). ^{195}Pt NMR established that bridging was head-to-head. Although the linkage has been drawn as N3,O2 on p. 59, the evidence is not incontrovertible. (Lippert,

---

1. Percent Pt obtained by Dr. S. W. Barr of the Analytical Laboratories, The Dow Chemical Co., Midland, MI.

after a detailed examination by NMR and vibrational spectroscopy of many platinum complexes with unsubstituted uracil concluded that only X-ray analysis permits an unequivocal assignment (55).) Microanalysis of Pl-MeUB revealed the following elemental composition:[1] C, 14.67%; H, 2.57; N, 13.89; O, not determined; Pt, 44.7 $\pm$ 1.1 (1s).[2] Comment on the fit of these latter percentages to proposed structures is deferred until later. Discussion of possible structures has already been given and will be returned to later.

Electrochemistry

The electrochemical techniques employed consisted of cyclic voltammetry (CV), fast cyclic voltammetry (FCV), differential pulse voltammetry (polarography, DPV or DPP), rotating disk voltammetry (RDV), controlled-potential coulometry (CPC), and electrosynthesis (by CPC). Platinum was most commonly used as the working electrode, although initial survey scans made use of other electrode materials as well. More-or-less standard electrochemical cell configurations were used, although all cells were custom built for Dr. Weaver's research group. For experiments in CV, DPP, and RDV, a Princeton Applied Research (PAR) Model 174 Polarographic Analyzer was used. FCV required a more involved setup, and will be described in the appropriate section. A PAR 173 potentiostat in conjunction with a

---

1. Performed by Dr. H. D. Lee of the Department of Chemistry, Purdue University, W. Lafayette, IN.

2. Percent Pt obtained by Dr. S. W. Barr of the Analytical Laboratories, The Dow Chemical Co., Midland, MI.

PAR 179 digital coulometer was used in CPC experiments. The reference electrode in all cases was the NaCl-saturated calomel electrode (ssce). Almost all work was done in aqueous solution. The supporting electrolyte was most often either sodium perchlorate or sodium nitrate (usually at a concentration of 0.1F). A conventional deaeration train with either N_2 or Ar was used, with deaeration provided both before and throughout a run. Recording was done with either a Hewlett Packard 7045A or Houston 2000 X-Y recorder.

Cyclic Voltammetry (CV) -

Various fritted cells of standard design were used with a three-electrode arrangement. A platinum flag electrode was most commonly used as the working electrode, although the use of gold, vitreous (glassy) carbon, and mercury were used where appropriate. A platinum wire was used as the counter (auxiliary) electrode, and the ssce as the reference. Platinum electrodes were ignited in the flame of a Meker burner immediately prior to use.

Fast Cyclic Voltammetry (FCV) -

Conventional cyclic voltammetry, as, for example, can be practiced using a PAR 174 Polarographic Analyzer and a standard servomotor-driven X-Y recorder, accommodates sweep rates up to about 500 mV/s. Beyond this range (and up to many volts per second), where fast cyclic voltammetry takes over, more complex instrumentation is required. A typical setup combines a signal generator and synchronizer (PAR 175 Universal Programmer), a driveable potentiostat (PAR 173), an oscilloscope (Nicolet Explorer I storage oscilloscope),

and an X-Y recorder. A schematic of the setup is given in Figure 1.

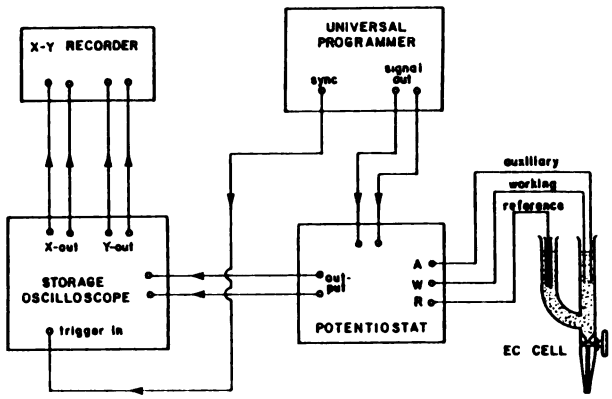

Figure 1. Arrangement for fast cyclic voltammetry.

The cyclic voltammetric responses of Pl-MeU and Pl-MeUB were studied at scan rates up to 20 V/s in an attempt to unravel their mechanistic behavior. Also, in order to relate peaks in the anodic and cathodic portions of the cyclic voltammogram, a series of cyclics was recorded over progressively narrower potential ranges.

Rotating Disk Voltammetry (RDV) -

Either Pt or Au disk electrodes (Pine Instrument Co, Grove City, Pa.), consisting of the metal embedded in a teflon insulator rod, were used in conjunction with a variable-speed rotator, also manufactured by Pine Instrument Co. Most experiments were conducted using a 3.8 mm-diameter Pt or a 2.2 mm-diameter Au electrode. Electrodes were abraded on a polishing wheel with sanding disc, using first 1.0μ jeweler's polishing alumina followed by 0.3μ alumina. Rotational frequencies were read directly from a ten-turn dial. The scan rate was typically 5 mV/s. Cells expressely designed for RDV

were used in all cases.

Differential Pulse Voltammetry (DPV) -

DPV was accomplished at both a dropping mercury electrode (DME) using conventional apparatus, and at a planar, platinum electrode. The scan rate was ordinarily 5 mV/s; pulse modulation amplitudes ranged from 5-50 mV.

Controlled-Potential Coulometry (CPC) -

Oxidative and reductive CPC were performed on Pl-MeU and Pl-MeUB in order to 1) determine n, the number of electrons transferred per molecule, and to 2) obtain mechanistic information. The electrolysis cells were of ~10 ml capacity, and contained two side arms, one for a coiled Pt auxiliary electrode, and the other for the ssce reference electrode, each separated from the working electrode by a fine frit. The working electrode consisted of a coiled (3 turns), 0.031 in.-diameter Pt wire. As mentioned, pretreatment consisted of ignition in the flame of a Meker burner. The most consistent performance was achieved by using a counter (auxiliary) electrode of larger area than the working electrode.

The earliest electrolyses were conducted in $NaClO_4$ supporting electrolyte (usually 0.1F), but because of precipitation problems (although the precipitation was also used to advantage in isolating an intermediate) with Pl-MeU, most of the remaining electrolyses were conducted in $NaNO_3$. As is customarily done in electrolysis work in order to shorten the electrolysis time, the solutions were kept agitated by magnetic stirring. In those experiments in which CV's

were recorded periodically throughout the course of an electrolysis, recording was by a Pt flag electrode. The electrolyses were under the control of a PAR 173 potentiostat; current measurement and integration were performed by a PAR 179 digital coulometer.

The oxidative electrolysis of Pl-MeU and Pl-MeUB was ordinarily conducted at +1.1 V vs ssce, although other potentials were used in special cases. The reductive electrolysis of Pl-MeUB was carried out at -0.1 V vs. ssce. The proper current setting on the PAR 179 was critical for reasons not fully understood. A too-low setting when electrolyzing Pl-MeUB would, as the current decayed to a small value, result in a flickering panel light (Over I light), thereby invalidating the registered value of the accumulated coulombic charge. On the other hand, the higher the setting, the lower the accuracy of the current integration. The explanation for this troublesome behavior probably lies in erratic current measurements stemming from an accumulation of precipitated or adsorbed Pl-MeUB on the electrode surface (vide infra). Pl-MeU, which has little tendency to precipitate or adsorb on platinum, presented no problem when electrolyzed in 0.1F $NaNO_3$. However, when electrolyzed in 0.1F $NaClO_4$, the Over I light would also flicker after the onset of precipitation.

Electrosynthesis -

Electrosynthesis was conducted in the same manner as CPC. The compounds isolated consisted of an intermediate electrolysis product of Pt(II,II)l-MeU (so designated to specify a +2 oxidation state for

each of the two Pt atoms), believed to be P(II,III)1-MeU, and a fully-electrolyzed product, believed to be P(III,III)1-MeU. The fully-electrolyzed Pl-MeUB, in which all platinums may be in the +3 oxidation state, was also isolated. P(II,III)1-MeU precipitated during electrolysis as the perchlorate salt from a 0.1F $NaClO_4$ supporting electrolyte. P(III,III)1-MeU and fully-electrolyzed Pl-MeUB were precipitated as the tetraphenylborate salt from aqueous solutions 0.1F in $NaNO_3$. Because fully-electrolyzed Pl-MeU tended to quickly revert back to a partial green color once the electrolysis was terminated, the precipitation was conducted in situ in the electrolysis cell. With the cell design and electrode configuration used, and when more than 20-25 mg of Pl-MeU were electrolyzed in 0.1F $NaClO_4$, the rate of electrolysis sometimes slowed drastically to the point that the electrolysis had to be interrupted to burn off (it did not wash off) the precipitated product from the electrode.

Work-ups. $[P(II,III)1\text{-}MeU](ClO_4)_3$ - After precipitation, the cell contents were centrifuged @ 700 rpm for 5 min., the supernatant then decanted. The solid was washed twice with 10 ml of MeOH to remove $NaClO_4$, centrifuged, and decanted. This was followed by drying in vacuo overnight. As a note, $[P(II,III)1\text{-}MeU]^{2+}$ could be isolated as the nitrate salt from D_2O.

$[P(III,III)1\text{-}MeU](BPh_4)_4$ - The workup was the same as for $[P(II,III)1\text{-}MeU](ClO_4)_3$ except that H_2O was substituted for MeOH in the wash step.

Fully-electrolyzed Pl-MeUB - The procedure was the same as for [P(III,III)1-MeU]$(BPh_4)_4$. Typical yields were 60% for the synthesis and workup of these three compounds.

Physical and Chemical Characterization

Elemental Analysis[1] -

[P(II,III)1-MeU]$(ClO_4)_3$: C, 12.29%; H, 2.27; N, 11.46; O, not determined; Cl, 10.49 (calc'd: 11.93, 2.20, 11.13, 10.56). Pt was not determined.

[P(III,III)1-MeU]$(BPh_4)_4$[2]:

Visible Spectrophotometry -

Solution measurements were made in aqueous solution in 1 mm cells. (Details of solution measurement are given on p. 80 .) Because solution spectra and solid phase spectra can be quite different, particularly for transition metal ions in which electronic levels are easily perturbed by surrounding counter ions, solid state spectra can be informative. In the absence of a reflectance attachment, transmission spectra were recorded of the platinum dimer [P(II,II)1-MeU]$(NO_3)_2$, of the perchlorate salt of the half-electrolyzed material, [P(II,III)1-MeU]$(ClO_4)_3$, and of the

---

1. Performed by Dr. H. D. Lee of the Department of Chemistry, Purdue University, W. Lafayette, IN.

2. Not determined; it was felt that since the tetraphenylborate counter ion, which was used without recrystallization, contributed the preponderance of the carbon and hydrogen content, the values would not be reliable.

fully-electrolyzed material, [P(III,III)1-MeU]$(BPh_4)_4$, all as their KBr pellets. Spectra were recorded on a Cary Model 17 spectrophotometer vs KBr.

A transmission spectrum of the mixed-valence compound is shown in Appendix C along with an absorption spectrum obtained in solution for contrast. As expected, these two spectra are approximate inverses of one another from 1200 nm to about 640 nm - i.e., where transmission is high in the transmission spectrum, absorbance is low in the absorption spectrum, and vice versa. In the solution absorption spectrum, there is a barely-detectable peak present as a shoulder, first apparent at about 640 nm. In the transmission spectrum of the solid, this peak is partially resolved. Barton et al. also reported an additional band, centered at 480 nm, for mull spectra (18).

Infrared Spectroscopy -

IR spectra of three KBr-pelletized compounds were recorded on a Perkin-Elmer Model 137 spectrophotometer: [P(II,II)1-MeU]$(NO_3)_2$, [P(II,III)1-MeU]$(ClO_4)_3$, and [P(III,III)1-MeU]$(BPh_4)_4$. Calibration was provided by polystyrene film. When a ligand is coordinated to a transition metal, absorptions which are sharp in the uncomplexed ligand are often broadened, thereby leading to lowered resolution. This was true for all three compounds run here. The observed bands are as follows: [P(II,II)1-MeU]$(NO_3)_2$. 3455 cm^{-1} (br, m)[1], 3265 (br, s) (due to N-H stretch and probably also to H_2O), 1635(s) (C=O

---

1. br = broad, s = strong, m = medium, w = weak.

stretch), 1514(m), 1480(m), 1380(s) (NO_3^-), 1150(w); additional absorptions below 1150 are indicative of ring vibrations.

[P(II,III)1-MeU]$(ClO_4)_3$. 3420-3470(br, m), 3205(br, s), 1631(s), 1521(m), 1481(m), 1423(w), 1377(s), 1324(w), 1104(br, s).

[P(III,III)1-MeU]$(BPh_4)_4$. ~3440(br, m), ~3205(m), 1631(s), 1526(m), 1479(m), 1428(m), 1372(m), 1330(m).

Mass Spectrometry -

The virtual proliferation of soft and desorption ionization techniques in mass spectrometry in recent years has extended the applicability of mass spectrometry to middle and large molecules, compounds with negligible vapor pressure. The successful use of ^{252}Cf plasma desorption in the elucidation of the molecular weight range of a platinum blue (40) was mentioned earlier. One of the most promising of these newer techniques is fast atom bombardment (FAB) mass spectrometry. An excellent description of this technique is given in ref. 82. The applicability of the FAB technique to the current study was tested with reference to Pl-MeU[1].

Analysis was by both positive and negative mass analysis on a Finnigan TSQ_2 mass spectrometer using the following general conditions:

---

1. The work was performed by Dr. J. Zakett and P. W. Langvardt of the Analytical Laboratories, The Dow Chemical Co., Midland, MI.

FAB Source - Ion Tech NB11F gun
Xenon gas
6 kV neutral energy, 20 μA

Mass Spec - Q_1 mass scans, alternate positive/negative ion scans
Mass range of 10-1000 amu scanned in 1.5 sec

Several supporting solvents were used on the probe tip in attempting the analysis: glycerol, glycerol/HCl, and triethanolamine.

The disappointing result was that none of the spectra showed the presence of any organic ion containing platinum above background levels. The data suggest that ionization did not occur under the analysis conditions used. It was suggested by J. Zakett that field desorption (FD) ionization be tried, but this was not done. As this FAB experiment was not successful on the platinum dimer (F.W. = 832.5), there was little point in attempting it on the blue.

Solubility -

A few solubility determinations were made. Most interest was in the mixed-valence compound.

[P(II,II)1-MeU]$(NO_3)_2$. This compound is soluble in H_2O, dimethylsulfoxide (DMSO), formamide, N-methylformamide, and ethylene glycol (dissolves slowly). It is also soluble in 5:1 N,N-dimethylformamide (DMF)/H_2O and 5:1 CH_3OH/H_2O. It is insoluble in methanol, acetonitrile, tetrahydrofuran, 1,4-dioxane, dioxanes,

acetone, DMF, N,N-dimethylacetamide (DMAC), and nitromethane.

[P(II,III)1-MeU]$(ClO_4)_3$. This mixed-valence compound has considerable solubility in H_2O (even though it was precipitated from H_2O; on p. 148 the K_{sp} is calculated to be ~$6x10^{-7}$). It is also soluble in DMSO (solution turns pink) and in formamide, which forms a colorless solution. It is insoluble in methanol, acetone, acetonitrile, DMAC, hexamethylphosphoramide, propylene carbonate, and nitromethane.

[P(III,III)1-MeU]$(BPh_4)_4$. This compound is insoluble in water. Its solubility in other solvents was not determined.

[Pl-MeUB]$^{n+}(NO_3)_n$. This platinum blue goes most readily into solution in water containing nitrate. It is also soluble in DMSO and DMF, but insoluble in acetonitrile and propylene carbonate.

Redox Titrimetry

Oxidative titrations were conducted using Ce(IV) as the titrant. Standard solutions, 1N in H_2SO_4, were prepared by direct weighing of predried (at 85°C for 4 hrs) and dessicated primary standard cerium(IV) ammonium nitrate, $(NH_4)_2Ce(NO_3)_6$. A typical Ce concentration was 0.025 N. The Pt compounds were ordinarily dissolved in 1.0 ml of 1.0N HCl; without Cl^- the kinetics of reaction were intolerably slow. Titrations were conducted in a #1-dram vial using a mini-stirring bar. Addition of titrant was via a microliter syringe. The titrations were monitored potentiometrically using a looped-Pt wire as the working electrode and Ag/AgCl as the reference electrode. The reference electrode was prepared according to the

instructions of Sawyer and Roberts (83). Prior to most runs the Pt electrode was ignited in a flame to provide a renewed and reproducible surface. Potential measurements were made with either a pH meter (on the mV scale) or a high-impedance digital voltmeter. No precautions were taken to regulate the temperature. Titration curves were drawn by hand from the recorded data. End points were determined both by the ΔV method and by eye, but usually by the latter.

Redox Titrimetry/EPR -

Redox titrimetry to be followed by EPR measurement was conducted by carrying out a new titration for each EPR determination to be made. The measurements were to be conducted on Pl-MeU only, in an effort to determine if the original Pt(II)-Pt(II) complex was oxidized all the way to Pt(IV)-Pt(IV). Samples were stored in EPR tubes in liquid N_2 until time of analysis[1]. Details concerning EPR measurements are given in the CPC/ESR section to follow.

Controlled-Potential Coulometry in Conjunction with Vis/NIR Spectroscopy

Electrolyses conducted at +1.1 V vs ssce were sampled at ~1/8 intervals for examination by visible and near infrared (NIR) spectroscopy. Sixteen mg of Pl-MeU in 6.0 ml of 0.1F $NaNO_3$ supporting electrolyte and 10.0 mg of Pl-MeUB in 10.0 ml were run. At each sampling, 500 µL was removed using a syringe with hypodermic

---

1. Unfortunately, not all samples were run.

needle. The spectra were run immediately in 1 mm quartz cells. All spectra were recorded on a Cary Model 17 spectrophotometer. The reference cell contained 0.1F $NaNO_3$ in water. Most scans covered the range from 1200 nm in the NIR down to about 375 nm, although scouts were made out to 2000 nm to ensure that there was no absorption above 1200 nm.

Controlled-Potential Coulometry in Conjunction with Electron Paramagnetic Resonance Spectroscopy

The electrolysis of both Pl-MeU and Pl-MeUB was followed by EPR by sampling the electrolyte at 1/4 intervals throughout an electrolysis. Samples were stored in 2.8 mm o.d. x 2.0 mm i.d. quartz EPR tubes in liquid N_2 until time of analysis. Electrolysis potentials between 0.65 V and 1.1 V were used, depending on the concentration of supporting electrolyte and on the rate of electrolysis desired. Initially, the electrolyses were carried out in 0.1F $NaNO_3$; the resulting EPR spectra revealed hyperfine structure. Later electrolyses performed in 0.01F $NaClO_4$ (low concentration used to avoid precipitation) led to simpler EPR spectra devoid of hyperfine structure. A typical concentration of Pl-MeU and Pl-MeUB used was 2 mg/ml. Samples in the solid state of starting and isolated materials were also run.

Spectra were recorded on either a Varian E-Line Century Series ESR spectrometer[1] or on a Bruker ER 200D ESR spectrometer[2], both with variable temperature accessories. All measurements were made in the X-Band (9.2-10.0 GHz). The microwave frequency was read from a digital counter; g factor calibration was with diphenylpicryl hyrazide (DPPH). Solid spectra were obtained at room temperature. Solution spectra were recorded at ~123 K or ~133 K in a liquid N_2 Dewar.

Controlled-Potential Coulometry in Conjunction with Paramagnetic Nuclear Magnetic Resonance Spectroscopy

Pl-MeU (6.0 mg/6.0 ml, 1.2×10^{-3}M) was electrolyzed in 0.02 F $NaNO_3$ in D_2O and sampled at the halfway point and after complete electrolysis. At the usual supporting electrolyte concentration of 0.1 F $NaNO_3$, precipitate formed during the electrolysis. On the other hand, Pl-MeUB (12.0 mg/6.0 ml) was electrolyzed in 0.1 F $NaNO_3$ in D_2O without problem. Nine-tenths of a ml were combined with 0.1 ml of a solution of a water-soluble reference compound (5×10^{-3}M DSS, 2,2-dimethyl-2-silapentane-5-sulfonic acid (Tier's salt) in D_2O) into an NMR tube and stored in liquid N_2 until time of analysis. ^1H NMR spectra were recorded on a Bruker 250 MHz Fourier-transform NMR spectrometer[3]. Ordinarily, 2000 scans were accumulated, and required about 45 minutes.

---

1. By Dr. J. D. Woollins
2. By Dr. P. O'Malley
3. By Dr. T. Li

X-ray Photoelectron Spectroscopy

Arrangements were made with The Dow Chemical Co. to have X-ray photoelectron spectra taken of several solid samples. Unfortunately, they were never run.

Liquid Chromatography (LC)

Ion-pair reversed phase LC (IPRPLC) was performed on the dimer Pl-MeU and its electrolysis products, and on the platinum blue Pl-MeUB. LC on Pl-MeU was designed to follow the appearance and disappearance of electrolysis products and also to study the effect of aging (autooxidation) on the disappearance of Pl-MeU, coincident formation of hydrolysis products, and formation of polymeric species. Pl-MeUB was examined to elucidate the distribution of oligomeric chains, as well as to follow its decomposition in solution.

Isocratic separations were achieved using a Waters Associates Model 6000A Solvent Delivery System; gradient separations were under the control of a Model 660 Solvent Programmer with the addition of a second pump, the Model M-45. Injection was by syringe using either a Model 7125 Rheodyne injector or a Model U6K Waters injector. A 20 μL injection volume via loop was typical. Detection was either in the visible or ultraviolet range using the Waters Model 440 Absorbance Detector. An interference filter with λ_{max} at 658 nm was used for the former, 280 nm for the latter.

Solvents were Sybron/Barnsted Organopure (Model D3600) water and Omnisolv^{R}-grade methanol (MCB Reagents). Ion-pairing agents used, depending on the intent, included ethane-, butane-, pentane-, hexane-, heptane-, and octanesulfonic acids (Aldrich Chemical Co.), most as their sodium salts. In addition, sodium dodecylsulfate (laurylsulfate) (Fisher Scientific Co.) was tried, in a variant known as soap chromatography. Tetrabutylammonium (TBA^+) ion was added as a peak sharpener and was prepared by neutralizing TBA^+OH^- (MCB, available as a 25% solution (w/w) in methanol) with 1 N HNO_3. Final pH adjustment was made with 0.1 N NHO_3 (an alkaline pH destroys silica-based packings).

All eluents were filtered through 0.22 μ Millipore filter Type GS and were degassed by vacuum just prior to use. When doing gradient elution, the A eluent had to first be passed through a C_{18} column to remove impurities introduced by the sulfonic acid and/or $TBA^+NO_3^-$. Most IPRP separations were conducted on a Whatman Partisil ODS-3 column with nominal 10 μ particles. Flow rates typically were 1.0 ml/min.

Isotachophoresis

Conditions suitable for the determination of $[P(II,II)1\text{-MeU}]^{2+}$ and its electrolysis products by isotachophoresis (ITP) were worked out by S. W. Barr of The Dow Chemical Co., Midland, Mich. The polymeric blue was not examined by ITP.

Instrument: Shimadzu IP-2A Isotachophoretic Analyzer

Leading Electrolyte: 5 mM $HClO_4$ in 40% acetone

Terminating Electrolyte: 5 mM Tetra(n-butyl)ammonium perchlorate in 40% acetone

Migration Current: 100 μA

Injected Volume: 5-10 μL

Output Format: 1. Potential Gradient (step)
2. Differential (peak)

RESULTS AND DISCUSSION

Electrochemistry

Cyclic Voltammetry (CV) -

Initially, cyclic scans were taken of Pl-MeU, Pl-MeUB, platinum benzoate blue (PBzB), and platinum phthalate blue (PPhB). The latter two are blues of a new kind prepared in the laboratory of Dr. Rosenberg by Dr. J. D. Woollins. Because these two experimental compounds are fundamentally different from the pyrimidine blues, or for that matter, from any others which have been described in the scientific literature, it was deemed of interest to investigate their electrochemical behavior along with that of Pl-MeU and Pl-MeUB. Not only is electrochemical characterization lacking, but there has been virtually no characterization of any kind on either PBzB or PPhB.

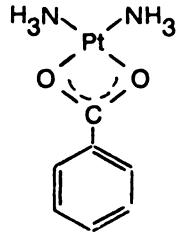

Basic unit of PBzB

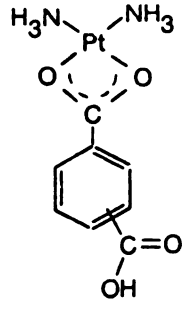

Basic unit of PPhB

Intitial Surveys. The very first scan made of Pl-MeU produced the cyclic voltammogram shown in Figure 2. A broad, two-component wave was obtained in each direction. The natural inclination would be to associate wave a with d and b with c. This first voltammogram proved to be somewhat of an aberration since such well-resolved waves and waves of such symmetry were rarely obtained, even with fresh solutions and fresh electrodes.

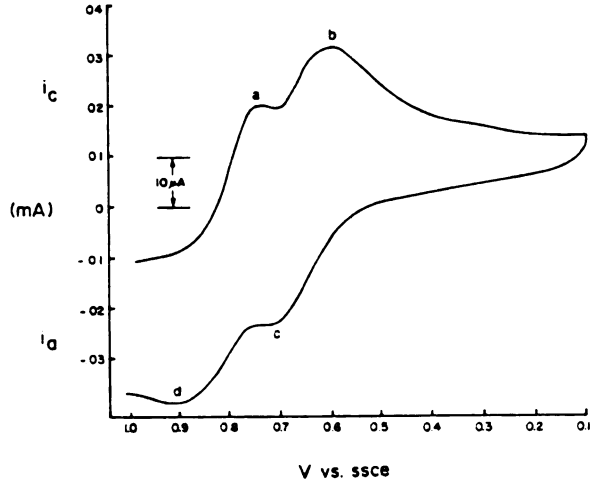

Figure 2. Initial cyclic voltammogram of platinum (II) 1-methyluracil (Pl-MeU, 9.7 mg/10 ml, 1.2 mM) obtained at Pt; scan rate (v) of 100 mV/s.

Within a matter of minutes, resolution for this same preparation of Pl-MeU was degraded to the point where only a single, very broad wave was detectable for both the reductive and oxidative components of the voltammogram (peaking at app. 0.64 and 0.83 V vs ssce, respectively). This more typical behavior is shown in Figure 3.

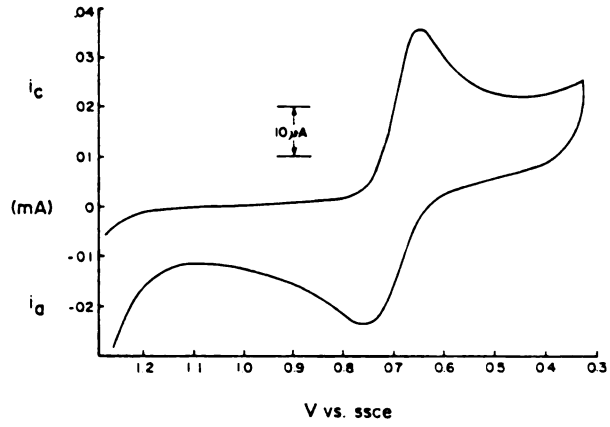

Figure 3. A more usual CV of Pl-MeU (2.4 mg/5.0 ml, 0.58 mM) over the same approximate potential range; v = 100 mV/s.

The instability of aqueous solutions of Pl-MeU (they sometimes gradually took on a violet, and then, often, a blue or purple tint) led to generally irreproducible changes in the CV's over the period of days and weeks, but this was not studied in a controlled fashion. The usual CV for Pl-MeUB, an example of which is shown in Figure 4, is similar to that of the aged Pl-MeU as shown in Figure 3.

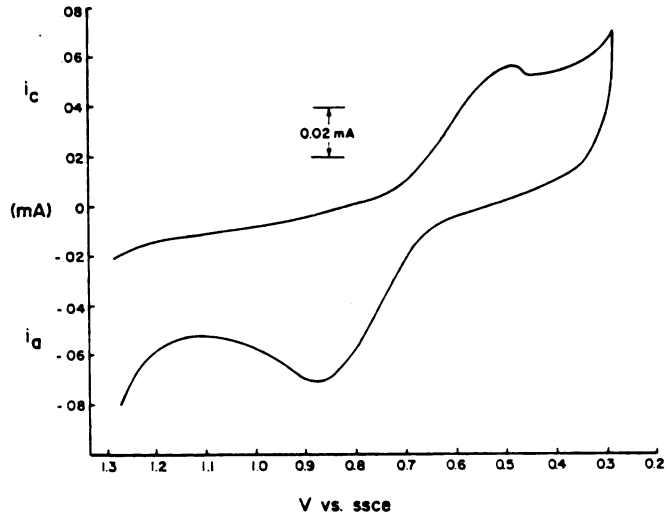

Figure 4. A representative CV of Pl-MeUB (10.0 mg/5.0 ml) at Pt over approximately the same limited potential range used in Figures 2 and 3; v = 100 mV/s.

There is no clear suggestion of two components to the wave in either direction, although the breadth is suggestive of more than a single component. PPzB, insoluble in water, but soluble in methanol, proved to be electroinactive, as did PPhB (soluble in 0.5% $NaHCO_3$), over the potential range accessible to Pt.

A more direct comparison of these compounds could be obtained if each was run in the same solvent/electrolyte system. Of the several electrochemically-compatible solvents tried, DMSO proved to be a suitable solvent for all four compounds. However, DMSO is an "unnatural" solvent for the blues and the related Pl-MeU since the biological system, which we wish to mimic, however crudely, is an aqueous one. Furthermore, DMSO, as a coordinating ligand, may exchange with the ammine groups, thereby altering the compounds. It may be this behavior that explains the change in color from dark blue

to yellow that takes place upon dissolution of PBzB or PPhB in DMSO. In any event, the cyclics obtained in DMSO were somewhat less descript (less well-defined) than those obtained in aqueous solution; hence, this approach was abandoned.

All four compounds were further examined at the hanging mercury electrode (HME) to ascertain their electroactivity at more negative potentials. In addition, CV's were recorded at glassy carbon, an electrode material that bridges the potential ranges of Pt and Hg, and at gold to see if the additional anodic range provided by gold would prove useful in the study of these platinum compounds.

In this dissertation it will be argued that Pt(II) and Pt(III) are the oxidation states that best account for the observed behavior of Pl-MeU and Pl-MeUB. Since the well-recognized Pt(II) and Pt(IV) oxidation states dominate platinum chemistry, the question arises - if the sweep potential is made more positive, will an additional wave corresponding to oxidation of platinum to the +4 state appear in the CV? By choosing Au as the electrode material, the potential range is extended by +0.2 V over Pt. It turned out that none of the four compounds exhibited an additional wave on Au. In general, background levels were higher with Au, and the CV's less well-defined.

Like gold, the use of vitreous carbon offered no advantage for the study of these compounds. Although vitreous carbon encompasses a wide usable potential range (~1.3-(-1.5)V vs ssce), the CV's were sloping despite the absence of electroactive substances (that is, for blanks). In the case of Pl-MeUB, a compound which readily yields a CV at Pt, a barely-detectable cyclic was obtained at vitreous carbon,

even at a concentration as high as 8 mg/ml. While Pl-MeU is better behaved at carbon than Pl-MeUB, delineation in the CV as observed at Pt was not obtained. This is made apparent by comparing the cyclics in Figure 5a, obtained at carbon, with those in 5b; the latter were obtained at Pt.

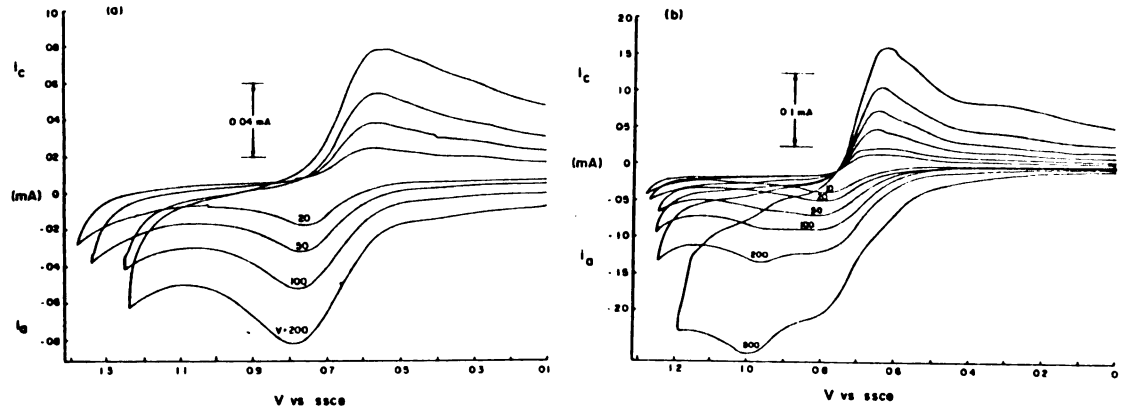

Figure 5. CV's of Pl-MeU (8.3 mg/5.0 ml, 2.0 mM) at a) vitreous carbon and at b) Pt as a function of v.

The emergence of a second anodic wave at high scan rates, discernible at Pt, is not discernible at carbon.

One interpretation of the CV behavior at carbon, as exemplified in Figure 5a, is that a second electron is not lost upon oxidation. A determination of n at carbon by controlled-potential coulometry, which would serve to either confirm or controvert this interpretation, was not made. An alternate, and probably more likely interpretation, is that the single peak represents a $2e^-$ transfer, and that transfer of the second electron is equally facile at all sweep rates, unlike the situation at Pt, as evidenced by Figure 5b.

Part of the explanation of the observed behavior at Pt (which will be expounded upon later) has to do with surface adsorption or precipitation of the partially-oxidized ($-1e^-$) intermediate, which acts to block access to the electrode to other reactants. It may well be that surface precipitation is less pronounced at carbon as compared to platinum, or is even entirely absent.

Assuming for the moment that the wave at carbon represents a $2e^-$ transfer, a calculation of the approximate E^o for the reaction $[P(III,III)1\text{-MeU}]^{4+} + 2e^- \rightleftarrows [P(II,II)1\text{-MeU}]^{2+}$ is possible. To make the calculation we assume reversible electrochemical behavior, although clearly, as Figure 5a shows, the system is not reversible. (Reversibility requires a peak separation of $59/n$ mV $\simeq$ 30 mV; see Appendix A.) With the assumption of reversibility, E^o is found midway between the peak potentials. In the present case we have $E^o_{[P(III,III)1\text{-MeU}]^{4+}} + 2e^- \rightleftarrows [P(II,II)1\text{-MeU}]^{2+} \simeq (0.735 + 0.575)/2 = 0.665 \rightarrow 0.66$ V (v = 20 mV/s) vs ssce. This translates to 0.90 V vs nhe. At v = 100, a value of $(0.775 + 0.560)/2 = 0.668 \rightarrow 0.67$ V is obtained. The close agreement at v = 20 and v = 100 suggests that even though the system is not reversible, the calculational procedure is a reasonable one.

In contrast to the CV's of Pl-MeU at Pt, the CV's of Pl-MeUB are not as well-delineated in either the anoidc or cathodic components, although the same tendency with increasing scan rate is suggested; this can be seen in Figure 6.

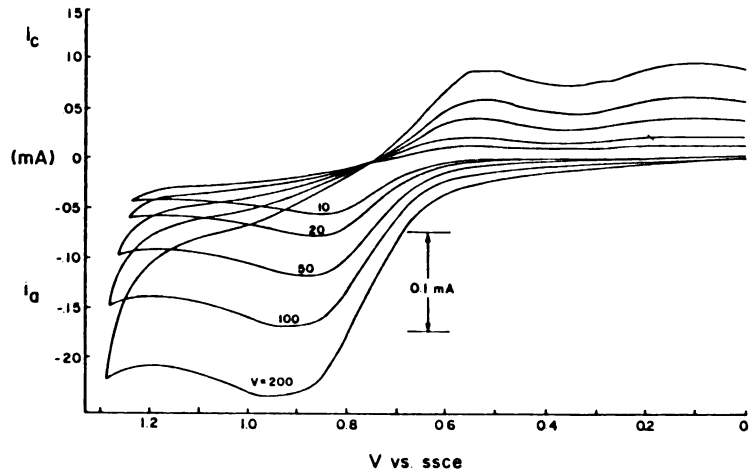

Figure 6. CV's of Pl-MeUB (39 mg/5.0 ml) at Pt as a function of v.

Evidence will be presented later for a mixed-valence state for Pl-MeUB with the average formal oxidation state being close to 2. Since Pl-MeUB consists of a mixture of oligomers (as will also be shown later), this means that, in contrast to the dimeric Pl-MeU in which only two Pt atoms are candidates for oxidation, many more Pt atoms are subject to oxidation in the polymeric Pl-MeUB. Because the platinums are not all in the same environment, and because some may exhibit sluggish kinetics, a broad wave is not unreasonable.

All four compounds exhibit irreversible behavior at Hg. The responses for Pl-MeU and Pl-MeUB are shown in Figures 7 and 8, respectively.

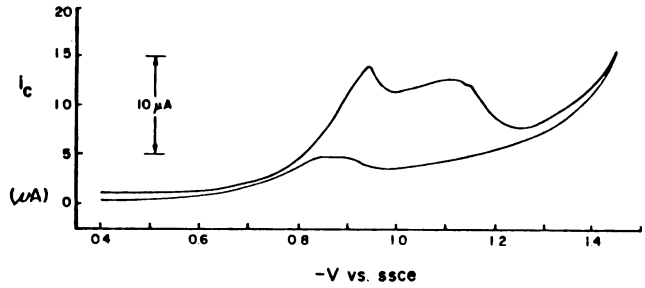

Figure 7. Double-sweep voltammogram of Pl-MeU (8.3 mg/5.0 ml, 2.0 mM) at a hanging mercury electrode (HME); v = 100 mV/s.

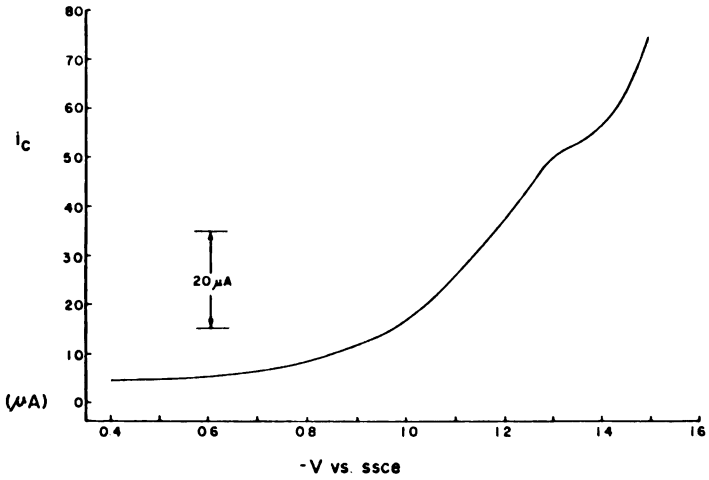

Figure 8. Single-sweep voltammogram of Pl-MeUB (39 mg/5.0 ml) at a HME; v = 100 mV/s. No peak was obtained in the reverse sweep.

For these compounds, the signal (current) may be due to the reduction of platinum to the metal, Pt(II) $\xrightarrow{2e^-}$ Pt(0), to a reduction of the uracil ligands, or to a combination of both. This question may, in principle, be addressed by ratioing the peak current density (i/A) for Pt(III) $\xrightarrow{e^-}$ Pt(II) at Pt to the current density at Hg at the more negative potential. If reduction at Hg is due solely to Pt(II) $\xrightarrow{2e^-}$ Pt(0), then $\frac{i_{c,Hg}}{i_{c,Pt}} \simeq 2$. This relationship is only approximate because reduction at Hg is seen to be totally irreversible, for which

eq. (5), Appendix A, applies, whereas the reduction at Pt is more nearly reversible, for which eq. (1), Appendix A, applies in the limit. When the two current densities are compared, it becomes clear that the ligands are undergoing reduction (ratio >> 2). The current contributed by reduction of Pt(II) to the metal could be determined by anodic stripping voltammetry, but this was not done. In Figure 7, which shows the response of Pl-MeU at Hg, the presence of a very broad wave (centered at ~ -1.1 V) following a sharper one also seems to implicate the ligands in the irreversible process.

Typical E^{o} values of inorganic platinum complexes for the reduction of Pt(II) to Pt(0) are well positive of the region shown in Figures 7 and 8 (14), and would ordinarily fall within the range accessible to platinum. Figure 8 shows the more complex behavior of Pl-MeUB. The response, which steadily increases out to the limit posed by the evolution of H_2, is suggestive of a massive breakdown of the complex. In earlier polarographic studies, no waves were observed for uracil (84,85) or for 1,3-dimethyluracil (84). In general, 2- and 4-substituted pyrimidines are found to be nonreducible or difficulty reducible, presumably because of tautomeric shifts which remove reduction sites, i.e., double bonds, in the ring (86).

PBzB and PPhB are electroinactive at Pt, and remain inactive well into the range of Hg; this is shown in Figure 9.

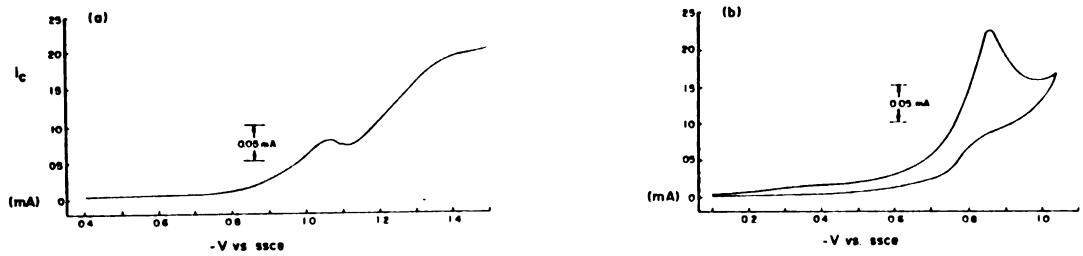

Figure 9. Single-sweep voltammograms of a) platinum phthalate blue (40 mg/5.0 ml) and b) platinum benzoate blue (40 mg/5.0 ml) at a HME; v = 100 mV/s. PPhB gave no peak on reversal.

If these two aromatic blues are true platinum blues and possess the mixed-valency characteristic of these compounds, then one is led to the conclusion that the platinum-carboxylate complexes provide an enhanced facilitation of the intermediate oxidation state, probably by increased electron delocalization through the polymer chain. In Figure 9b, which shows a cyclic of PBzB at Hg, the shape and breadth are reminiscent of the cathodic wave obtained for Pl-MeU and Pl-MeUB at more positive potentials. (The region at more negative potentials is not shown, because the interpretation is confounded by a background signal due to the methanol.) The cyclic for PPhB is not as well defined as that of PBzB, as is apparent from a comparison of Figures 9a and b. This may owe to the presence of the unbound carboxylate moiety which may be reduced.

Because of the contrasting nature of the cyclics obtained for PBzB and PPhB on the one hand and Pl-MeU and Pl-MeUB on the other, two additional compounds were run for further comparison: cis-PBzB-Cl_2 and cis-PPhB-Cl_2, analogs of PBzB and PPhB in which the

ammine ligands have been replaced by chlorine. Substitution of chlorine for ammonia rendered both of these compounds water soluble, probably because of the ready aquation of the complex (Cl^- is a better leaving group than NH_3). Comparison of the benzoates and phthalates was made at the same concentration - 8 mg/ml.

Figures 10 and 11 reveal the sharp contrast between PPhB-$(NH_3)_2$ & PPhB-Cl_2 and between PBzB-$(NH_3)_2$ & PBzB-Cl_2.

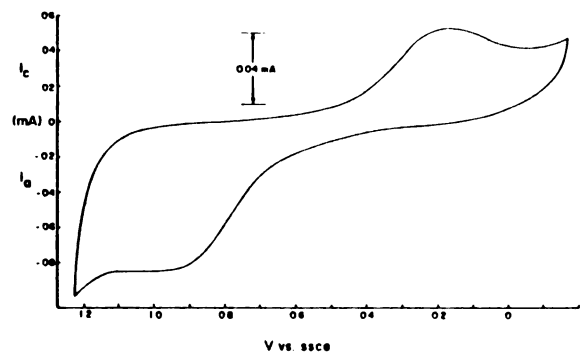

Figure 10. CV of platinum phthalate blue containing Cl ligands (PPhB-Cl_2) (35 mg/5.0 ml); v = 100 mV/s.

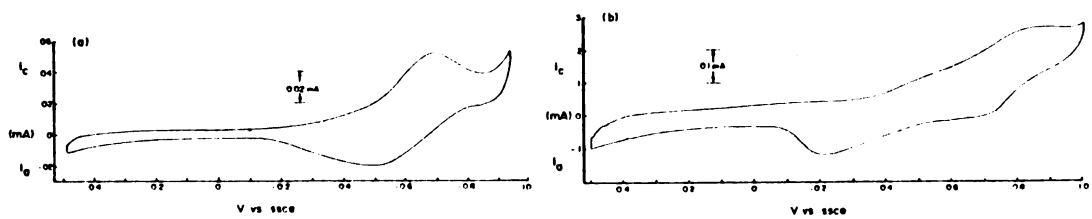

Figure 11. CV's of a) platinum benzoate blue containing Cl ligands (PBzB-Cl_2) (30 mg/5.0 ml) and b) platinum phthalate blue containing Cl ligands (PPhB-Cl_2) (35 mg/5.0 ml), both at Pt; v = 100 mV/s.

Whereas PPhB-$(NH_3)_2$ gave no response at positive potentials on Pt,

this is not the case for PPhB-Cl_2 (Figure 10), although a ΔE_p of ~0.7 V indicates a high measure of irreversibility. The situation is the same for PBzB-Cl_2 (not shown). It may be that Cl^- binds to the electrode surface and provides a bridge for electron transfer. In Figure 11a the CV for PBzB-Cl_2 at more negative potentials is seen not to be totally irreversible, also in contrast to the behavior of PBzB-$(NH_3)_2$. The CV for PPhB-Cl_2 over the same region is even more interesting in that a 2-component wave was obtained in both directions scanned; this is shown in Figure 11b. Obviously there is room for further investigation here, to study in a rigorous fashion the relative effects of Cl and NH_3 upon the cyclic voltammograms. These preliminary results suggest that ammine ligands have a stabilizing effect on the partially-oxidized character of the platinums (perhaps by not effectively removing electrons from the molecular orbital defined by the platinum chain) whereas chloride has the opposite effect (perhaps by competing for these same electrons).

In the preceding paragraphs, the overall features of the electrochemical behavior of Pl-MeU, Pl-MeUB, PBzB, and PPhB were presented. There will be little additional discussion of the last two. Unanswered at this point is the question of what is the mechanism responsible for the observed CV behavior - whether 1, 2, or more electrons are involved in the redox behavior of Pl-MeU. We already know that the mechanistic behavior for Pl-MeUB will be harder to address. Examination of Pl-MeU by DPV at Pt at modulation amplitudes ranging from 5-50 mV gave only a single peak, perhaps a

little broad (~.145 V full width at half maximum), but without even a suggestion of two as had been hinted at by CV (see Figure 5b). Similarly for Pl-MeUB, measurement by DPV also yielded a single, but broader peak (.25 V fwhm). This is not to be unexpected in light of the earlier comparison of CV's. As will be shown in following sections, investigation by FCV and RDV proved useful in elucidating the mechanistic process for these two systems.

All electrochemical procedures have a dependence on n, the number of electrons transferred in a given operation. While n appears in the equations describing virtually every electrochemical technique, its determination usually depends on the knowledge of other parameters - e.g., diffusion coefficients. Only controlled-potential or controlled-current coulometry is independent of all these variables, since in coulometry (electrolysis) conditions are chosen such that all, or a good portion, of an electroactive species is electrolyzed. In this work controlled-potential coulometry was used to determine (or estimate) n in Pl-MeU and Pl-MeUB. While suitable potentials for oxidative and reductive electrolysis can often be selected by inspection of the cyclic voltammograms, where there is ambiguity, RDV is more suited for this purpose. As was mentioned in the preceding paragraph, RDV proved to be of interest in its own right by helping to elucidate the electron transfer process.

Fast Cyclic Voltammetry (FCV) -

To this point very little interpretation of the CV's of Pl-MeU and Pl-MeUB has been attempted. It has been noted, though, that the

CV for Pl-MeU exhibits an increasingly well-delineated anodic doublet as the scan rate increases. In contrast, an unresolved, broad, anodic wave is obtained at all scan rates for Pl-MeUB. Without further experimentation, meaningful interpretation of the CV's was not possible. With the aim of elucidating the electrochemical (or coupled chemical/electrochemical) mechanism, FCV was employed.

CV's for Pl-MeU at scan rates ranging from 20 mV/s to 10 V/s are shown in Figure 12.

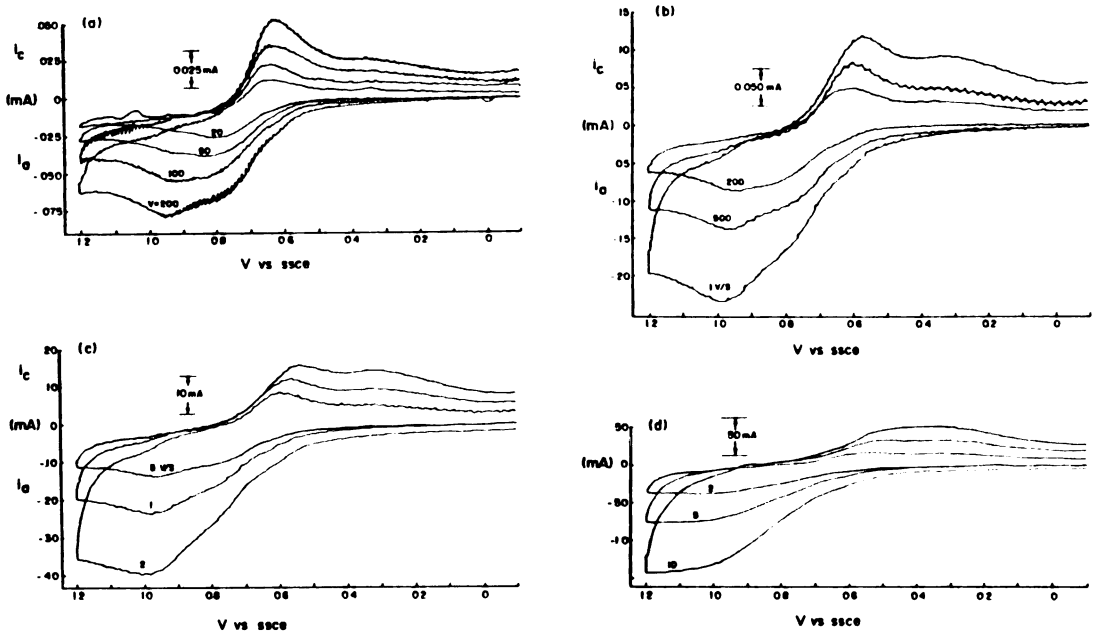

Figure 12. CV's of Pl-MeU (8.2 mg/5.0 ml, 2.0 mM) at Pt over the sweep range v = 20 mV/s to 10 V/s.

Scan rates lower than about 10 mV/s are not practical because convective effects begin to set in; at very rapid scan rates double layer charging effects become increasingly important. Each scan in

Figure 12 was initiated at -0.1 V vs ssce, a potential at which the intrinsic Pt(II) oxidation state of Pl-MeU is undisturbed. The changing appearance of the anodic wave with scan rate alluded to in the previous paragraph - i.e., the emergence of a second peak at 0.95 V - is again apparent. At scan rates in excess of ~1 V/s, the first anodic component, which peaks at 0.8 V, is engulfed by the second so that a broad, undelineated wave results.

For ease of discussion, let us define the peak potentials of these two anodic components by E_{pa1} (less positive) and E_{pa2}. Comparison of the cathodic responses at the low and high scan rates reveals a broad cathodic wave centered at ~0.35 V (call it pc2) that is obviously coupled to pa2. The less negative cathodic wave (pc1) is centered at ~0.65 V. At about 5 V/s and above, pc1 and pc2 are merged into a broad, unresolved wave. While ΔE_{pa} ($= E_{pa2}-E_{pa1}$) is on the order of 150 mV, ΔE_{pc} ($= E_{pc1}-E_{pc2}$) is slightly larger, on the order of 0.20 - 0.23 V.

The correspondence between peaks pa2 and pc2 on the one hand and pa1 and pc1 on the other is further demonstrated by reference to Figure 13.

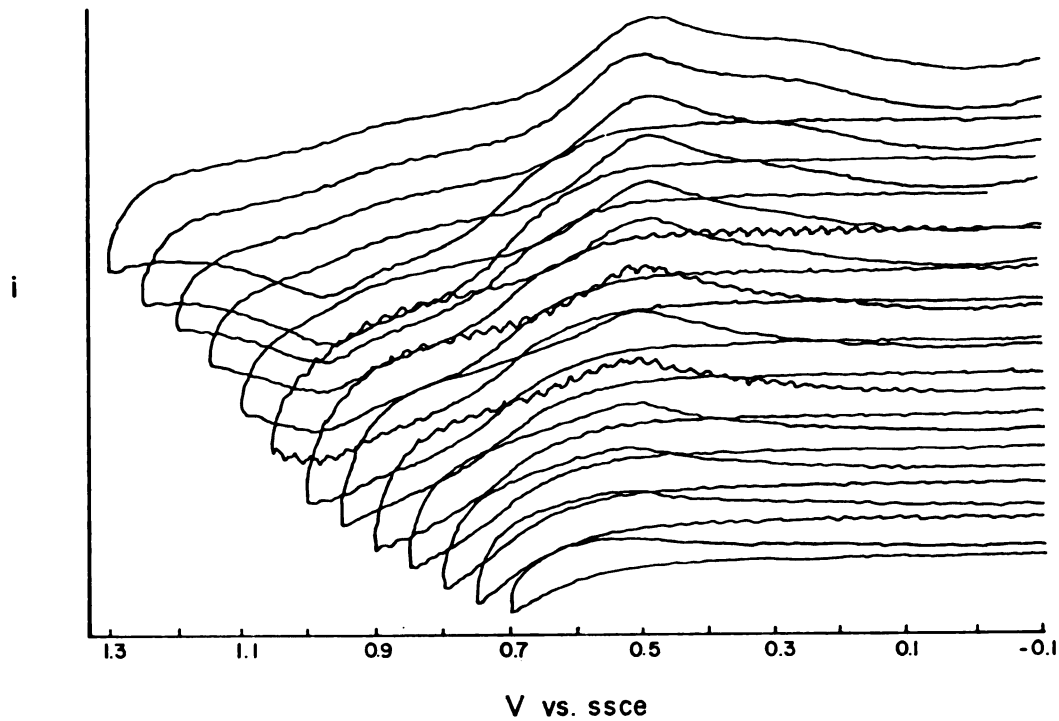

Figure 13. Correspondence of cathodic and anodic peaks in the CV's of Pl-MeU; v = 500 mV/s.

By gradually shifting the potential of reversal to less positive potentials (in 0.05 V increments), a correspondence is demonstrated between pa2 & pc2 and pa1 & pc1, since, as pa2 disappears, so does pc2; pa1 and pc1 remain. Further support for the correspondence of these two pairs of peaks is provided by coulometric analysis in conjunction with cyclic voltammetry (vide infra). (A series of CV's similar to those in Figure 13, except that they were initiated at increasingly negative potentials from -0.1 to -0.8 V, reveals an additional cathodic peak at -0.30 V, but it is irreversible, as there is no corresponding anodic peak.)

At the initiation of a scan at -0.1 V (as in Figure 12), both Pt

atoms in Pl-MeU are in the +2 oxidation state. The first wave - pal - must therefore correspond to the oxidation of Pt(II). From coulometry it is known that 2 electrons are given up per molecule in the oxidation of P(II,II)l-MeU @ +1.1 V vs ssce. If we can accept on faith at this point that cyclic voltammetric experiments in conjunction with other evidence suggest that pal represents the transition P(II,II)l-MeU → P(II,III)l-MeU + e^- (vide infra), then, correspondingly, pcl results from the reverse reaction: P(II,III)l-MeU + e^- → P(II,II)l-MeU. Let us summarize at this point the remainder of the interpretation and then offer the supporting evidence in the paragraphs that follow. Peak pa2 is due to P(II,III)l-MeU → P(III,III)l-MeU + e^- and peak pc2 corresponds, in part, to the reverse reaction P(III,III)l-MeU + e^- → P(II,III)l-MeU. Only in part, because if we start with P(III,III)l-MeU exclusively, and then reduce it in two successive $1e^-$ transfer steps to P(II,II)l-MeU,

$$\text{P(III,III)l-MeU} + e^- \rightarrow \text{P(II,III)l-MeU} \qquad E_1^{\circ}$$

and

$$\text{P(II,III)l-MeU} + e^- \rightarrow \text{P(II,II)l-MeU} \qquad E_2^{\circ},$$

and if P(II,III)l-MeU is more readily reduced than P(III,III)l-MeU (meaning in this case that $\Delta E = E_2^{\circ} - E_1^{\circ} > 0$ and/or the overpotential is less for the former)[1], then only a single wave

---

1. Ease of reduction depends on both thermodynamic and kinetic factors; it is the former that predominates and orders the "ease" of reduction for these two couples.

results. (This has been shown by Polcyn and Shain (87), although their treatment deals with strictly reversible systems and does not consider kinetic complications as we must.) This means that the wave for the reduction P(II,III)1-MeU + $e^- \rightarrow$ P(II,II)1-MeU lies under the wave for P(III,III)1-MeU + $e^- \rightarrow$ P(II,III)1-MeU. Why then the peak pc1? A peak at pc1 can only result from the direct reduction of P(II,III)1-MeU to P(II,II)1-MeU - i.e., from P(II,III)1-MeU that was not electrolyzed all the way to P(III,III)1-MeU during the forward scan. This will be elaborated on below. We will now turn to the fast cyclics and examine them in detail to see if the explanation offered here is a reasonable one.

The usual diagnostic criteria used to unravel voltammetric data include the measurement of anodic and cathodic currents, i_{pa} and i_{pc}, the ratio of i_{pa} to i_{pc}, peak potential E_p, or half-peak potential $E_{p/2}$, $\Delta E_p = E_{pa}-E_{pc}$, and the ratio $i_p/v^{1/2}$ as functions of the scan rate v. Both ΔE_p and $i_p/v^{1/2}$ are invariant with v in a nernstian (reversible) system, with the former equaling 59/n mV; $i_{pa}/i_{pc} = 1$ (see Appendix A).

Measured potentials and currents for the CV's of Figure 12 are listed in Table 1. Peak potentials are seen to be only very slightly dependent on scan rate at modest scan rates ($\leq$500 mV/s). ΔE_{pac1} ($=E_{pa1}-E_{pc1}$) is on the order of twice that expected for a reversible process (see Appendix A), while ΔE_{pac2} ($=E_{pa2}-E_{pc2}$) is considerably larger. Anodic currents exceed their cathodic counterparts, although the ratio i_{pa1}/i_{pc1}, as best as can be determined, appears to

Table 1
FCV Data for Pl-MeU

v(mV/s)	$E_{pa1}^{(1)}$(V)	E_{pa2}	ΔE_{pa}	E_{pc1}	E_{pc2}	ΔE_{pc}	ΔE_{pac1}	ΔE_{pac2}
20	0.78	-(2)		.65	.34	.31	.13	
50	.78	-(2)		.64	.34	.30	.14	
100	.78	.94	.16	.64	.34	.30	.14	.60
200	.78	.96	.18	.63	.34	.29	.15	.62
500	-(2)	.97		.61	.34	.27	-(2)	.63
1000	-(2)	.98		.57	.34	.23	-(2)	.64
2000	-(2)	.99		.53	.33	.20	-(2)	.66

(1) vs ssce

(2) indiscernible

v	$i_{Pa1}^{(2)}$	$i_{pa2}^{(3)}$	i_{pc1}	i_{pc2}	i_{pa1}/i_{pc1}	i_{pa2}/i_{pc2}
20	18	-	13.0	4.5	1.4	
50	26.7	-	20.0	4.0	1.3	
100	33.2	-	27.0	4.5	1.2	
200	43.8	-	42.0	5.0	1.0	
500	-(1)	-	54.0	8.0		
1000	-(1)	-	70.0	10.5		
2000	-(1)	-	78.4	16.0		

(1) indiscernible

(2) in arbitrary units

(3) not possible to estimate

decrease as the scan rate increases. Both the i_{pa1}/i_{pc1} and ΔE_p values point to the irreversibility of the Pl-MeU system. An explanation will be offered below for the larger-observed anodic currents; unequal cathodic and anodic currents are understandable in terms of nonsymmetrical barriers which are scaled by the transferring electron. A corresponding ratio cannot be obtained for i_{pa2}/i_{pc2}, since no meaningful measurement of i_{pa2} is possible. As is characteristic of cyclic voltammograms, the appearance of the CV was the same, regardless of the direction of the initial sweep.

Because the sweep rate may be varied over a wide range in cyclic voltammetry, mechanistic information covering the time scale from $\sim 10^{-4}$s to ~5s may be obtained (88). In certain cases, mechanisms involving coupled chemical steps can also be elucidated. One may, for example, wish to postulate an intervening step involving an association reaction of the P(II,III)l-MeU intermediate, or perhaps ligand rearrangement, prior to transferring a second electron to the electrode. In general terms this may be represented as

$$A - e^- \rightarrow B \quad (1)$$

$$B \rightarrow C \quad (2)$$

$$C - e^- \rightarrow D \quad (3),$$

the so-called ece mechanism. Of the three reactions, (1) and (3) are directly observable by electrochemistry, but (2) is not. Whether or not the chemical step $B \rightarrow C$ is deducible from electrochemical measurements depends on the time window of the EC technique, the rate

of the chemical step, and the equilibrium constant for B → C. Rotating disk voltammetry, to be discussed later, covers the approximate window from 10^{-3} - 0.3 s. Coulometry, also used here, is generally less useful in kinetic and mechanistic problems, having a time window ranging roughly from 100-3000 s. However, coulometry has other crucial advantages which were exploited in this work.

Before continuing with our discussion of the CV's of Pl-MeU, an additional piece of information needs to be mentioned. When sweeping toward more positive potentials at the lower scan rates (100-200 mV/s and less), a stream of green product could be seen descending from the electrode. When scanning at 10 or 20 mV/s, the stream was discernible before the point of potential reversal was reached. When sweeping at 50 mV/s and above, the delay was such that the stream was not in evidence until both sweeps were completed. The observed behavior was the same in either 0.1 F $NaClO_4$ or 0.1 F $NaNO_3$. Also, the CV's were indistinguishable in these two media. (A difference in behavior in these two electrolytes could have significance since the product is isolable as its perchlorate salt; see under Electrosynthesis in the Experimental section.) Before we are in a position to consider what effect this behavior might have on the appearance of the CV's, we need first to understand the interpretation of CV's generated for well-behaved systems. A relevant example is the following.

Consider

$$A + e^- \rightleftarrows B \qquad E_1^o \quad (1)$$

$$\text{and} \quad B + e^- \rightleftarrows C \qquad E_2^o \quad (2),$$

a two-step process in which one electron is transferred in each of two successive, reversible steps. Four general shapes of the resultant voltammograms may be distinguished, the particular shape being dependent on the value of ΔE_{12}^o; see Figure 14 (87).

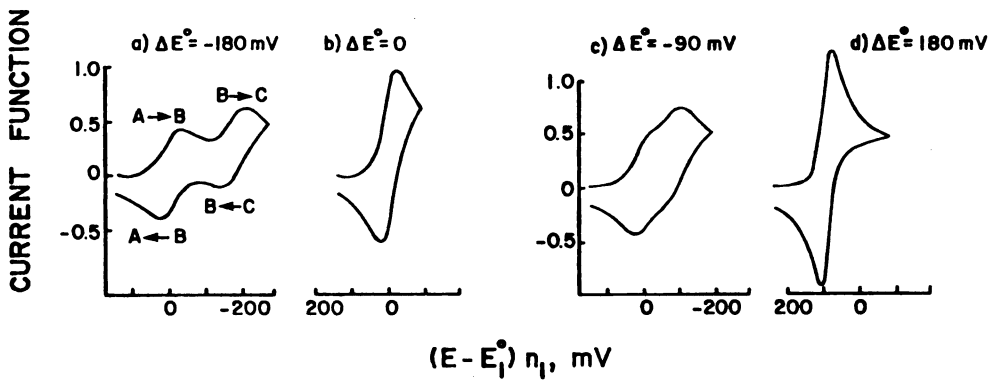

Figure 14. Possible cyclic voltammograms for two-step reversible process (taken from ref. 87).

The voltammograms may be more complex when coupled chemical reactions are considered and also when kinetic complications arise (i.e., for nonreversible systems). Taking Figure 14 as an example - as A is reduced to B, B begins to diffuse out into the diffusion layer. As the potential is made more negative, a second reduction wave appears which is made up, in part, of a direct $2e^-$ reduction of A to C as well as a $1e^-$ reduction of B to C, B now diffusing back to the electrode as it is removed by electrochemical conversion to C at the increasingly negative electrode potential. Because within the time

domain of the experiment B does not diffuse beyond the limits of the diffusion layer (δ) (the absence of convection is assumed), the shape of the wave and the current due to the reduction $B + e^- \rightarrow C$ is the same as that for $A + e^- \rightarrow B$. (The current corresponding to the second wave is measured by extending the baseline from the first wave (not shown in the figure); the first wave is ordinarily assumed to decay as $t^{-1/2}$.) Again, because the electrolyzed material has not diffused beyond the border of the diffusion layer, and because additional B and C are continuously generated as long as the potential remains sufficiently negative, the currents upon reversal are equal to those obtained in the forward scan. This is the situation that obtains when no kinetic or other complications intervene.

For a planar electrode, the diffusion layer width, δ, is measured orthogonal to the electrode surface. The flux of electroactive species is the same at any point in a plane at a distance d from the electrode. As the potential is swept, the uniformity of the concentration profile (flux) at any distance d from the electrode ensures that the current density on the electrode surface is the same everywhere. However, in the present instance, because of the stream of intermediate product descending from the electrode, this, apparently, is not the case for the Pl-MeU dimer.

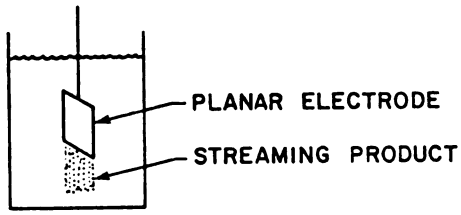

Evidence will be presented later showing that as the scan rate decreases, the number of electrons transferred is closer to 1, whereas at the highest scan rates the number is closer to 2. The fact that the intermediate electrolysis product - believed to be P(II,III)1-MeU - can be seen streaming downward from the planar (Pt flag) electrode, argues that a uniform flux normal to the surface, which in turn leads to a uniform current density over the surface of the electrode, does not obtain for P1-MeU. For this dense material, without mixing, the influence of gravity (sedimentation) prevails over the laws of diffusion. All other things being constant, the rate of fall at low velocities is proportional to the difference (d_1-d_o) between the density d_1 of the descending species and d_o of the medium. At the lowest scan rates, the second electron transfer contributes less current than it otherwise would because not all of the intermediate remains in the diffusion layer. Part of the second anodic wave derives from a direct $2e^-$ oxidation and part from the further oxidation of P(II,III)1-MeU. This convective influence on the diffusion layer violates a tenet upon which CV is based, and

therefore makes straightforward interpretation more difficult.

An additional explanation for the comparatively smaller contribution from the second electron transfer, one which follows a different line of reasoning and will be expounded upon momentarily, has to do with surface precipitation on the electrode. The fact that there is a considerable lag time before the descending stream is evident, suggests a surface precipitation of the intermediate product. As surface precipitate blocks access to the electrode surface to other reactants, further electron transfer is impeded. Even though the peak current increases with increasing scan rate in cyclic voltammetry ($i \propto v^{1/2}$), the overall charge transferred is lower since the duration of the de facto microelectrolysis is shorter ($q \propto t$). Therefore, since the surface film is less well developed at higher sweep rates, blockage due to localized precipitation is lower, the result of which is an enhanced pa2.

Upon potential reversal, the magnitude of i_{pc1} is less than that of i_{pa1} for the reasons that 1) additional amounts of intermediate have passed out of the diffusion layer under the influence of gravity and 2) some of the Pt(II)Pt(III) intermediate was oxidized to the Pt(III)Pt(III) state. In general, $i_{pc} \neq i_{pa}$ for irreversible systems due to slow electron transfer. For the fully-oxidized material, the subsequent reduction wave for Pt(II)Pt(III) $\xrightarrow{e^-}$ Pt(II)Pt(II) is buried under the peak for Pt(III)Pt(III) $\xrightarrow{e^-}$ Pt(II)Pt(III) centered at ~0.30 V. As indicated, there may also be kinetic factors at work. The fact that the magnitude of i_{pc1}, though smaller, is roughly

comparable to that of i_{pa1}, derives largely from the continuous generation of P(II,III)1-MeU as long as the electrode potential is sufficiently positive.

Support for the argument that surface precipitation plays a role in the observed CV behavior may be provided by the observation that the perchlorate salt of $[P(II,III)1\text{-MeU}]^{3+}$ is less soluble in aqueous solution than $[P(II,II)1\text{-MeU}]^{2+}(ClO_4)_2$. As suggested, precipitation on the electrode surface would inhibit the transfer of electrons from solution reactants. If the rate at which nucleation (precipitation) occurs places it within the time window of the scan, then the subsequent oxidation will not occur extensively. However, as the scan rate becomes relatively faster, then a second electron transfer becomes more competitive, pa2 becomes more pronounced, and i_{pa2} grows accordingly. It is relevant to point out here, though, that the visible, green stream did not appear to contain any insoluble matter. The molar absorptivity of the green P(II,III)1-MeU was determined to be 5.1×10^3 M^{-1} cm^{-1} (see p. 216).

Enhanced adsorption (precipitation) of the intermediate P(II,III)1-MeU on the electrode surface relative to the starting P(II,II)1-MeU should not have an exclusively inhibitory effect on further electron transfer, but, in fact, would be expected to facilitate transfer of a second electron for the adsorbate, and increasingly so at higher scan rates, providing no limiting chemical step intervenes. While at the same time facilitating complete oxidation to the Pt(III)Pt(III) state for the adsorbate, to repeat,

transfer of a second electron from unadsorbed (dissolved) P(II,III)l-MeU would be less effective through the adsorbed layer, thereby leaving unoxidized P(II,III)l-MeU in solution which can then be reduced back to the starting material upon scan reversal. This reduction is manifested in the $1e^-$ wave centered at 0.64 V.

Consistent with what has been said so far, a full two electrons, on average, are not removed from P(II,II)l-MeU during the CV experiment. This will be argued below, mostly by reference to RDV data. As hinted at previously, a full consideration of the CV behavior of the Pl-MeU system must not ignore kinetic factors. We are dealing with a quasi-reversible system, a state that may result from the intervention of heterogeneous kinetic effects alone, from chemical complications, or from a combination of both. A perhaps extreme example of a chemical step is given by the dimer → tetramer reaction observed in the electrochemistry of α-pyridone blue (41). No direct evidence was obtained in this work to support a similar dimerization or higher order association reaction; EPR and other measurements to be discussed later can all be accounted for by considering only the dimer. If we are to gauge the kinetic factor (extent of irreversibility) from shifts in the various peak potentials, then the effect is slight over the sweep range investigated. Examination of i_{pa}/i_{pc} current ratios is perhaps more telling. Unfortunately, at those scan rates at which two cathodic peaks are discernible, the anodic envelope is without sufficient resolution to permit calculation of the current ratios. Also, at the

highest scan rates used (2V/s and above), the anodic wave does not peak before reaching the anodic limit on Pt, hence again precluding a calculation of current ratios.

It was mentioned above that at intermediate scan rates (50-100 or 200 mV/s), the P(II,III)1-MeU intermediate was also evident as a descending stream, although the intensity of the stream was lower (to the naked eye) than that at lower scan rates. Because of the lag time, also mentioned, the descending stream was not apparent until after the double-sweep scan was concluded. Since the amount of material formed in an electrolysis at a given current is directly proportional to the time of electrolysis (Faraday's law), it is readily understood why less intermediate is evident at the higher sweep rates.

In considering the redox behavior of the Pl-MeU system, the question naturally arises whether the site of electron transfer can be localized (i.e., at which Pt atom does it occur?) in the molecule. Consider again the structure (head-to-head):

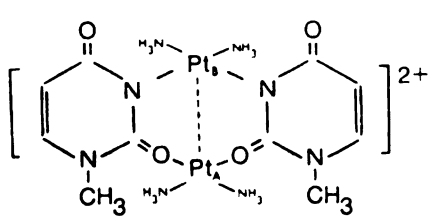

Pl-MeU(N^3,O^2)

or possibly

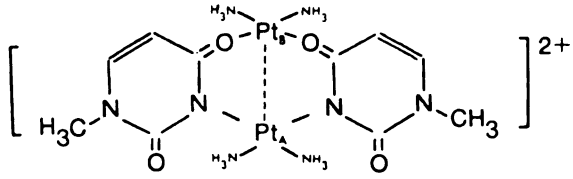

Pl-MeU(N^3,O^4)

While tautomeric structures may be drawn for uracils (2,4-dihydroxyuracil ↔ uracil-2,4-dione) or resonance forms drawn for the corresponding uracilate anions,

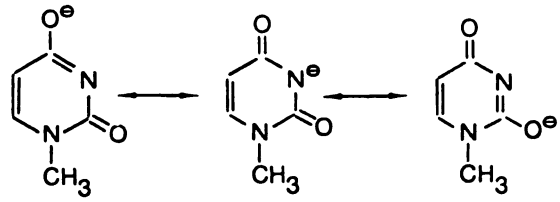

Resonance forms for uracilate

similar structures are not possible when the uracilates are bonded to platinum. Therefore, because the immediate environments of the two Pt atoms are not the same, their $E^{o\prime}$s may be expected to differ. (However, distinct environments or inequivalent Pt's is not a requirement for unequal $E^{o\prime}$s. Even if the complex were head-to-tail rather than head-to-head, if there is interaction between the Pt

sites, the E^{o}'s will differ.) The relevant question, though, is by how much do the E^{o}'s differ? Depending on the extent of Pt-Pt bonding, electron delocalization may not permit a distinction between Pt_A^{II}-Pt_B^{III} and Pt_A^{III}-Pt_B^{II}; an apt representation in this case, an <u>average</u> representation, is given by $Pt^{2.5}$-$Pt^{2.5}$. For very rapid interatomic (intervalence) electron transfer it would not be correct to associate one E^{o} with one Pt center and the second E^{o} with the other. What this would mean in terms of the cyclic voltammograms presented is that pal is not to be associated with the oxidation of a particular atom, and the same for pa2. Actually, the representation Pt_A^{II}-Pt_B^{III} $\underset{\text{fast}}{\overset{\text{very}}{\leftrightarrow}}$ Pt_A^{III}-Pt_B^{II}, which describes a partially-localized system (a so-called trapped-ion system), is most fitting; this representation is supported by Hush model calculations (<u>vide infra</u>).

CV's of Aged Pl-MeU -

The cyclic voltammetric behavior of freshly-prepared Pl-MeU and of somewhat aged Pl-MeU was contrasted in Figures 2 and 3. Similarly, the material giving rise to the CV's in Figure 12 was rerun three days later, yielding the CV's shown in Figure 15.

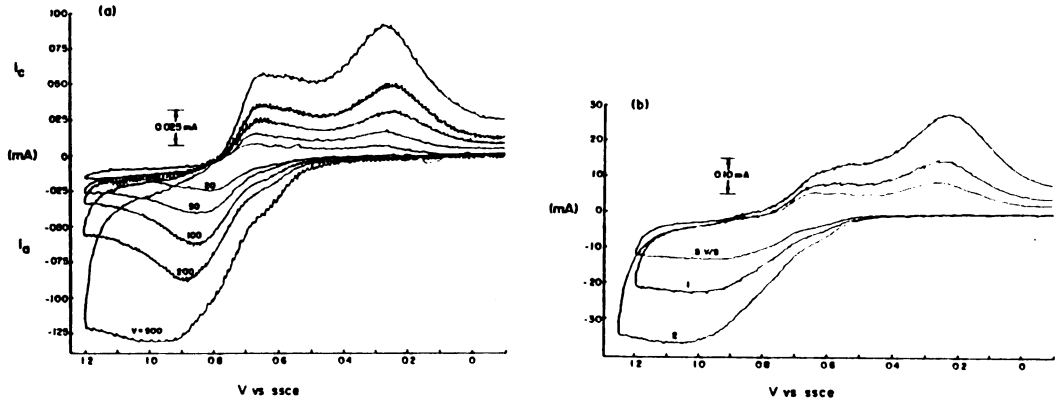

Figure 15. CV's from 20 mV/s - 2 V/s of aged P1-MeU (8.2 mg/5.0 ml, 2.0 mM), to be contrasted with Figure 12.

Several differences are apparent: 1) the presence of two components to the anodic wave is not apparent; 2) E_{pa} for the single anodic peak shifts markedly toward more positive potentials with increasing scan rate; 3) pc2 is more prevalent, and at the highest scan rates, i_{pc2} is of the same order of magnitude as i_{pc1}. E_{pc1} appears not to shift with scan rate whereas E_{pc2} shifts slightly, at first toward more positive potentials and then toward more negative ones. Although three days elapsed between the measurements shown here, the same changes were also observed to take place in as little as 12 hours.

Since a case has already been made for a correspondence between pc1 & pc2 and the anodic waves, and since the positions of pc1 and pc2 are observed to be relatively independent of scan rate in Figure 15, then, by deduction, the positions of the corresponding pa1 and pa2 peaks should also be fixed. In fact, as can be seen below in the accompanying figure, two waves juxtaposed as shown will give rise to

the observed behavior:

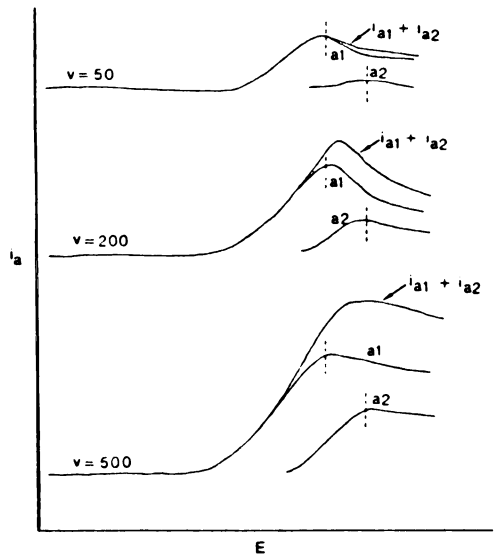

Dissection of i_a into i_{a1} and i_{a2} components

However, there is more to it than this. Aqueous, saline solutions of Pl-MeU would sometimes acquire a violet tinge upon standing (in sealed vessels, not protected from light). It was shown by liquid chromatography that polymeric species not unlike those comprising Pl-MeUB formed (vide infra). Although there was only a very light violet tinge to the solution giving rise to the CV's in Figure 15 (perhaps due primarily to the slight electrolysis achieved in the course of conducting CV experiments three days previous), air oxidation of Pl-MeU in electrolyte solution may have led to some slight polymerization with attendant partial oxidation. Hence, more than two platinum atoms per molecule may contribute to the observed anodic wave, as a pronounced anodic peak, and one shifted toward more positive potentials, is reminiscent of the CV of Pl-MeUB (see, for example, Figures 6 and 16). Also, the heightened response of pc2 (@

~0.26 V) suggests that oxidation beyond the P(II,III)1-MeU state is facilitated in the aged solution. Normally, cyclic voltammetry does not reflect the relative proportion of oxidation states in solution, as the appearance of the CV is independent of the potential at which the scan is initiated. This is not necessarily true, though, in a highly irreversible system, and is not true in the present case, as will become abundantly clear later when a joint elctrolysis/CV experiment is described. The changes as exemplified in going from Figure 12 to 15, were observed to occur in either perchlorate or nitrate media. It warrants mentioning that while CV's of aged Pl-MeU varied somewhat from preparation to preparation and may depend somewhat on the method of storage and on the extent of exposure to air, CV's of freshly-prepared Pl-MeU were reproducible.

FCV Applied to Pl-MeUB -

CV's of Pl-MeUB are shown in Figure 16, and may be compared with those of aged Pl-MeU in Figure 15.

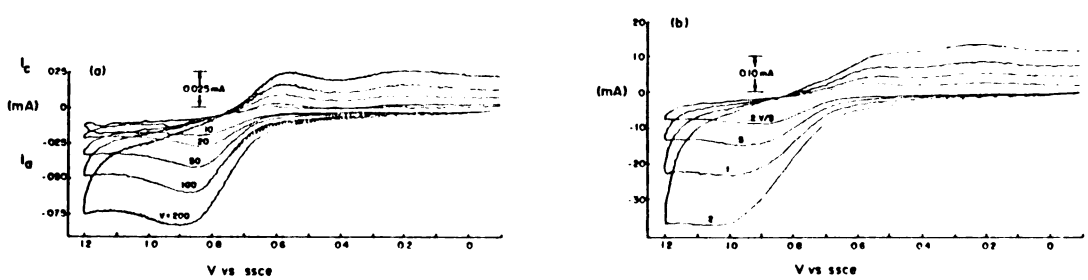

Figure 16. CV's of Pl-MeUB (24.4 mg/5.0 ml) over the sweep range 10 mV/s - 2 V/s.

The general features are the same although the relative magnitude of i_{pc2} is larger in the latter (Figure 15). A lack of reversibility for

Pl-MeUB is apparent, just as for Pl-MeU. However, as mentioned above, different preparations of Pl-MeU that were permitted to age, rarely yielded superimposable CV's. In this sense the CV's in Figure 15 should only be taken as illustrative.

Note from the current scales in Figures 12, 15 and 16 and from the appropriate concentrations that i_p/C^* (where C^* denotes the concentration in the bulk) is greater roughly by a factor of three for Pl-MeU than for Pl-MeUB. If certain simplifying assumptions are made, an expression can be derived relating peak current to molecular weight in a polymer containing noninteracting electroactive centers (89). Obviously, the requirement of noninteracting centers does not hold for the blues, since some Pt-Pt bonding is regarded as one of their characteristic features (and will also be shown to apply to Pl-MeUB in later sections). As pointed out by Flanagan et al. (89), a number of factors can complicate the theoretical treatment of a polymeric system: interactions between the electroactive centers, slow electron transfer at the electrode, structural changes upon oxidation and/or reduction, adsorption or precipitation of reactants or products at the electrode surface, and a difference in diffusion coefficients between reactants and products. The fact that most molecules bearing identical electroactive groups exhibit multiple waves rather than a single wave, as would be expected in the absence of any complication, may attest to the intervention of one or more of the above factors.

As mentioned, interaction between Pt centers may be assumed to be

extant in Pl-MeUB (evidence will be presented for it). The high degree of irreversibility, as especially exemplified by the large potential difference between the outer peaks (ΔE_{pac2}) is indicative of slow electron transfer. The possibility of structural changes in Pl-MeU upon oxidation at the electrode was alluded to earlier, and may hold even more for the polymeric Pl-MeUB. The anticipated effects from precipitation or adsorption were also described. Experiments to be discussed later have demonstrated that Pl-MeUB is strongly adsorbed at the Pt surface. A change in the diffusion coefficient upon oxidation is probably not so important.

The lower i_p/C^* noted for the polymeric system is probably explainable primarily in terms of a significantly lowered diffusion coefficient relative to Pl-MeU. The breadth and undelineated nature of the anodic wave due to Pl-MeUB is understandable in terms of the range of oligomeric species as well as their variable composition. For this complex system, and without knowledge of molecular weights, an estimate of the number of electrons transferred is not possible.

Comparison with CV's of Related Complexes -

Pt(III) is not a widely-recognized species in platinum chemistry. Those relatively few compounds known are listed in the Literature Review under Binuclear Platinum(III) Complexes. Evidence has been advanced above for the existence of a Pt(III) state in electrolyzed Pl-MeU - represented by P(II,III)l-MeU and P(III,III)l-MeU - and in Pl-MeUB, as deduced, in part, from their cyclic voltammograms. It is of interest to compare these cyclics

with those of related platinum compounds.

<u>cis</u>-$Pt(NH_3)_2(1\text{-}MeU)_2 \cdot 2H_2O$ was used in the synthesis of Pl-MeU, as reported by Woollins and Rosenberg (80) (mentioned on p. 66).

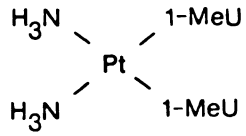

<u>cis</u>-$Pt(NH_3)_2(1\text{-}MeU)_2$

The valence state of Pt is 2 in this compound. CV's taken in perchlorate and sulfuric acid have the appearance shown in Figure 17.

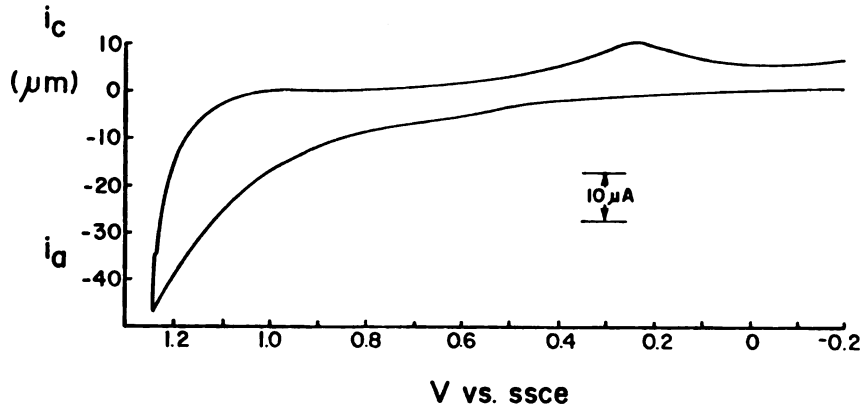

Figure 17. CV of <u>cis</u>-$Pt(NH_3)_2(1\text{-}MeU)_2$ (3.0 mg/5.0 ml, 1.2 mM) at Pt; v = 100 mV/s.

By analogy to the CV's obtained for Pl-MeU, and obtaining n=2 for this compound by redox titrimetry (<u>vide infra</u>), the cathodic peak centered at ~0.24 V vs ssce may be assigned to Pt(IV) $\xrightarrow{2e^-}$ Pt(II).

The corresponding anodic peak for the transition $Pt(II) \xrightarrow{-2e^-} Pt(IV)$ occurs at too positive a potential to be distinguished from the current due to the anodic limit on Pt. An attempted electrolysis at a potential as positive as 1.25 V vs ssce, conducted at a pH of 1.5, proceeded only at a trifling rate. It is of interest that, in one instance, a solution of Pl-MeU that stood for several days eventually yielded a CV very similar to that shown in Figure 17, and hence suggests hydrolysis to this mononuclear platinum complex (this is supported by LC). We may conclude from this comparison of the CV's of Pl-MeU and the mononuclear cis-$Pt(NH_3)_2(1\text{-MeU})_2$ that the latter compound cannot stabilize the +3 intermediate oxidation state.

Another compound, $[(NH_3)_2Pt(OH)_2Pt(NH_3)_2](NO_3)_2$,

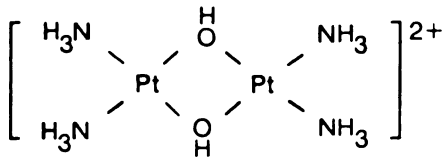

Hydroxo-bridged platinum dimer

an isolated "diaquo" species (72), yielded no CV at Pt at a concentration of 1.16 mg/ml (1.88 mM). When titrated with Ce(IV), this compound displayed a clean, single break corresponding to the transition $2Pt(II) \xrightarrow{-4e^-} 2Pt(IV)$ (vide infra). Perhaps a CV would be discernible at Au, but this was not tried. Both the absence of a cyclic and the titration results rule out an intermediate +3 oxidation state for this dimeric platinum species. Although a Pt(III) state cannot be stabilized in this compound, the Pt(II) state

is, apparently, lent additional stability by the bridging groups since the wave for the transition Pt(II) $\xrightarrow{-2e^-}$Pt(IV) is not accessible at Pt. Comparing the structure of this hydroxo-bridged dimer with the structure of the Pt(III)Pt(III) dimer derived from Pl-MeU, seems to mitigate against the Pt(III) state in those complexes containing saturated ligands in which electron delocalization is not possible. Also, the Pt-Pt interaction in $[(NH_3)_2Pt(OH)_2Pt(NH_3)_2]^{2+}$ is not likely to be strong, as the Pt-Pt internuclear separation is reported to be 3.085 Å (72).

Determination of n for Pl-MeU -

It was argued earlier that at the lowest scan rates, the number of electrons transferred per molecule of Pl-MeU approaches 1. An experiment comparing the behavior of a well-characterized system and that of Pl-MeU provides support for this contention.

Cyclics were obtained at 10 mV/s, 20 mV/s, and 2 V/s for the model compound $[Ru(NH_3)_6]Cl_3$, one known to exhibit reversible behavior, and for Pl-MeU. The CV's are shown in Figure 18. Pertinent measured currents and potentials are tabulated in Table 2.

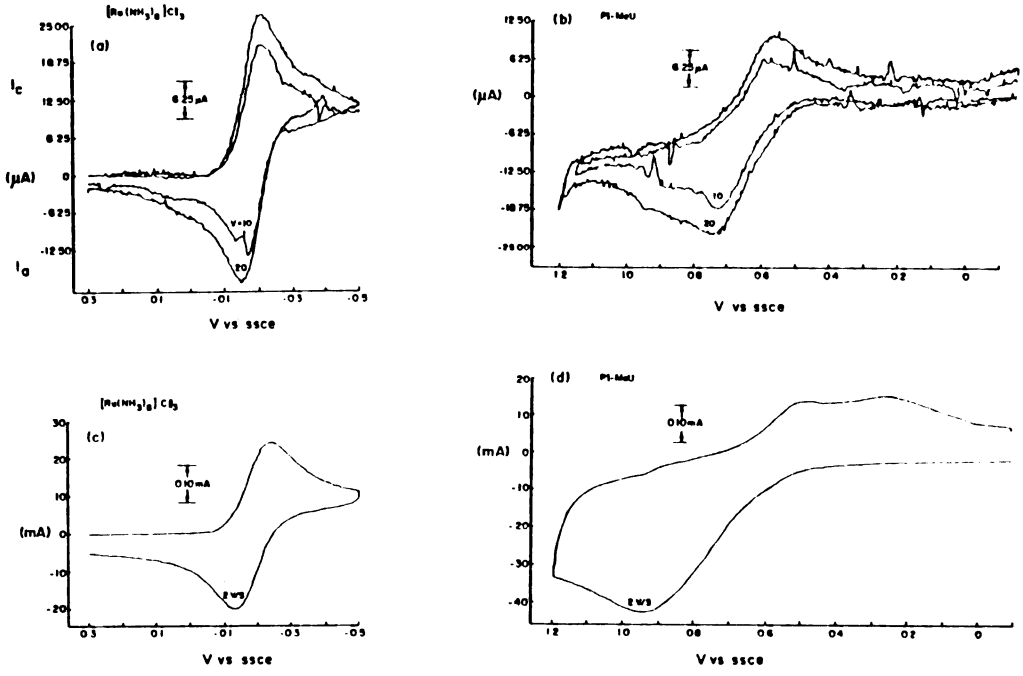

Figure 18. CV's of model compound $[Ru(NH_3)_6]Cl_3$ (4.7 mg/5.0 ml, 3.0 mM) and of Pl-MeU (8.2 mg/5.0 ml, 2.0 mM) taken at v = 10 mV/s, 20 mV/s, and 2 V/s for the purpose of calculating n, the number of electrons transferred per molecule of Pl-MeU. The noisy CV's at v = 10 and 20 mV/s stem from the high magnification used.

Table 2
CV Data for the Calculation of n in Pl-MeU

Compound	v(mV/s)	$i_{pa}^{(1)}$	i_{pc}	i_{pa}/i_{pc}	$E_{pa}^{(2)}$	$E_{pc}^{(2)}$	ΔE_{pac}
(3)$[Ru(NH_3)_6]^{3+}$	10	63(4)	69.5	0.91	-.15	-.21	.060
	20	82	85.5	.96	-.15	-.21	.060
	2000	695	760	.92	-.136	-.238	.10
$[Pl\text{-}MeU]^{2+}$	10	59	42	1.40	.775	.635	.14
	20	70	59.5	1.18	.78	.61	.17
	2000	1185	-		.95	-	

(1) arbitrary units

(2) vs ssce

(3) the couple swept was $[Ru(NH_3)_6]^{3+} + e^- \rightarrow [Ru(NH_3)_6]^{2+}$ and $[Ru(NH_3)_6]^{2+} - e^- \rightarrow [Ru(NH_3)_6]^{3+}$

(4) estimated, noisy CV

The shift in ΔE_p between 10 mV/s and 20 mV/s noted for Pl-MeU is typical of irreversible systems as is the large value of ΔE_p (= 0.59/n mV for a reversible system). The closest approach to reversible behavior for a partially-irreversible system is always at the slowest scan speeds.

For a reversible system, $i_p = (2.69 \times 10^5)\, n^{3/2} A D^{1/2} v^{1/2} C^*$. Then $AD^{1/2}v^{1/2} = \dfrac{i_p}{2.69 \times 10^5\, n^{3/2}\, C^*}$. This factor can be obtained for the known ruthenium system for which n = 1. Making the assumption that $D_{[Pl\text{-}MeU]^{2+}} = D_{[Ru(NH_3)_6]^{3+}}$, and carrying through the algebra, one can solve for $n_{Pl\text{-}MeU}$:

$$n_{Pl\text{-}MeU}^{3/2} = \frac{i_{p,Pl\text{-}MeU}}{i_{p,Ru}} \cdot \frac{C^*_{Ru}}{C^*_{Pl\text{-}MeU}} \cdot n_{Ru}^{3/2}.$$

For $C^*_{[Ru(NH_3)_6]^{3+}} = 3.04 \times 10^{-1}$ mol/cm^3 and $C^*_{[P(II,II)1\text{-}MeU]^{2+}} = 1.97 \times 10^{-1}$ mol/cm^3, $n_{Pl\text{-}MeU}^{3/2} = 1.54 \times \dfrac{i_{p,Pl\text{-}MeU}}{i_{p,Ru}}$

($i_{p,Pl\text{-}MeU}$ is anodic current while $i_{p,Ru}$ is cathodic in this equation.) Calculated n values are as follows:

v(mV/s)	$n_{calc.}$(Pl-MeU)
10	1.20
20	1.19
.	
.	
.	
2000	1.85

Note: ΔE_p for $[Ru(NH_3)_6]^{3+}$ @ v = 2V/s = 0.10 → no longer totally reversible.

The potential at which $i_{p,Pl\text{-}MeU}$ is measured at the two lowest scan rates is 0.17 V less positive than the potential used for the measurement at v = 2V/s (see Figure 18). This difference reflects the greater contribution of the second electron transfer at the scan rate of 2V/s. A value of n that increases with v is in agreement with our earlier qualitative discussion. The most straightforward interpretation of this effect lies in postulating surface precipitation, as previously discussed.

Rotating Disk Voltammetry (RDV) -

The use of rotating disk voltammetry (RDV) served several purposes in the present study: 1) inspection of RDV's allowed the selection of appropriate potentials for exhaustive electrolysis of both Pl-MeU and Pl-MeUB (although one must be aware that the voltammetric experiment does not necessarily translate directly to macroscale electrolysis because the time scales of the two experiments are so different; stated differently, a voltammogram and a so-called coulogram may be shifted from one another by several tenths of a volt), 2) by comparing RDV's with CV's, confirmation of peaks in the CV's as "real", and not artifacts of the CV experiment, was possible, 3) by once again employing the $[Ru(NH_3)_6)^{3+}$ model system, the number of electrons, on average, transferred from Pl-MeU as a function of rotational velocity could be determined, and then, by analogy, related to the scan rate dependence in cyclic voltammetry, 4) by making various assumptions, an estimate of the

average molecular weight of Pl-MeUB could be made, 5) information about the comparative adsorptive behavior of Pl-MeU and Pl-MeUB was obtained by noting the rate of decrease of the limiting current due to adsorption in successive sweeps as a function of the rotational speed, and 6) by generating RDV's at various stages of an exhaustive electrolysis and comparing these with the corresponding cyclics, additional conclusions regarding the electrochemical behavior of Pl-MeU and Pl-MeUB could be made.

RDV's of Pl-MeU and Pl-MeUB, taken at 500 rpm, are shown in Figure 19 along with the RDV of the supporting electrolyte.

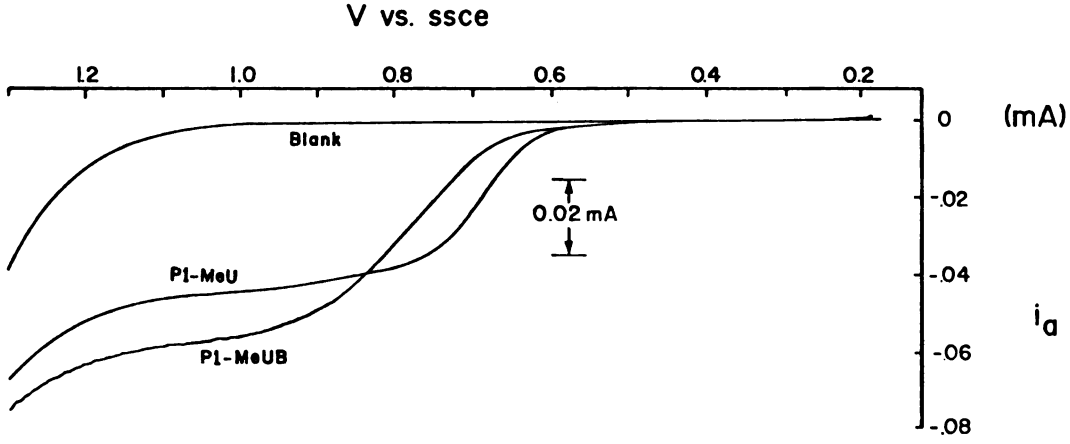

Figure 19. Rotating disk voltammograms of Pl-MeU (5.6 mg/10 ml, 0.67 mM) and Pl-MeUB (22.3 mg/10 ml) taken at 500 rpm (ω = 52 rad/s).

The voltammogram for the more complex Pl-MeUB is shifted toward more positive potentials, a manifestation of the greater irreversibility of this system. Notice that the curve for Pl-MeUB is smooth while the curve for Pl-MeU has an inflection (subtle, see also Figure 21b).

The inflection will be related to two discernible electron transfer steps, in analogy to the CV's for Pl-MeU. The RDV's of Figure 19 show that a potential of 1.0 V vs ssce is a satisfactory choice to ensure complete oxidative electrolysis, but since the background current is still slight at 1.1 V, the latter is a better choice in kinetic systems such as the two we are concerned with here. Since Pt is in the +2 oxidation state in native Pl-MeU and since it has an average oxidation state close to 2 in Pl-MeUB (to be demonstrated later), no cathodic current is apparent at potentials more positive than 0.2 V. Partially- or exhaustively-electrolyzed Pl-MeU or Pl-MeUB, in contrast, yields a cathodic current (not shown) at positive potentials, but not a limiting current plateau. Rather, the current continues to rise gradually in a nondescript fashion out to the cathodic limit on Pt. However, dc polarography did exhibit a plateau from about -1.0 V to -1.35 V ($E_{1/2} \cong$ -0.8 V vs ssce) for exhaustively-electrolyzed Pl-MeUB; there was no corresponding plateau for unelectrolyzed material.

Determination of $\underline{n}$ by RDV -

RDV is a mass transport limited technique. Agitation of the solution brings reactant to a distance d from the electrode by convection, where d is the thickness of the hydrodynamic diffusion layer. By the same action, product is swept out into solution by the rotating electrode. In the diffusion layer itself, though, convection is absent.

The concentration profile of reactant is shown in Figure 20 (88).

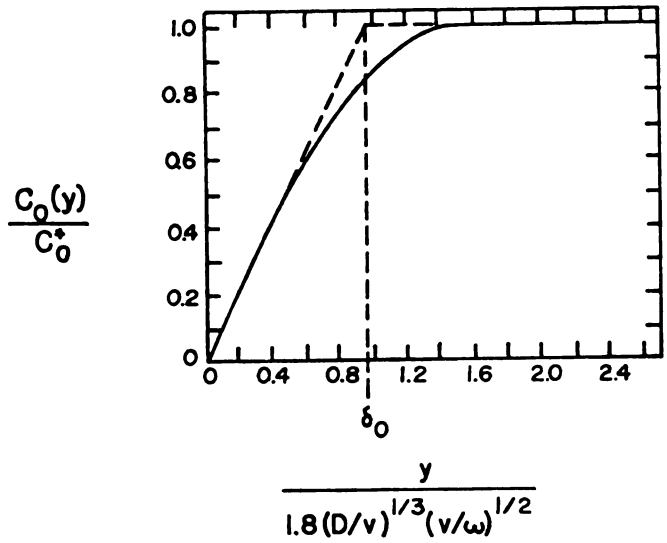

Figure 20. Concentration profile of electroactive species in RDV in terms of dimensionless coordinates (taken from ref. 88).

The profile of the product is the inverse of the reactant profile. The greater the angular frequency of rotation ω (in rad/s), the sharper the profile, i.e., the narrower the diffusion layer thickness. In the CV's we observed that as the scan rate was increased, transfer of a second electron to the electrode was more effective. Two divergent views might be offered as to what effect ω would have on the effectiveness of the second electron transfer in RDV. The first is that, just as at higher scan rates the intermediate product is able to diffuse away a shorter distance per ΔE sweep of the potential, in RDV at higher ω the product is more closely constrained to the electrode (i.e., the concentration profile is sharper). Likened to the CV experiment, a larger contribution from the second electron transfer may be anticipated because of the

proximity of the intermediate to the electrode. The other view states that as ω increases, the product is more rapidly swept out into solution and that consequently there is less time allotted for transfer of the second electron.

To study this question, RDV's were obtained as a function of ω for the model compound $[Ru(NH_3)_6]Cl_3$ and for Pl-MeU. The RDV's are shown in Figures 21a and 21b. While the Pt disk electrode was cleaned and polished prior to commencing a series of runs, it was not polished betwen runs. To do so was both too time consuming and led to irreproducible RDV's. Two runs were made at each frequency in the order shown. This was followed by an additional run at each frequency in reverse order as a check on repeatability. It can be seen that there was some dimunition in response over the course of the experiment. However, because it was gradual, no compensation was made for it. Only the two runs made during the forward traversal were used in the calculations to follow.

The analysis here relies on the use of the Levich equation (see Appendix B): $i_\ell = 0.620nFAD^{2/3}\omega^{1/2}\nu^{-1/6}C^*$. Making the assumption that $D_{[Ru(NH_3)_6]^{3+}} = D_{[Pl\text{-}MeU]^{2+}}$, we first solve for $AD^{2/3}\nu^{-1/6}$ in terms of the remaining parameters which are either known or measured. Plugging this into the Levich equation for $[Pl\text{-}MeU]^{2+}$, we get

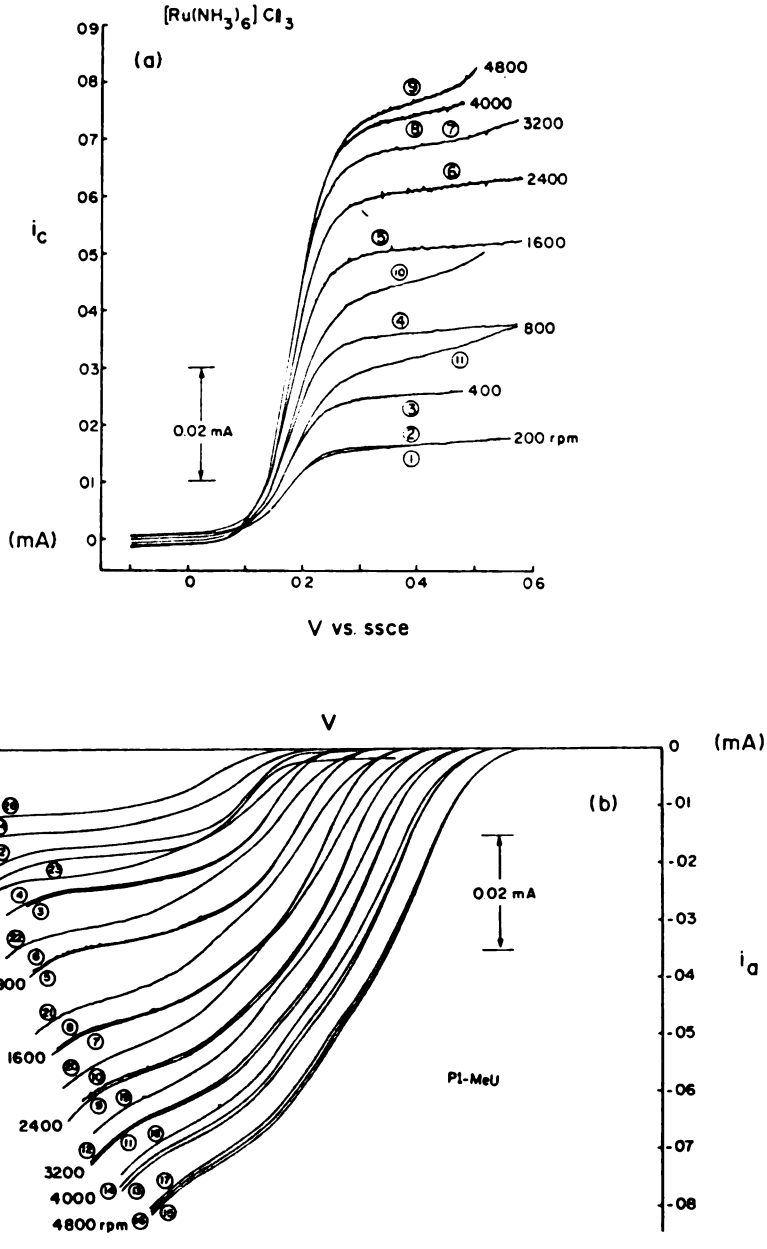

Figure 21. RDV's of a) model compound $[Ru(NH_3)_6]Cl_3$ (2.4 mg/10 ml, 0.78 mM) and b) P1-MeU (4.2 mg/10 ml, 0.50 mM) as a function of ω for the purpose of calculating n. In b) the runs are offset for the sake of clarity; each scan was from 0.4 - 1.2 V vs ssce. The circled numbers correspond to the order in which the runs were made (see text).

$$n_{Pl\text{-}MeU} = \frac{i_{\ell,Pl\text{-}MeU}}{i_{\ell,Ru}} \cdot \frac{C^*_{Ru}}{C^*_{Pl\text{-}MeU}} \cdot n_{Ru}$$

For $C^*_{Ru} = 7.75\text{x}10^{-1}$ mol/cm^3 and $C^*_{Pl\text{-}MeU} = 5.04\text{x}10^{-1}$ mol/cm^3,

$$n_{Pl\text{-}MeU} = 1.54 \cdot \frac{i_{\ell,Pl\text{-}MeU}}{i_{\ell,Ru}}$$

The data from Figures 21a and b and calculated n values are listed in Table 3. In an earlier experiment a value of n = 1.57 had been obtained at f = 500 (ω = 7.24).

A plot of i_ℓ vs $\omega^{1/2}$ was linear through $\omega^{1/2} \cong 18$ for both $[Ru(NH_3)_6]^{3+}$ and $[Pl\text{-}MeU]^{2+}$, as expected from the Levich equation. From the trend shown in n vs f in Table 3, apparently the interpretation that the electrolysis product is quickly swept out into solution at the higher angular velocities is the correct one. The calculated n vs f values do not plot to a smooth curve. Although the number of electrons transferred is calculated to be lower at higher ω, the RDV's at high ω more clearly show that more than one electron step is involved (because they are not smooth). It is of interest to note that RDV's for Pl-MeUB are smooth at all values of ω - see Figure 22 for an example at a single value of ω.

An approach similar to the one used here would not be informative in the case of Pl-MeUB because 1) the molecular weight(s) is unknown, and 2) the assumption that $D_{[Ru(NH_3)_6]^{3+}} = D_{[Pl\text{-}MeUB]^{n+}}$ is not a good one. (An estimate of $D_{Pl\text{-}MeUB}$ is given later.) In this case the fuller expression

Table 3
RDV Data for the Calculation of n for Pl-MeU

f(rpm)	$\omega^{1/2}(s^{-1/2})$	$i_{\ell,Ru}^{(2)}(\mu A)$	$i_{\ell,Pl\text{-}MeU}^{(3)}(\mu A)$	$n_{Pl\text{-}MeU}$
140[1]	3.83	14.5	17.7	1.88
400	6.47	22.5	21.5	1.47
800	9.15	33.5	32.2	1.48
1600	12.9	48.5	45.4	1.44
2400	15.8	60.0	53.8	1.38
3200	18.3	67.5	60.6	1.38
4000	20.5	74.0	65.0	1.35
4800	22.4	77.0	68.8	1.38

(1) measured; the remaining values were read off the dial

(2) cathodic, measured @ -0.4 V vs ssce

(3) anodic, measured @ +1.1 V vs ssce

$$n_{Pl\text{-}MeUB} = \frac{i_{\ell,Pl\text{-}MeUB}}{i_{\ell,Ru}} \cdot \frac{C^*_{Ru}}{C^*_{Pl\text{-}MeUB}} \cdot \frac{D^{2/3}_{Ru}}{D^{2/3}_{Pl\text{-}MeUB}} \cdot n_{Ru}$$

would have to be used. But since Pl-MeUB consists of a distribution of oligomers (vide infra), a mean n, $\bar{n}$ - based on a mean concentration (which in turn is based on a mean molecular weight) and on a mean D - would have little meaning.

A Calculation of the Mol. Wt. of Pl-MeUB from RDV Data -

By making RDV measurements on a model compound, $[Ru(NH_3)_6]^{3+}$, and on Pl-MeU and Pl-MeUB under identical conditions, and by making certain assumptions, a calculation of an average molecular weight for Pl-MeUB is possible. While not identical to, the treatment to be given here was inspired by the publication of Smith, Kuder, and Wychick (90), which deals with the voltammetric behavior of poly(vinylferrocene). Theirs appears to be one of the relatively few applications of electrochemistry to polymer science.

By applying the Levich eq.,

$$i_\ell = 0.620nFAC^*D^{2/3}\nu^{-1/6}\omega^{1/2}$$

to the reduction $[Ru(NH_3)_6]^{3+} + e^- \rightarrow [Ru(NH_3)_6]^{2+}$, and using $D = 7.5\times10^{-6}$ cm^2/s and $\nu = 0.01$ cm^2/s, a value of 0.114 cm^2 was obtained for the area of the disk electrode. Making the same calculation discussed in the preceding section, at a value of $\omega = 52.4$ rad/s (f = 500 rpm), and again making the assumption that $D_{[Pl\text{-}MeU]^{2+}} = D_{[Ru(NH_3)_6]^{3+}}$ (the diffusion coefficients of small molecules differ

little), a value of n = 1.57 is obtained.

If a value of D can be obtained for Pl-MeUB, then an estimate of the molecular weight is possible through application of the Einstein-Stokes equation: $D = (2.96 \times 10^{-7}/\eta)(d/M)^{1/3}$. In this equation η is the viscosity of the solution and d is the density of the electroactive species. In utilizing the equation, the assumption is made that the electroactive molecules are spherical and are much larger than the solvent molecules. In the present case, the first assumption may be questionable, its goodness depending on chain length and extent of coiling. It is further assumed that there be no significant dipolar or hydrogen-bonding interaction between the electroactive species and the solvent, most certainly a poor assumption in the present instance (solvent - water).

To obtain the diffusion coefficient, solve the Levich eq. for D:

$$D^{2/3} = i_{\ell}/(0.62nC^{*}FA\nu^{-1/6}\,\omega^{1/2})$$

F, A, ν, and ω are known, n and C^{*} are not. At this point, another assumption needs to be made. A possible structure for platinum uracil blues consists of alternate singly-bridging uracil anions (12). (As previously discussed, double bridging is not likely, as it would confer no flexibility to the chain, although even if double bridging were assumed, the calculation to follow would hardly change at all.) A possible structure was shown earlier (p. 39) and is repeated, with slight modification, here (91).

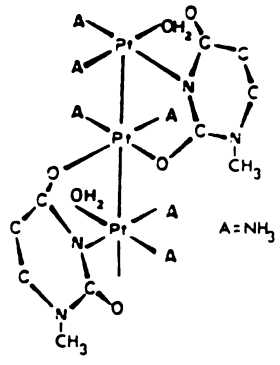

A possible structure for Pl-MeUB

The depiction shown begins at one end of the chain and proceeds through 3 atoms. Redrawn without regard to the stereochemistry, we can identify the repeating unit between dashed lines; it consists of 2 Pt's, 4 ammines (A), and 2 1-MeU groups:

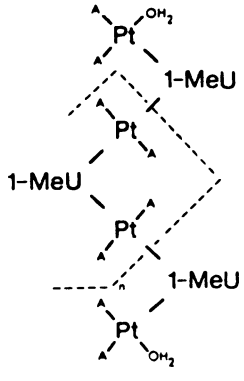

Also to repeat, the structure of the dimer may be represented as

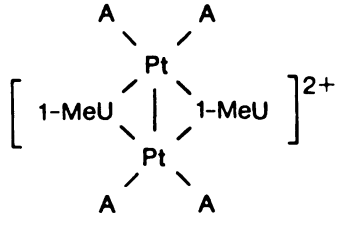

Over the length of the chain, there is one fewer 1-MeU group than there are Pt atoms. Then, for a chain length of 15-20 units or so, the difference in concentration per repeating unit in the blue compared with that in the dimer is negligible:

$$\frac{[\text{blue/repeating unit}]}{[\text{dimer}]} \sim 1$$

This also ignores the additional (presumed) coordinated water at each end of the chain (a negligible effect). For each repeating unit in the blue, assume n to be the same as for the dimer. That is, if under the experimental conditions used, $n_{Pl\text{-}MeU} = 1.6$, then assign $n_{Pl\text{-}MeUB/(repeating\ unit)} = 1.6$. This assumption may not be so bad, but the uncertainty in the 1.6 figure may be considerable, as we saw earlier. (Coulometric analysis, to follow, will also show that $1 < n < 2$.) Actually, the Pt atoms in Pl-MeUB are more difficult to oxidize, so that $n_{Pl\text{-}MeUB/(rep.\ unit)} < n_{Pl\text{-}MeU}$. Nevertheless, with these assumptions made ($n_{Pl\text{-}MeUB/(rep.\ unit)} = n_{Pl\text{-}MeU}$), a value for D may be obtained from the measured i_ℓ corresponding to a known weight of Pl-MeUB:

$$D = 1.36\text{x}10^{-6} \rightarrow 1.4\text{x}10^{-6}\ cm^2/s$$

If, rather, a value of n = 1 were to be used, then $D = 2.7\text{x}10^{-6}$ cm^2/s; for n=2, $D = 1.0\text{x}10^{-6}$ cm^2/s.

For use in the Einstein-Stokes eq., a viscosity, η, equal to 1.0 cp was taken (valid for dilute solutions). The density d was determined by volumenometry (92), and was found to be 2.5 gm/cm^3. Substituting these values and $D = 1.36\text{x}10^{-6}$ cm^2/s into the Einstein-Stokes eq., a value M = 25,465 was obtained. The formula wt. for each repeating unit in Pl-MeUB, taken to be the same as in the dimer, is 832. The mean number of repeating units is then calculated to be 25,465/832 = 30. If the value of D corresponding to n=1 is substituted in the equation, M = 3,365 is obtained. Hence,

this determination is critically dependent on n.

By way of comparison, an upper limit of 5000 amu, obtained by sedimentation studies, was reported for a platinum thymine purple (19), and an upper limit of 3000, by gel chromatography (procedure unpublished), for a Pt-thymine blue (5). Based on a liquid chromatographic study (vide infra), the value 30 seems a little high. A value closer to 20 would conform better to current belief (18). While a number of assumptions were made in this treatment, the uncertainty in n is most limiting. Also, the assumptions conditional to use of the Einstein-Stokes equation may not be well met.

Adsorptive Behavior by RDV -

A number of electrochemical techniques can be used to study adsorption. One of the most common is chronocoulometry which yields the surface excess Γ (in mol/cm^2) directly. Adsorption affects the outcome of all electrochemical measurements; the experimenter needs always to be wary. The relatively strong tendency of Pl-MeUB to adsorb on platinum became apparent during controlled-potential coulometry experiments (vide infra). Likewise, behavior observed in the course of recording RDV's was best explained by invoking adsorption on the electrode surface.

Figure 22 shows a series of consecutive runs of Pl-MeUB on Pt by RDV made without polishing the electrode between runs.

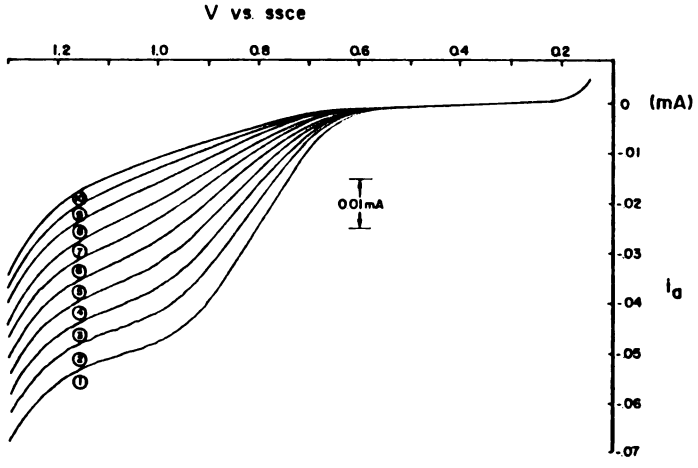

Figure 22. Consecutive RDV's of Pl-MeUB (27.0 mg/10 ml) in perchlorate medium generated at $\omega = 42\ s^{-1}$.

It is to be noted that in each succeeding scan in Figure 22 the limiting current has decreased. Similar series were generated at rotational frequencies ranging from 200-3200 rpm. As the plot in Figure 23 shows, the fractional drop in limiting current in succeeding runs increases with ω. (The drop is even more pronounced at Au.) This dimunition in current may be accounted for by postulating adsorption.

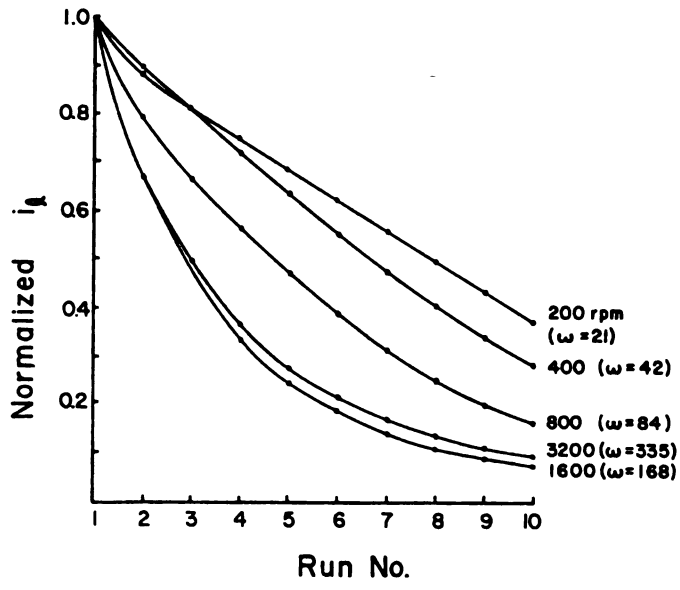

Figure 23. Limiting current by RDV for successive runs of Pl-MeUB as a function of ω.

As surface coverage by adsorption increases, the path a reactant takes to reach the surface may not be a direct one, but may require hopping about to find a vacant site. The current will be reduced because of the lower surface area available ($I = i_d \times A$, where I is the measured current and i_d is the current density). As the rotational speed increases, there is less time for reactant to seek out the imposed circuitous (hindered) path to the surface, and hence a proportionately greater dimunition in the current is observed (Figure 23). No surface experiments were conducted in an attempt to elucidate the nature of the adsorbed Pl-MeUB. As mentioned, the electrode surface was not cleaned and abraded between runs. However, it was cleaned and polished each time the rotational frequency was changed.

A Pl-MeUB concentration of 2.7 mg/ml in 0.1 F $NaClO_4$ was used to generate the curves of Figure 22. It was mentioned earlier that

Pl-MeU had been observed to precipitate in a perchlorate medium, although this never occurred with Pl-MeUB. Nevertheless, a check on the adsorption behavior was made in nitrate medium; the result was the same. A comparison with Pl-MeU by RDV made at a lower concentration (in perchlorate) contrasts the adsorptive behavior of these two systems, and is shown in Figure 24. This contrasting behavior was confirmed by coulometric analysis.

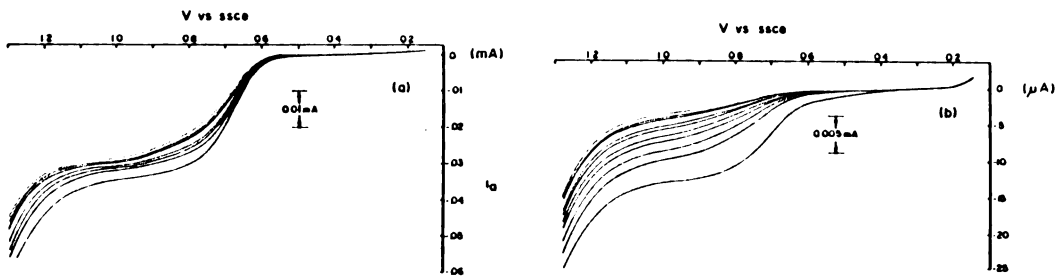

Figure 24. Comparative adsorptive behavior in perchlorate medium by RDV of a) Pl-MeU at a concentration of 5.1 mg/10 ml (0.61 mM) and b) Pl-MeUB, also at 5.1 mg/10 ml; ω = 42 s^{-1}. Successive runs were made as per Figure 22.

Controlled-Potential Coulometry (CPC) (93-96) -

Controlled-potential coulometry (CPC) is a bulk electrolysis technique in which accumulated charge is measured at a fixed potential difference, ordinarily in an exhaustive electrolysis. It is contrasted with nonbulk techniques in that the concentrations of electroactive species in the bulk solution are appreciably altered. This is a direct consequence of the large A/V ratio employed (where A is electrode area and V is solution volume), of rapid mass transport provided by vigorous agitation of the solution, and of the long time

scale of the experiment (minutes and even hours). This lengthened time window for CPC makes it generally less useful as a mechanistic probe compared with other electrochemical techniques. The primary usefulness of CPC lies in its ability to establish n, the number of electrons transferred per molecule, through the application of Faraday's law.

CPC of Pl-MeU. CPC of Pl-MeU was ordinarily conducted in either 0.1 F $NaClO_4$ or 0.1 F $NaNO_3$. Electrolysis in 0.1 F $NaClO_4$ led to the precipitation of the green partial-oxidation product $[(NH_3)_2Pt(II)(C_5H_5N_2O_2)_2Pt(III)(NH_3)_2](ClO_4)_3$, referred to as P(II,III)l-MeU. This was useful in the isolation of this product, but in most trials a nitrate supporting electrolye was used.

The electrolysis behavior of P(II,II)l-MeU in $NaNO_3$ is exemplified in the curves of Figure 25.

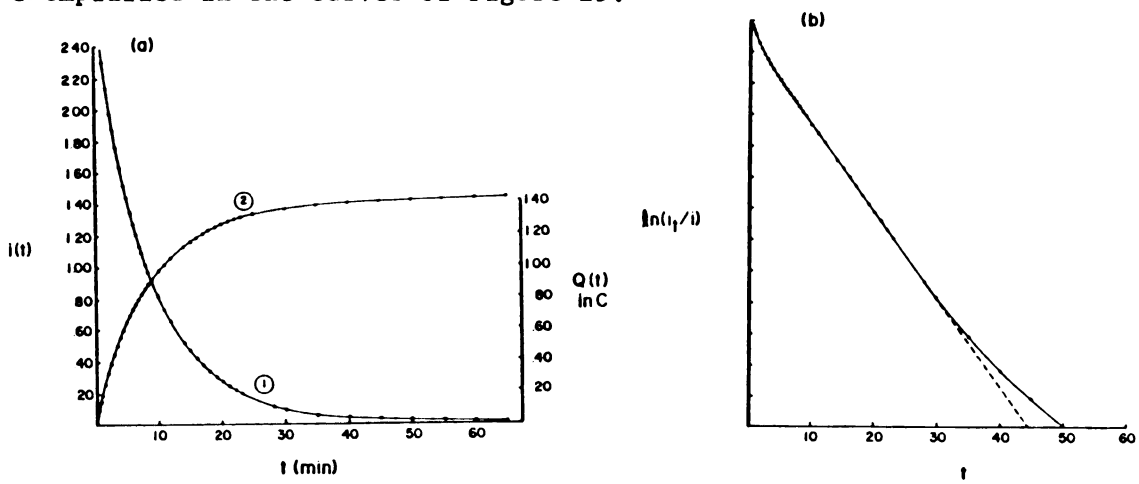

Figure 25. Controlled-potential electrolysis curves for Pl-MeU (5.9 mg/5.0 ml, 1.4 mM) conducted in 0.1 F $NaNO_3$: a) current-time curve (1) and charge-time curve (2); b) the corresponding ln i-vs-t plot. The electrolysis potential was maintained at +1.1 V vs ssce throughout the electrolysis.

As the Q(t)-vs-t curve is the integral of the i(t)-vs-t curve - $Q(t) = \int_0^t i dt$ - these two curves are the inverse of one another. The electrolysis giving rise to these curves was conducted at +1.1 V vs ssce. The color passed from essentially colorless (maybe a very pale yellow) through an intense green to a golden yellow.

In a first-order system, one in which there are no kinetic complications or serious adsorptive effects, both the concentration and current decay exponentially: $C^*(t) = C^*(0)e^{-k_e t}$ and $i(t) = i(0)e^{-k_e t}$ (* refers to bulk). These equations assume 100% current efficiency. The parameter k_e can be described in terms of a nernstian diffusion-layer model, $k_e = \frac{DA}{\delta V}$ (or $k_e = \frac{mA}{V}$ where m, the mass transfer coefficient, equals D/δ), where δ is the diffusion-layer thickness; k_e may be thought of as a first-order rate constant. Here it can be seen more formally that the ratio (electrode surface)/(solution volume) should be kept large and δ small (by vigorous stirring or ultrasonication) in order to shorten the electrolysis time. The equations also reveal a characteristic feature of CPC, and that is that the time of electrolysis is independent of the initial concentration. For a first-order system, a plot of ln i(t) vs t is linear with slope $-k_e$. A ln i(t)-vs-t plot for the electrolysis graphed in Figure 25a is shown in 25b.

At 99% completion, $C^*(t)$ and i(t) have decreased to 1% of their initial values so that $i(t)/i(0) = 0.01$, and at 99.9% completion, $i(t)/i(0) = 0.001$. Hence, CPC is capable of a high degree of accuracy (and precision) in a well-behaved system - that is, one in which the

background is negligible. In practice, the current decays to the level of the background, a level that should be made as small as possible.

A closer examination of Figure 25b reveals that there is a relatively short settling-in period (due in small part to double layer charging effects) before the linear portion of the curve is reached, and following this linear portion the curve curves upward. At lower electrolysis potentials (where the applied overpotential is less), the settling-in period is longer. The upward shift of the curve following the linear portion stems from the proportionately greater contribution of the solvent(H_2O)/supporting electrolyte - i.e, from the background current. The fact that the exponential approach of Q(t) is nearly flat beyond about 40 min on the scale of Figure 25a, signals that the electrolysis is, practically speaking, complete. The contrasting behavior of Pl-MeUB will be noted later. Graphical techniques applicable to first-order systems exist for estimating the point of completion of an electrolysis without actually carrying it to completion. Alternatively, one can read the accumulated charge corresponding to a preselected degree of completion (corrected for the background). n is then calculated from Faraday's law.

Using the latter approach, a value of 2.04 $\pm$ 0.05 was obtained for Pl-MeU. Employing the four most commonly-used graphical techniques (94, 97-101), values of 1.97, 2.07, 2.06, and 2.08 were obtained. Of these four, the last two are generally considered the

most reliable (94). These results translate to either $Pt(II)Pt(II) \xrightarrow{-2e^-} Pt(III)Pt(III)$ or to $Pt_A(II)Pt_B(II) \xrightarrow{-2e^-} Pt_A(IV)Pt_B(II)$ (or $Pt_A(II)Pt_B(II) \xrightarrow{-2e^-} Pt_A(II)Pt_B(IV)$). For either of the latter two situations to obtain, Pt atoms A and B have to be energetically very different. Arguments will be advanced to support the transition $Pt(II)Pt(II) \xrightarrow{-2e^-} Pt(III)Pt(III)$ as the extant one.

It is instructive to examine the electrolysis curve of Pl-MeU, as the ln i-vs-t plot, as a function of potential. In the region where both oxidations are mass-transport controlled, and assuming that there is no intervening chemical reaction, the overall reaction approaches $P(II,II)l\text{-}MeU - (n_1 + n_2)e^- \rightarrow P(III,III)l\text{-}MeU$, where $n_1 = n_2 = 1$ - i.e., by controlled-potential coulometry, the reaction is indistinguishable from a direct $2e^-$ transfer. The result is a linear ln i-vs-t plot. In this mass transport-controlled region, the electrolytic rate constants k_{e1} and k_{e2} are equal; if they were not, the plot would be curved either upward or downward (102). The rate constant may be calculated from either current or charge measurements, but the latter approach is more accurate (102). Taking the mean of 9 calculations made using the equation $k_e = - 1/t \ln \frac{Q_R}{Q_\infty}$ where $Q_R = Q_\infty - Q_t$ (102), a value of $k_e = 1.99 \times 10^{-3} \pm 0.02 \times 10^{-3}$ s^{-1} was obtained.

As the potential is reduced below the limiting region, the second electron transfer (and eventually the first, also) becomes sufficiently sluggish so that the P(II,III)l-MeU intermediate has

time to diffuse out into the bulk solution before a second electron can be transferred. This is a sort of ece mechanism. Deviation from linearity in the i-t curve is to be expected, and is, in fact, diagnostic. For either reversible or totally irreversible systems, the ln i-vs-t plot should be dissectable into two linear portions, the first corresponding to the more facile transfer and the second to the slower transfer (at long t), with a curved portion in between where both transfers are contributing. Hence, overall, the curve is concave upward. The corresponding quasi-reversible case appears not to have been worked out. Electrolysis curves for Pl-MeU generated at +1.1, 0.80, 0.75, and 0.70 V vs ssce are presented in Figure 26.

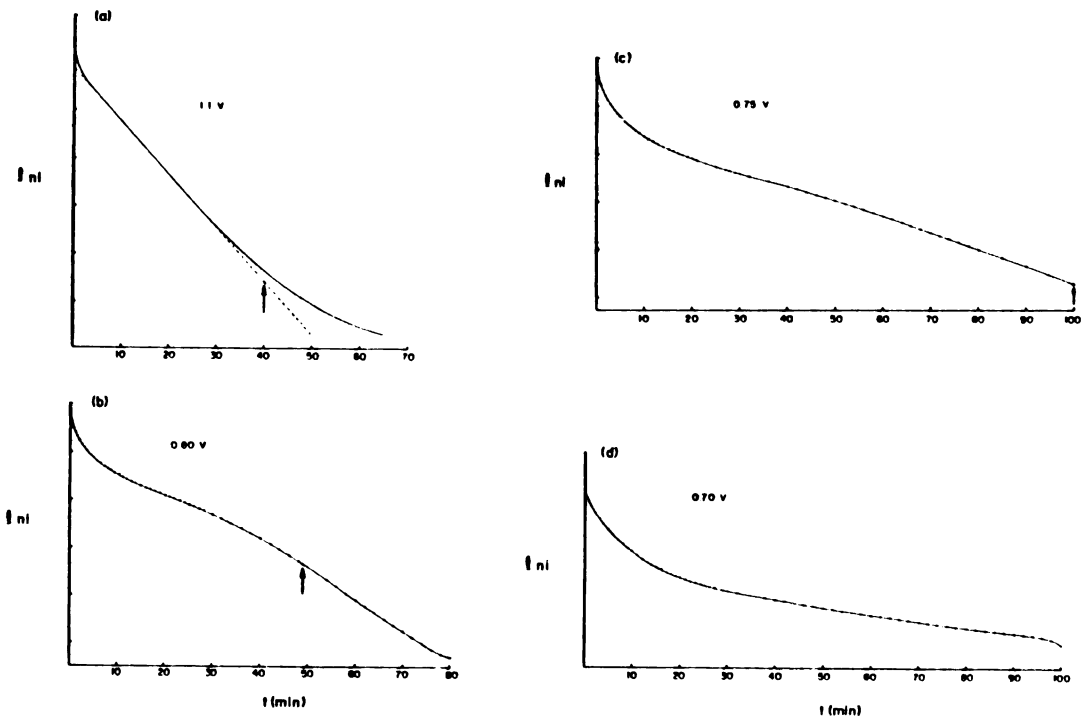

Figure 26. Electrolysis curves of Pl-MeU (as ln i-vs-t plots) at a concentration of 1.4 mM at +1.1, 0.80, 0.75 and 0.70 V vs ssce. The arrow denotes the point at which the electrolysis is judged to be complete (by the color); the electrolysis at 0.70 V was not carried to completion.

The slower rate of oxidation at the three lower potentials is evident from the smaller slopes. While the electrolysis curve at 1.1 V is linear (or nearly so) to the point of completion, the other three are shaped differently, but similarly. Rather than exhibiting concaveness upward, they are concave downward. Is there an explanation for this?

Both Meites (95) and Bard & Santhanam (93), in their reviews of controlled-potential coulometry, report that, depending on the relative magnitudes of the rate constants k_{e1}, k_{e3}, and k_2, consecutive electrode reactions with an intervening chemical step (ece mechanism) can give rise to ln i-vs-t plots which are concave downward. A fundamental paper is due to Gelb and Meites (102). These analyses were made for the case where both electrolytic steps are mass transport limited (103). This is certainly not the case here since the potential has been deliberately reduced below that corresponding to the limiting region. The case where the rate of electron transfer is not mass transport limited appears not to have been worked out. Nevertheless, based on the cited reviews, we might be tempted to conclude that for our system, in which $k_{e3} < k_{e1}$ at the lower potentials (i.e., the second step is slower than the first), an intervening chemical step is required to produce a concave downward ln i-vs-t plot for Pl-MeU. However, since both electrolytic steps are not mass transport limited at the lower potentials, such a conclusion is only speculative. In any event, how the behavior at lower potentials relates to an electrolysis conducted in the limiting

region (i.e., at 1.1 V, which is what is really of interest) where the ee mechanism is assumed to be operative, is unknown, since the extent of dc reversibility was not determined at the lower potentials. (As will be shown shortly, exhaustive oxidative electrolysis at 1.1 V followed by exhaustive reductive electrolysis at -0.1 V returns the system to its initial state, or nearly so.)

Determination of K_{sp} for [P(II,III)1-MeU]$(ClO_4)_3$ - The solubility product constant, K_{sp}, for the reaction $[P(II,III)1\text{-MeU}]^{3+} + 3ClO_4^- \rightleftarrows [P(II,III)1\text{-MeU}](ClO_4)_3$ can be determined by slowly electrolyzing P(II,II)1-MeU, plotting ln i(t) vs t and then noting the point where there is an abrupt change in the slope. A slow electrolysis is achieved by electrolyzing at lower potentials or by decreasing the magnitude of A/V. Only an estimate can be made from the work done here, since, under the electrolysis conditions employed, too few points were recorded prior to the break to permit accurate and precise assignment of the break point. Values of K_{sp} ranging from 4×10^{-7} - 8×10^{-7} were obtained. A K_{sp} in the range of 10^{-7} attests to water solubility sufficient to require special precautions when attempting to isolate small quantities from aqueous solution.

Chemical Reversibility of Precipitation of $[P(II,III)1\text{-MeU}]^{3+}$ with ClO_4^- - It is of interest to study the chemical reversibility of the precipitation of $[P(II,III)1\text{-MeU}]^{3+}$. If our earlier interpretation of the CV's is correct, a potential of +0.4 V vs ssce (see Figure 15,

for example) should be adequate to reverse this process - i.e., to regenerate $[P(II,II)1\text{-MeU}]^{2+}$ from $[P(II,III)1\text{-MeU}]^{3+}$. As a test, P(II,II)1-MeU in perchlorate medium was electrolyzed at 1.1 V until, practically speaking, the electrolysis had come to a halt; $7.392\text{x}10^{-1}$C of charge was passed. At this point the agitated solution was an intense green and was murky, with $[P(II,III)1\text{-MeU}](ClO_4)_3$ having precipitated out. Dropping the potential from +1.1 V to +0.4 V, $3.95\text{x}10^{-1}$C of charge could be passed, with the current being of the opposite sign. During the reversal, the color went from the dark, murky green to a light, murky green. Switching back to +1.1 V, an additional $3.792\text{x}10^{-1}$C was accepted, again with sign reversal. The color was now a decidedly darker green.

This behavior supports the earlier-made contention that the more positive cathodic wave (pc1) in the CV represents $[P(II,III)1\text{-MeU}]^{3+} \xrightarrow{e^-} [P(II,II)1\text{-MeU}]^{2+}$ since at 0.4 V the second cathodic wave (pc2) is barely evident. The fact that not all the precipitate redissolves may suggest the presence of some $[P(III,III)1\text{-MeU}](ClO_4)_4$ co-precipitated, which could interfere with the redissolution of $[P(II,III)1\text{-MeU}](ClO_4)_3$. This suggestion, though, may not be consistent with the observation that, in almost every case, the charge accepted in the oxidation of $[P(II,II)1\text{-MeU}]^{2+}$ was somewhat less than that expected for complete conversion of P(II,II)1-MeU to P(II,III)1-MeU. As three examples of this - where quantitative $1e^-$ transfer required the passage of 0.85 C, 0.70 was

passed; in a second case it was 0.74 out of 0.79 C, and 0.97 out of 1.17 in a third. Actually, as has already been indicated, transfer of the second electron appears to occur at all potentials at which the first electron is transferred, only at a slower rate.

By oxidatively electrolyzing P(II,II)1-MeU at progressively less positive potentials, improved selectivity toward P(II,II)1-MeU→P(II,III)1-MeU, as opposed to complete oxidation to P(III,III)1-MeU, is to be expected. Of course at some point as the potential is decreased the electrolysis becomes prohibitively slow. Electrolyses conducted at +0.75 V vs ssce and above proceeded to completion (i.e., to the P(III,III)1-MeU state) in less than 90 min. At lower potentials, the time required to achieve complete electrolysis was unacceptably long. One of the goals that evolved in this study was to compare the P(II,III)1-MeU/P(III,III)1-MeU selectivity as a function of electrolysis potential, to be determined by sampling the electrolyte periodically throughout an electrolysis and then extracting the P(II,III)1-MeU/P(III,III)1-MeU ratio by liquid chromatography. Unfortunately, it was discovered (surmised) that in the all-metal LC system used, on-column reduction of both P(III,III)1-MeU and P(II,III)1-MeU to P(II,II)1-MeU was occurring (vide infra), hence precluding the study (with the equipment available).

Electrolysis of P1-MeU Coupled with CV. P1-MeU was oxidatively electrolyzed at +1.1 V vs ssce, and CV's recorded at 1/8 intervals throughout the electrolysis. The traces shown in Figure 27 were

obtained.

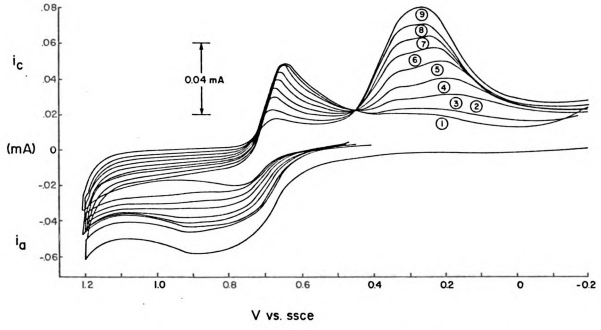

Figure 27. Cyclic voltammograms of Pl-MeU (5.7 mg/6.0 ml, 1.14 mM) recorded throughout an oxidative electrolysis conducted at +1.1 V vs ssce; v = 100 mV/s. Cyclics 2 - 9 were recorded at app. 1/8 increments throughout the electrolysis; 1 was taken prior to the electrolysis.

Upon subsequent reductive electrolysis at -0.1 V, the series of CV's shown in Figure 28 was generated.

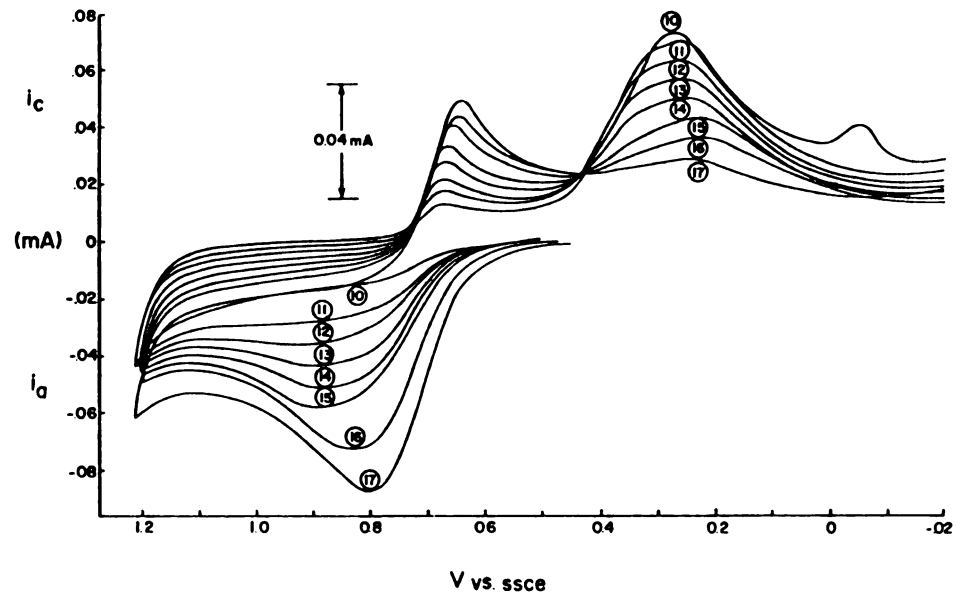

Figure 28. CV's of P1-MeU (5.7 mg/6.0 ml, 1.14 mM) obtained during reductive electrolysis at -0.1 V conducted subsequent to the oxidative electrolysis of Figure 27; v = 100 mV/s. 10 is the CV prior to reductive electrolysis, 17 the CV at the completion of electrolysis.

Trace 1, the CV prior to electrolysis (Figure 27), has the same general shape as those previously discussed. Note that at the potential of sweep initiation (0.40-0.45 V), no fully-electrolyzed material is reduced prior to initiating a scan. The fact that even at the conclusion of the oxidative electrolysis (trace 9) there is yet a small wave for the transition P(II,II)1-MeU $\xrightarrow{-e^-}$ P(II,III)1-MeU probably stems from the thermodynamic instability of the P(III,III)1-MeU state relative to the partially-oxidized, mixed-valent P(II,III)1-MeU intermediate state. At the moment that the electrolysis potential is removed prior to recording a CV, there is some reversion of P(III,III)1-MeU to P(II,III)1-MeU.

As we proceed through the electrolysis (from trace 1 to trace 9), pc2 grows as pc1 subsides. This is consistent with our earlier interpretation of the cyclics. (RDV's were also consistent; for the fully-electrolyzed material, there was no anodic current, but there was cathodic current.) However, for the first time, we notice that, at least in this experiment, pc2 is composed of two (at least) components. Of course this does not necessarily mean that they are the result of two (or more) species. Their separate origin is unknown at this time. Notice that between pc1 and pc2 all CV's pass through a common point at +0.45 V. This "isopotential" point is reminiscent of the isosbestic point in visible or UV spectrophotometry[1]. At the isopotential point the current in each trace is the same as P(II,III)1-MeU reduced to P(II,II)1-MeU diffuses away from the electrode surface. If we disregard trace 10 in Figure 28, the isopotential point defined by the CV's obtained during reductive electrolysis is equally sharp.

---

1. Although not common, isopotential points have been reported on several occasions (104 and references therein). Apparently, they can be diagnostic of surface adsorption or deposition. A theoretical treatment of various surface conditions which can give rise to isopotential points is given by Untereker and Bruckenstein (104). Because a detailed understanding of this manifestation is not central to the discussion at hand, this topic will not be developed here.

The cyclics obtained during reductive electrolysis at -0.1 V (traces 10 - 17 in Figure 28) are not exactly superimposable on their counterparts obtained during oxidative electrolysis. Note particularly the disproportionately large i_{pa1}/i_{pc1} in trace 17 compared with trace 1. The large deviation from $i_{pa}/i_{pc} = 1$ suggests a less reversible system immediately after sequential forward and reverse electrolysis compared to the system prior to electrolysis. It is interesting, though, that upon standing undisturbed in the electrolysis cell overnight, a CV virtually idential to 1 was obtained. The same behavior was noted in the RDV's - that is, the limiting current obtained immediately upon conclusion of the reductive electrolysis was less than that recorded prior to electrolysis, but after standing overnight, the initial and final RDV's nearly overlayed one another. This behavior indicates accompanying chemical changes.

In a separate experiment, exhaustive oxidative electrolysis was followed by exhaustive reductive electrolysis with a single CV taken between the two electrolyses. A total charge of 1.280 C was passed during oxidation and 1.271 C during reduction. Using background values previously obtained, these were corrected to 1.24 C and 1.25 C, respectively. The CV's before, between, and after the electrolyses are shown in Figure 29.

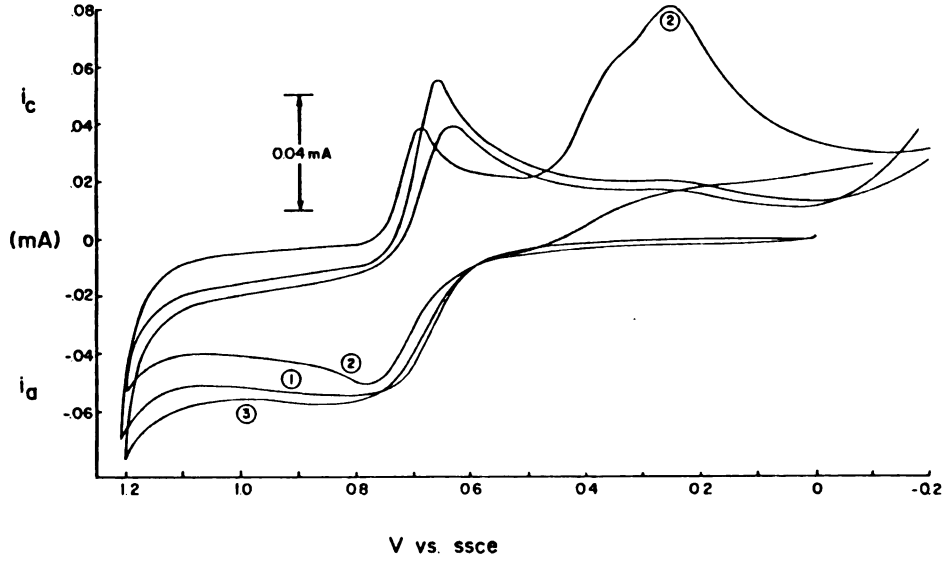

Figure 29. CV's before (1), between (2), and after (3) oxidative and reductive electrolysis of P1-MeU (5.8 mg/6.0 ml, 1.16 mM); v = 100 mV/s.

It is seen that without the disturbances introduced by taking numerous CV's throughout an electrolysis, the initial and final CV's are very similar. CV's of the final electrolysis product, taken as a function of v, exhibited the same behavior as noted previously for unelectrolyzed material. Hence, the system is reversible in a dc electrochemical and chemical sense.

During oxidative electrolysis conducted at 1.1 V, the color proceeded in the fashion colorless → light green → intense green → green-yellow → golden yellow. During the following reduction the color sequence was slightly different: yellow → green-yellow → light green → colorless; the color did not pass through a dark green. The slight difference in the color progressions may furnish further substantiation of the proposed interpretation of the CV's: because the intermediate P(II,III)1-MeU is more readily reduced than

P(III,III)1-MeU, relatively less of the green product is present in solution during the reductive electrolysis at -0.1 V than during the oxidative electrolysis at +1.1 V. An ln i-vs-t plot of the return, reductive electrolysis shows it to follow first-order behavior, just as in oxidative electrolysis. As a final note, the oxidative and reductive electrolyses proceeded at about the same rate at the selected potentials.

CPC of Pl-MeUB. The controlled-potential coulometry of Pl-MeUB is not as well-behaved, and therefore not as straightforward to interpret as that of Pl-MeU. An asymptotic approach for Q(t) vs t was never apparent, even when the electrolysis (oxidative) lasted many hours or even days, although certainly dQ(t)/dt was greatly diminished with time. The lack of an asymptote (after correction for background contributions) means that first-order behavior is absent. Complicating the interpretation in the case of Pl-MeUB is its far greater tendency to adsorb (precipitate) on Pt when compared with Pl-MeU. This tendency was illustrated earlier by RDV.

An example of an electrolysis curve for Pl-MeUB, plotted on two different time scales, is given in Figure 30.

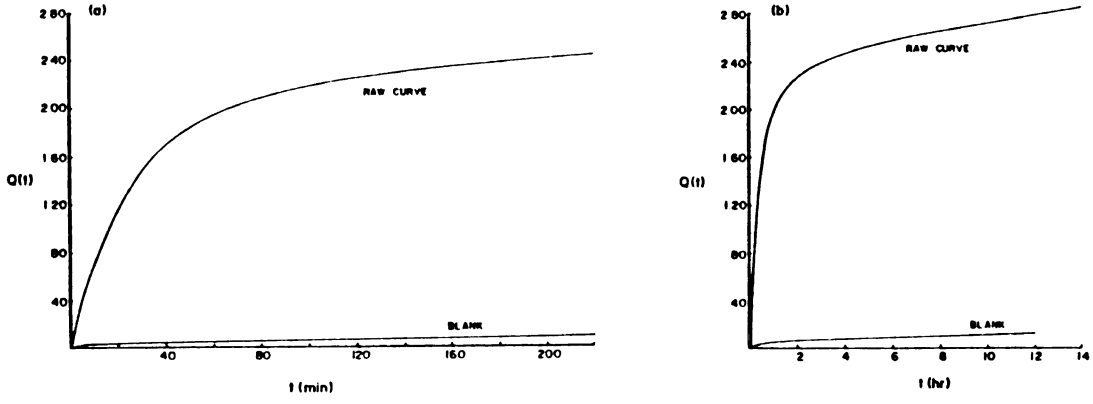

Figure 30. Electrolysis (oxidative) curves for Pl-MeUB (13.25 mg/6.0 ml): a) over ~4 hrs, b) over 14 hrs.

In Figure 30a the electrolysis is shown out to nearly 4 hrs, and in b out to 14 hrs. At all times the slope of the electrolysis curve exceeds the slope of the background (blank) curve. This is equivalent to saying that the current has not diminished to the level of the background. Knowing from earlier studies that Pl-MeUB tends to adsorb on Pt, one might suspect that the effect of adsorption or precipitation is responsible for the nonasymptotic profile. Although RDV experiments demonstrated the greater tendency of Pl-MeUB to adsorb on Pt relative to Pl-MeU, confirmation by CPC was sought.

Adsorption of Pl-MeUB on Pt. In a simple experiment, a Pt wire electrode was immersed to a depth d in an aqueous solution of Pl-MeUB, and an oxidative electrolysis carried out for a time t. The current was noted at time t. The electrode was then lowered an additional distance d. As the current in coulometry is given by $i(t) = nFAmC^{*}(t)$, the current would be expected to double upon lowering

the electrode in accordance with the doubled electrode surface area; that is, in the absence of adsorptive effects. However, if there is an adsorptive coating (or layer of precipitate) on the electrode, which in turn results in a lower potential on the solution side of the interface, then the current, prior to lowering the electrode, will be lower than it would otherwise be. In this case, the current will more than double when the electrode is lowered an additional amount d.

In performing this experiment on Pl-MeU, the current increased by about a factor of 3, depending somewhat on the concentration/surface area ratio. This result demonstrates a susceptibility to adsorption of Pl-MeU on Pt. For Pl-MeUB the current jumped from 13 to 29 times, again showing some dependence on the ratio of concentration to surface area. The comparison, plotted as Q(t) vs t, is shown in Figure 31.

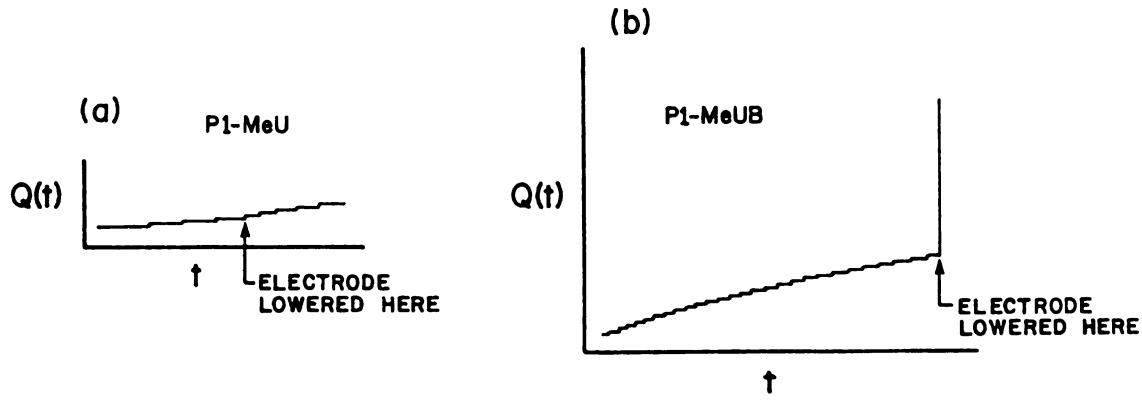

Figure 31. Relative adsorption of a) Pl-MeU and b) Pl-MeUB at Pt. The relative adsorption is gauged by noting the change in slope of the electrolysis curve when an electrode is lowered an additional length d. If there were no adsorptive effect, the instantaneous slope would double.

Clearly there is significant adsorption (or precipitation) of Pl-MeUB on the Pt electrode surface, although this does not necessarily implicate adsorption as the cause of the nonasymptotic profile in the electrolysis curves. This is because, regardless of the extent of adsorption, one would expect that eventually the curves would flatten out.

One approach to gauging the effect of adsorption of Pl-MeUB is to compare electrolysis curves generated over a range of concentrations. The lower the concentration (i.e., the lower C/A is), the less severe the anticipated effect. Electrolysis curves generated at concentrations ranging from 0.048 mg/ml to 5.79 mg/ml are shown in Figure 32. At the lowest concentration (0.048 mg/ml), we see the closest approach to an asymptote in the electrolysis curve, but the uncertainty in the corrected curve may be considerable because of the relatively large magnitude of the background current. Figure 33 shows the relative approach of dQ(t)/dt to background levels at each concentration for periods up to four hours. A similar plot out to as many as 20 hrs shows, likewise, that the background level is never reached.

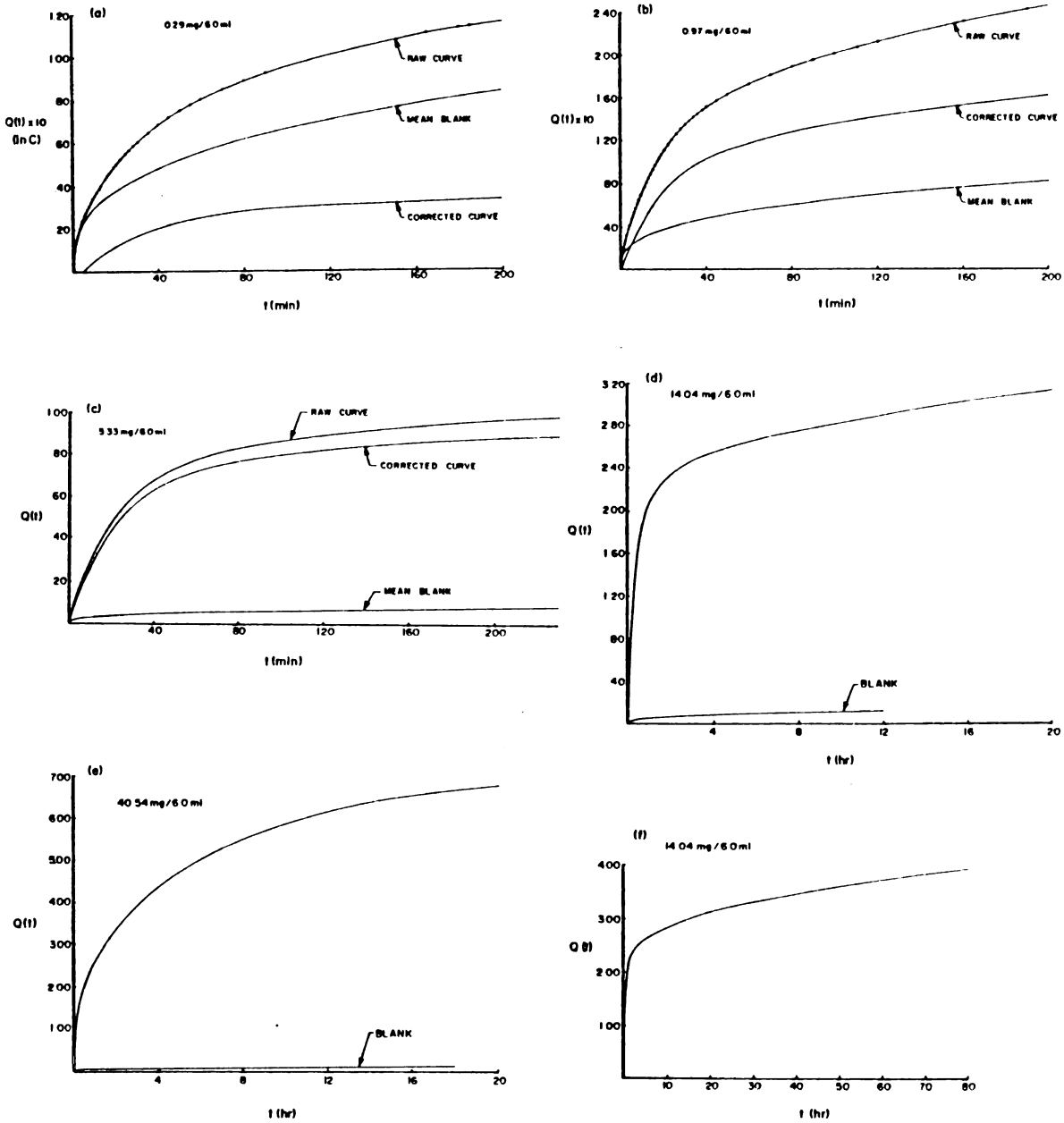

Figure 32. Electrolysis curves of Pl-MeUB generated over the concentration range 0.048 mg/ml to 5.79 mg/ml.

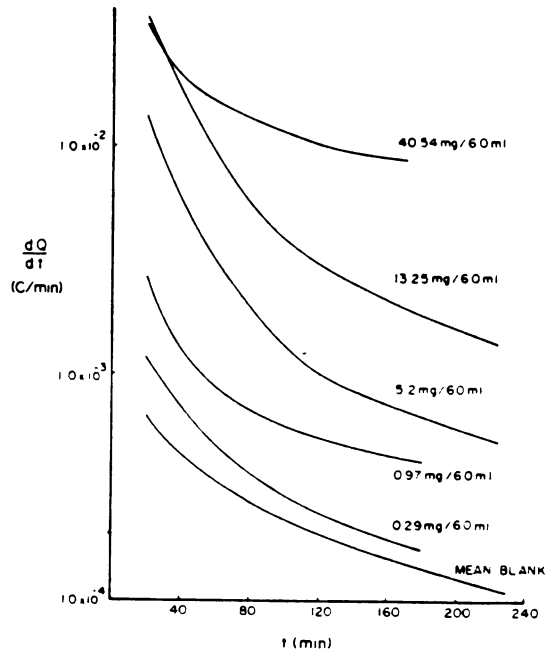

Figure 33. Slopes (dQ/dt) of electrolysis curves of Pl-MeUB and of the blank plotted out to ~4 hrs.

There is, clearly, an effect due to adsorption on the shapes of the Q-vs-t electrolysis curves. However, since all curves exhibit the same general feature - namely, a nonasymptotic profile - it would appear that an interpretation invoking more than adsorption is required to explain the shapes of the curves. There is a caveat to this reasoning, though, and that is that if only a monolayer is required for the inhibiting effect of adsorption to be manifested, and if even at the lowest concentration of 0.29 mg/6.0 ml (0.048 mg/ml) there is a sufficient number of molecules to coat the electrode a monolayer thick, then adsorption could still be the cause of slow electron transfer. Another experimental observation supports the conclusion that the effect of adsorption is relatively less

important: For several different concentrations of Pl-MeUB, at a point when the electrolysis was proceeding very slowly, the electrolysis was interrupted and the electrode ignited to burn off any adsorbed material. Upon resumption, the electrolysis proceeded at the same slow rate in each case. Finally, it bears mentioning that the effect of adsorption is given very short shrift by authors reviewing the field of coulometry. By omission, if for no other reason, readers are led to belive that adsorption is not generally troublesome to accurate and precise coulometry. Other interpretations of the CPC behavior of Pl-MeUB will be considered in the next section.

The ln i-vs-t plots drawn for Pl-MeUB exhibit a central linear region, just as for Pl-MeU. However, the graphical analysis techniques alluded to in conjunction with Pl-MeU may be applied only if the current decay (corrected for background, if necessary) is known to be exponential. If that is the case, the time of electrolysis is independent of concentration (mentioned previously). In the ln i-vs-t plots of Pl-MeUB, when the linear portion is extended to the abscissa (time axis), the point of intersection moves toward longer times with increasing concentration - decidedly nonfirst-order behavior. This may be a manifestation of adsorption, of mechanistic (kinetic) effects, or both. One check on the reasonableness of applying first-order analysis is to compare the ratio of predicted charge (graphical analysis in CPC is known as predictive coulometry) to the ratio of concentrations from separate

experiments. Two comparisons are given: $\frac{5.33 \text{ mg}}{0.97 \text{ mg}} = 5.49$ vs $\frac{0.846 \text{ C}}{0.127 \text{ C}} = 6.66$ (a sizeable blank for 0.97 mg lends some uncertainty to the value 0.127 C) and $\frac{13.25 \text{ mg}}{5.33 \text{ mg}} = 2.48$ vs $\frac{2.17 \text{ C}}{.846 \text{ C}} = 2.56$.

CPC is potentially a powerful tool in the study of the mixed-valence Pl-MeUB because it should allow an assignment of a formal oxidation state of Pt to be made. This may be accomplished by ratioing the charge consumed during oxidative and reductive electrolyses. Also, if the molecular weight distribution or an average molecular weight is known, then n can be calculated. Alternatively, if the charge can be accurately determined, then the combination(s) of n and molecular weight which, through the application of Faraday's law, calculate(s) to the measured charge, can lead to postulations about structure. While (a) combination(s) of n and molecular weight may be obtained by this procedure, this would not be a terribly productive approach since, in actuality, Pl-MeUB consists of a distribution of oligomers.

Further Interpretations of CPC Behavior of Pl-MeUB. The effect of adsorption on the CPC behavior of Pl-MeUB was discussed previously. Other explanations to assist in the interpretation of the electrolysis curves of Pl-MeUB are considered in this section. It was proposed earlier, by analogy, that the anodic wave in the CV of Pl-MeUB arises from the combined oxidation of unknown numbers of Pt(II) to Pt(III). As Pt(IV) is an historically- and much wider-recognized oxidation state for Pt than Pt(III), the possibility of Pt(III) being slowly oxidized to Pt(IV) needs to be considered.

Evidence pertaining to this question was acquired by redox titrimetry and by analogy to the redox and EPR behavior of Pl-MeU, and will be consider later in the appropriate section. Even without that evidence, though, we might predict that since slow, further oxidation does not complicate the CPC behavior of Pl-MeU, we should not expect it to do so for Pl-MeUB; particularly since, judging from the CV's of Pl-MeU and Pl-MeUB, the Pt(III) oxidation state is attained at a slightly more positive potential in the latter than in the former.

One piece of evidence against further oxidation beyond Pt(III) that may pertain and will be presented here, is that as the electrolysis continues at a dawdling pace, there is no further color change. Earlier in the electrolysis the color changes from deep blue-green to a honey brown. This color change is associated, presumably, with the transition from the mixed-valence state to a (largely) Pt(III) state. Oxidation to Pt(IV) may require ligand reorganization about Pt to an octahedral arrangement, which in turn should manifest itself as a change in color since the electronic energy levels of Pt become perturbed. This rearrangement may not be easily accomplished along the constrained, bridged Pt chain.

A more likely explanation for the continuous, slow rise in the electrolysis curve is that not all Pt(II) centers are oxidized to Pt(III) at comparable rates. This is not an unreasonable hypothesis considering the complexity and size of Pl-MeUB, as its stereochemical configuration may pose certain stereoscopic or proximity limitations on the heterogeneous electron transfer. Presently we believe this to

be the predominant cause of the slow electron transfer at long electrolysis times. The postulation of a kinetic complication is supported by the fact that in the slowly rising portion of the electrolysis curve (i.e., at long t), the rate of electrolysis was independent of the rate of stirring.

Mechanistic Treatment of CPC of Pl-MeUB. With reference to the literature, mechanisms are considered in this section which may shed additional light on the interpretation of the electrolysis data for Pl-MeUB. The Pl-MeUB system being considered here is generally more complicated (displays slow kinetics at all accessible potentials) than those which have been treated theoretically. Hence, although this section reviews treatments that relate to the problem at hand, no new interpretation of the CPC behavior of Pl-MeUB is offered in this section. Hence, if the reader so desires, he can move on to the next section with no loss in continuity.

As has been mentioned, the simplest case to treat in controlled-potential coulometry is the nernstian reaction which is mass transport controlled (no kinetic complications), one with no side reactions and with no coupled homogeneous reactions, either preceding or following. If the electrolysis of a nernstian system is not carried out in the limiting region, then the back reaction needs to be considered, although the current still decays in an exponential manner. However, for a process that is irreversible and inherently slow at all potentials, there is no back reaction to consider. In a totally irreversible system, the current also decays exponentially,

but at sufficiently small electrolysis potentials, the potential-dependent rate constant acquires a magnitude where the electrolysis rate is no longer dependent on the stirring rate - i.e., the process is no longer mass transfer controlled. As is always the case in electrochemistry, the quasi-reversible system is the least straightforward to treat; yet it also exhibits first-order behavior, but the rates of both the forward and reverse reactions need to be considered.

While a plot of ln i vs t is linear in each of these cases, this is not necessarily the case for more involved processes where parallel or consecutive electrochemical reactions or those coupled with chemical steps need to be considered. Depending upon the relative magnitudes of the rate constants constituting the several steps, the current-time curves may be perturbed from that of a single electron transfer step. If the rate is the same throughout an electrolysis, then ln i vs t is linear. The best gauge of a complication in an electrolysis is nonlinearity in the ln i-vs-t plot.

Nonfirst-order time dependence arises from the intrusion of slow steps, either electrochemical or chemical. When the apparent value of k_e (in $i = i_o e^{-k_e t}$) decreases as the electrolysis proceeds, the ln i-vs-t plot is concave upward. A very prolonged electrolysis, as is observed for Pl-MeUB, most likely arises from the intrusion of one or more very slow steps, as already discussed. If a slow step is an intervening chemical one, as in $A - n_1e^- \rightarrow B \rightarrow C - n_2e^- \rightarrow D$, that

step would have to be very slow indeed to escape detection by CPC. It is through the variation of the potential, whereby the rates of the two electrochemical steps can be made to vary, while the rate of the chemical step remains invariant, that CPC can prove an elucidative tool.

A number of cases which give rise to nonlinear ln i-vs-t plots are treated by Bard and Santhanam (93) and Meites (95), as previously mentioned. The most common deviation is upward concaveness. Reaction mechanisms giving rise to concave upward ln i-vs-t plots include catalytic reactions, preceding reactions, consecutive reactions, and ece reactions. The case, as apparently represented by Pl-MeUB, for which electron tranfer is slow at all potentials, appears not to have been considered. As more than one mechanism can give rise to the same type of deviation from linearity, CPC does not have the capacity to permit a mechanistic assignment based on ln i-vs-t data alone. Several authors argue that the slope of a ln i-vs-t plot is a more sensitive indicator of a kinetic complication than the current-time curve itself (105, 106).

Several ln i-vs-t plots of Pl-MeUB are given in Figure 34. For Pl-MeUB several mechanisms might be considered: 1) the parallel oxidation of noninteracting sites. (This possibility was raised earlier in the discussion of the cyclic voltammetric behavior of Pl-MeUB.) This situation is representable by

$$\cdots XXR_1XX\cdots \rightarrow \cdots XXO_1XX\cdots + e^-$$

$$\cdots XXR_2XX\cdots \rightarrow \cdots XXO_2XX\cdots + e^-$$

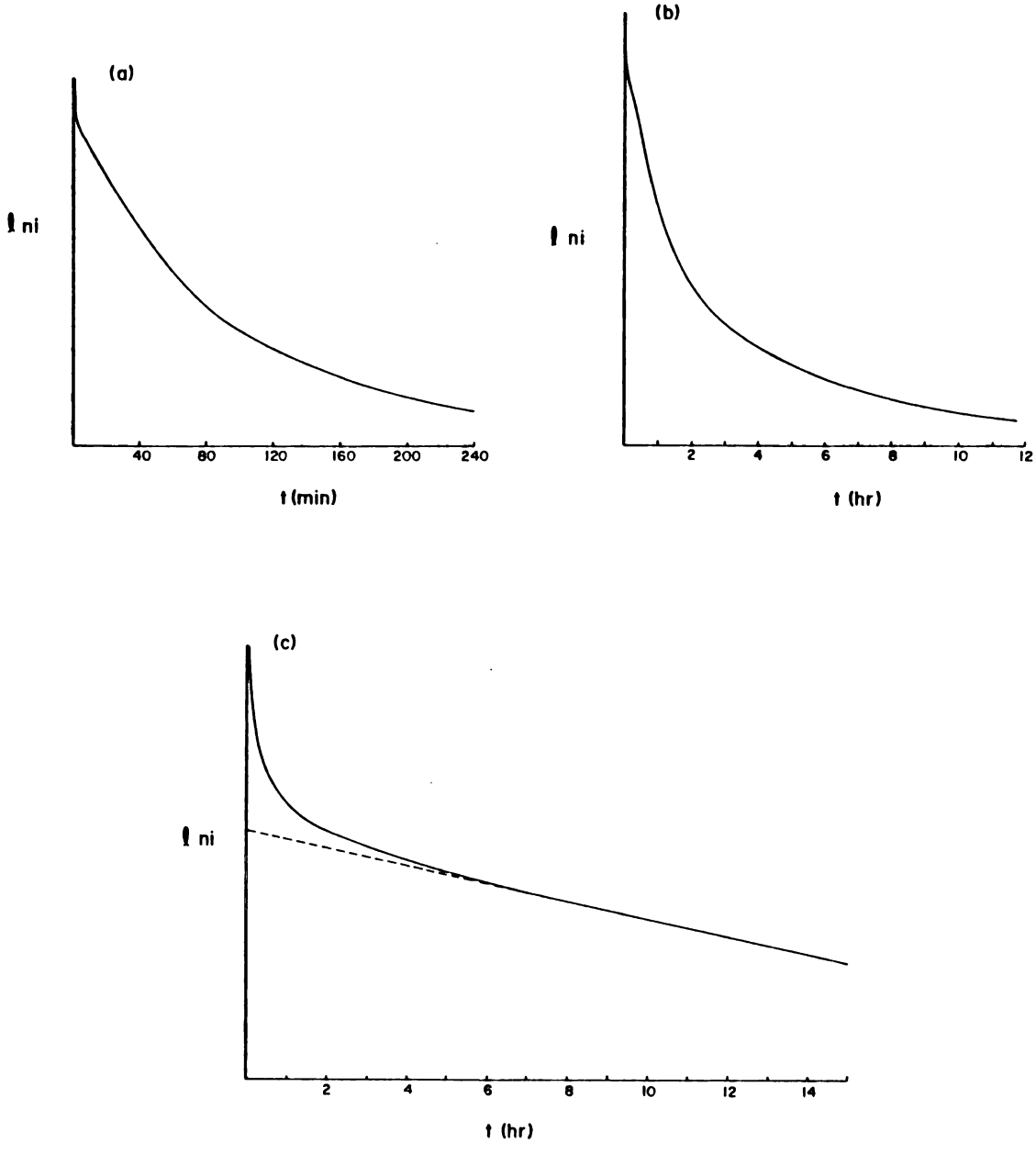

Figure 34. Electrolysis curves of Pl-MeUB plotted as ln i-vs-t: a) 5.33 mg/6.0 ml, b) 13.25 mg/6.0 ml, c) 40.54 mg/7.0 ml.

for two noninteracting centers, and is analogous to the simultaneous oxidation of two chemically unrelated species:

$$R_1 \rightarrow O_1 + e^-$$
$$R_2 \rightarrow O_2 + e^-$$

For the depicted case, where only 2 electrons are transferred, the ln i-vs-t curve can be dissected into two linear segments. Where more than two electrons are involved, only the last segment (and possibly the first) can be dissected. Since the properties of the blues are believed to be due in part to the interaction between platinum centers, this variant of the ee mechanism is not a probable one.

A more probable mechanism involves 2) consecutive electrode reactions, also an ee mechanism:

$R \rightarrow I_1 + n_1e^-$ where I is an intermediate,

$I_1 \rightarrow I_2 + n_2e^-$

$\vdots$

$I_{n-1} \rightarrow O + n_ne^-$

In principle, if the potential is sufficiently negative, the ln i-vs-t curve can be dissected as above for the $2e^-$ case. Where there are many consecutive steps, this is not possible. When a second or subsequent electron transfer is sufficiently slow so that intermediate I can diffuse away from the electrode, the situation can be likened to an ece (or ...ece...) mechanism. Expressions for current have been derived for the case where all reactions are in the mass transport controlled region and a) the process is nernstian or

b) the process is totally irreversible (for a two-step mechanism) (93). To the author's knowledge, a treatment has not been given for quasi-reversible reactions.

A mechanism involving 3) consecutive reactions at interacting Pt sites with intervening chemical reactions cannot be ruled out for Pl-MeUB. In the simplest case, this is an ece mechanism. One possibility might be disproportionation leading to a redistribution of oligomeric species. With an intervening chemical step between each electron transfer, the mechanism expands to ecece.... The shape of an ln (i_t/i_o)-vs-$k_e t$ plot for an ece mechanism, where k_e is the apparent rate constant for the electrolysis, depends on the value of k/k_e, where k is the rate constant for the chemical step. For k/k_e = 0.01 ($k_e = k_{e1} = k_{e2}$), the plot is concave upward.

The ln i-vs-t plots in Figures 34a and b exhibit a linear portion through the first hour or so. During this portion of the electrolysis, those Pt centers for which electron transfer is most facile dominate the electrolysis. At the end of 4 hrs the curves are curved upward at all concentrations. It is unclear, because of a lack of data points, whether or not the final portion of the curve in Figure 34b is also linear. In Figure 34c it may be after 6 hrs or so, although more data points would have better defined the curve. (At the very high concentration of 40.5 mg/7.0 ml (c), the current due to background is at all times negligible.) Linear or not, the most reasonable interpretation is that more difficultly oxidizable Pt centers are giving up electrons to the electrode during the latter

stages of electrolysis. This is simply to repeat our earlier interpretation. If one assumes linearity after 6 hrs in Figure 34c, then first-order analysis, as used previously, may be applied. When done, the fact that a figure was obtained for Q_∞ well under that which was accumulated during 21 hrs of electrolysis, strongly suggests that additional "reluctant" Pt centers continue to very slowly transfer electrons to the electrode. Recalling once again the mixed polymeric nature of this platinum pyrimidine blue, this is not surprising. The effect of elevated temperature on the shape of the electrolysis curve was not studied.

A few additional comments are in order before leaving this topic. After concluding this work, the author encountered several articles dealing with the electron transfer properties of large biological molecules, compounds which may exhibit intolerably slow electron transfer kinetics (for example, see refs. 107, 108). Thin-layer cells have been found to be useful in a number of these studies. Thin-layer cells have the advantages of speed and simplicity, and are generally free of complicating secondary reactions between electrode reaction products and parent reactants (109). The need for suitable electrochemical methods for the study of kinetically-limited biomolecules has spurred development in thin-layer spectroelectrochemistry (107, 110, 111), applicable to molecules containing the requisite chromophores; in spectroelectrochemistry, electrochemical and spectral measurements are combined, often on short-lived species. In some cases, indirect,

coulometric titration through the use of so-called mediator titrants has been found to be useful in the facilitation of electron transfer between the redox system and the electrode (107, 108).

In a study on a not-so-large molecule - hypoxanthine - behavior not unlike that observed for platinum 1-methyluracil blue in this study was reported (112).

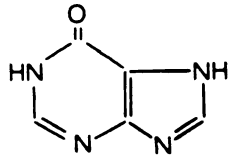

Hypoxanthine
(6-hydroxypurine)

Using a normal electrolysis cell, electrolyses were reported to take more than 12 hrs to reach completion. A quite positive electrolysis potential was used, and a large background correction was required. The authors stressed that the n-value, which was determined to be ~6e, "should be regarded as approximate". In contrast, with a thin-layer cell, the electrolyses were complete within 15 min; a value of n = 4 was obtained. In attempting to reconcile the apparent discrepancy, the authors concluded that "some form of slow chemical and/or electrochemical reaction follows the initial 4e transfer".

Calculation of Valence of Pt in Pl-MeUB. It was mentioned earlier that, in principle, by comparing the charge accumulated during oxidative and reductive electrolyses, an average formal oxidation

state may be assigned to Pt. We now know that for Pl-MeUB it has not been possible to reliably determine Q_∞. As the curves in Figure 35 reveal, a reductive electrolysis behaves like an oxidative one, except that the current (and charge) is considerably lower, a reflection of an average formal oxidation state considerably closer to 2 than to 3.

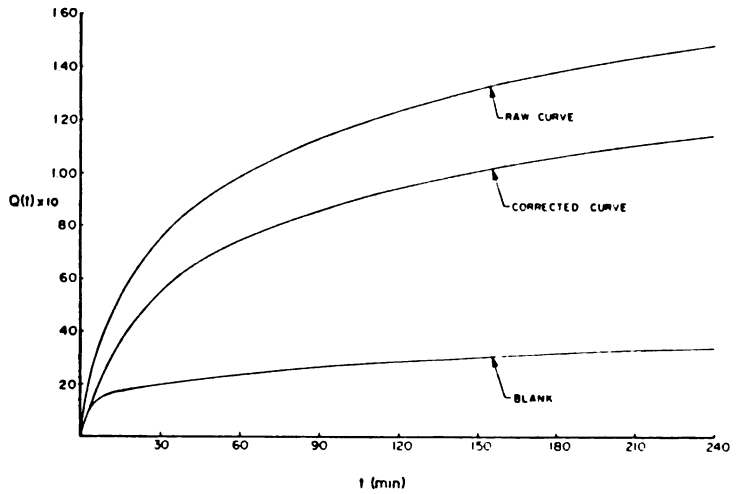

Figure 35. Reductive electrolysis curve for Pl-MeUB conducted at -0.1 V vs ssce.

If we can assume that the shapes of the oxidative and reductive electrolysis curves for Pl-MeUB are similar because of the same underlying kinetic factors, then first-order graphical analysis applied to the early, linear portion of the ln i-vs-t plots should apply. (Actually, we know from earlier-discussed work that the situation is not quite the same at the oxidative (+1.1 V) and reductive (-0.1 V) potentials used, since the cyclic voltammograms exhibit a small current at the latter potential due (presumably) to the slow reduction of the ligand groups.)

When first-order graphical analysis was applied, values of Q_{oxid} = 0.846 C and Q_{red} = 0.0775 C were obtained for a solution containing 5.32 mg of Pl-MeUB. Then

$$\frac{Pt(II)}{Pt(III)} = \frac{0.846}{0.0755} = 10.9 \rightarrow 11$$

This means that, on average, one Pt in 12 is in the +3 valence state, so that the average formal oxidation state of platinum in platinum 1-methyluracil blue is 2.08. This agrees with the range of 2.08 $\pm$ 0.15 reported for platinum uracil blue (PUB) by Lippard et al. (18). Apparently, the perturbation of a substituted nitrogen (Pl-MeUB vis-a-vis PUB) has no effect on the extent of mixed-valency. This would have been difficult to predict since the bonding possibilities are greater for PUB than for Pl-MeUB.

Electrolysis of Pl-MeUB Coupled with CV. Cyclic voltammograms of Pl-MeUB were recorded at ~1/8 intervals throughout an exhaustive, oxidative electrolysis conducted at +1.1 V vs ssce and again during a subsequent exhaustive, reductive electrolysis at -0.1 V. As a precaution, because of the greater adsorptiveness of Pl-MeUB on platinum, the working electrode was ignited between oxidative and reductive electrolyses. The CV's obtained during the oxidation cycle are shown in Figure 36. Those obtained during the reduction cycle are shown in Figure 37.

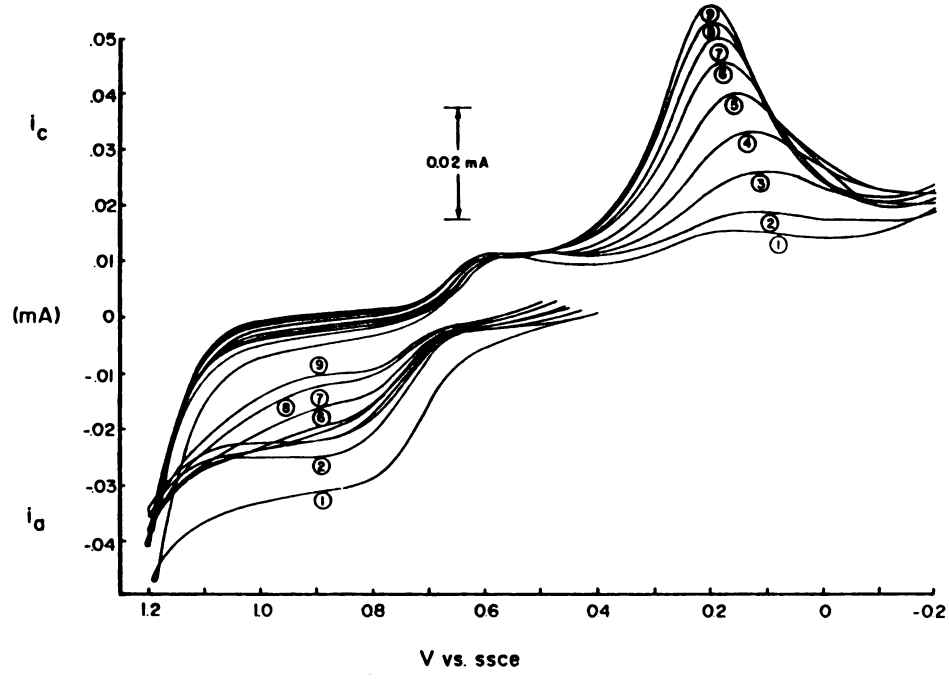

Figure 36. Cyclic voltammograms of Pl-MeUB (5.4 mg/6.0 ml) recorded throughout an oxidative electrolysis conducted at +1.1 V vs ssce. Cyclics 2 - 9 were recorded at ~1/8 increments throughout the electrolysis; 1 is the CV prior to electrolysis.

Comparison of these CV's with those of Pl-MeU and Pl-MeUB obtained as a function of v (Figures 12 and 16, respectively) and with those of Pl-MeU obtained during exhaustive, oxidative and reductive electrolysis (Figures 27 and 28, respectively), allows us to expand upon our earlier interpretation of the cyclic voltammetric behavior of Pl-MeUB.

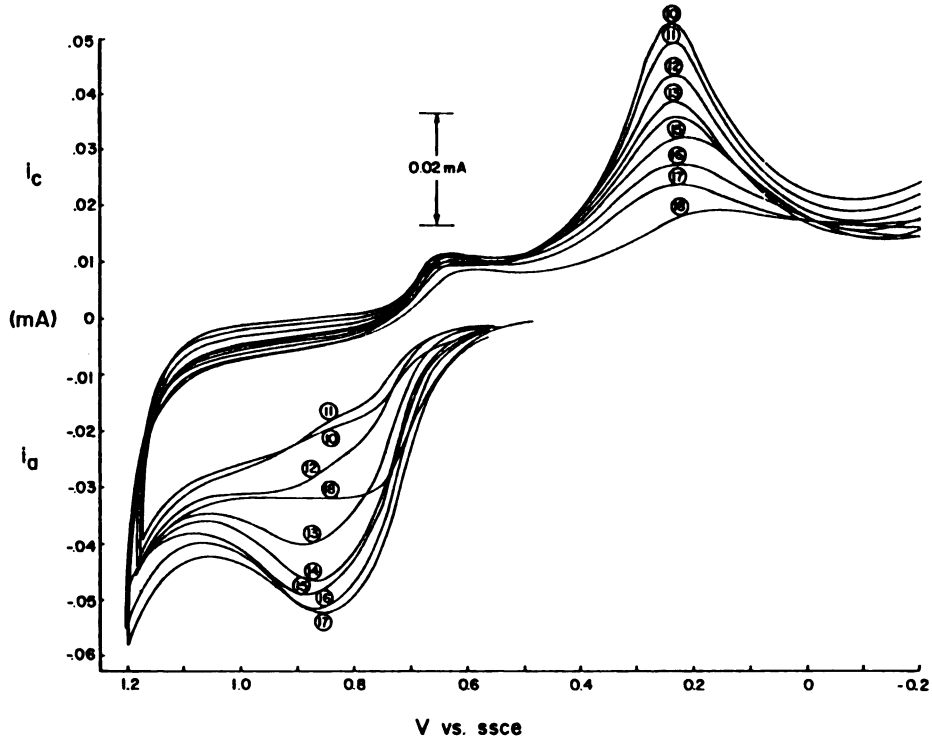

Figure 37. CV's of Pl-MeUB (5.4 mg/6.0 ml) obtained during reductive electrolysis conducted at -0.1 V subsequent to the oxidative electrolysis of Figure 36. 10 was taken prior to reductive electrolysis, 17 is the CV at the conclusion of the electrolysis, and 18 is the CV after standing overnight.

As the electrolysis proceeds, i_{pc1} falls, although the effect is less pronounced than for Pl-MeU. pc1 derives from the presence of Pl-MeU impurity (shown by LC) and perhaps in part from one or two Pt atoms in Pl-MeUB, those which are most easily reduced, but more likely from the former. As previously noted for Pl-MeUB, the anodic peak occurs at more positive potentials than for Pl-MeU. This simply means that the large majority of the electrons in the polymer are not as readily transferred as the first in Pl-MeU. This, presumably, is a result of the stability accorded the Pt atoms through interaction along the polymeric chain. Again we see the growth in pc2 as the

electrolysis proceeds, but the effect is greater for Pl-MeUB than for Pl-MeU (see Figure 27). Interestingly, E_{pc2} moves inward (toward more positive potentials) rather than outward. This inward shift may be the result of competition between two (or more) components which together constitute pc2. (This was the case for Pl-MeU; see Figure 27.) Indeed, the last Pt centers to be oxidized (those most difficultly oxidizable) are the first to be reduced (perhaps because of more positive $E^{o'}$s and/or because smaller overpotentials are required). Overall, E_{pc2} is slightly less positive (by ~0.1 V) than for Pl-MeU, a manifestation of the greater irreversibility of the platinum blue. This is a reflection of slow steps in the electron transfer process. For this more complex system, there is no isopotential point. The color sequence during oxidation follows the pattern deep blue-green → dark green → green-brown → brown-green → brown → honey brown.

CV's 10 - 18 in Figure 37 chart the course of the subsequent reductive electrolysis. Similar to the situation previously noted for Pl-MeU, i_{pa}/i_{pc1} grows to about twice the value it had prior to electrolysis (trace 1). Trace 18 is the CV after the solution stood overnight undisturbed (no deaerating gas flowing), and matches quite well the CV obtained prior to electrolysis. This behavior is very similar to that observed earlier for Pl-MeU, and again implicates an accompanying chemical change. Also as before, the initial RDV and that obtained after the overnight period matched very well (not shown). There was no cathodic current apparent in the RDV's except

in the oxidized material, and in that case, there was no plateau, only a slowly rising current beginning at about 0.7 V and proceeding to the cathodic limit on Pt.

Although what follows is sheer speculation, perhaps upon reduction there is some disproportionation of the polymeric platinum blue, thus generating smaller fragments which diffuse more rapidly, thereby contributing a larger i_{pa}. Upon standing, an equilibrium distribution may reassert itself, a condition manifested in similar (but not identical) initial and final CV's. However, since Pl-MeU exhibits similar behavior, and since disproportionation is a less likely prospect there, perhaps another explanation begs.

Close inspection of the initial and final CV's for Pl-MeUB (trace 1 in Figure 36 and trace 18 in Figure 37) reveals that, while the reversibility (in a chemical sense) is considerable, it is lower for this complex system than for the simpler Pl-MeU. That is, the initial and final CV's match less well for Pl-MeUB than for Pl-MeU. This is no surprise. What is perhaps surprising is that a system that reflects such a high degree of irreversibility in its CV's can, in fact, be reversed by electrolysis to the extent that it can. As comparison of Figure 38 with Figure 16 attests, the final electrolysis product of Pl-MeUB after sequential, exhaustive oxidative and reductive eletrolysis is not identical to the starting material.

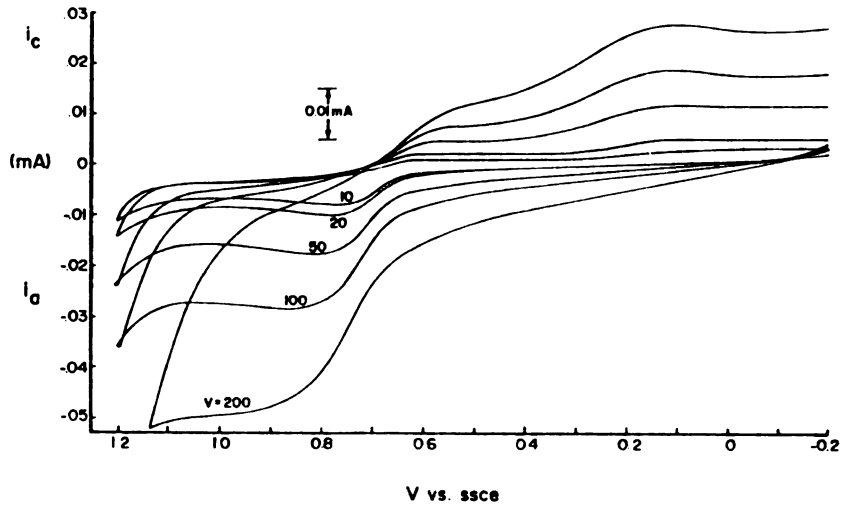

Figure 38. CV's of Pl-MeUB (5.4 mg/6.0 ml) as a function of v after sequential oxidative and reductive electrolysis. These may be compared with the CV's in Figure 16.

Based on the greater predominance of pc2 after the sequential electrolyses, it appears that not all of the Pt atoms oxidized to Pt(III) are reduced back to Pt(II). Perhaps more light could have been shed on the reversibility of the Pl-MeUB system by making use of reversal coulometry at progressively lower potentials. The color sequence upon reduction of the oxidized material follows the order honey brown → brown-green → dark green → green-blue, although the final green-blue is lighter than the original, more like that observed when Pl-MeUB is reduced directly.

In a separate experiment in which an exhaustive, oxidative electrolysis (conducted for 4 hrs) was followed by exhaustive, reductive electrolysis (also for 4 hrs), 0.89 C of charge was passed during oxidation (after correcting for the blank contribution) and 0.85 C during reduction. (The electrode was not ignited between electrolyses; it is not necessary to do so.) Again, it was only

after the solution stood overnight that the final CV approximated the initial CV. Recall that when this same experiment was performed on Pl-MeU, an overnight, quiescent period was not required for the initial and final CV's to match.

Summary of Electrochemical Findings -

The primary techniques used to characterize the redox behavior of the dimer Pl-MeU, the polymer Pl-MeUB, and several related compounds consisted of cyclic voltammetry (CV), rotating disk voltammetry (RDV), and controlled-potential coulometry (CPC). CV at platinum revealed a scan rate dependence for Pl-MeU, with a second electron transfer becoming increasingly competitive at higher sweep rates. This behavior was attributed to 1) the convective influence of a dense intermediate (P(II,III)l-MeU) and to 2) adsorption (or precipitation) of the intermediate on the electrode surface. The outer cathodic and anodic peaks were shown to correlate with one another, as were the inner peaks. The first electron transfer is somewhat irreversible, whereas the second is highly irreversible. The CV's were accounted for by postulating the transitions Pt(II)Pt(II) $\rightarrow$ Pt(II)Pt(III) $\rightarrow$ Pt(III)Pt(III). On average, the number of electrons transferred during a scan was between 1 and 2, with 1 being approached at the lowest scan rates and 2 at the highest rates. Supportive evidence for a fluctuating n was obtained by RDV.

The CV's of Pl-MeUB are similar to those of Pl-MeU, but are less well delineated, a reflection of the greater complexity of the polymeric blue. Separation between cathodic and anodic peaks is

greater, implying a less reversible system. Interestingly, the CV's of aged solutions of Pl-MeU resemble closely the CV's of Pl-MeUB. As was done for Pl-MeU, the platinum III state was also invoked to explain the CV behavior of Pl-MeUB. Neither platinum benzoate blue (PBzB) nor platinum phthalate blue (PPhB), two blues in which Pt is coordinated through carboxylate oxygens, is electroactive at a platinum electrode. Contrastingly, both PBzB and PPhB in which ammine ligands were replaced by Cl, exhibited electroactivity at Pt. All compounds examined displayed irreversible behavior at mercury at the most negative potentials.

Adsorption or precipitation of Pl-MeUB on platinum is particularly acute. This was studied by both RDV and CPC. This coating of the electrode proved to be problematic in the CPC study of Pl-MeUB. Unlike the Pl-MeU dimer, which exhibited first-order kinetics by CPC (n=2), Pl-MeUB was decidedly nonfirst order, displaying a prolonged (seemingly endless) asymptotic profile in its Q-t curve. Consequently, a value for Q_∞ could not be obtained. Sluggish kinetics arising from less-accessible platinum sites in the Pl-MeUB polymeric chain is believed to be at least as important as adsorption in determining the shapes of the electrolysis curves. Cyclic voltammograms recorded at regular intervals throughout sequential, exhaustive, oxidative and reductive electrolysis of both Pl-MeU and Pl-MeUB revealed a considerable degree of <u>chemical</u> reversibility in both cases, somewhat surprising considering the high degree of irreversibility of their cyclic voltammograms, and perhaps

even unexpected for the polymer considering its far greater complexity.

Through the use of the Stokes-Einstein equation and by making certain assumptions, an estimate of the molecular weight for Pl-MeUB in solution was made. Unfortunately, the uncertainty in the calculated value is high because the "effective" number of electrons transferred, on average, per monomeric unit in an RDV experiment, a number required to make the molecular weight estimation, is also uncertain. A result of fundamental significance is the calculation of the average formal oxidation state of platinum in the mixed-valence blue; a value of 2.08 was obtained. This calcultion relies on first-order behavior in the early portion of both the oxidative and reductive electrolysis curves.

Redox Titrimetry - Oxidative Titrations Using Ce(IV)

Redox titrimetry was used to study several questions. Controlled-potential, oxidative electrolysis of Pl-MeU showed that two electrons are transferred per molecule - i.e., n = 2. Starting from P(II,II)1-MeU, this means that either P(III,III)1-MeU or P(II,IV)1-MeU (or P(II,IV)1-MeU $\leftrightarrow$ P(IV,II)1-MeU) is the end product. Arguments have already been advanced (and will later be expanded upon) for the former, P(III,III)1-MeU. Regardless of its form, the question arises, can further oxidation to the Pt(IV)-Pt(IV) state be effected?

As regards Pl-MeUB, there were several questions to be addressed: 1) can an equivalence point be identified for this mixed-valence,

polymeric system? 2) if so, knowing the percent Pt composition, what are the possible average formal oxidation states that account for the titration data? 3) if an equivalence point is discernible, and if it can also be presumed to correspond to all Pt(III), can further oxidation to Pt(IV)l-MeUB be effected? Finally, several additional compounds were titrated to acquire more information about blues and related compounds (recall the recording of cyclic voltammograms of related compounds presented earlier).

Ce(IV) is a frequent oxidant of choice in redox titrimetry. Among its attributes are high oxidizing strength, which is somewhat medium dependent, and a simple stoichiometry - Ce(IV) + e^- → Ce(III). In the present work, Ce(IV) solutions were prepared in 1N H_2SO_4. $E^{o'}$, the formal potential is +1.44 V vs the nhe in 1N H_2SO_4 or 1.20 V vs the ssce. While a direct comparison of a cerium titration with a controlled-potential electrolysis is not possible since the $E^{o'}$s of Pl-MeU and Pl-MeUB are not precisely known, and since the potential of the Ce/Pl-MeU/Pt or Ce/Pl-MeUB/Pt system changes as the titration progresses, nevertheless, we can be sure that $E^{o'}$ = 1.20 > 1.10 (the potential used in the electrolyses) provides adequate oxidizing strength to address in a meaningful way the questions posed above.

The most satisfactory results were obtained when 1N HCl was used to dissolve the sample. Chloride is required to prevent the redox reaction from being prohibitively slow, particularly in the vicinity of the end point; it may act by serving as a bridge between the

oxidant and the reductant. It may also be that the response of the potentiometric indicator electrode (Pt) is facilitated by chloride bridging. (If this is so, perhaps the CV's could be altered in the presence of low concentrations of Cl^-.) In the literature review presented earlier it was mentioneed that some workers conducted titrations in 4.5N HCl. The present author found this to be wholly unsatisfactory, as consistently high (i.e., excessive Ce(IV) titrant was consumed) values were obtained on model compounds, presumably because some Cl^- was oxidized by the cerium. Additionally, the titration curves exhibited anamolous behavior, displaying dips. As will be made apparent shortly, 1N HCl also makes a contribution to the blank, albeit a smaller one, but a concentration of 1N provides a suitable compromise between speed and accuracy. If the reaction rate is too slow, the end point cannot be precisely discerned.

Prior to conducting the redox titrations, cyclic voltammograms were recorded for each compound to evaluate stabilities in acid media. (Cerium titrations must be conducted in a fairly concentrated acidic medium; see, for example, ref. 113.) Both sulfuric and hydrochloric acid were used in the titrations, but only the former could be used to assess stabilities at a Pt electrode since Cl^- was oxidized at the most positive potentials needed to record the CV's. Since sulfuric is the more strongly-oxidizing of the two acids, its use alone sufficed in assessing by CV resistance to acid-catalyzed decomposition. Neither nitric ($E^{o'}$ of 1.61 V for Ce(IV) in 1N HNO_3) nor perchloric ($E^{o'}$ of 1.70 V in 1N HC104) acid was suitable for the

titration because each led to partial oxidation of the platinum dimer in the absence of Ce oxidant. Cyclic voltammograms of both the dimer and platinum blue were stable over the course of an hour in 5N H_2SO_4, although the response (current) was depressed somewhat relative to lower concentrations. Because 5N solutions gave low results for the test compound cis-$Pt(NH_3)_2Cl_2$ in a titration (due, presumably, to slow oxidation by the sulfuric acid), a concentration of 1N H_2SO_4 for the Ce titrant was settled upon.

As the presence of acid extends the anodic range on platinum, it was of interest to note whether by cyclic voltammetry an additional wave or waves corresponding to complete oxidation of Pt would appear. In neither $HClO_4$ nor H_2SO_4, at concentrations to 1.0N in the former and 5.0N in the latter, was there any indication of further oxidation of Pl-MeU. Perhaps significant, no green intermediate was observable in 1.0N $HClO_4$, although it was observable at a 5.0N concentration in H_2SO_4. This suggests decomposition in $HClO_4$; there was no precipitation of any decomposition product. In general, there were enough bulges in the CV's due to acid alone, whatever the acid, that attempted complete interpretation would not be a profitable (nor germane) exercise.

The accuracy and precision of the adopted titration procedure was gauged by titrating cis-platinum - cis-$Pt(NH_3)_2Cl_2$ - purported to be >99% pure (114). While it does not necessarily follow that the accuracy and precision obtained on a known, well-behaved system will translate to an unstudied system, particularly one where kinetic

complications may obtain, it does indicate the best that can be expected. Titrations were conducted on 1.0 ml of titrand using a microliter syringe as the titrant dispenser; slightly more than 500 μL of titrant was required. The titration was followed potentiometrically using a Pt electrode. The results of the study are compiled in Table 4. A sample titration curve is presented in Figure 39.

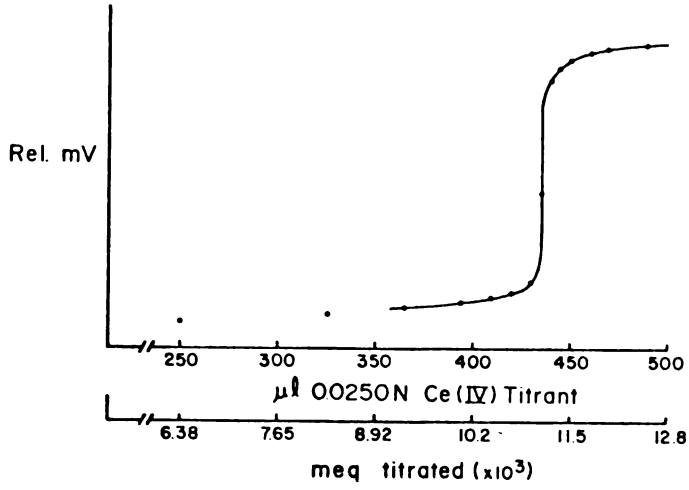

Figure 39. A titration curve for the Ce(IV) titration of <u>cis</u>-$Pt(NH_3)_2Cl_2$.

Conclusion: Either 1N or 2N HCl provides the best choice. Choice: All subsequent titrations were conducted with 0.0250N Ce in 1N H_2SO_4 as titrant and with the analyte dissolved in 1.0 ml of 1N HCl.

Table 4
Precision Study on cis-Pt

Run #	Titrand	Titrant	% Rel. Error	Mean Rel. Error
1	1.53 mg in 1 ml 1N HCl (5.10 mM)	0.02005 N Ce in 1N H_2SO_4	+11.1	
2	1.53 mg in 1 ml 1N HCl (5.10 mM)	0.02005 N Ce in 1N H_2SO_4	+11.8	10.9 ± 1.0
3	1.53 mg in 1 ml 1N HCl (5.10 mM)	0.02005 N Ce in 1N H_2SO_4	+9.8	
4	5.10 mM in 1N HCl	0.03024 N Ce	+7.2	
5	5.10 mM in 1N HCl	0.03024 N Ce	+10.4	8.7 ± 1.6
6	5.10 mM in 1N HCl	0.03024 N Ce	+8.5	
7	5.10 mM in 1N HCl	0.04004 N Ce	+12.4	12.1
8	5.10 mM in 1N HCl	0.04004 N Ce	+11.8	
9	5.00 mM in {0.4N HCl, 0.6N H_2SO_4}	0.02020 N Ce	+11.3[1]	
10	5.00 mM in {0.4N HCl, 0.6N H_2SO_4}	0.03024 N Ce	+11.3	
11	5.10 mM in 2N HCl	0.02550 N Ce	+7.2	
12	5.10 mM in 2N HCl	0.02550 N Ce	+7.8	7.5 ± 0.8
13	5.10 mM in 2N HCl	0.02550 N Ce	+6.5	
14	5.10 mM in 2N HCl	0.02550 N Ce	+8.5	
15	5.20 mM in 2N HCl	0.02550 N Ce	+7.0	
16	5.20 mM in 2N HCl	0.02550 N Ce	+6.4	7.0 ± 0.4
17	5.20 mM in 2N HCl	0.02550 N Ce	+7.4	
18	5.20 mM in 2N HCl	0.02550 N Ce	+7.0	
19	5.80 mM in 4.5N HCl	0.02550 N Ce	+17.2	
20	5.80 mM in 4.5N HCl	0.02550 N Ce	+2.9[2]	
21	5.80 mM in 4.5N HCl	0.02550 N Ce	-[3]	

[1] too slow to be practical, especially near the end point; even though the error arising from the oxidation of Cl^- should be lower, the uncertainty of the end point due to slow kinetics leads to low accuracy.

[2] too few points taken near the end point to be certain of this number

[3] erratic behavior in the vicinity of the end point

Titration of Pl-MeU -

Between 2.8 and 4.2 mg (3.4-5.0 mM) of the platinum dimer was titrated. A titration curve obtained early in this work is shown in Figure 40a. The "eyeballed" end point for this titration is 10% high, slightly higher than that obtained in the previous study on cis-platinum. LC (to be discussed later) revealed little in the way of impurities and/or hydrolysis products for the freshly-prepared solution. However, mononuclear platinum-containing impurities or hydrolysates would contribute to a high value since each platinum would react with 2 moles of Ce in going from Pt(II) to Pt(IV) as compared to only a univalent change (Pt(II) → Pt(III)) for each platinum in the dimer (vide infra). The second inflection point at 545 μL in Figure 40a is an anamoly, caused by an abrupt, unexplained shift in potential. A typical titration curve from a set of four generated nearly six months after that of Figure 40a is shown in 40b. The titration shown in Figure 40b was conducted on a freshly-prepared solution, as was that in a. It was the solid material that had stood for an additional six months, not a solution. The solid dimer had been synthesized approximately one year prior to obtaining the curve in a.

While a calculation of the percent positive error in the titration depicted in Figure 40a follows directly from a comparison of the number of mequiv titrated with the number of mgm weighed, in b the calculation has to account for that (those) compound(s) giving rise to the sharp inflection at 302 μL. That the first break at 276

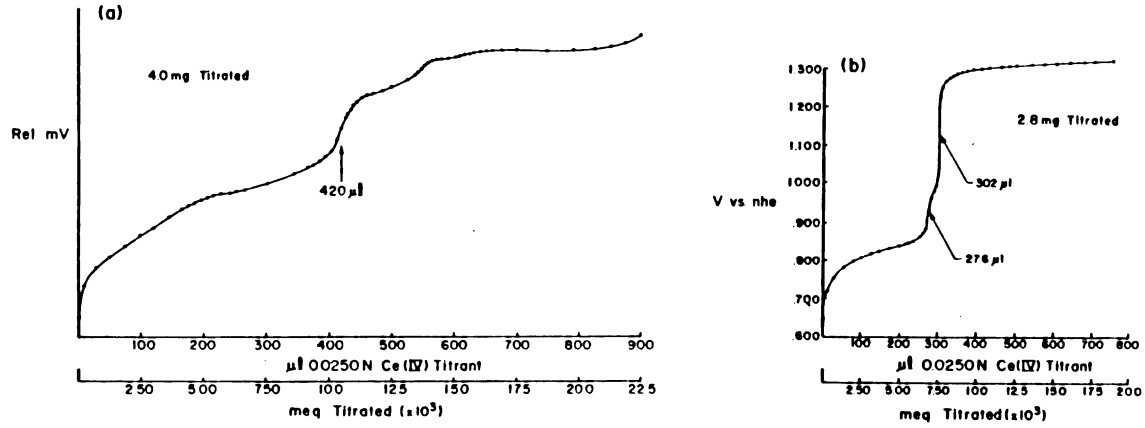

Figure 40. Titration curves for the titration of platinum(II) 1-methyluracil (Pl-MeU) with Ce(IV) taken nearly six months apart. Plot a) was drawn from readings made on the mV scale of a pH meter, while b), generated six months after a), was obtained using a high input impedance digital voltmeter.

µL is, in fact, due to the dimer, and not the second, follows by analogy to the curve in a, but more convincing evidence is provided by an abrupt change in color to a golden yellow (the color observed for the fully-electrolyzed material by CPC) observed to coincide with the inflection at 276 µL. The abruptness of the second shift is typical of a Pt(II) $\xrightarrow{-2e^-}$ Pt(IV) transition, as typically seen in mononuclear Pt compounds. An example is afforded by the titration curve of the related compound <u>cis</u>-$Pt(NH_3)_2(1\text{-MeU})_2$, shown in Figure 41 (to be discussed momentarily).

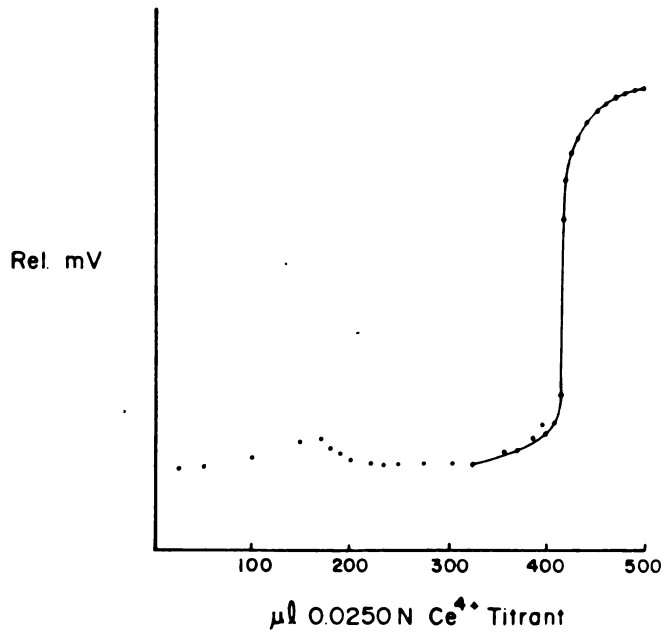

Figure 41. Titration curve for $Pt(NH_3)_2(1\text{-MeU})_2$. The break corresponds to 2 equivalents of electrons, thereby implicating a Pt(II) $\xrightarrow{-2e^-}$ Pt(IV) transition.

An explanation for the sharp break at 302 μL in Figure 40b and its absence in a (again, the curves were generated nearly six months apart, and on freshly-prepared solutions) is to postulate the decomposition $[(NH_3)_2Pt(1\text{-MeU})_2Pt(NH_3)_2](NO_3)_2 \rightarrow Pt(NH_3)_2(1\text{-MeU})_2 + Pt(NH_3)_2(NO_3)_2$ in the <u>solid</u> phase. The sharp end point is then assumed to arise from the $2Pt(II) \xrightarrow{-4e^-} 2Pt(IV)$ transition of these two product compounds. Correcting for this decomposition reaction, a calculation of percent error may be made. Doing this, the positive errors incurred in these five titrations were 9.2% in the first one, and 12.4, 6.3, 7.9, and 12.5 in the remaining four, for an average error of 9.7%.

The number of equivalents titrated through the equivalence point

was equal to 2(n=2), implying either

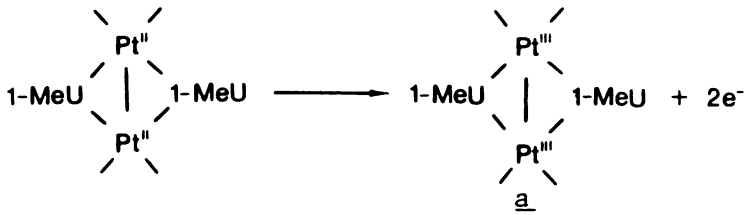

a

or

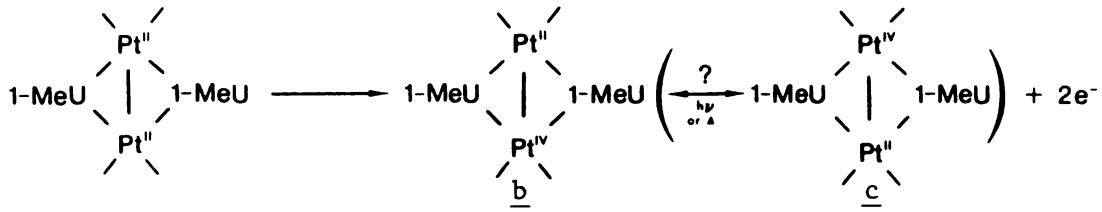

b c

Two representations of the titration of Pl-MeU

The 2 equivalents of electrons given up is in agreement with the results of controlled-potential electrolysis.

Product b in the above scheme is unlikely, as previously discussed, and the intervalence shift represented by b and c even less so. In the review by Allen and Hush on mixed-valence inorganic compounds (115), many examples are given of complexes in which the oxidation state of homonuclear species differs by two. It appears that in every such case for which the structure has been determined, a single bridging atom is interposed between metallic centers, thereby precluding direct metal-metal bonding. The platinum dimer under discussion here has two 1-methyluracil bridging ligands between platinums, but very likely also has direct bonding betwen platinum centers. Support for the last statement lies in a structural analogy to both a head-to-head platinum(II) 1-methylthymine dimer (d_{Pt-Pt} =

2.909 Å (50)) and to a head-to-tail platinum(II) 1-methyluracil dimer (d = 2.954 Å (74)). These internuclear distances are believed short enough to involve some Pt-Pt bonding. Furthermore, these compounds may be looked upon as precursors of platinum blues (although more direct routes of synthesis are used in practice), which, consensus says, exhibit properties characteristic of partial metal-metal bonding. Additional evidence for direct bonding in Pl-MeU will be given later in conjunction with a discussion of electrolysis/visible spectrophotometry and of electrolysis/EPR.

For directly bonded Pt atoms to differ in oxidation state by two, a very high degree of stabilization, sufficient to offset the energetic unfavorability of a Pt(II)-Pt(IV) arrangement, would have to be provided by the difference in environment around the two platinums in Pl-MeU. A two electron intervalence shift as represented by $Pt_A(II)-Pt_B(IV) \xrightarrow{h\nu \text{ or } \Delta} Pt_A(IV)-Pt_B(II)$ (see b and c in the schematic representation above), or, in general, by $M^{n+}-M^{(n+2)+} \xrightarrow{h\nu \text{ or } \Delta} M^{(n+2)+}-M^{n+}$, is, apparently, not known to exist. Rather, with a bridging atom A interposed between metallic centers, the intervalence transfer occurs as $M^{n+}-A-M^{(n+2)+} \rightarrow M^{(n+1)+}-A-M^{(n+1)+}$. An example is given by $Sb^{V} + Sb^{III} \rightarrow Sb^{IV} + Sb^{IV}$ (115). If the interconversion represented by b and c actually took place (upon absorption of light of suitable wavelength or by thermal activation), then the further oxidation by cerium(IV) to the Pt(IV)-Pt(IV) state (n=4) should occur as well.

ESR spectra taken prior to titration, at several points during

titration, and at the equivalence point, had the expected appearance (not shown): The ESR spectrum of untitrated Pl-MeU displayed no paramagnetic signal, in accordance with a low-spin d^8-d^8 electron configuration (see the section on electrolysis/EPR for a fuller accounting of the magnetic properties of Pl-MeU). At a point half-way to the equivalence point, the ESR signal was at a maximum, indicating maximum nonpairing. This corresponds to a Pt(II)-Pt(III) configuration (d^8-d^7) having one unpaired electron, and suggests delocalization; otherwise an inflection point should be discernible corresponding to half way on the titration curve. At the equivalence point, the EPR signal had vanished. Either a pairing up of spins in a Pt(III)-Pt(III) configuration (d^7-d^7) or a Pt(II)-Pt(IV) (d^8-d^6) arrangement would produce no net spin. However, a Pt(II)-Pt(IV) configuration is not consistent with the appearance, growth, dimunition, and disappearance of an EPR signal observed in proceeding toward the end point. (A much more detailed examination of ESR data will be given in the section on CPC/ESR).

The Hush model applied to this system will argue for considerable interaction (although not complete delocalization) between the Pt centers. In the case of the Pt(II)-Pt(III) intermediate, this means that both Pt_A(II)-Pt_B(III) and Pt_A(III)-Pt_B(II) must be invoked for a realistic and accurate representation of the system. Independent of the ESR results cited above, the improbability of Pt_A(II)-Pt_B(IV) $\rightarrow$ Pt_A(IV)-Pt_B(II) has been noted. It was also mentioned that for a Pt(II)-Pt(IV) state to be attained without

intervalence transfer, a very high degree of stability would have to be accorded either $Pt_A(II)-Pt_B(IV)$ or $Pt_A(IV)-Pt_B(II)$. Since this does not occur for a Pt(II)-Pt(III) state, it is even less likely to occur for a Pt(II)-Pt(IV) state, for which the difference in charge between platinums is greater.

The color progression observed in the titration with Ce(IV) was not quite the same as that noted during controlled-potential electrolysis. In the latter case the pattern was colorless → light green (lime) → intense green → green-yellow → golden yellow. With Ce(IV) the color changed according to the sequence green (momentary) → green-blue → blue → deep blue → purple → wine red → maroon → orange → lustrous yellow. The difference in color progression is in part probably a reflection of the difference in ionic environment (Cl^- from 1.0N HCl as opposed to NO_3^- from 0.1F $NaNO_3$), whose effect is to modulate the electronic distribution about the Pt atoms. The electrolysis was not run in 1.0N HCl as a check. Another factor may have to do with the oxidizing potential: the electrode in CPC may enable certain intermediates to propagate vis-a-vis Ce titration, as the thermodynamics are inherently more variable under electrochemical control.

The titration, as represented by Figure 40a, was rapid through the end point and beyond for a short distance - that is, equilibrium was rapidly achieved after the addition of each aliquot of titrant. At a volume corresponding to about 2/3 of an equivalent beyond the end point, the titration began to proceed very slowly, with the

potential jumping to a high value immediately upon addition of titrant, and then slowly drifting down toward an equilibrium (presumably) value. Gradually, the drift became intolerably slow, although this procedure was followed to well beyond where the second equivalence point would have occurred. In the end, more than 2 hrs elapsed between additions of titrant. (A practice adopted by some experimenters on similarly kinetically-limited systems has been to wait a fixed time after the addition of titrant before recording a value, but this is a questionable practice, since, as the equivalence point is approached, a slow titration reaction becomes even slower.) The color in the end was a distinct yellow, no doubt in part imparted by the color of Ce(IV)/Ce(III).

Post end-point behavior was not the same as just described in the titrations represented by Figure 40b; the attainment of equilibrium was rapid with no jumps in potential being observed. However, as noted earlier, in this case there was a second end point postulated to arise from the transition Pt(II) → Pt(IV), which served to shift the potential into a region where its value is dictated by the [Ce(IV)]/[Ce(III)] couple (vide infra). "Well-behaved" systems, as, for example, cis-Pt, exhibit rapid equilibrium in the post end-point region where the electrode is poised by the [Ce(IV)]/[Ce(III)] couple.

The potentiometric behavior beyond the break in the titration curve as exemplified in Figure 40a suggests that further oxidation is occurring, but at a very slow rate, at a rate far too slow to result

in a second break in the curve. It is, perhaps, a bit curious that the rate of attainment of equilibrium did not slow immediately after the equivalence point was reached, but rather began about 1/3 of the way toward where the second equivalence point would be. A separate titration using Ce prepared in HNO_3, a more strongly oxidizing medium, gave similar results, although there was a hint of a second inflection point at about the appropriate volume. However, because, as with the Ce/H_2SO_4 titrant, the readings made were dependent on the time waited (although the decay was not as slow as with Ce/H_2SO_4), and because the same behavior was manifest beyond the second inflection, to call this inflection an end point would be a dubious claim. The titration represented by Figure 40b gave no evidence of further oxidation of Pl-MeU beyond its end point. The greater oxidizing strength of $Ce/HClO_4$ could not be tested, as the platinum dimer precipitated out, presumably as the perchlorate salt. As to the common oxidants permanganate or dichromate, there is little reason to think that their use would be any more illuminating; their stoichiometries are complicated. However, use of a $2e^-$ oxidant, which could potentially remove two electrons directly from a given platinum atom, might be instructive.

Additional information as to the further oxidizability of Pl-MeU could be furnished by ESR spectra taken beyond the equivalence point. Toward this end, an excess of Ce(IV) equal to one equivalent beyond the equivalence point was added (i.e., 50% beyond the equivalence point - would correspond to Pt(III)-Pt(IV)). Four hrs

were allowed for any reaction to take place before transfer to an EPR tube and storage in liquid N_2. A second experiment corresponding to two equivalents beyond the equivalence point was also perfomed (i.e., 100% beyond the equivalence point - would correspond to Pt(IV)-Pt(IV)). Had further oxidation occurred, this would be reflected in the ESR spectra[1].

Based on the titration data (but, unfortunately, without benefit of ESR measurements), the conclusion is drawn that high stability is accorded the Pt(III)-Pt(III) configuration by the doubly-bridging ligands vis-a-vis Pt(IV)-Pt(IV). Perhaps a rationalization could be given in terms of a molecular orbital description of the system.

Calculation of $E^{o'}$ -

The titration curve of Figure 40b may be used to calculate the formal potential, $E^{o'}$, for the half-reaction $[P(III,III)1\text{-MeU}]^{4+} + 2e^- \rightleftarrows [P(II,II)1\text{-MeU}]^{2+}$. It can be shown using nernstian analysis that $2E^{o'}_{P(III,III)1\text{-MeU}} = 3E_{eq} - E^{o'}_{Ce^{4+}}$ where E_{eq} is the potential at the equivalence point and $E^{o'}_{Ce^{4+}}$ is the formal potential for the Ce^{4+}/Ce^{3+} couple (see, for example, ref. 116). (An alternate and simpler approach, which makes use of the equation $E^{o'} = E^{1/2}_{eq}$, a relationship that also follows from nernstian analysis, is probably not applicable in the present case for the reason that the equivalence point reflects two reactions - $[P(II,II)1\text{-MeU}]^{2+} \xrightarrow{-e^-} [P(II,III)1\text{-MeU}]^{3+}$ and $[P(II,III)1\text{-MeU}]^{3+} \xrightarrow{-e^-} [P(III,III)1\text{-MeU}]^{4+}$

---

1. Unfortunately, neither of these tubes was run.

- instead of the one required to use this simple relationship.) Referring to Figure 40b, we can calculate that

$$E^{o'}_{Ce^{4+}} = \frac{0.276}{1.00 + .276} \times 1.44 + \frac{1.00}{1.00 + .276} \times 1.28 = 1.31 \text{ V}$$

where 1.44 is the formal potential for Ce^{4+}/Ce^{3+} in 1N H_2SO_4 and 1.28 is the correponding formal potential in 1N HCl. Then reading E_{eq} = 0.928 V from the curve, $E^{o'}_{P(III,III)1\text{-MeU}}$ = (3x0.928-1.31)/2 = 0.74 V. This value translates to 0.74-0.236 = 0.50 V vs ssce.

Since this calculation applies to a nernstian (reversible) system, how it relates to the electrochemical behavior as monitored in the CV's is not entirely clear. Reference to Figure 27 reveals that 0.5 V is approximately midway between the two reduction peaks for P1-MeU. The value 0.74 V vs nhe does not agree well with the value 0.90 V estimated from cyclic voltammetry at carbon (p. 91). However, as the reader may recall, there was some uncertainty associated with the interpretation of the CV's at carbon. If we overlook the underlying irreversible behavior, then the calculated $E^{o'}$ can be taken to represent the formal potential for the overall reduction of the (III,III) species to the (II,II) state.

Beyond the equivalence point the potential can be calculated on the basis of the Ce^{4+}/Ce^{3+} couple by using the Nernst equation. When this is done at a point corresponding to 500 µL of titrant added, a value of 1.32 V is obtained. This agrees very well with the value 1.31 read from the plot. Unfortunately, in the early stages of this

work, when curves represented by Figure 40a were obtained, a voltmeter was not used (the rel. mV scale on a pH meter was used); unfortunately, because the measured potential may have had diagnostic value. However, direct comparison of Figures 40a and b leads to the conclusion already given that grudgingly slow further oxidation takes place beyond the observed end point.

Ce(IV) Titration of Related Compounds -

We concluded earlier from the cyclic voltammetric behavior of cis-$Pt(NH_3)_2(1\text{-MeU})_2$ that a $2e^-$ transfer corresponding to $Pt(II) \xrightarrow{-2e^-} Pt(IV)$ accounts for the behavior of this complex, and that the mononuclear cis-platinum diammine bis(1-methyluracilate) cannot support the +3 oxidation state. The titration of this compound supports the earlier conclusion, with a sharp break in evidence for the $Pt(II) \xrightarrow{-2e^-} Pt(IV)$ transition, but without even a hint of a break corresponding to $Pt(II) \xrightarrow{-e^-} Pt(III)$. Its titration curve was shown in Figure 41.

Titration of the "diaquo" bridged dimer $[(NH_3)_2Pt(OH)_2Pt(NH_3)_2](NO_3)_2$ yielded a single break corresponding to $2Pt(II) \xrightarrow{-4e^-} 2Pt(IV)$. An interpretation of this result as well as of the absence of any cyclic voltammetric response at Pt was given earlier. The gist was that, taken together, these measurements argue against the tervalent state in this complex. It may be that the absence of unsaturation in the bridging ligands and the 3.085 Å Pt-Pt separation (72) mitigate against the Pt(III) state.

Titration of Pl-MeUB with Ce(IV) -

The titrimetric behavior of Pl-MeUB was similar to that of Pl-MeU, although with the former the long equilibration times began almost immediately after the equivalence point. A typical titration curve is shown in Figure 42. As with the dimer, only a single end point was obtained.

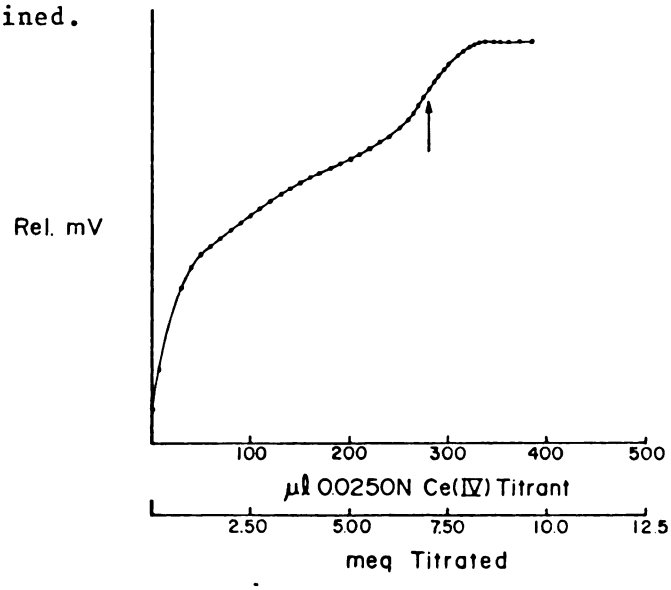

Figure 42. A titration curve for the Ce(IV) titration of Pl-MeUB. The end point was taken at the point marked by the arrow.

When voltage readings were taken during the titration, the equivalence point potential was 0.93 V vs nhe (not shown), the same as was observed for the dimer. As the curve flattened out after the equivalence point, the potential reading was 0.99 V, well below the value which would be dictated by the Ce^{4+}/Ce^{3+} couple were no further oxidation taking place. Again, this is indicative of further oxidation, no matter how slow. For the polymeric, stabilized blue, the indication is that the barrier toward continued oxidation of platinum beyond Pt(III) is even greater than for the dimer. The

color change during titration followed the pattern observed in the electrolysis: blue-green → brown → honey-brown. Well beyond the equivalence point the color was an orange-brown, presumably a reflection of the color of the excess Ce titrant.

By analogy to Pl-MeU and to the earlier CV and CPC results, let us take the equivalence point to correspond to the Pt(II) atoms in Pl-MeUB going to Pt(III). If this is the case, a correspondence may be expected between the Ce titration shown in Figure 42 and oxidative electrolysis of this compound. Taking for instance electrolyses conducted on 5.33, 14.04, and 40.54 mg, and correcting the titration curve in Figure 42 (generated from 2.90 mg) for a 10% blank contribution (0.00700 meq → 0.00636 meq), then the equivalent charge for each of the three electrolyses would be $\frac{5.33}{2.90}$ x (0.00636×10^{-3} eq x 96487 C/eq) = $\frac{5.33}{2.90}$ x 0.614 = 1.13 C; $\frac{14.04}{2.90}$ x 0.614 = 2.97 C; $\frac{40.54}{2.90}$ x 0.614 = 8.58 C. Reference to Figure 32 shows that these calculated equivalent charges would correspond to many hours of electrolyzing (out of range in two of the figures). When the electrolyses shown in Figure 32 were carried out to, and past the points of calculated equivalent charge, there was no suggestion of completion of electrolysis in any of the electrolysis curves.

The fact that the Q-t curves continue to rise beyond the calculated equivalence points at rates exceeding the background contribution may beg that the interpretation which attributes the slow, prolonged rise in the electrolysis curves to very slow kinetics be amended. One argument, though, is supported, and that is the

argument against the further oxidation (substantial) of Pt(III) to Pt(IV): based on the titrations of Pl-MeU and Pl-MeUB, which showed that continued titration beyond the equivalence point was at least as difficult for Pl-MeUB as for Pl-MeU, then if the further oxidation Pt(III)→Pt(IV) does not complicate the electrolysis of Pl-MeU, then it should also not complicate the electrolysis of Pl-MeUB. Perhaps the expectation of a close correspondence between the electrolysis and titration curves is not fully warranted, in that these experiments are not alike. As was pointed out in the earlier discussion of the electrolysis behavior of Pl-MeUB, various factors and several mechanisms can give rise to the observed shapes of the electrolysis curves.

Calculation of the Extent of Mixed-Valency of Pl-MeUB by Titrimetry -

Accurate determination of the equivalence point should make possible assignment of an average formal oxidation state for platinum in Pl-MeUB. One approach is to assume a structure - a singly-bridged Pt chain - as we have done previously:

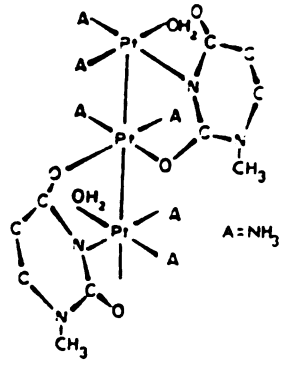

Assumed structure of Pl-MeUB for calculational purposes

or in simplified schematic fashion (disregarding the cis stereochemistry):

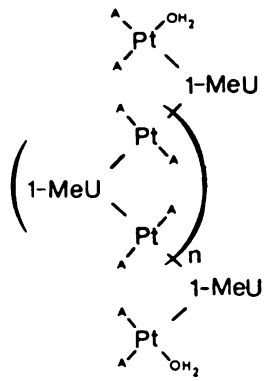

An alternate representation

For a given chain length, say 12 Pt atoms, the formula weight, taking 1 Pt per chain to be in the +3 state, and the remaining 11 to be in the +2 state (see p. 174)[1], is given by

$$11(1\text{-MeU}) + 12Pt + 24NH_3 + 2H_2O + 14NO_3$$

$$= 11\times125.1 + 12\times195.1 + 24\times17.0 + 2\times18.0 + 14\times62 = 5029.$$

---

1. It may seem a contradiction of purpose to initially assume an average oxidation state (1 Pt(III) in every 12 Pt atoms) in a section entitled Calculation of the Extent of Mixed-Valency.... Actually, the effect of one additional nitrate group (F.W. = 62), required by the lone Pt(III), is essentially negligible compared to 5029 (see above). To be fully rigorous, the procedure described should be replaced by an iterative process: once an average oxidation state is calculated, the calculation is repeated, replacing 5029 with the adjusted value, and so on for successive iterations. However, the precision of the data do not warrant the time that would be required to carry out the successive calculations.

For w mg titrated, the expected number of mequiv used in the titration of Pt(II) to Pt(III) is equal to 11 x $\frac{w}{5029}$. Rather than having the molecular weight (which we do not), if we know the number of mequiv from a titration (corrected downward for its positive error due to the oxidation of some Cl^-) and the weight of sample titrated, then the combination of n and F.W. that best fits the data can be calculated. This is done in Table 5 (listed as # Pt(II)'s rather than as n) for four replicate titrations of Pl-MeUB. The best five fits with the best of these underlined are listed for each titration. The formal oxidation state that corresponds to the calculated n value is listed in the last column.

The spread in the number of Pt(II) atoms calculated is considerable; there is a corresponding spread in the calculated oxidation state. Earlier we obtained a value of 2.08 (1 Pt(III) in every 12 Pt's) by comparing oxidative and reductive electrolyses. We could take into account the percent impurity in Pl-MeUB contributed by Pl-MeU (can be estimated by LC, vide infra), and then recalculate the # Pt(II)'s and the mean oxidation state. However, as reference to Figure 58 (to be discussed later in the appropriate section) will attest, to obtain a reliable figure for the percent Pl-MeU in Pl-MeUB by integration would tax even the best of modern-day integrators. Woollins and Rosenberg reported a figure of 5-10% Pl-MeU in Pl-MeUB (80). For only a 5-10% contribution, and because the mean oxidation state in Pl-MeUB is very close to 2, an adjustment made by including the contribution of Pl-MeU, in which the oxidation state of platinum

is 2, would be very slight. Considering the error inherent to the determination of the equivalence point in the titration of Pl-MeUB, it would serve no useful purpose to make this adjustment.

Note that the formula weights calculated and listed in Table 5 are considerably lower than the 25,500 value reported earlier, a value obtained by combining RDV data with the Einstein-Stokes equation. The average of the four values shown in Table 5 is 9290 $\pm$ 3030 (1 std. dev.). This value translates to 9290/832 = 11 units, a value consistent with current thinking on platinum blues (18).

Table 5
Average Formal Oxidation State for Platinum
in Pl-MeUB Based on Assumed Structure

Run #	mg Spl.	meq Titrant	meq/mg	10% Corr. meq[1]	[# Pt(II)'s]$_{calc}$	F.W.[2]	Mean Pt Ox. State
1	2.90	0.00700	2.41×10^{-3}	.00636	9.20,10.11,<u>11.02</u>,11.94,12.85	5027	2.083
2	2.70	.00680	2.52×10^{-3}	.00618	20.08,21.04,<u>21.99</u>,22.94,23.89	9607	2.043
3	2.70	.00775	2.87×10^{-3}[3]				
4	2.62	.00662	2.53×10^{-3}	.00602	22.08,23.03,<u>23.99</u>,24.94,25.90	10439	2.040
5	2.76	.00702	2.54×10^{-3}	.00638	26.06,<u>27.02</u>,<u>27.98</u>,28.95,29.91	12104	2.035

Mean (mean Pt ox. state) = 2.050 → 2.05 $\pm$ 0.02 (1s)

[1] corrected downward for the 10% positive error determined from 5 titrations of Pl-MeU

[2] corresponds to underlined value

[3] rejected on the basis of the Q test

A more direct calculation of oxidation state, one that relies on no assumptions regarding structure, is based on percent Pt composition. Any of several methods may be used to determine percent

platinum: flameless atomic absorption, atomic emission (most notably inductively coupled plasma (ICP) atomic emission), X-ray fluorescence, and neutron activation, to name four. Using the last of these, a value % Pt(Pl-MeUB) = 44.7% ± 1.1% was obtained[1]. If one takes the same 10% error correction used to generate Table 5, then for the same four runs listed in Table 5, using % Pt(Pl-MeUB) = 44.7, Table 6 may be generated.

Table 6
Average Formal Oxidation State for Platinum
in Pl-MeUB Based on Percent Platinum. I.

Run #	mg Spl.	mg Pt[(1)]	meq Titrant	10% Corr. meq	$\frac{Pt^{II}}{Pt^{II}+Pt^{III}}$	Mean Pt Ox. State
1	2.90	1.30	0.00700	.00636	.96	2.04
2	2.70	1.21	.00680	.00618	1.00	2.00
3[(2)]						
4	2.62	1.17	.00662	.00602	1.00	2.00
5	2.76	1.23	.00702	.00638	1.01	2.00
						Av. = 2.01

[(1)] sample contains 44.7 ± 1.1% Pt

[(2)] see Table 5

The value 2.01 shown is surprisingly low (recall the 2.08 figure generated previously by comparing oxidative and reductive electrolysis curves (p. 174); in fact, because of the uncertainty

---

1. Analysis performed by Dr. S. W. Barr of The Dow Chemical Co., Midland, MI.

associated with this figure (vide infra), it is statistically indistinguishable from 2.00.

In making these calculations, the relevant question to be asked is, how reliable is the correction factor being applied to the number of mequiv consumed in the titrations? The figure of 10% used was arrived at by rounding off the average of five determinations made on Pl-MeU (see p. 190): (9.2 + 12.4 + 6.3 + 7.9 + 12.5)/5 = 9.7 ± 2.7(1s) or 5.4(2s). If we calculate the average oxidation state corresponding to the +1s(12.4) and +2s(15.1) deviations (to make calculations at the -1s and -2s deviations would produce an average oxidation state < 2.0), the values in Table 7 are obtained.

Table 7
Average Formal Oxidation State for Platinum in Pl-MeUB Based on Percent Platinum. II.

Run #	mg Spl.	mg Pt[1]	meq Titrant	12.4% Corr. meq	15.1% Corr. meq
1	2.90	1.30	0.00700	.00622	.00608
2	2.70	1.21	.00680	.00604	.00591
4	2.62	1.17	.00662	.00588	.00575
5	2.76	1.23	.00702	.00624	.00610

		$[\frac{Pt^{II}}{Pt^{II}+Pt^{III}}]_{12.4\%}$	$[\frac{Pt^{II}}{Pt^{II}+Pt^{III}}]_{15.1\%}$	$[\text{Mean Pt Ox. State}]_{12.4\%}$	$[\text{Mean Pt Ox. State}]_{15.1\%}$
1	2.90	.93	.91	2.07	2.09
2	2.70	.97	.95	2.03	2.05
4	2.62	.98	.96	2.02	2.04
5	2.76	.99	.96	2.01	2.04
				Av. = 2.03	Av. = 2.06

[1] sample contains 44.7 ± 1.1% Pt

Summarizing - from Tables 6 and 7 we may write that, based on a measurement of percent platinum in Pl-MeUB, the average formal oxidation state of

$$Pt = \begin{matrix} 2.01 \pm 0.02(1s) \\ 2.01 \pm 0.05(2s) \end{matrix}$$

Again, the range encompassed by these values is somewhat less than the value of 2.08 obtained by comparison of oxidative and reductive electrolysis curves. There is no valid reason to suspect that the error figure of ~10% (due to the blank) arrived at by titrating Pl-MeU, is not also valid for Pl-MeUB, since the blank contribution arises from the slow oxidation of Cl^- (source: 1N HCl), and its magnitude should only be dependent on the duration of the titration; as has been previously described, Pl-MeU and Pl-MeUB behaved similarly when titrated. The values for the average formal oxidation state of platinum calculated here suggest a very weak paramagnetism to Pl-MeUB, a result consistent with EPR measurements (vide infra).

It is of interest to note that the value determined for percent Pt in Pl-MeUB (=44.7 ± 1.1%) is not significantly (nor statistically) different from the value determined for percent Pt in Pl-MeU (=44.4 ± 1.1% (p. 67)). Their equivalence is consistent with probable structures that have been shown for Pl-MeUB from time-to-time throughout this thesis - structures based on repeating diamminated platinum units linked by alternate, single 1-MeU bridges.

An assignment of an average oxidation state could, in principle,

also be based on reductive titrimetry, but this was not attempted. As reported in the Literature Review section earlier, the reductive titration procedure used by Barton et al. (18) was plagued by a high blank and attendant high uncertainty in the assigned oxidation state. That is not to say that their procedure could not be improved upon.

Ce(IV) Titration of Other Blues -

The cyclic voltammetry of platinum benzoate blue (PBzB) and platinum phthalate blue (PPhB) was discussed earlier. The complete absence of a voltammetric response over the accessible range on Pt was pointed out. Upon dissolution (with the aid of gentle heating) in 1N HCl, the benzoate blue turned yellow. PBzB dissolved more readily in MeOH/1N HCl than in aqueous HCl solution, but its potentiometric behavior was erratic and unusable. In 1N HCl (aq) the benzoate blue acted much like Pl-MeUB during titration, except that there was no color change. Based on a single titration of PBzB, the average formal oxidation state for Pt in this compound was calculated ala the procedure used for Pl-MeUB in the previous section; calculated values are given in Table 8. The titration curve is shown in Figure 43.

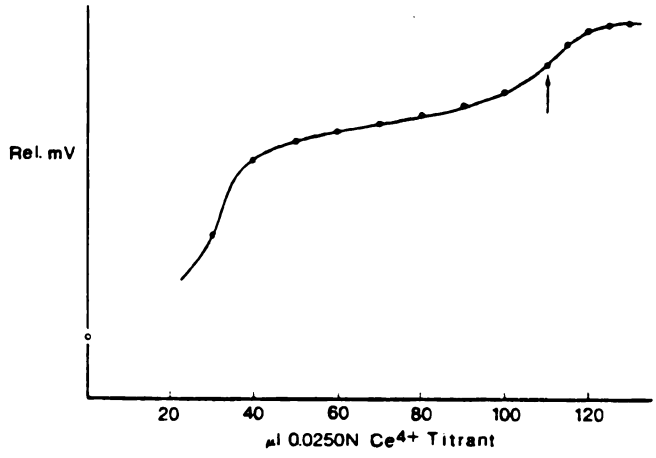

Figure 43. A titration curve for the Ce(IV) titration of PBzB. The end point was taken at the point marked by the arrow.

Table 8
Average Formal Oxidation State of Platinum in Platinum Benzoate Blue Based on Percent Platinum

mg Spl.	mg Pt[1]	meq Titrant	9.7% Corr. meq	12.4% Corr. meq	15.1% Corr. meq
2.62	1.12	0.00275	.00251	.00245	.00239

$[\frac{Pt^{II}}{Pt^{II}+Pt^{III}}]_{9.7\%}$	$[\frac{Pt^{II}}{Pt^{II}+Pt^{III}}]_{12.4\%}$	$[\frac{Pt^{II}}{Pt^{II}+Pt^{III}}]_{15.1\%}$
.44	.43	.42

$[\text{Mean Pt Ox. State}]_{9.7\%}$	$[\text{Mean Pt Ox. State}]_{12.4\%}$	$[\text{Mean Pt Ox. State}]_{15.1}$
2.56	2.57	2.58

[1] Percent Pt = 42.7 ± 1.7% - courtesy of Dr. S. W. Barr, the Analytical Laboratories, The Dow Chemical Co., Midland, MI.

This is a fascinating result, in that for this very different blue, the average oxidation state of platinum is considerably higher than for Pl-MeUB. According to this result, roughly half of the Pt atoms

are in the II state and half are in the III state. Unlike the case for Pl-MeUB, no ESR measurements - which could have lent confirmation to this finding - were made.

When the ammines in PBzB were replaced by chlorines,

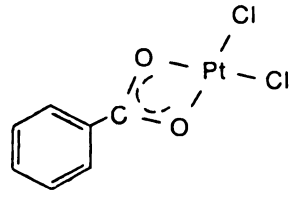

vs

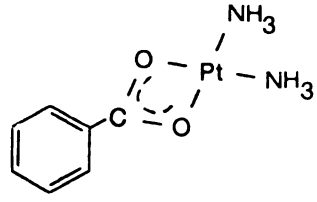

an exchange that conferred ready water solubility to the benzoate blue, the titrimetric behavior was less straightforward. Although as the titration proceeded the period required for equilibration greatly increased, as was also the case for the ammine-containing PBzB, no end point was discernible in the titration curve. There was no color change from the original brown solution (the solid is deep blue) other than a lightening from the added cerium. The cyclic voltammetric behavior was equally inconclusive.

Platinum phthalate blue (PPhB),

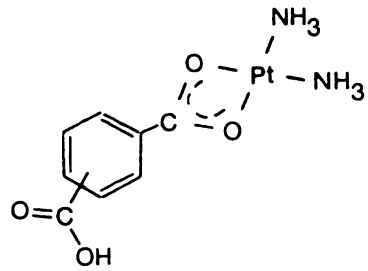

is not water soluble; the Cl-for-NH_3-substituted analog is. Like its benzoate analog, it gave no discernible end point. Unlike the benzoate, the initially-brown solution turned yellow of its own accord in a matter of minutes. It is apparent that the blues are capable of producing a plethora of colors. This brief glimpse into related blues seems to suggest a difference in behavior between ammine-substituted and chlorine-substituted blues, although the reason for the difference is not certain.

Summary of Titrimetry Findings -

Acidic solutions of Ce(IV) were used in the oxidative titration of Pl-MeU, Pl-MeUB, and related compounds. The Pl-MeU dimer displayed a single end point which was assigned to $[P(II,II)1\text{-MeU}]^{2+} \rightarrow [P(III,III)1\text{-MeU}]^{4+} + 2e^-$. Evidence obtained by EPR was used to support this assignment. The absence of even a hint of an inflection at the halfway point (1 eq of titrant added) argues against the selective formation of the mixed-valent $[P(II,III)1\text{-MeU}]^{3+}$ (i.e., against a strongly-localized Pt(II) and Pt(III)) in the highly-oxidizing medium. This is consistent with the CPC observations discussed previously.

Titration of $[P(III,III)1\text{-}MeU]^{4+}$ beyond the equivalence point was sluggish, indicative of very slow (inconsequentially slow after a point) further oxidation to $[P(III,IV)1\text{-}MeU]^{5+}$ and $[P(IV,IV)1\text{-}MeU]^{6+}$. EPR measurements, which could have confirmed the absence of significant further oxidation, were, unfortunately, not obtained. Titrations of Pl-MeU conducted six months apart, but on fresh solutions in each case, revealed an apparent decomposition of the dimeric complex, a decomposition which had taken place in the solid state. An $E^{o'}$ value for the half-reaction $[P(III,III)1\text{-}MeU]^{4+} + 2e^- \rightleftarrows [P(II,II)1\text{-}MeU]^{2+}$ was calculated from titrimetry to be 0.74 V vs nhe. Titration curves for two related compounds, one mononuclear - <u>cis</u>-$Pt(NH_3)_2(1\text{-}MeU)_2$ - and the other a doubly-bridged binuclear species - $[(NH_3)_2Pt(OH)_2Pt(NH_3)_2]^{2+}$ - were interpreted in terms of a Pt(II) → Pt(IV) transition.

Titration of the polymeric Pl-MeUB also revealed a single end point, and exhibited a titration curve similar in appearance to that of Pl-MeU; they both yielded an E_{eq} of 0.93 V vs nhe. As with the dimer, the end point was ascribed to Pt(II) → Pt(III). The sluggish behavior exhibited by Pl-MeU beyond the end point was exacerbated for Pl-MeUB - i.e., with each addition of titrant, after an initial jump in potential, there ensued a protracted decline in the magnitude of the potential. No meaningful data could be collected. This behavior is interpreted to be a manifestation of exceedingly slow further oxidation beyond the all III state.

An average formal oxidation state for Pt in Pl-MeUB, based on

titrimetry, was calculated by 1) assuming a structure and by 2) measuring percent Pt. A value of 2.05 $\pm$ 0.02 was obtained by the former approach, a value of 2.01 $\pm$ 0.05 by the latter. A related compound, platinum benzoate blue (PBzB), yielded an average oxidation state of 2.56 based on a single determination; the calculation was based on measured percent Pt. The average oxidation state of Pt in platinum phthalate blue (PPhB) was not determined, as this compound is water insoluble. Interestingly, when the ammines were replaced by Cl, neither PBzB nor PPhB gave a discernible end point.

CPC/Vis-NIR Spectroscopy

Oxidative electrolyses were conducted on Pl-MeU and Pl-MeUB at +1.1 V vs ssce, and the solutions sampled at ~1/8 intervals for recording of their visible and near infrared (NIR) spectra. One reason for doing this was to get both a qualitative and quantitative description of the change in absorption character with a change in the valence state. A second was to apply the Hush model treatment to the mixed-valence state and to thereby gauge the extent of interaction between platinum centers. Conclusions drawn from the Hush treatment may then be compared for consistency with other results - viz., those from combined electrolysis/EPR studies.

Pl-MeU -

Figure 44 shows the series of spectra obtained for the dimer Pl-MeU. The magnitude of the molar absorptivity @ 742 nm as a function of the extent of electrolysis is given in Table 9.

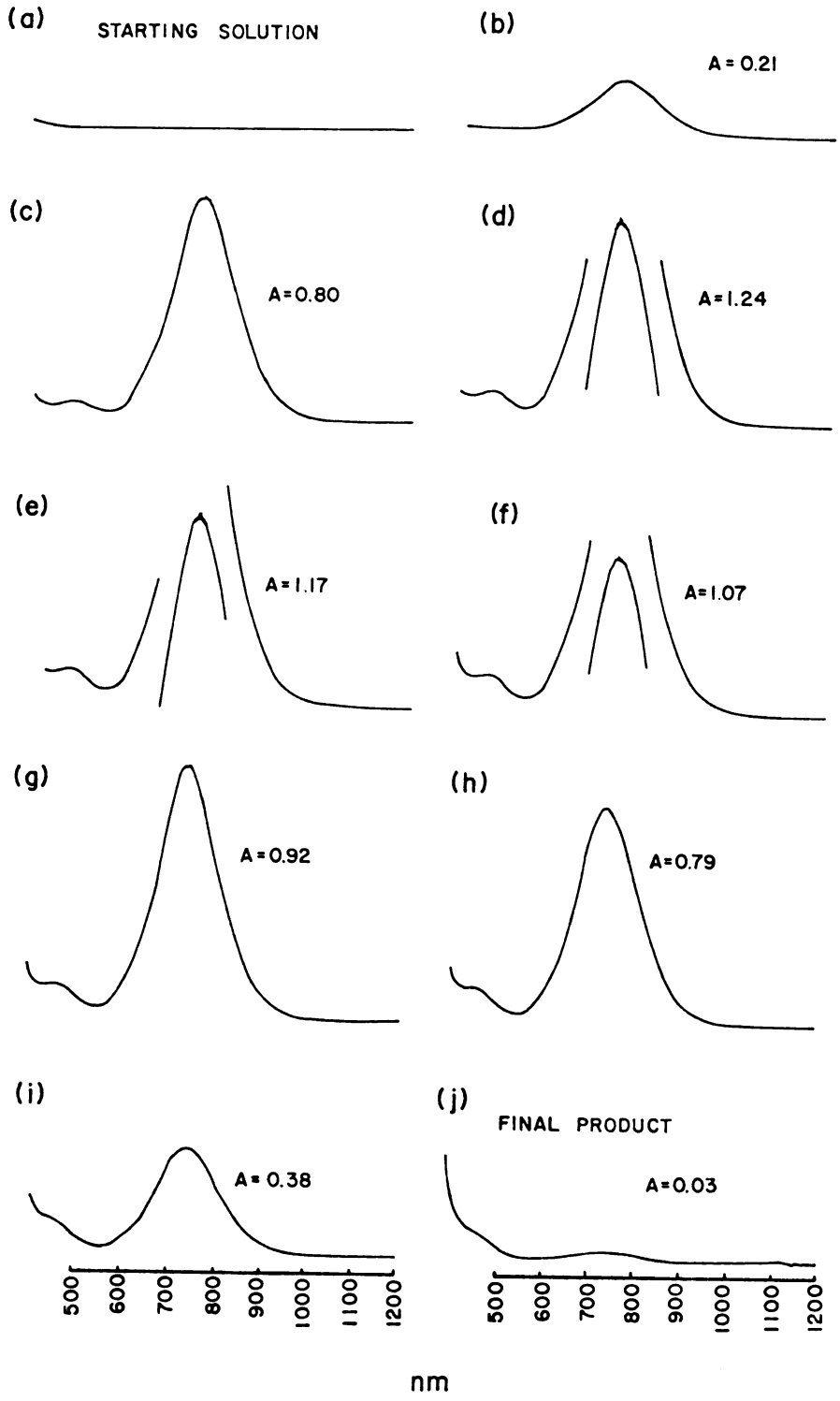

Figure 44. NIR/Vis spectra of Pl-MeU (2.4 mM) taken at 1/8 intervals throughout an oxidative electrolysis; senstivity, 1.0 AUFS.

Table 9

Molar Absorptivity, ε_{742}, of Pl-MeU as a Function of the Extent of Electrolysis

Fractional Completion of Electrolysis	ε_{740} (M^{-1} cm^{-1})
0	~0
0.13	9.20×10^2
.25	3.30×10^3
.36	5.11×10^3
.46	4.82×10^3
.55	4.40×10^3
.62	3.78×10^3
.68	3.24×10^3
.84	1.57×10^3
~1.0	1.23×10^2

The intense color (green) which forms during electrolysis is presumed due to the intervalence electron transfer associated with the Pt(II)-Pt(III) state:

$$[(NH_3)_2Pt^{II}(1\text{-MeU})_2Pt^{III}(NH_3)_2]^{3+} \xrightarrow{h\nu} [(NH_3)_2Pt^{III}(1\text{-MeU})_2Pt^{II}(NH_3)_2]^{3+*}.$$

The broad band which peaks at about 740 nm is the intervalence transfer band. Were the Pt(II)-Pt(III) species formed to the exclusion of any other (viz., to the exclusion of Pt(III)-Pt(III) during the first half of the electrolysis), then a maximum value of the molar absorptivity would be expected at the halfway point in the electrolysis. The fact that ε peaks before the electrolysis is 50% complete, is probably a reflection of the contribution of the final

electrolysis product - $[P(III,III)1\text{-}MeU]^{4+}$ (which is yellow, not green). One might also wish to conjecture about the effect of rearrangement or disproportionation on ε. However, recalling the high degree of chemical reversibility displayed upon sequential oxidative and reductive electrolysis, it is unlikely that a coupled chemical step is a major factor in defining the ε-vs-extent of electrolysis profile. We have already seen that the transition $P(II,II)1\text{-}MeU \xrightarrow{-e^-} P(II,III)1\text{-}MeU$ occurs more readily (at lower potential) than the following $P(II,III)1\text{-}MeU \xrightarrow{-e^-} P(III,III)1\text{-}MeU$. Nevertheless, the latter oxidation reaction also takes place at an appreciable rate over the entire potential range used (+0.70 V to +1.1 V) in the course of conducting these electrolyses. Hence, a contribution from the P(III,III)1-MeU species throughout virtually the entire electrolysis is not surprising.

Hush Model Treatment of Pl-MeU (117-119). It was pointed out in the Introduction of this dissertation in the section on Mixed-Valence Compounds that a scheme has been devised which classifies mixed-valence compounds according to the degree of interaction between metal centers (36). While some interaction is usually direct through metal-metal bonding, the intervening ligands may also provide a path for electron transfer, and at the very least, serve to modulate the interaction between metal centers. Electron transfer may be initiated by either optical absorption or thermal activation; a unified, general theory dealing with both types of transfer has been developed (117, 118). Intervalence transfer can take place in

both the solid state and in solution, and techniques are available for studying both. What follows is a treatment according to the method of Hush (117) applied to the mixed-valence P(II,III)1-MeU system. Hush has also presented a review of known, colored inorganic mixed-valence systems (115), including several Pt(II)-Pt(IV) compounds. It is interesting to read in that review that compounds in which platinum was originally believed to exist in the tervalent state, were later reassigned as mixed valent containing Pt^{II} and Pt^{IV} (115).

The degree to which an electron can be taken as being localized at a particular metal (donor) site in the ground state is fundamental to the Hush treatment. The extent of delocalization from one metal nucleus to another depends on 1) the extent of direct overlap of the orbitals of the two atoms and 2) on the degree of metal-ligand overlap through either σ- or π-type metal-ligand bonding. A certain degree of localization is required; otherwise, a "collective" description is appropriate, and the system will exhibit typical metallic properties. In a quantitative way, this is expressed in terms of overlap integrals.

The transition in question is given by $[(NH_3)_2Pt^{II}(1\text{-MeU})_2\text{-}Pt^{III}(NH_3)_2]^{3+} \xrightarrow{h\nu} [(NH_3)_2Pt^{III}(1\text{-MeU})_2Pt^{II}(NH_3)_2]^{3+*}$. In the Hush intervalence charge transfer theory, the energy is postulated to be absorbed almost completely into the phonon system, rather than into electron levels. A consequence of this is that in returning to the ground state, there is no corresponding radiative emission

(fluorescence and phosphorescence are not possible). In the calculations to follow, the absorbance spectrum in which ε is a maximum (Figure 44) was used.

The maximum absorbance is at λ = 742 nm = λ_{max}. This corresponds to $\bar{\nu}_{max} = \frac{1}{\lambda_{max}} = 1.35 \times 10^4$ cm^{-1}. The bandwidth at half-height, $\Delta\bar{\nu}_{1/2}$, equals 0.27×10^4 cm^{-1}; the band is assumed to be Gaussian. The molar absorptivity $\varepsilon_{max} = 5.10 \times 10^3$ M^{-1} cm^{-1}. The approximate extent of delocalization in the ground state is given by the valence delocalization coefficient α: $\alpha^2 = \frac{(4.2 \times 10^{-4})\varepsilon_{max}\Delta\bar{\nu}_{1/2}}{\bar{\nu}_{max} \cdot d^2 \cdot g^2}$ (219.1), where d is the interatomic (interplatinum) distance in Å and g is the difference in oxidation state of the two metal centers. The crystal structure has not been determined for this compound, as the isolated perchlorate salt was not suitable for X-ray crystallographic analysis (81); consequently, d is unknown. However, Pt-Pt distances are known in several related compounds: A head-to-tail Pt(II) dimer with 1-methylthymine bridging ligands has a Pt-Pt distance of 2.974 Å (49). In the corresponding head-to-head dimer, the Pt-Pt distance is 2.909 Å (50). In a head-to-tail Pt(II) dimer containing 1-methyluracilate ligands, the interatomic Pt-Pt distance is 2.954 Å (74). The compound under discussion here is the head-to-head 1-methyluracilate dimer, but the $[\cdot Pt(II)-Pt(III)\cdot]^{3+}$ rather than the $[\cdot Pt(II)-Pt(II)\cdot]^{2+}$. As 1-methylthymine and 1-methyluracil differ only in a methyl group,

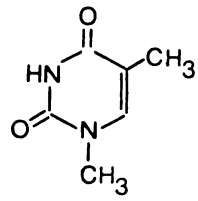

1-Methylthymine

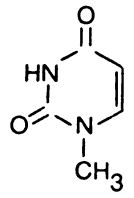

1-Methyluracil

to assume a value of 2.91 Å for the interplatinum distance in the head-to-head platinum(II) 1-methyluracil dimer would probably be only slightly in error. As the Pt oxidation state increases, the internuclear distance becomes shorter. This is exemplified by Pt(III)-Pt(III) dimers (54) and by platinum α-pyridone blue (2.779 Å); in the latter compound the average formal oxidation state of platinum is 2.25 (18). Let us use a value somewhat less than 2.91 Å, say 2.88 Å. Then, using eq. 219.1 ,

$$\alpha^2 = \frac{4.2\times10^{-4}\times5.10\times10^{3}\times0.27\times10^{4}}{1.35\times10^{4}(2.88)^2 \times 1^2} \rightarrow \alpha = 0.23$$

If, rather, a value of d = 2.80 Å is used, α = 0.24. Crudely, this (α = 0.23) means that an electron is localized to a particular Pt atom 77% of the time.

If the localization is sufficiently large (α < 0.25 (120)), the

complex is referred to as a trapped valence complex. With $\alpha = 0.23$, the compound fits the class II description, barely - partially-localized, but certainly not to the extent of, for example, biferrocene[Fe(II)Fe(III)] picrate ($\alpha = 0.9\text{-}1.4\times10^{-2}$) (120) or of Creutz's and Taube's well-known ruthenium complex, $[(NH_3)_5Ru^{II}(\text{pyrazine})Ru^{III}(NH_3)_5]^{5+}(1.70\times10^{-2})$ (121), although Beattie, Hush, and Taylor argue that, based on physical evidence provided by the NIR mixed-valence band, vibrational spectra, and X-ray photoelectron spectroscopy, the ruthenium-pyrazine ion is best characterized as a delocalized system with symmetrical ground state (122). (This interpretation for the ruthenium system runs counter to the generally-accepted view.)

The lower α in biferrocene and in Creutz's and Taube's complex relative to Pl-MeU is understandable, at least in simplistic terms, by reference to their structures: The evidence argues for Pt-Pt overlap in Pl-MeU (primarily based on CPC/EPR results to be given in a following section). In Creutz 's and Taube's complex a pyrazine group intervenes between metal centers. Biferrocene consists of two ferrocene units linked through cyclopentadienyl rings, so that two organic groups are interposed between the Fe ions.

Borderline class II-class III is probably a more apt classification for the 1-methyluracil platinum dimer. This is the same description accorded several platinum blues by Chang et al. (24). The high value for α reported here for Pl-MeU is not inconsistent with the value Chang et al. obtained for a platinum

blue - platinum phthalimide blue ($\alpha \cong 0.12$, vide infra).

In the Hush model, the activation energy for the thermal electron-transfer process is equal to or greater than one-fourth the energy of the optical transition: $E_{op} \leq 4E_{th}$. In the case of a symmetrical ion such as $[(NH_3)_2Pt^{II}(1\text{-MeU})_2Pt^{III}(NH_3)_2]^{3+}$, the equality obtains. From $E_{op} = \bar{\nu}_{max}$, we can calculate $E_{th} = 9.6\text{x}10^3$ cal mol^{-1}. Given this, the maximum thermally-activated unimolecular electron-transfer rate constant can be estimated from

$$k_{th} = \frac{kT}{h} \exp\left[\frac{-E_{op}/4}{RT}\right]$$

where $E_{op} = \bar{\nu}_{max}$. This calculates to $k_{th} = 5.4\text{x}10^5$ sec^{-1}, assuming no activation entropy and a transmission coefficient of unity. This value may be compared with a calculated rate constant of $1.3\text{x}10^{10}$ sec^{-1} for biferrocene[Fe(II)Fe(III)] picrate.

A higher α implies a correspondingly higher k_{th}. Relative to the biferrocene system, we see the opposite trend. The discrepancy between the biferrocene and 1-methyluracil systems argues that the Hush model does not fit the 1-methyluracil system well. Also, the higher the delocalization coefficient, and the more symmetrical the ground state, the farther into the near infrared would be the expected position of the intervalence band. It is of interest that for the Creutz-Taube ion mentioned above, with $\alpha = 1.7\text{x}10^{-2}$, a system, which according to Beattie et al. should be classified as delocalized (122) (not a trapped-valence system), the intervalence

band peaks at 1570 nm, well into the near infrared region. In the present instance, for $[P(II,III)1\text{-MeU}]^{3+}$, for which $\alpha \cong 0.23$ was obtained, the intervalence band is largely in the visible region, peaking at 740 nm. A scan out to $\lambda = 2000$ nm revealed no additional absorption bands. It is appropriate here to point out that the Hush theory is based on a weak-interaction model (i.e., low delocalization) and hence would be expected to fit less well the higher α is.

As a further check on the suitability of the Hush model to P(II,III)1-MeU, observed and calculated values of $\Delta\bar{\nu}_{1/2}$ can be compared using the equation $\bar{\nu}_{max} = (\Delta\bar{\nu}_{1/2})^2/2310$ ($\bar{\nu}_{max}$ and $\Delta\bar{\nu}_{1/2}$ in cm^{-1}), also derived by Hush (117). Using this equation, a value $(\Delta\bar{\nu}_{1/2})_{calc'd} = 5.58\times10^3\ cm^{-1}$ was obtained. Then $(\Delta\bar{\nu}_{1/2})_{obs} = 2.7\times10^3\ cm^{-1} < (\Delta\bar{\nu}_{1/2})_{calc'd} = 5.58\times10^3\ cm^{-1}$. Powers and Meyer report $(\Delta\bar{\nu}_{1/2})_{calc'd} < (\Delta\bar{\nu}_{1/2})_{obs}$ for a series of Ru ions (123) and biferrocene ions (124), although their ratio did not exceed 1.4. On the other hand, Creutz and Taube reported $(\Delta\bar{\nu}_{1/2})_{calc'd} = 6(\Delta\bar{\nu}_{1/2})_{obs}$ for the ruthenium ion $[Ru^{II}(pyrazine)Ru^{III}]^{5+}$ (125). In the former case, the discrepancy was attributed to the use of a single oscillator model in deriving the equation; in the latter, the high-temperature limit criterion, $2RT > h\nu$, where $h\nu$ is the energy associated with a metal-ligand vibrational transition, was not met.

Beattie, Hush, and Taylor have modified the Hush model to account for the relatively narrower bandwidth as delocalization increases (122). In the Hush model the half-bandwidth is predicted to decrease

as the temperature is lowered. The modification predicts that the bandwidth will increase more slowly with temperature as a system becomes more delocalized, so that narrow bandwidth suggests a delocalized rather than a localized state. In further studies of the theoretical limitations of the Hush model, Schatz et al. have concluded that if a mixed-valence system is a class III compound, Hush's formulas cannot be applied to the intervalence absorption profiles (126,127).

An additional check on the applicability of the Hush model can be made by obtaining spectra in a series of solvents. Hush has predicted that E_{op} for the intervalence transfer band varies linearly with $(1/n^2 - 1/D_s)$ where n^2 and D_s are the optical (refractive index) and static dielectric constants of the solvent. Unfortunately, since [P(II,III)l-MeU]$(ClO_4)_3$ is either insoluble or unstable in virtually all solvents other than water (see Experimental section), this study could not be made.

Pl-MeUB -

Figure 45 shows the series of spectra obtained in the course of an oxidative electrolysis of the platinum blue complex.

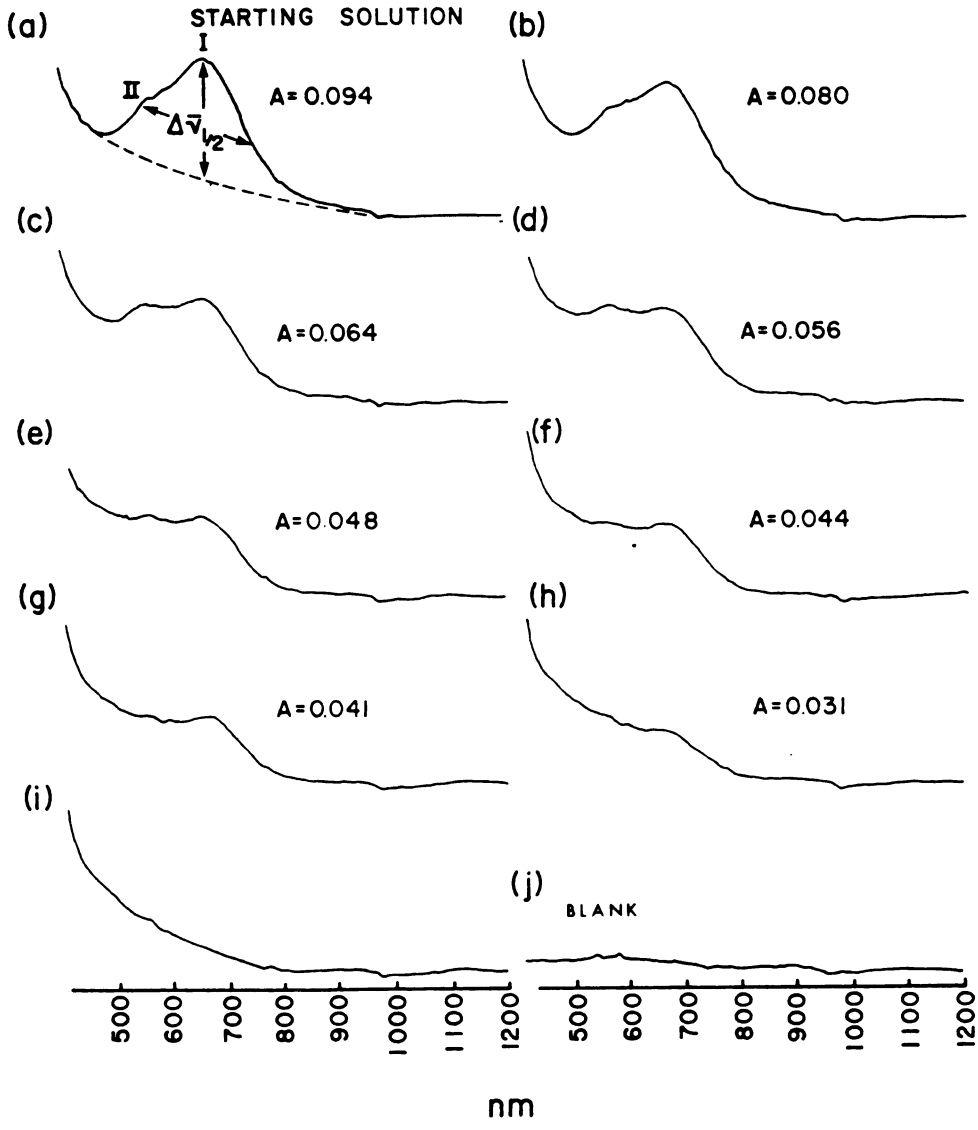

Figure 45. NIR/Vis spectra of Pl-MeUB (conc. of 1 mg/ml) taken at 1/8 intervals throughout an oxidative electrolysis; sensitivity, 0.2 AUFS.

Prior to electrolysis, a band with λ_{max} at 660 nm (band I) is evident with a shoulder (band II) at lower wavelength. As band I recedes, band II grows. From about 25% completion to 60% completion, the ratio of band I to band II is relatively constant. Beyond this point, the contribution of I becomes smaller, and a gradual rise in the absorption curve, but with no resolution between bands, is noted until the absorbance is off scale. This follows the color progression from green-blue →→ honey-brown. The spectrum of reductively electrolyzed Pl-MeUB (not shown) reveals, by comparison, faint absorbance above ~480 nm.

A figure for ε can only be estimated since the molecular weight (avg.) of Pl-MeUB is not accurately known. We can note, however, that the maximum absorbance (ε_{max}) was recorded for the unelectrolyzed material. As the electrolysis proceeds, the absorption spectrum changes from one dominated by intervalence transfer to a conventional one in which electrons are promoted between electronic levels. Note that the position of the band I maximum is unchanged throughout the electrolysis. It bears mentioning that Chang et al. estimated that the molar absorptivities of platinum blues are generally greater than 500 M^{-1} cm^{-1} (24), although the basis of their estimate is unknown to the present author since the molecular weights of platinum blues are not accurately known; neither did they provide any estimates of molecular weight. In the first publication on platinum pyrimidine blues, Rosenberg et al. estimated molar absorptivities on the order of 500-1000 M^{-1} cm^{-1}

for several uracil and thymine blues (2). Barton et al. estimated molar absorptivities of several hundred for a platinum uracil blue and a platinum hypoxanthine green and estimated ε = 1100-1500 M^{-1} cm^{-1} for platinum acetamide blue (18).

In an earlier section, by use of RDV and the Einstein-Stokes equation, the average molecular weight of Pl-MeUB was estimated to be ~25,500 (p. 137). This corresponds to a mean number of repeating units equal to 30. However, the uncertainty in the calculated molecular weight is considerable because the value of n ($1 < n < 2$), obtained by RDV, is uncertain. n is required to calculate D, the diffusion coefficient, which in turn is one of the parameters in the Einstein-Stokes equation. Since a value of 20 for the number of repeating units appears to be in better conformity with current belief (18), this value will be used to estimate $\bar{\varepsilon}$ (mean ε) for native Pl-MeUB. Twenty repeating units corresponds to a molecular weight of app. 20x832 = 16640. From Figure 45 it can be seen that the absorbance of a 1.0 mg/ml $\rightarrow \frac{1.0 \text{ mg}/1.0 \text{ ml}}{16640 \text{ mg/mmol}} = 6.0\text{x}10^{-5}$ M solution of Pl-MeUB is 0.094; a cell of 1 mm pathlength was used to make the measurement. Then $\bar{\varepsilon} = 0.094/(0.1 \text{ cm} \times 6.0\text{x}10^{-5} \text{ M}) = 15667 \simeq 15{,}500$ M^{-1} cm^{-1}, a very high value compared to the estimates of Rosenberg and Barton reviewed above. Considering that the compounds for which their estimates were made included platinum uracil blues, it is obvious that an accurate estimate (theirs and ours) is contingent on a reliable figure for the average molecular weight.

As indicated, band I may be assigned as an intervalence transfer

band. Band II appears to be associated with the presence of Pt(III), but does not grow in proportion to the concentration of Pt(III). Using the $\bar{\varepsilon}$ value just calculated, Hush model calculations will be made, thereby allowing us to gauge the extent of delocalization (α) along the polymeric chain. Chang et al., by apparently making an assumption regarding the average molecular weight for platinum phthalimide blue, obtained the result $\alpha \tilde{=} 0.12$. This value led these authors to classify this system as class II-class III borderline. It is of interest to note that their calculated bandwidth of 6300 cm^{-1} (using $\bar{\nu}_{max} = (\Delta\bar{\nu}_{1/2})^2/2310$) exceeded the measured value of 3900 cm^{-1}.

Hush Model Treatment of Pl-MeUB. As the magnitude of $\bar{\varepsilon}$ for Pl-MeUB is known with so little certainty, the calculations to follow are to be regarded only as being indicative. They should not be assumed to possess the same degree of accuracy as in the earlier section on the well-characterized Pl-MeU.

The absorbance maximum for native Pl-MeUB is at $\lambda = 660$ nm $= \lambda_{max}$ (band I, first spectrum in Figure 45). Then $\bar{\nu}_{max} = \frac{1}{\lambda_{max}} = 1.52\text{x}10^4$ cm^{-1}. The bandwidth at half-height was estimated as shown in the figure: $\Delta\bar{\nu}_{1/2} = 0.44\text{x}10^4$ cm^{-1}. From above, $\bar{\varepsilon}_{max} = 15.5\text{x}10^3$ M^{-1} cm^{-1}. Again,

$$\alpha^2 = \frac{(4.2\text{x}10^{-4})\ \bar{\varepsilon}_{max}\Delta\bar{\nu}_{1/2}}{\bar{\nu}_{max}\cdot d^2\cdot g^2} \qquad (219.1)$$

We will use a value d = 2.91 Å (see p. 219); g, the difference in

oxidation state, = 1. Then

$$\alpha^2 = \frac{4.2\times10^{-4}\times15.5\times10^{3}\times0.44\times10^{4}}{1.52\times10^{4}\ (2.91)^2\cdot1^2} \rightarrow \alpha = 0.47$$

If, on the other hand, a more conventional value of $\bar{\varepsilon}$ were used, say 1000 M^{-1} cm^{-1}, a value more in keeping with the ranges reported by Rosenberg and Barton, then a delocalization value $\alpha = 0.12$ is obtained. This is the same as the value reported by Chang et al. for platinum phthalimide blue, mentioned above. These authors classified their system as class II. For an $\alpha = 0.47$, the system is class III, roughly 50% delocalized, no longer a trapped-ion system.

Continuing with the Hush model calculations, $E_{op} = \bar{\nu}_{max} \leq 4E_{th}$ leads to $E_{th} \geq 10.8\times10^{3}$ cal mol^{-1}. Then $k_{th} = \frac{kT}{h} \exp\left[-\frac{E_{op}/4}{RT}\right] \rightarrow k_{th} = 7.1\times10^{4}$ sec^{-1}. These values are consistent with those obtained earlier for the dimer precursor. A check on the appropriateness of the Hush model is provided by $\bar{\nu}_{max} = (\Delta\bar{\nu}_{1/2})^2_{calc'd}/2310$ ($\bar{\nu}$ in cm^{-1}). Using this equation, a value $(\Delta\bar{\nu}_{1/2})_{calc'd} = 5.9\times10^{3}$ cm^{-1} is obtained. This compares quite well with the $(\Delta\bar{\nu}_{1/2})_{observed} = 4.4\times10^{3}$ cm^{-1}. On the other side of the ledger, for $\alpha > \sim0.25$ (class III designation), the suitability of Hush's formulae has been called into question (126,127).

Controlled-Potential Coulometry Coupled with Electron Spin Resonance Spectroscopy (128-131)

A brief discussion of the application of ESR to platinum blues was presented in the Literature Review. All authors attribute any

observed paramagnetism to the unpaired spin of the d^7 platinum. Further, varying amounts of delocalization along the Pt chain are postulated to account for the observed hyperfine structure. In this section the ESR spectra of platinum 1-methyluracil blue, Pl-MeUB, acquired at various stages of electrolysis, will be discussed. In addition, spectra of the platinum 1-methyluracil dimer, Pl-MeU, also taken throughout an electrolysis, will be treated. The simpler dimer better lends itself to a rigorous treatment than does the less-well characterized, polmeric Pl-MeUB, and will therefore be dealt with first. The author is unaware of any ESR studies of dimeric platinum compounds similar to Pl-MeU. This is understandable, since, without perturbation (as, for example, is afforded at an electrode), these compounds exist either as Pt^{II}-Pt^{II} or Pt^{III}-Pt^{III} dimers, and are diamagnetic.

The conjoining of electrochemistry and ESR spectroscopy is a natural couple since electrochemistry, through the appropriate choice of electrochemical technique and potential/current setting, offers a high degree of control in the generation of paramagnetic species. By far, the greatest application has been to the generation of organic free radicals, those both of a transitory nature and those longer-lived. For the most stable species, ESR measurement may be off-line, with electrogeneration in this case most often by controlled-potential electrolysis. For transient species, the electrochemical cell and EPR measuring vessel may be incorporated into the same device. In this case, the electrochemical technique is

often of a more transient nature, as in polarography. Two detailed treatments dealing with the combination of electrochemistry and ESR in organic chemistry have been published (130, 131). Many inorganic ions, particularly transition metal ions, with their partially-filled d orbitals, have been widely studied by EPR, and, in fact, have provided much fodder for the theoretical development of the technique. However, the generation of paramagnetic inorganic ions for EPR study by electrochemical means has been relatively sparse compared to its much wider use in the generation of free radicals in organic chemistry. No discussion of the principles of ESR spectroscopy will be given here, as many monographs and texts are available on the subject.

ESR of Pl-MeU -

In taking ESR spectra of Pl-MeU in solution, two decidedly contrasting sets of spectra were obtained - one displayed hyperfine structure, the other was devoid of hyperfine structure. The former situation is evident in the spectra of Figure 46, which shows the spectra of the unelectrolyzed compound, and of the 1/4-, 1/2-, 3/4- and fully-electrolyzed material; the latter situation is shown in Figure 47. An accounting of this difference will be deferred until later.

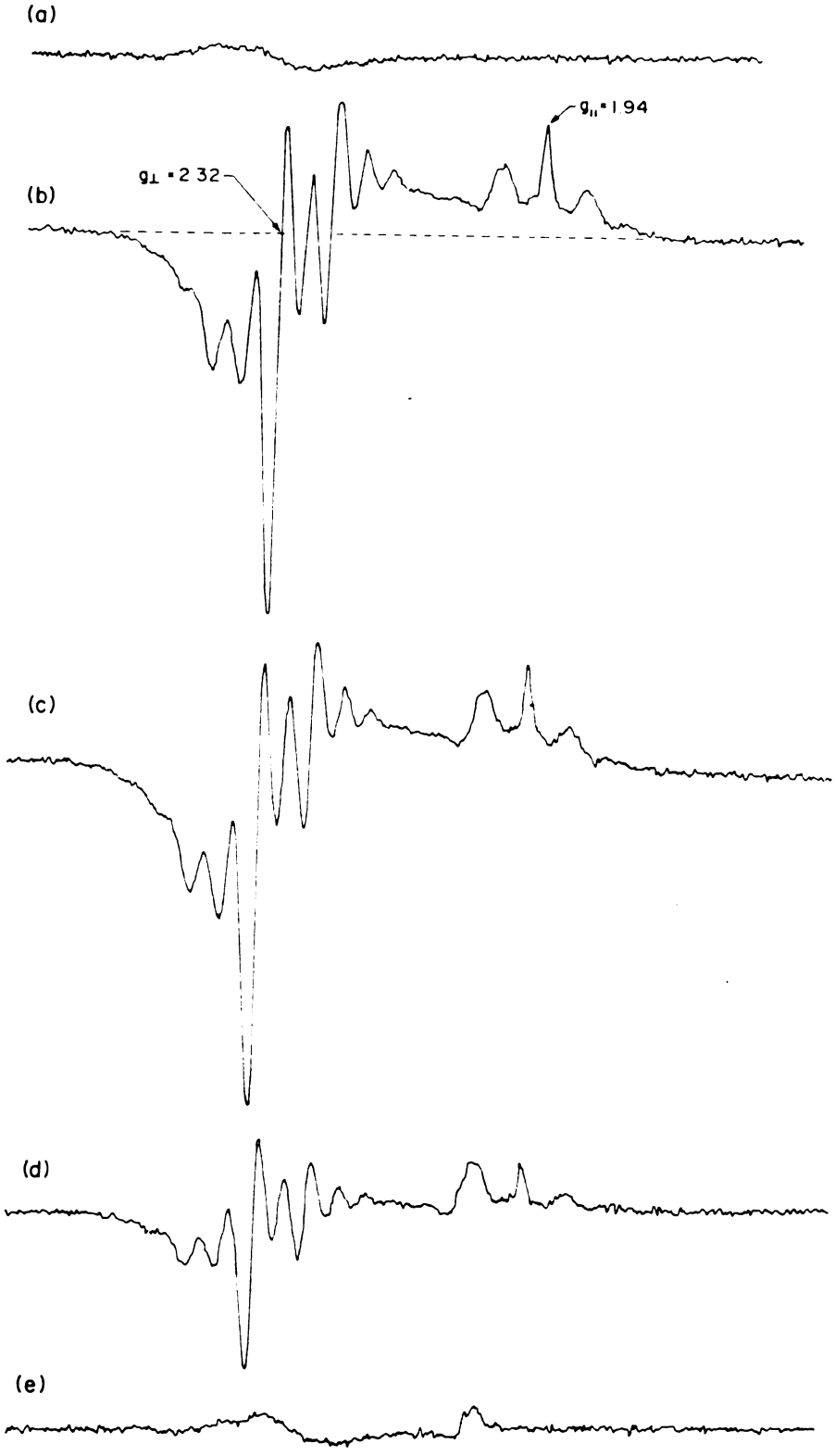

Figure 46. ESR frozen-solution (~-140°C) spectra of a) native (unelectrolyzed), b) 1/4-, c) 1/2-, d) 3/4-, and e) fully-electrolyzed Pl-MeU (2.4 mM) in nitrate (0.1F) medium. X band, freq. = 9.14×10^9 Hz, field set at ~3270 G, mod. freq. = 100 kHz, mod. amp. = 25 G, microwave power = 30 mW.

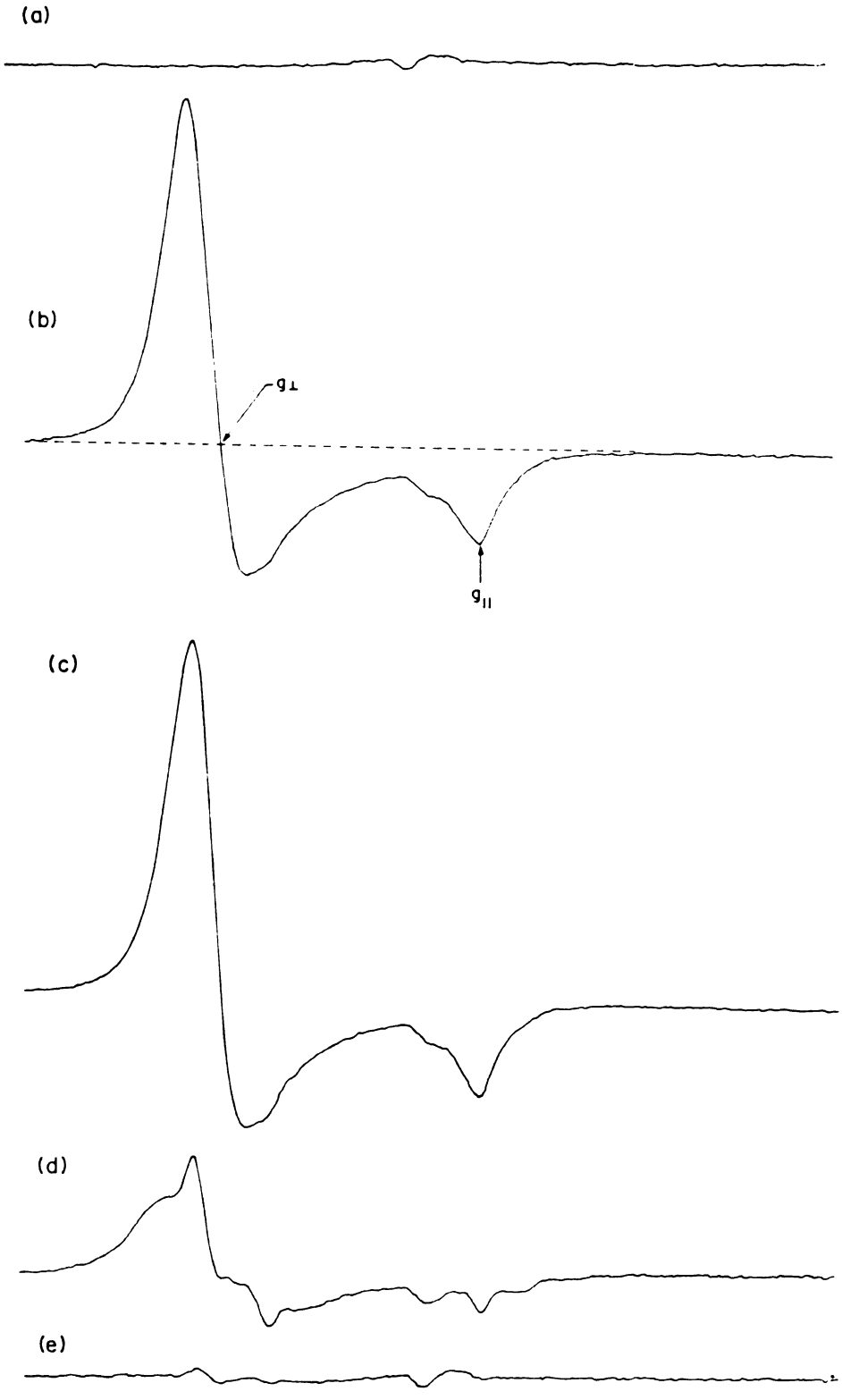

Figure 47. ESR frozen-solution (~ -150°C) spectra of a) native (unelectrolyzed), b) 1/4-, c) 1/2-, d) 3/4-, and e) fully-electrolyzed Pl-MeU (2.4 mM) in perchlorate (0.02F) medium. X band, freq. = 9.52×10^9 Hz, field set at ~3400 G, mod. freq. = 100 kHz, mod. amp. = 32 G, microwave power = 15.8 mW. The differential presentation shown here is the usual one; that in Figure 46 is inverted.

The important thing to note now is that in both of these situations, the initial spectrum, that for P(II,II)1-MeU, exhibits no EPR signal. Somewhere between the 1/4 and 1/2 points in the electrolysis, the perpendicular component of the signal (whether split or unsplit), for which $g_{\perp} \tilde{=} 2.32$ (vide infra), has peaked. At the 3/4 point the amplitude is decreasing until the final electrolysis product is reached, where once again there is no ESR signal.

Accurate quantification of the intensity of the ESR signal requires double integration since the usual differential presentation(as in Figures 46 and 47) is the approximate first derivative of the true absorbance. Nevertheless, if all instrumental conditions are kept constant from run to run, then the peak-to-peak amplitude of the derivative curve is a reasonable gauge of absorption intensity (132). The peak-to-peak amplitude (in arbitrary units) of the most intense peak as a function of the extent of electrolysis is shown for both cases in Table 10.

Table 10
Peak-to-Peak Amplitude[1] of Differential Signal vs Percent Electrolysis for P1-MeU

Percent Electrolyzed	Split (Fig. 46)	Unsplit (Fig. 47)
0	0	0
~25	1.0	0.98
~50	0.90	1.0
~75	0.47	0.36
100	0	0

[1] in arbitrary units

In the section on CPC/Vis it was pointed out that the color intensity reaches a maximum at app. 3/8 of the way through the electrolysis. (The electrolysis was sampled eight times in conjunction with the electronic absorption measurements whereas only four samplings were made for EPR analysis.) Those results combined with the ones here suggest that the electronic absorption intensity and EPR signal intensity behave in parallel fashion, which further implicates the unpaired electron as the source of both observations. This is reasonable since, according to the Hush model, the intensity of the absorption band is ascribed to intervalence transfer. As an analysis to follow will show, the intervalent electron is an unpaired electron. This same dual behavior had been previously noted by Barton et al. in an experiment on platinum α-pyridone blue (PPB), a tetramer, in which the reduction in the intensity of the blue color upon titration with Ce(IV) paralleled the reduction in unpaired spin intensity as measured by EPR (18).

Interpretation of Spectra. The EPR spectrum of $[P(II,III)1\text{-MeU}]^{3+}$ is that characteristic of axial symmetry, with anisotropic g values of $g_{\perp} \tilde{=} 2.31$ and $g_{\parallel} \tilde{=} 1.94$ either as the solid or as the frozen aqueous solution. This type of spectrum may be described by the following axial spin Hamiltonian (18, 31, 59):

$$H = \beta[g_{\parallel}S_zH_z + g_{\perp}(S_xH_x + S_yH_y)] + A_{\parallel}S_zI_z + A_{\perp}(S_xI_x + S_yI_y) \quad (235.1)$$

where β is the Bohr magneton, S is the spin operator (with S = 1/2), H is the magnetic field, A is the hyperfine tensor, and I is the

nuclear angular momentum operator. The anisotropy results from coupling of the spin and orbital angular momenta, which is appreciable, and is typical of heavier paramagnetic transition metal ions (platinum is a fifth row element). In dilute solution, an isotropic spectrum is usually obtained, with average values for g (and for a, the hyperfine coupling constant). However, when the solution is frozen (as here), an anisotropic spectrum is usually obtained, particularly for transition metal ion complexes, because the resulting spectra are not those of a motionally-averaged system. If there were no spin-orbit coupling, the isotropic value $g = g_e = 2.0023$ would always be observed.

Having just mentioned PPB in the previous subsection, it is pertinent to note the similarity of the ESR spectrum of PPB (avg. formal oxidation state of 2.25) (18) and that of $[P(II,III)1\text{-MeU}]^{3+}$ exhibiting hyperfine structure. For PPB, and in fact, for all platinum blues for which EPR spectra have been obtained, the spectra are explained by invoking axial symmetry containing both parallel and perpendicular orientations, with the unpaired spin located in a d_{z^2} atomic orbital (5, 12, 18, 30, 31, 33, 34, 47, 56, 57, 58). Although this postulation is probably correct, the same symmetry arguments which apply to the original model referenced by all authors - that developed by Krigas and Rogers (59) - do not strictly apply to the blues. Let's see what arguments can be brought to bear to account for the EPR behavior observed for Pl-MeU. Throughout this discussion keep in mind the structure of Pl-MeU, surmised in part from analogs

whose structures have been crystallographically determined (50, 74), but also from direct spectroscopic measurement (80); this structure has been shown several times previously and is repeated here.

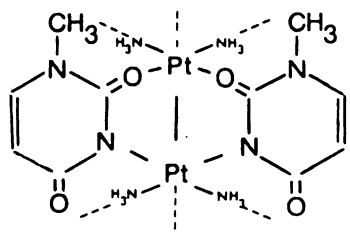

Pl-MeU

Krigas and Rogers showed that γ-irradiation of K_2PtCl_4 at 77 K led to the formation of radicals giving rise to ESR spectra. The crystal structure of K_2PtCl_4 consists of square-planar units stacked in alternate lamellae along the z axis with four potassium ions in between. The distance between lamallae is 4.13 Å, while the Pt-Cl distance is 2.33 Å. The symmetry point group for each Pt atom is D_{4h}. One type of ESR spectrum obtained showed axial symmetry and was postulated to arise from $[(PtCl_4)_2]^{3-}$, a d^{15} species ($d^8 + d^7$). To order the d atomic orbitals and consequent molecular orbitals, ligand field theory was applied.

The energy ordering of the five metal d orbitals in proceeding from an octahedral to a tetragonal (square-planar) field is shown in Figure 48.

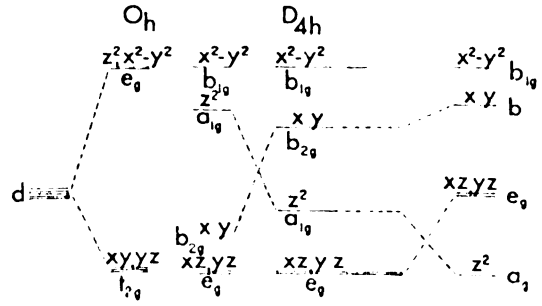

Figure 48. Ordering of the five d orbitals in an octahedral field with increasing axially-elongated tetragonal distortion from left to right (taken from ref. 59).

The intermediate states correspond to tetragonal distortion due to axial elongation. Which of the three orderings applies depends on the extent of interaction between ligand and metal. Using a crystal field method, g values corresponding to these three possibilities were calculated. Two pairs were consistent with the experimentally-obtained order $g_{\perp} > 2 > g_{\parallel}$: $g_{\perp} > 2 = g_{\parallel}$ for the d_{z^2} orbital containing the unpaired electron and $g_{\perp} > 2 > g_{\parallel}$ for d_{xy}. Since at the large separation (4.13 Å) between consecutive platinum nuclei, the small overlap between d_{xy} orbitals along the z axis could not possibly alter the energy levels to the extent required by the g values, it was concluded that only d_{z^2} was consistent with the evidence.

Taking the case of extreme tetragonal distortion, the following molecular orbital energy diagram was proposed (Figure 49).

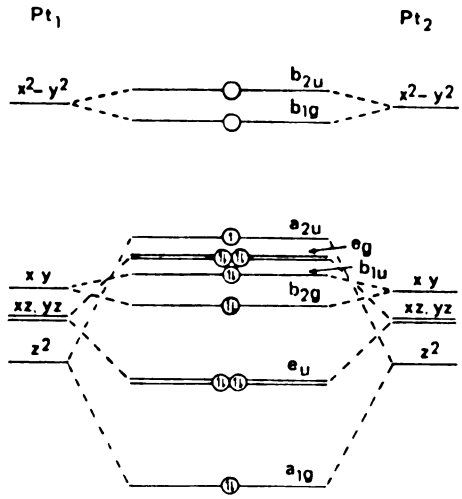

Figure 49. Possible molecular orbital energy level scheme for tetragonally-distorted octahedral field (taken from ref. 59).

Apparently, the ordering of electronic levels from absorption studies (in the ultraviolet and visible regions), which could serve to confirm the proposed ordering, is uncertain because it is difficult to assign an absorption band to a certain transition between multiplets, due to the presence of strong spin-orbit coupling (60). For the γ-irradiated crystal, removal of an electron from the $d^*_{z^2}$ or a_{2u} orbital results in a hole-like state. Strict application of Krigas' and Rogers' results requires a symmetry point group no lower than C_{4v}.

Amano and Fujiwara also produced Pt(III) ions upon γ-irradiation of divalent and quadrivalent homonuclear, crystalline complexes (60). Also using ligand field theory, they calculated g values expected for the different ground states possible for a low-spin d^7 configuration in a structure undergoing uniaxial elongation (133). Their conclusion

was that $g_{\perp} > g_{\parallel} = 2$, corresponding to a $^2A_{ig}$, implicating tervalent platinum, with the unpaired electron residing in the $5d_{z^2}$ orbital. Furthermore, they predicted that the parallel axial component should be much weaker than the perpendicular one.

As far as Pl-MeU is concerned, the symmetry about each Pt (as drawn on p. 237) is not D_{4h}, but rather C_{2v}. However, an analogy can be drawn between the arrangement about each platinum in Pl-MeU and that in cis-$Pt(py)_2Cl_2$, one of the systems treated by Amano and Fujiwara (60) (vide supra). These authors point out that, although this compound does not have a fourfold axis, the electronic state can be explained approximately in terms of D_{4h}; the ligand field of cis-type complexes has D_{4h} symmetry, contrary to their geometrical symmetry (134). The large g-shift ($g_{\perp} = 2.54$) of cis-$Pt(py)_2Cl_2$ shows that, despite the lack of a fourfold axis in geometrical structure, the complex, nevertheless, has D_{4h} or C_{4v} symmetry.

We now have the information necessary to render an interpretation to the ESR behavior of Pl-MeU. There is a caveat, though, in that the ligand field model for tetragonal distortion via axial elongation from an octahedral field assumes six identical substituents, which is not the case for Pl-MeU. Obviously then, the ligand field calculations, if they could be made at all, would differ somewhat from the idealized case, but here we will assume the effects of this perturbation to be negligible.

To apply axial-elongation arguments to Pl-MeU is reasonable. One-half of the structurally-characterized platinum α-pyridone blue

is much like Pl-MeU, with double-bridging of the α-pyridone groups through O and N between Pt atoms (see the structure on p. 27). In this compound the interatomic distances are Pt-Pt - 2.774 Å (within each dimeric unit), mean Pt-N (N from ammine groups) - 2.027 Å, Pt-N (N of α-pyridone group) - 2.026 Å, Pt-O (O of α-pyridone group) - 2.019 Å, and Pt-O (O from capping NO_3^- counter ion) - 3.321 Å. The first and last bond distances represent axial elongation. Similarly, in the head-to-tail bis(μ-(1-methyluracilato-N^3,O^4))-bis(cis-diammineplatinum(II)) dinitrate trihydrate, the Pt-Pt distance is 2.954 Å; Pt-N distances (to both ammine and uracil nitrogens) range from 2.03-2.08 Å, and Pt-O distances to uracil span 2.03-2.07 Å; the distance between Pt and the nitrate counter ion is not given (74). In the latter compound the bonds about each platinum form a square plane, with one square plane lying roughly over the other.

Invoking the tetragonal distortion of Figure 48 and the orbital ordering of Figure 49, which for P(II,III)1-MeU is supported by axial symmetry and $g_\perp \cong 2.31 > g_\parallel \cong 1.94 \cong 2$, the interpretation made then is that in going from $[P(II,II)1\text{-MeU}]^{2+}$ to $[P(II,III)1\text{-MeU}]^{3+}$, an electron is lost from the $d^*_{z^2}$ (a_{2u}) molecular orbital, thereby generating a $1e^-$ bond between Pt centers. The magnitude of the perpendicular g factor suggests that the unpaired electron is largely associated with platinum since platinum has a large spin-orbit coupling constant, and corresponds to that expected for $5d_{z^2}$ holes with admixture, due to the spin-orbit interaction, from the degenerate $d_{xz,yz}$ level. Placing the odd electron in the d_{z^2} orbital

is the only conclusion consistent with the experimental evidence.

Mehran and Scott also postulated localized d_{z2}-like states in the "one-dimensional" metal-chain, semiconductor compound - Magnus's green salt, $Pt(NH_3)_4PtCl_4$ (135). Similarly, the g factors observed for the mixed-valence platinum complex $K_2Pt(CN)_4Br_{1/3}\cdot 3H_2O$ also implicate d_{z2}-like hole states, again with an admixture, due to spin-orbit interaction, of the degenerate e_u ($5d_{xz,yz}$) states (136).

The EPR behavior of Pl-MeU during electrolysis can be accounted for by reference to Figure 46. P(II,II)l-MeU is diamagnetic because all electrons are paired; the configuration of each platinum atom is low-spin $d^8(d^2_{z2}, d^4_{xz,yz}, d^2_{xy})$. In general, four-coordinate, square-planar complexes of Pt(II) have the low-spin d^8 configuration, and hence given no ESR signal. In P(II,III)l-MeU the odd electron is found in the $a_{2u}(5d^*_{z2})$ molecular orbital. In proceeding to P(III,III)l-MeU, the odd electron is given up, which leaves all electrons paired (d^7-d^7); hence the complex is EPR silent. Conversely - and this is an important point - the fact that the Pt(III)Pt(III) complex is EPR-silent, implicates Pt-Pt overlap. Without the aid of ligand/M.O. theory, the EPR behavior could not be explained, since in a (d^7,d^7) system, without invoking coupling between platinums and pairing of electron spins, the EPR signal intensity would be expected to increase over its intensity in P(II,III)l-MeU rather than falling to zero. Finally, the M.O. picture in Figure 49 is not a complete one, since ligand orbitals have not been included. However, the overlap of d_{z2} orbitals with

ligand orbitals is very slight. Intuitively, we would expect that the electrons given up during electrolysis are primarily associated with the metal sites.

Improved g Values. It was mentioned in the discussion above that the use of crystal (ligand) field theory allows the calculation of g values. An improved set of g values may be obtained by including perturbation calculations to the first-order (31), or better yet, by including second-order perturbation terms (59). For an unpaired electron in the d_{z^2} orbital, the equations are $g_{\parallel} = 2$ and $g_{\perp} = 2 + \frac{6\xi}{\Delta E}$ for first-order adjustment, and

$$g_{\parallel} = 2N^2 - 3N^2(\xi/\Delta E)^2 \qquad (243.1)$$

and

$$g_{\perp} = 2N^2 + 6N(\xi/\Delta E) - 6N^2(\xi/\Delta E)^2 \qquad (243.2)$$

for second-order adjustment (137). In these equations N is the normalization coefficient of the zero-order configuration in the wavefunction that arises from the spin-orbit interaction, ξ is the spin-orbit coupling constant, and $\Delta E = E(e_u) - E(a_{2u})$ is the average energy separation between the d_{z^2} and degenerate d_{xz}, d_{yz} states. Substituting $g_{\perp} = 2.328$ and $g_{\parallel} = 1.944$ (obtained for the solid) into eq. 243.1 and 243.2, $N = 0.989$ and $\xi/\Delta E = 0.068$ are obtained for P(II,III)1-MeU. The parameters ξ and ΔE are not separately determinable by EPR. These values for N and $\xi/\Delta E$ may be compared with those obtained for several other compounds as shown in Table 11; g values are also given.

Table 11
Comparison of N and $\xi/\Delta E$ Values

Compound	N	$\xi/\Delta E$	$g_\perp$	$g_\parallel$	Ref.
$K_2Pt(CN)_4Br_{1/3}\cdot 3H_2O$	0.99	.067	2.336	1.946	136
Pt(IV)-doped $[Pt(NH_3)_4][Pt(CN)_4]$	.99	.10	2.504	1.939	135
$[(PtCl_4)_2]^{3-}$	.964	.180	2.723	1.770	47
Platinum α-pyridone blue (PPB)	.997	.071	2.380	1.976	59
P(II,III)1-MeU	.989	.068	2.328	1.944	This work

A decrease in the magnitude of $g_\perp$ may be interpreted as a reflection of <u>increased</u> delocalization of the unpaired spin. This suggests that γ-irradiated K_2PtCl_4, which results in the production of $[(PtCl_4)_2]^{3-}$, is considerably localized (Pt-Pt separation is 4.13 Å), whereas the α-pyridone blue (Pt(1)-Pt(2) - 2.774 Å, Pt(2)-Pt(2′) - 2.877 Å, where primed and unprimed refer to the two units comprising the tetramer) and P(II,III)1-MeU are much less so. The smaller $g_\perp$ factors and smaller $(\xi/\Delta E)$ values may be taken to reflect increased d_{z^2} character, and less mixing with the d_{xz}, d_{yz} states as reflected in an increased energy level separation, $\Delta E = E_{d_{z^2}} - E_{d_{xz}, d_{yz}}$.

<u>Hyperfine Splitting in P(II,III)1-MeU</u>. The differences in the two sets of spectra in Figures 46 and 47 were previously noted. The spectrum of the solid $[P(II,III)1\text{-}MeU](ClO_4)_3$ is as in Figure 50a - i.e., a broad signal with no hyperfine splitting. The spectra of the solid in pure water and of the solid dissolved in aqueous solution containing perchlorate are virtually identical and are somewhat

broader than the spectrum of the solid; they are exemplified by the spectrum in Figure 50b.

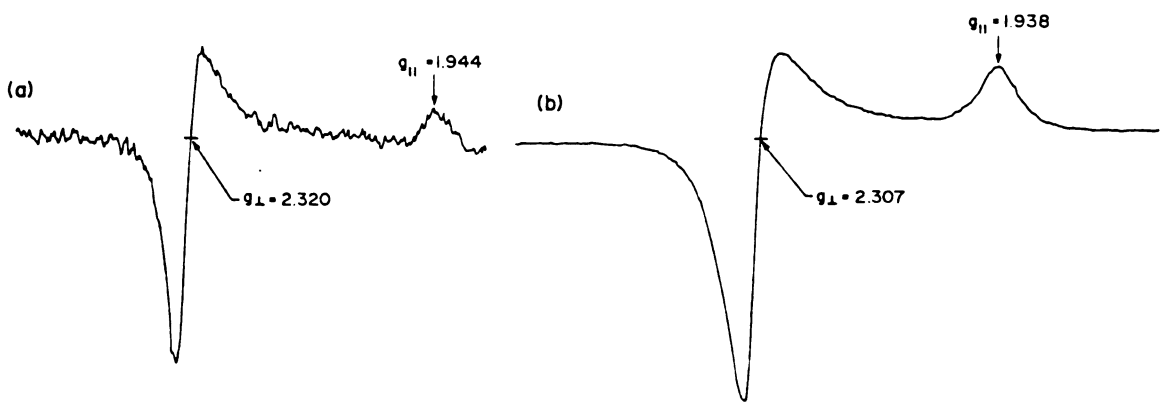

Figure 50. ESR spectra of a) [P(II,III)1-MeU]$(ClO_4)_3$ as the solid and of b) the solid in aqueous frozen solution (~-140°C). Measured g values are shown. Instrumental settings were as in Figure 46.

Hyperfine structure results from the interaction of the electron and nuclear spin moments. The regularity of the splitting pattern in Figure 46 suggests that only one type of nuclear species is causing the splitting, most probably ^{195}Pt (33% abundant, I = 1/2), and not the inequivalent nitrogens ($I_{^{14}N}$ = 1) contributed by the ammines and uracil groups, although the width of each line may be limited ultimately by unresolved superhyperfine interactions with the ligand nitrogens. No other naturally-occurring isotope of platinum (^{194}Pt, ^{196}Pt) has a nonzero nuclear moment. The hyperfine coupling constants measured in Figure 46d, given by $a(g/g_e)$ (138), where a is the separation between peaks in gauss, and g and g_e are the g factors of the species in question and of the electron, are given in Table 12 along with the values for platinum α-pyridone blue (PPB) reported by

Barton et al. (18).

Table 12
Comparison of Splitting Constants for
P(II,III)1-MeU and PPB

Platinum 1-methyluracil[1]		Platinum α-pyridone blue[2]	
a	$a(g/g_e)$	a	$a(g/g_e)$
60 G	70	68 G	81
66	76	65	77
58	67	63	75
49	57	65	77
62	72	58	69
49	57	70	83
56	65	66	78

[1] $g = 2.321$ [2] $g = 2.380$

Those authors assigned the hyperfine coupling to the interaction of the unpaired spin with the ^{195}Pt nuclei. There as here, assignment of the hyperfine splitting to ligand nuclei would not be reasonable given the small overlap of d_{z^2} and ligand orbitals, particularly in light of the large coupling constants obtained.

For localization to a single platinum atom, a 1:4:1 line pattern is expected. This is because platinum, with I = 1/2, is 33.7% abundant. Were the ^{195}Pt nearly 100% abundant, then the familiar 1:1 pattern would be obtained, as, for example, for an electron split by ^{1}H in an organic free radical. For delocalization over two

equivalent platinum atoms, a 1:7.9:1:16.5:7.9:1 intensity distribution is calculated (58, 59), a result following from both the statistical distribution of ^{195}Pt nuclei over the two centers and from superposition of lines. The splitting pattern in Figure 46d does not agree particularly well with the theoretical calculation. As we have other evidence that supports the delocalization of the electron over the two platinums (the EPR evidence given in the previous section and the Hush model calculations), we might therefore expect the theoretical distribution of lines. The deviation of the line pattern from the theoretical may, perhaps, be best explained by postulating nonequivalence of the two platinum atoms in this head-to-head dimer, a condition that would lead to nonequal spin densities on the two atoms. Allowance should also be made for the weak spectra of Figure 46, which makes accurate intensity determinations difficult and somewhat uncertain. Actually, water, the solvent used here, and similarly high-dielectric solvents, are not solvents of choice in EPR spectroscopy because they strongly absorb microwave power. A difference in relaxation rate (line broadening) and the introduction of second-order splitting can also affect the intensities of lines (18).

Hyperfine vs No Hyperfine. As to why hyperfine splitting is apparent in frozen solutions in the presence of nitrate but absent in a perchlorate medium and in the solid with perchlorate as anion - this has not been answered to this point, and is not a trivial question. To explain this behavior is not central to the main thrust of EPR as

it applies to the overall characterization of Pl-MeU, but regardless, it is of interest in its own right. To succintly summarize the experimental observations: A broad, unsplit perpendicular component was obtained for the solid [P(II,III)l-MeU]$(ClO_4)_3$ at room temperature and for the solid dissolved in water or in 0.02F $NaClO_4$. (Use of a higher perchlorate concentration, such as 0.1F, during the electrolysis led to precipitation of the mixed-valence product.) The electrolysis of P(II,II,)l-MeU in 0.1F $NaNO_3$ led to hyperfine-split spectra as exemplified in Figure 46.

A broad, unresolved signal is often observed in solid state ESR spectra, particularly when the unpaired spin density is high, although the variation in spin-lattice relaxation times in different systems can be quite large. The spin-lattice interaction is high in the compact solid state, T_1 (the spin-lattice relaxation time) is small, and consequently, the signal is a broad one. In contrast, resolved spectra can often be obtained in frozen solution. Such was the case for <u>cis</u>-diammine platinum α-pyridone blue (18, 47).

Nitrate is a more strongly ligating group than perchlorate, or equivalently for the purposes of this discussion, the nucleophilicity toward Pt^{II} (or Pt^{IV}) is in the order $ClO_4^- < H_2O < NO_3^-$ (139). When [P(II,III)l-MeU]$(ClO_4)_3$ is dissolved in water, perchlorate can be assumed to be only loosely associated with the cation. Then, just as repeating units are believed to be stacked in the platinum blues, they may similarly align themselves end-to-end in solution in the absence of a strongly ligating group. This, then, may result in

increased spin-lattice relaxation arising from interaction of spin magnetic dipoles at the relatively high concentration used here, and may also lead to electron spin exchange between neighboring ions; both effects would lead to broadened lines. Electron spin exchange processes can drastically influence line width and spectral appearance, particularly at higher concentrations. In the presence of the much stronger ligating NO_3^- ion, the axial positions are occupied by this ion. Therefore, line broadening by these two mechanisms is greatly diminished, and the hyperfine structure is manifest. The fact that a solution of 0.02F ClO_4^- concentration was used whereas a 0.1F concentration of NO_3^- was used, served to heighten this effect.

Instead of postulating end-to-end stacking of Pt units, we might alternatively postulate that in strictly aqueous solution and in perchlorate medium, the axial positions are dominated by water molecules. This intimate contact with water provides a path for spin-lattice interaction between the platinum compound and the solvent, and results in line broadening. In a nitrate medium, intimate contact with water molecules is precluded.

EPR of Pl-MeUB -

Figure 51 shows the five EPR spectra taken throughout the electrolysis of Pl-MeUB. The pre- and post-electrolysis spectra in a and e, respectively, are essentially those contributed by the noise of the system. The vanishingly weak spectrum of the native (unelectrolyzed) platinum 1-methyluracil blue offers additional support for the presence of relatively few Pt(III) ions compared to the number of Pt(II) entities present - i.e., the average formal oxidation state of Pt is close to 2. Even without examining the spectra, we might therefore anticipate considerable delocalization of the unpaired electron(s) in this compound. Unlike the situation for Pl-MeU, we cannot predict where the maximum should lie in a plot of integrated signal intensity vs extent of electrolysis. To be able to do so, we would need to know the extent of delocalization, the ratio of Pt(II) to Pt(III) over the delocalized chain, and would need to be able to describe the interaction among platinums in terms of molecular orbitals to account for spin-pairing of the Pt(III)'s formed during electrolysis. Using the peak-to-peak height of the approximately differential signal, the relative signal intensities at the approximate 1/4, 1/2, and 3/4 points in the electrolysis were 0.93, 1.0, and 0.83. At the 3/4 mark in the electrolysis of Pl-MeU, the relative intensity was below 0.5.

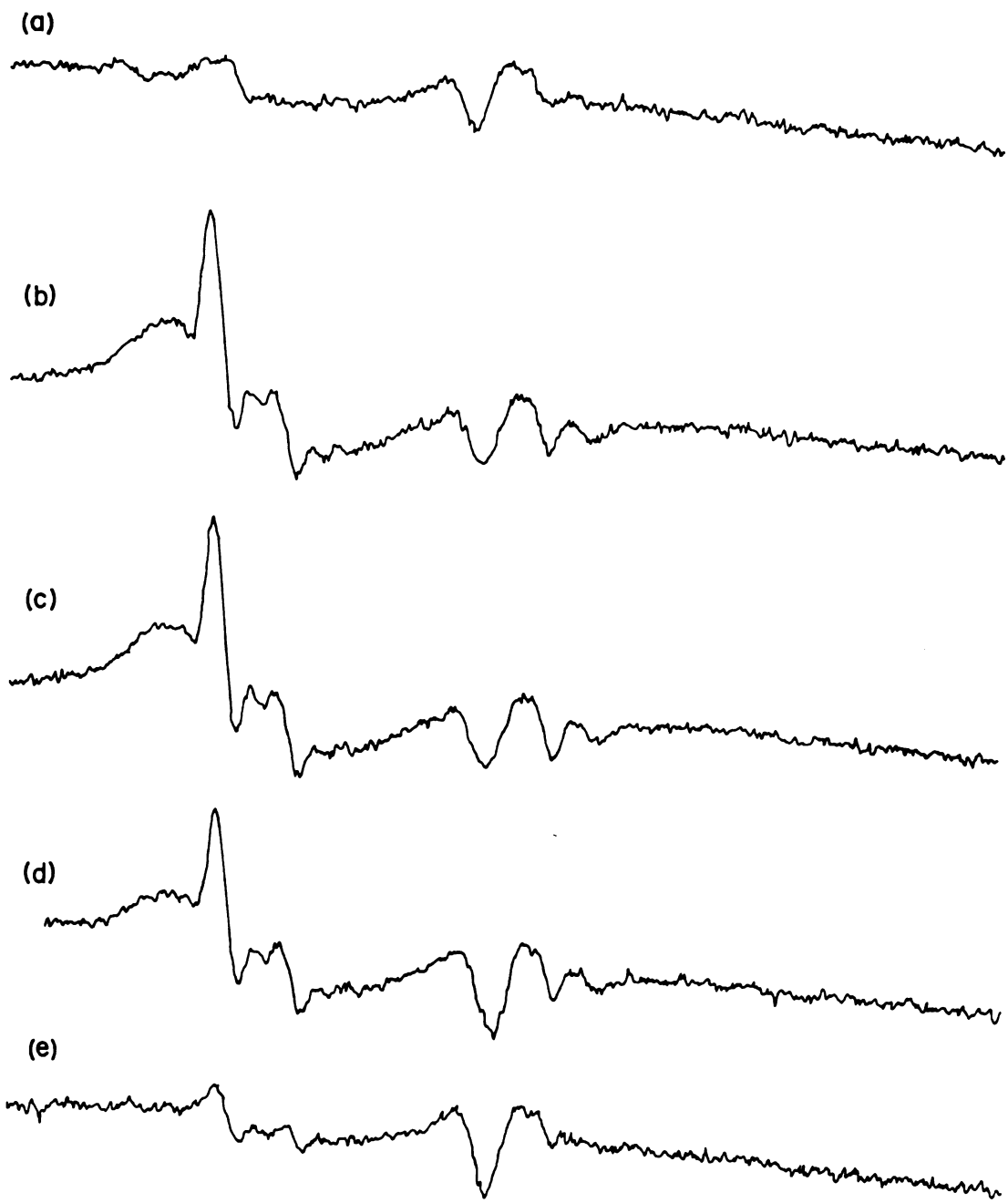

Figure 51. ESR frozen-solution (~-150°C) spectra of a) native (unelectrolyzed), b) 1/4-, c) 1/2-, d) 3/4-, and e) fully-electrolyzed P1-MeUB (2.0 mg/ml) in perchlorate (0.02F) medium. Instrumental settings were as in Figure 47.

Although the symmetry arguments applied to the interpretation of the ESR spectra of Pl-MeU are less applicable in the case of the blue, Pl-MeUB, the relationship of Pl-MeUB to Pl-MeU and the order $g_{\perp} = 2.275 > g_{\parallel} = 1.948 \tilde{=} 2$ argue for the same interpretation - i.e., the unpaired electron(s) is associated primarily with the overlapping $5d_{z^2}$ atomic orbitals along the Pt axis of the oligomeric chain. Hence, a columnar stacking of Pt units is postulated. Again, the primary ($\perp$) absorption suggests considerable spin-orbit coupling of the odd electron, which is to be expected for a heavy transition metal ion such as platinum. The spin Hamiltonian given by eq. 235.1 is again applicable. The same analysis involving second-order perturbation effects in describing g values used in the analysis of Pl-MeU can be made for the platinum blue. Substituting the values $g_{\perp} = 2.275$ and $g_{\parallel} = 1.948$ into eqs. 243.1 and 243.2, the values $N = 0.989$ and $\xi/\Delta E = 0.058$ are obtained. These values suggest <u>greater</u> delocalization for Pl-MeUB relative to Pl-MeU, consistent with what we would expect. Values of $g_{\perp}$, $g_{\parallel}$, N, and $\xi/\Delta E$ are compiled in Table 13 and compared with literature values.

Table 13
Comparison of $g_{\perp}$, $g_{\parallel}$, N, and $\xi/\Delta E$ Values for Platinum Blues

Compound	$g_{\perp}$	$g_{\parallel}$	N	$\xi/\Delta E$	Ref.
Platinum α-pyridone blue	2.380	1.976	0.997	.071	47
Platinum asparagine blue	2.39	1.97	$.99_2$	$.07_0$	33
Platinum (1-methylnicotinamide, guanosine) blue	2.41_8	1.97_9	.998	.076	30
Platinum glutamine blue	2.44	1.99	1.00(1)	.077(1)	34
Platinum 6-methyluracil:					
type O (oxidized)	2.394	1.991	1.00(1)	.071(1)	58
type R (reduced)	2.375	1.983	.999(1)	.068(1)	
Platinum cytosine blue	2.394	1.970	.996(1)	.073(1)	23
Platinum thymine blue	2.378	1.995	1.00(1)	.066(1)	23
Platinum 1-methyluracil blue	2.275	1.948	.989	.058	This work

(1) calculated by present author

Splitting Pattern of Pl-MeUB. EPR solution spectra of Pl-MeUB were obtained only in perchlorate medium, and not in pure water or in the presence of nitrate, so that the comparisons made for Pl-MeU cannot be made for Pl-MeUB. Intuitively, we might anticipate that line broadening by either of the mechanisms invoked to explain line broadening for Pl-MeU in solution - i.e., spin-lattice relaxation or spin-exchange between ions - will be less prevalent because of the lower unpaired spin density in Pl-MeUB. That is, because of the greater delocalization of an unpaired electron due to its being shared by a greater number of platinum atoms, the probability of interaction of the unpaired electron at a given site with either another platinum ion complex or with the solvent is reduced. This expectation is borne out in the spectra of Figure 51, which were taken with perchlorate as the counter ion. Recall that Pl-MeU gave

no hyperfine structure in the presence of perchlorate.

To attempt to make a definitive interpretation from the poorly-resolved, and generally ill-defined perpendicular component in these spectra is probably not well advised. The 1:4:1 and 1:7.9:1:16.5:7.9:1 intensity distributions were previously mentioned as those resulting from interaction of an unpaired spin over one and two equivalent platinums, respectively. A trimeric system would give an additional 1:4:1 splitting of each of the lines in the dimeric system; in a tetramer the expected intensity distribution is 0.2 : 4:23:68:100:68:23:4:0.2, and so on.

It is pertinent to note that in the structurally-characterized tetramer cis-diammineplatinum α-pyridone blue, neither the spectrum calculated assuming equivalent platinums nor that calculated assuming inequivalent platinums (although with the proviso that the coupling constants are integrally related in the latter case) agreed with the observed spectrum. In the case of the more complex Pl-MeUB, for which the evidence is that approximately 1 Pt in 12 or more is in the +3 oxidation state, the most that can be said is that the unresolved spectrum is suggestive of extensive delocalization over unknown numbers of platinums. It would, in fact, be unrealistic to expect a sharp, well-resolved spectrum, since the extent of delocalization may be expected to differ in chains of varying length. The delocalization noted here is a feature common to nearly all platinum blues. An exception is provided, apparently, by the blue involving 1-methylnicotinamide and guanosine as ligands in which the unpaired

electron appears to be much more localized, in fact, over just two platinums (30). The actual length of the chains cannot be determined from these spectra. Because of the low signal-to-noise ratio, the parallel component in the spectra of Pl-MeUB is not helpful in interpretation.

Summary of ESR Results -

Pl-MeU. ESR in conjunction with oxidative electrolysis has been instrumental in allowing the assignment of the III valence state in both Pl-MeU and Pl-MeUB. Native (unelectrolyzed) P(II,II)l-MeU is diamagnetic, each Pt being low-spin d^8. The P(II,III)l-MeU electrolysis intermediate is paramagnetic, while the fully-electrolyzed P(III,III)l-MeU is again diamagnetic. This behavior can be explained by invoking symmetry and ligand field arguments ala Krigas and Rogers (59) and Amano and Fujiwara (60, 133). For the case of tetragonal distortion in the ligand field due to axial elongation, a situation which obtains for Pl-MeU, M.O. theory may be used to postulate paired electron spins in the (II,II) and (III,III) species, and an odd electron with unpaired spin residing primarily in a $5d_{z^2}$ (a_{2u}) orbital in the (II,III) species. Conversely, the pairing up of spins and consequent vanishment of the EPR signal in the (III,III) complex implies significant Pt-Pt overlap, an important finding.

The EPR spectrum of $[P(II,III)l\text{-}MeU]^{3+}$, taken either on the solid or on the frozen solution, is that characteristic of axial symmetry, with anisotropic g values of $g_{\perp} \tilde{=} 2.31 > g_{\parallel} \tilde{=} 1.94$. The magnitude of

$g_{\perp}$ suggests that the unpaired electron is associated largely with platinum and further suggests delocalization. The values taken together correspond to those expected for a $5d_{z^2}$ hole with admixture, due to spin-orbit interaction, from the degenerate $d_{xz,yz}$ level. Separate electrolysis/Vis-NIR and electrolysis/EPR experiments suggest that the electronic absorption intensity and EPR signal intensity behave in parallel fashion, which further implies that the unpaired electron is the source of both the paramagnetism and the color in the $[P(II,III)1\text{-MeU}]^{3+}$ ion.

Two decidedly contrasting sets of EPR spectra were obtained for Pl-MeU - one exhibiting hyperfine structure and the other devoid of hyperfine interaction. In the solid state and in frozen solution, where the solution consisted of either water alone or of a 0.02N perchlorate aqueous solution, a broad, featureless spectrum was obtained. However, with nitrate as the supporting electrolyte, a well-resolved spectrum resulted. This difference was explained in terms of spin-lattice interactions, spin-exchange processes, and in terms of relative ligating strengths of anionic ligands. The hyperfine splitting pattern, which arises from the interaction of electron and nuclear spin moments, is indicative of splitting by ^{195}Pt with only secondary contributions from ligand nitrogens. Failure of the pattern to agree with theoretical distributions can be explained by postulating EPR-nonequivalent Pt atoms, a reasonable postulation in the head-to-head dimer. Since spin densities on nonequivalent atoms are not the same, a deviation from theoretical

distributions is to be expected.

Pl-MeUB. A very weak EPR spectrum for the native polymer reveals that platinum 1-methyluracil blue is only weakly paramagnetic. This qualitative result tends to corraborate earlier calculations, based on oxidative/reductive electrolysis and on redox titrimetry, that the average formal oxidation state in Pl-MeUB is close to 2. Since we believe there to be at least 11 Pt^{II}'s for every Pt^{III} (vide supra), considerable delocalization of an unpaired electron might be expected. The application of second-order perturbation effects in the calculation of g values (from which N and $\xi/\Delta E$ values are obtained), supports greater delocaliztion in Pl-MeUB than in Pl-MeU.

In general, the same arguments invoked to interpret the spectrum of P(II,III)1-MeU can be applied in the case of Pl-MeUB, although in a somewhat less rigorous fashion because the overall symmetry is lower. The spectrum is again that of an axially-symmetric system containing both parallel and perpendicular orientations. g values of $g_{\perp} = 2.275 > g_{\parallel} = 1.948$ are again indicative of considerable spin-orbit coupling. They further imply that the unpaired electron(s) is primarily associated with overlapping $5d_{z^2}$ atomic orbitals along the Pt axis of the oligomeric chain. Hence, platinum blues are generally believed to consist of a columnar stacking of Pt units.

Under solvent/supporting electrolyte conditions where the spectrum was totally unresolved in the case of the dimer, Pl-MeUB displayed hyperfine structure, although the spectrum was not well

resolved. The incomplete resolution suggests extensive delocalization over an unknown number of Pt centers. The absence of well-resolved peaks is not unexpected in the inhomogeneous polymer since the extent of delocalization may be expected to differ in chains of varying length.

Controlled-Potential Coulometry in Conjunction with Paramagnetic Nuclear Magnetic Resonance Spectroscopy (141)

Examination of NMR spectra in conjunction with ESR studies can prove useful for paramagnetic species because of the complementary nature of these two techniques. In particular, the disappearance of nuclear magnetic resonance coincident with the emergence of absorption due to electron paramagnetic resonance is doubly diagnostic of paramagnetism. Because the electron spin moment is large relative to the nuclear magnetic moment, the former may cause rapid relaxation of the nuclear excited state, which in turn leads to a short T_1 (spin-lattice relaxation time) and consequent line broadening, which, in extreme cases, vanishes into the baseline. Indeed, in the early days of NMR it was thought not to be possible to detect an NMR signal in paramagnetic transition metal ions. However, it is now recognized that this is not necessarily the case, and, in fact, many paramagnetic complexes yield NMR spectra.

In ESR slow relaxation (long T_1) results in a long-lived excited state and a corresponding narrow line width. If the relaxation is fast, the peaks are broad. When the electron relaxation is rapid, the nuclear relaxation mechanism is less efficient, thereby

lengthening T_1 and providing sharp lines. But when the nuclear relaxation is promoted by a sustained electron spin, T_1 is shortened, and the lines eventually disappear into the baseline. Hence the complementary nature of the techniques. In favorable (extreme) cases (from the standpoint of this experiment), where there is an NMR spectrum, there is no ESR spectrum, and vice versa.

CPC/PNMR of Pl-MeU -

In Figure 52 are shown the NMR spectra of native Pl-MeU (prior to electrolysis) (·Pt(II)-Pt(II)·), of the half-electrolyzed material (·Pt(II)-Pt(III)·), and of the fully-electrolyzed dimer (·Pt(III)-Pt(III)·). Referring to the lettering scheme shown in the accompanying drawing, the resonances in the native compound are as follows: N-C$\underline{H}_3$, a singlet, δ = 3.37; $\underline{H}_a$, a doublet, δ = 5.86; and $\underline{H}_b$, a doublet, δ = 7.43.

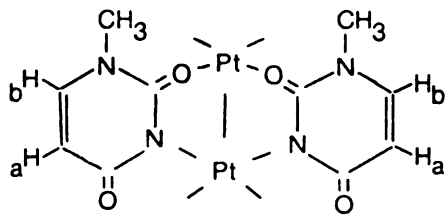

The large absorbance at δ = 4.76 is due to H_2O impurity in the D_2O. The broadband absorptions centered at δ = 0.62, 1.76, and 2.92 arise from methylenes in the DSS reference compound; DSS itself absorbs 0.015 ppm downfield of TMS.

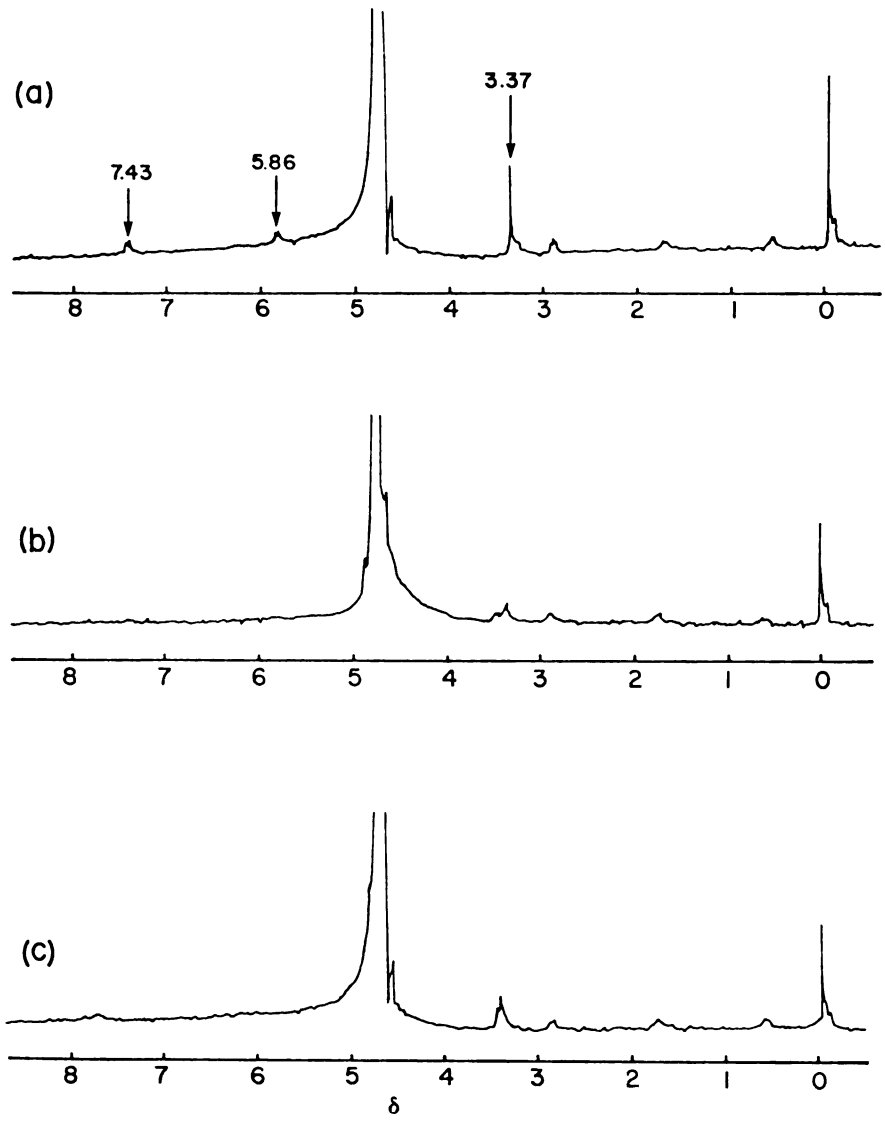

Figure 52. NMR spectra of a) native, b) half-electrolyzed, and c) fully-electrolyzed P1-MeU (6.0 mg/6.0 ml, 1.2 mM) in 0.02F $NaNO_3$ in D_2O; 2000 scans accumulated.

Figure 52b shows the NMR spectrum of half-electrolyzed Pl-MeU. In the ESR section, half-electrolyzed Pl-MeU was shown to yield an ESR spectrum. In Figure 52b the resonances due to the two protons in the ring have vanished. Also, the absorption at $\delta = 3.27$, due to the methyl protons, is greatly diminished. (It should also be noted that, inexplicably, the accumulated signal due to DSS is reduced by 40%.) In the fully-electrolyzed material (Figure 52c), there is still no resonance due to the H_a or H_b protons, but a weak, broadened peak has emerged for the methyl protons.

The spectacular effect would have been to have the spectrum vanish in b and to have a and c strong and identical. However, the effect observed in b is not inconsistent with the ESR results: The NMR spectra were measured in D_2O containing 0.02 F $NaNO_3$ at room temperature. The corresponding EPR spectra, taken of frozen solutions, showed hyperfine structure (Figure 46). Had ESR spectra also been taken at room temperature, very likely the absorptions would have been both weaker and broader (142). The explanation for the increased breadth, to repeat, lies in a shortened relaxation time (T_1). As was explained above, this tends to produce a sharper NMR absorption; hence the appearance of an NMR spectrum. Were the electron spin relaxation times long in the room temperature experiment, then we might expect the total vanishment of the NMR signal. The gist is that a marginal ESR spectrum begets a marginal NMR spectrum.

The fact that the fully-electrolyzed Pl-MeU also shows evidence

of paramagnetism is not surprising, in that, it is very difficult to avoid some reversion of the Pt(III)-Pt(III) product to the paramagnetic Pt(II)-Pt(III), and, apparently, it requires only a trace of paramagnetic impurity to lead to deterioration in the NMR spectrum (129). In contrast to the situation here, binuclear Pt(III) compounds which have been synthesized (54 and references therein), presumed to have paired spins in their molecular orbitals, and which therefore would be expected to produce no EPR signal, yield sharp, well-defined NMR spectra. While the observed chemical shifts in paramagnetic metal ions are often large relative to those of the uncoordinated ligand (as in the lanthanide shift reagents, for example), such was not the case here. As a final note, because of the broadband absorption typical of paramagnetic ions, high rf power is often employed. Since the T_1's are shorter, there is little danger of saturating the resonance.

CPC/PNMR of Pl-MeUB -

Weak NMR spectra were obtained for Pl-MeUB in the CPC/NMR experiment; the spectrum of the native material is shown in Figure 53. This spectrum serves to point out a certain incompatibility in the requirements of successful NMR and analytical scale electrolysis for this blue. While a reasonable charge requirement (1.68 C were passed in the complete electrolysis) as well as other considerations (including solubility limitations) dictate the amount of material that can be accommodated in an electrolysis, this amount obviously is too little to furnish a strong NMR signal within a reasonable period

of time (2000 scans, 45 min).

Evidence based on ESR measurements, redox titrimetry, and controlled-potential electrolysis point to a very weak paramagnetism in Pl-MeUB. NMR measurements of native, half-electrolyzed, and fully-electrolyzed polymer (the latter two spectra are not shown) revealed a weak, diffuse band at δ = 3.37, which, in the case of the platinum dimer, was attributed to the N-methyl protons. In the spectrum of Pl-MeUB, this absorbance may arise from Pl-MeU contamination (shown to be present by LC), or may derive from the same protons in the polymer. If it is the latter, the broadening may arise from an oligomeric distribution. A second, sharp peak observed upfield at δ = 2.23 decreased in amplitude as the electrolysis proceeded, but did not broaden. It is possible that this absorption is due to the N-methyl protons; if so, it shows that, despite Pl-MeUB consisting of a mixture of oligomers, the chemical shift is the same in all oligomers. Accepting that this absorption is due to the methyl protons, the reason for higher shielding in the polymer is not immediately obvious. No resonance was obtained for the two ring protons. Having made these observations, and recalling the ESR spectra of Pl-MeUB (Figure 51), it is apparent that a comparison of the NMR and ESR results is not particularly illuminating for this more complex case.

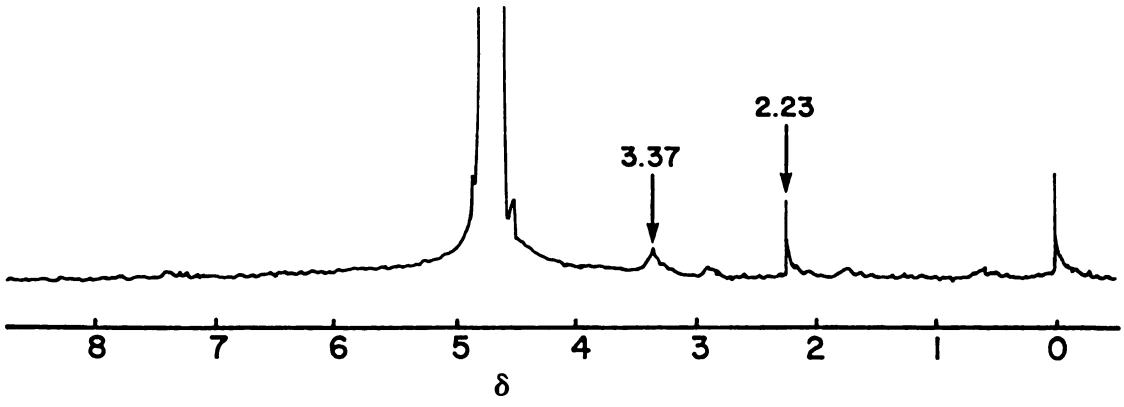

Figure 53. NMR spectrum of native Pl-MeUB (12.0 mg/6.0 ml) in 0.1F $NaNO_3$; 2000 scans.

X-ray Photoelectron Spectroscopy[1]

Liquid Chromatography[2] (144-146)

Goal -

Liquid chromatography (LC) has a number of potential uses in the study of blues and related compounds: The purity of a synthetic preparation is readily determined by LC. As aqueous solutions of the Pl-MeU dimer were sometimes noted to take on a violet or purple color with time, LC could be used to monitor the changes occurring. An

---

1. The application of X-ray photoelectron spectroscopy (XPS), with its unique ability to probe oxidation states in the solid state, would, undoubtedly, have proven a valuable asset in this study. Unfortunately, the samples were never run.

2. Because the application of LC to the study of blues has been virtually ignored in the literature, this topic was not introduced in the Literature Review, and hence, is developed here.

obvious use of LC in the current work was to examine the chromatographic profile and to obtain information about the oligomeric distribution of Pl-MeUB. To obtain concurrently an estimate of the molecular weight range would be valuable. LC could also prove useful in comparing different preparations of blues and could be used to examine their degradation in solution with time. As a final application of LC, periodic examination of the electrolyte during an oxidative electrolysis of Pl-MeU would allow a distinction to be made between the processes 1) $[P(II,II)1\text{-MeU}]^{2+} \xrightarrow{-e^-} [P(II,III)1\text{-MeU}]^{3+} \xrightarrow{-e^-} [P(III,III)1\text{-MeU}]^{4+}$ and 2) $[P(II,II)1\text{-MeU}]^{2+} \xrightarrow{-2e^-} [P(II,IV)1\text{-MeU}]^{4+}$ (n was shown to equal 2 by controlled-potential coulometry). This would furnish information complementary to that already discussed. If the LC mode is suitably chosen, a distinction between 1) and 2) can be made on the basis of retention time (charge) and on the number of major peaks observed (3 in 1), 2 in 2)). Based on LC alone, a distinction cannot be made between 1) and the sequence $[P(II,II)1\text{-MeU}]^{2+} \xrightarrow{-e^-} [P(II,III)1\text{-MeU}]^{3+} \xrightarrow{-e^-} [P(II,IV)1\text{-MeU}]^{4+}$. An argument against the latter sequence (which has not been considered before in this thesis) is that, as far as the author knows, no III → IV transition has ever been reported for a platinum compound.

Introduction -

With the renaissance experienced by liquid chromatography in the last dozen years or so, and considering the rather obvious candidacy of the blues and their precursors to LC examination, the paucity of

reported applications of LC to these groups of compounds is surprising. Other than a few attempts at electrophoresis, there appears to be only a single report on the application of high performance liquid chromatography (HPLC) to the blues, that by Woollins and Rosenberg (147).

For the sake of reference, those compounds which were desired to be studied by HPLC in the current study are listed here. First the dimer P(II,II)1-MeU and its electrolysis products:

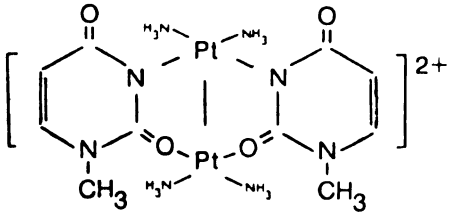

P(II.II)1-MeU

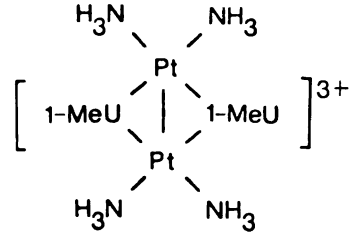

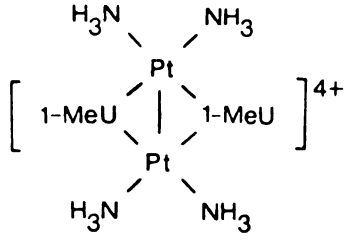

where 1-MeU =

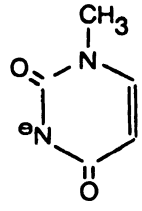

Second, the platinum blue Pl-MeUB, believed to be formed from a stacking of the pictured (below) unit along a chain:

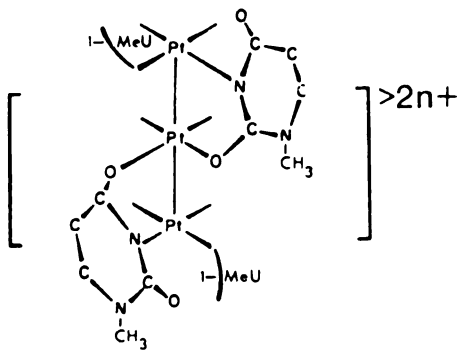

where n is the repeating unit consisting of 2Pt, 2 1-MeU, and $4NH_3$ groups.

Pl-MeUB

In choosing (an) appropriate LC mode(s) for the examination of these compounds, the following points are relevant: 1) there are metallic (Pt) sites over which positive charge is distributed; 2) organic character is contributed by the 1-methyluracil groups, which are 48% heteroatomic in composition (confers "polarity" to them); and 3) the species to be separated are cations ranging in weight from 832 (as the nitrate salt) for Pl-MeU to the several thousands (presumably) for the blue.

In planning a separation, several LC modes might be reasonably considered. Ion exchange carried out on a strong cation exchange column is an obvious choice because of the ionic nature of these solutes. For the three valence states of Pl-MeU, the requirement is to separate cations of +2, +3, and +4 charge, a not unreasonable expectation with modern ion-exchange packings. For the polymeric blue the situation is not so staightforward. As has been discussed

previously, and as will be discussed again momentarily, the platinum 1-methyluracil blue is believed to consist of a continuous distribution of oligomers over a range m, m+1, ..., n-1, n, where each number from m to n represents the number of repeating units per oligomer (each unit contains two platinum atoms). In this continuous distribution, an oligomer with n repeating units differs in charge by ~2 from one with n-1 and from one with n+1 units. As n increases, the fractional change in charge per added unit becomes smaller. The expected consequence of this is decreased resolution between oligomers by ion-exchange. Also, the larger the molecule, the more doubtful it is that each charged site in the molecule (that is, each platinum) participates in the ion exchange process; this is because of a steric mismatch between the platinum sites and the exchange sites on the packing. Consequently, predicting the order of retention may not be possible.

A further complication in ion exchange chromatography results from adsorptive interactions between solute organic groups and active sites on the surface of the support. This interaction can occur with both lipophilic and hydrophilic groups, but may be expected to be particularly strong with hydrophilic groups (such as the 1-methyluracil moiety) because of the attraction to underivatized silanol groups on the silica support. The larger the molecule, that is, the larger the number of methyluracil groups present, the more confounding this effect may be. The dual consequences of this effect are 1) an inability to predict the order of elution, and 2) far from

optimal ("bad") chromatography. Partly because of the aforementioned reasons, but just as much because of the lower efficiency of and lack of reproducibility in preparing ion-exchange packings, the use of a relatively newer LC technique for ionic species - ion-pair reversed phase high performance liquid chromatography (IPRPLC) - has in many applications supplanted ion-exchange chromatography.

In ion-pair chromatography an ionic solute is converted to an ion-pair using an appropriate ion-pairing reagent. The process may be depicted as $R^+ + C^- \rightleftarrows (RC)_{ip}$ where R is a monovalent cationic solute (although R does not have to be monovalent), C is the counter ion (or ion-pairing agent; the use of the term counter ion follows the parlance of LC), and RC is the ion-pair. For a hydrophilic solute the process may be represented as $R^+_{aq} + C^-_{aq} \rightleftarrows (RC)_{aq} \rightleftarrows (RC)_{org}$. In a solvent extraction into an organic layer, $(RC)_{org}$ would represent the species which has partitioned into the organic layer as the ion-pair. In a chromatographic system, $(RC)_{org}$ is the pair partitioning into the bonded alkyl (usually) phase, and as such identifies the process as ion-pair reversed phase LC.

For the sake of the purist, it deserves mention that there is some controversy over the actual mechanism of the partitioning process. The question is, does the pair form in the mobile phase and then partition as the pair into the organic stationary phase, or does the pairing agent position itself with its long hydrophobic tail immersed in the stationary phase and its hydrophilic, charged end facing outward, with the exchange mechanism then being one of ion

exchange? In fact, depending on the situation, it appears that each mechanism can prevail (148, 149). A less restrictive, so-called ion-interaction model has also been proposed (150); judging from the most recent literature, ion-interaction seems to be catching on as a term. Excellent discussions of ion-pair chromatography have been given by Gloor and Johnson (151) and Bidlingmeyer (152). Because of the large selection of column types available for reversed phase LC (reversed phase LC is by far the most widely utilized mode in LC), the chromatographer is afforded considerable flexibility in the design of a reversed phase separation.

IPRPLC will be developed more fully later as it applies to the investigation at hand; however, a few additional comments are in order at this point. Retention may be controlled by varying the amount of organic modifier in the mobile phase (most often methanol or acetonitrile) as in standard reversed phase LC. Additionally, the retention may be affected through the choice of ion-pairing reagent and by varying its concentration. For basic solutes, pH is another important parameter. In the present instance, the nitrogens in 1-methyluracil are so weakly basic, that within a tolerable (to the column) pH range, pH has no effect.

A third LC mode that might be considered, at least for the blues, is size-exclusion chromatography (SEC). Vast improvements have occurred in column development in recent years so that SEC is applied not only to higher molecular weight compounds (synthetic and bio-polymers, for example), but is now commonly applied to lower

molecular weight compounds as well (M.W. of a few thousand and less). However, SEC is not readily applied to ionic compounds (such as salts). This is because of strong attractive forces that develop between charged sites on the solute and the support, forces that preclude a separation based on size alone. This problem as well as others is considered by Yoza in a review article (153).

Pertinent Literature on LC -

Separations based on differential migration in an electrical field (electrophoresis) have been briefly covered earlier in the Literature Review section and will be mentioned again under Isotachophoresis. A single report in the literature deals with the LC examination of a blue - a pyrimidine blue, platinum thymine blue (147). Several blue components were separated from white components by introducing a tetrabutylammonium salt in a step-gradient fashion into a strictly aqueous phase in a reversed phase mode (not an ion-pair mechanism). The authors speculated that the blues were eluted by an ion-exchange mechanism with exchange occurring at nonderivatized Si-OH sites.

Study of the literature reveals few reports on related compounds. Various thymine complexes of Pt(II) were separated by reversed phase LC on LiChrosorb RP 18 with distilled water as the eluent (154). Several studies on nonionic metal cluster compounds show that to elute these compounds, essentially no variation in the standard reversed phase format is required (155, 156). A useful contribution comparing normal phase (not considered in the

Introduction above) and reversed phase LC on the retention behavior of various organometallic complexes (but not including Pt) was given by Gast and Kraak (157); interaction with the silica was strong in the normal phase mode, as might be predicted. Various schemes for the determination of cis-platinum-derived Pt in urine have been developed (158,159), but these depend on a derivatization reaction, a procedure not directly relevant to the LC needs in the current study.

Several studies point toward the utility of a paired-ion approach. Bushee et al. separated various denuded metal ions as their ion-pairs by reversed phase LC (160). Valenty and Behnken paired various derivatives of tris(2,2'-bipyridyl)ruthenium(II) with either methanesulfonate or n-heptanesulfonate anions and obtained separations on a C_{18} bonded column in an aqueous tetrahydrofuran mobile phase (161). O'Laughlin (162) and O'Laughlin and Hanson (163) made thorough studies of ion-pair separations of 1,10-phenanthroline chelates of a number of divalent metal ions.

Detection -

Various detection schemes may be used for metal compounds including UV/Vis (where applicable), electrochemical in its various forms (primarily amperometric or coulometric, polarographic to a lesser extent), and atomic spectroscopic using either atomic absorption spectrophotometry or inductively-coupled plasma emission. The use of electrochemical detection will be touched upon later.

The spectra of P1-MeU and P1-MeUB, shown in Figures 44 and 45, respectively, demonstrate the suitability of ultraviolet and/or visible detection for these compounds. For P(II,III)1-MeU, the absorption maximum is at 740 nm. At the center frequency (λ =658 nm) of the interference filter available, the value of A_{658}/A_{740} is 0.37. There is also a sharp peak at λ =278 nm due to the 1-methyluracil moiety. The value of A_{280}/A_{658} for P(II,III)1-MeU is approximately 6.5. Conveniently, the absorption maximum of P1-MeUB is at 660 nm. The ratio of the absorbances at 280 and 658 nm in P1-MeUB is $A_{280}/A_{658} \cong 17$.

Method Development -

IPRP chromatography places stringent demands on column packings because of the aggresive nature of the ion-pairing reagents. (They tend to slowly attack packing materials.) In the current work, the most satisfactory performance was achieved on a Partisil ODS-3(OctaDecylSilane, Whatman), which has a 10.5% carbon loading. Of several organic modifiers tried in the aqueous mobile phase, best overall performance was achieved with methanol. Ion-pairing candidates were selected from the series of alkylsulfonic acids (ordinarily as their sodium salts). Selected chromatograms will be shown that demonstrate the variation in retention time afforded in going from ethanesulfonic acid to octanesulfonic acid.

In addition to these sulfonic acids, sodium dodecylsulfate, commonly known as sodium laurylsulfate, was also tried. When laurylsulfate is used as the ion-pairing agent, the separation mode

is known as soap chromatography. An advantage to using the soap as the ion-pairing reagent is that the high comparative lipophilicity of the C_{12} agent overwhelms the more hydrophilic uracil groups, thereby dominating the retention process in the C_{18} stationary phase. In this manner, when the solvent conditions are suitably adjusted, the adjusted retention time t_R' ($t_R' = t_R - t_0$ where t_R is the measured retention time and t_0 is the retention time of unretained components (i.e., the solvent front)) for a given species $(R_a^+C^-)_{ip}$ would be expected to be roughly one half that of $(R_b^{2+}C_2^-)_{ip}$ where C is the ion-pairing reagent. Analogously, the t_R''s of $[P(II,II)1\text{-MeU}]^{2+}$, $[P(II,III)1\text{-MeU}]^{3+}$, and $[P(III,III)1\text{-MeU}]^{4+}$ should be distinguishable, for when the divalent species elutes at $t_R'(2+)$, then $t_R'(3+) \cong 1.5t_R'(2+)$ and $t_R'(4+) \cong 2t_R'(2+)$. As it turned out, sodium laurylsulfate proved to be too retentive at reasonable methanol concentrations. (If the methanol concentration was too high, solubilization of the unpaired cationic solutes was impaired.) However, this did not prove to be a problem since, at a methanol concentration of 50% (v/v), octanesulfonic acid fulfilled the same function.

In the early days of IPRPLC, this mode of LC was notorious for producing poorly-shaped, badly-tailing peaks. A probable reason for this, as was hinted at in the Introduction to this section, may be attributed to a strong interaction between the charged solute and the support, very likely through an ion-exchange mechanism with residual, exposed, anionic $\underline{SiO}^-H^+$ groups, although dissociation of the ion-pair in the organic phase may also contribute (164). While the addition of

low concentrations of salt as peak sharpeners can be effective, the addition of an ion-pairing sharpener such as tetrabutylammonium ion (TBA^+)(164) in conjunction with the alkylsulfonate ions is more effective with hydrophilic cationic solutes. Interestingly, TBA is not effctive as a tail-reducer with more hydrophobic solutes (164,165). The TBA^+/SO^-_3 ion-pairs prevent the damaging, strong interaction between solute and underlying support by displacement since these act as competing ion-pairs for partitionment into the stationary phase. Or if, rather, the dissociative mechanism alluded to is operative, it may act to suppress the disturbing dissociation.

Satisfactory chromatographic performance was achieved with a mobile phase composed of 0.01M sodium octanesulfonate and 0.005M tetrabutylammonium nitrate in 50% (v/v) $MeOH/H_2O$ adjusted to pH 3.0 with HNO_3. That, indeed, an ion-pair mechanism was operative with this mobile phase is demonstrated by the three chromatograms of Figure 54.

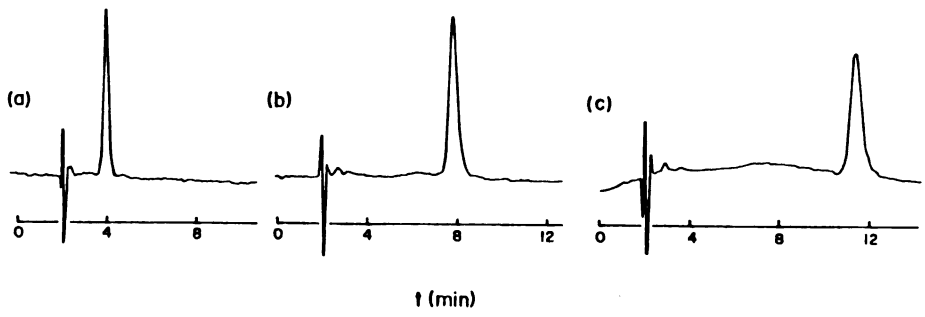

Figure 54. Three chromatograms illustrating the operability of the ion-pair reversed phase mode in the analysis of $[P(II,II)1\text{-}MeU](NO_3)_2$: a) 50% MeOH/0.01 M $HepSO_3Na$/0.005 M TBA^+, b) 50% MeOH/0.01 M $OctSO_3Na$/0.005 M TBA^+, c) 45% MeOH/0.01 M $OctSO_3Na$/0.005 M TBA^+.

In b a retention time of ~7.7 min was obtained using the above-mentioned mobile phase. When heptanesulfonate was substituted for octanesulfonate, the peak moved toward a shorter retention time (a, ~3.9 min), in accordance with expectation based on the reduced lipophilic character of the ion-pairing agent. The fact that the retention time was invariant over the pH range 6-2, supports the contention that ion-pairing occurs exclusively at platinum, and not at all in the uracilate groups. Also as predicted, when the methanol concentration was reduced from 50% to 45%, the peak moved out (to ~11.3 min), as shown in c. Hence, the behavior is consistent with that expected in an IPRPLC mode.

Electrolysis/LC of Pl-MeU -

As mentioned under Goals above, one of the intents of the LC phase of this project was to follow the oxidative electrolysis of P(II,II)1-MeU. The ion-pairing mode should allow a distinction between the possible reactions: 1) $[P(II,II)1\text{-}MeU]^{2+} - e^- \rightarrow [P(II,III)1\text{-}MeU]^{3+} - e^- \rightarrow [P(III,III)1\text{-}MeU]^{4+}$ and 2) $[P(II,II)1\text{-}MeU]^{2+} - 2e^- \rightarrow [P(II,IV)1\text{-}MeU]^{4+}$. A (hopefully) strong case has already been made for the former. Nevertheless, confirmation by LC would be welcome. If pathway 1) obtains, then peaks at three different retention times, each successively longer, should be obtained throughout the electrolysis, whereas in 2) only two peaks will be observed.

By invoking the reasoning applied earlier to the prediction of retention times in IPRPLC when the ion-pairing agent dominates the

process, we not only can predict the number of peaks expected for each pathway, but can calculate expected adjusted retention times, as was done on p. 274: $t_R'([P(II,II)1\text{-MeU}]^{2+}) = 0.67t_R'([P(II,III)1\text{-MeU}]^{3+}) = 0.50t_R'([P(III,III)1\text{-Meu}]^{4+}) = 0.50t_R'([P(II,IV)1\text{-MeU}]^{4+})$. Note that no distinction based on retention time is to be expected between the latter two ions. However, if the $[P(II,IV)1\text{-MeU}]^{4+}$ species is formed as in sequence 2) above, then, as mentioned, only two peaks will be obtained during the course of an electrolysis. For the predicted t_R''s to obtain, the retention time of $[P(II,II)1\text{-MeU}]^{2+}$ when coupled to a weakly-lipophilic pairing ion (such as methane- or ethanesulfonic acid) must be that of the solvent front - i.e., $t_R'([P(II,II)1\text{-MeU}]^{2+} = 0$. That this condition was met in the present instance is evident from Figure 55, which may be compared with Figure 54.

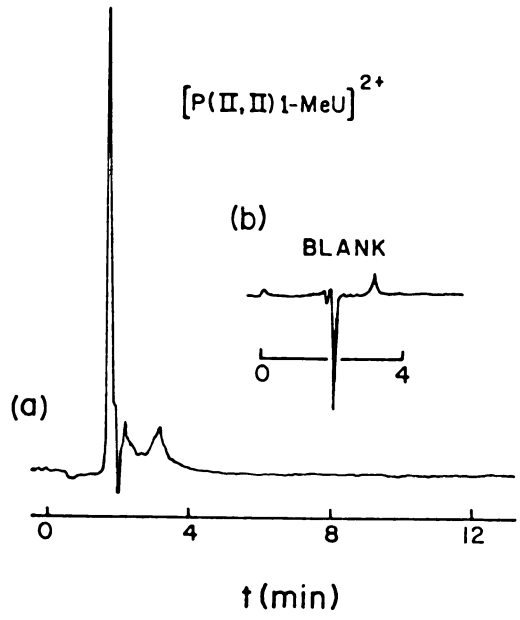

Figure 55. Chromatograms of a) $[P(II,II)1\text{-MeU}]^{2+}$ as the ethanesulfonate ion-pair and of b) the solvent front.

The electrolysis of $[P(II,II)1\text{-MeU}]^{2+}$ was sampled at 1/8 intervals for LC analysis. The outcome of the experiment was a disappointing one: there was only a single peak in each chromatogram, and the retention time was unchanged regardless of the extent of electrolysis. This is shown via selected chromatograms in Figure 56.

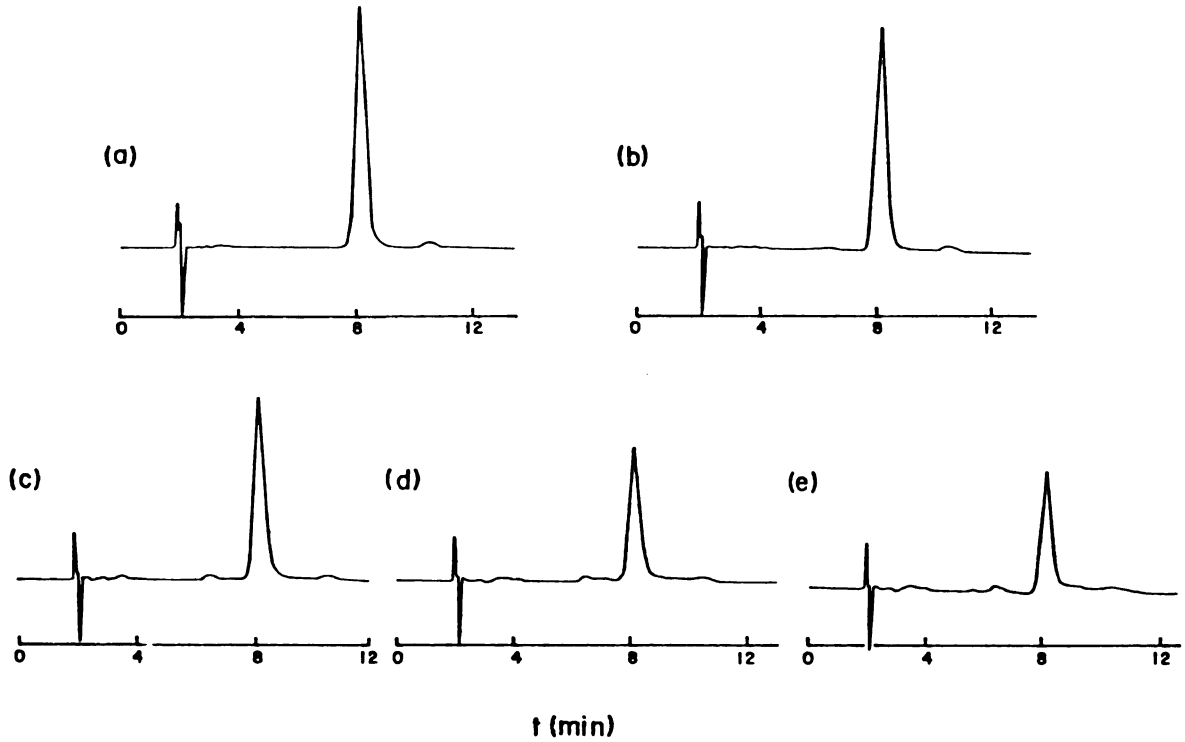

Figure 56. Chromatograms obtained a) prior to, and at the b) 1/4, c) 1/2, d) 3/4, and e) 4/4 points in the oxidative electrolysis of P1-MeU (λ = 280 nm). The reduced peak intensity with extent of electrolysis is real, not artifactual.

In none of these runs was there a response at λ = 658 nm (chromatograms not shown); at roughly the midway point of the electrolysis, when (ideally) the only species in solution is $[P(II,III)1\text{-MeU}]^{3+}$, the ratio A_{280}/A_{658} should equal ~6.5. Since the sensitivity setting for λ =658 was 10X that of λ =280 (0.01 $AUFS_{658}$

vs 0.1 $AUFS_{280}$), the lack of a response at λ =658 furnishes evidence that the mixed-valence species did not emerge from the column. Even when the amount of material introduced onto the column was increased 15-fold, there was still no response at λ =658.

The presumed explanation for this unanticipated behavior is that both the Pt(II)-Pt(III) and Pt(III)-Pt(III) species were reduced on-column back to the Pt(II)-Pt(II) state upon exposure to the metallic (iron) surface of the stainless steel column. In addition, the injector and all connecting tubing were also made of stainless steel. While the E^{o}'s for the Pt(II)-Pt(III) and Pt(III)-Pt(III) systems are not precisely known (but they are well positive), the E^{o} for $Fe^{2+} + 2e^{-} \rightleftarrows Fe$ can be read from a table of standard potentials:

$$E^{o}_{Fe^{2+} + 2e^{-} \rightleftarrows Fe} = -0.41 \text{ V vs nhe or } -0.65 \text{ V vs ssce.}$$

Clearly, on thermodynamic grounds, reduction of platinum by the free iron metal is a plausible explanation. Direct confirmation of this hypothesis could have been obtained through electrochemical detection of the LC effluent: if only the $[P(II,II)1\text{-MeU}]^{2+}$ species is emerging from the column, then a response would be expected for oxidative mode detection, but no signal for detection in the reductive mode (at carbon). An electrochemical detector was not available to the author during this work; furthermore, this experiment would only have provided negative information, and would have solved nothing. One solution to the problem of on-column reduction would be to use an all glass system (available from Pharmacia Fine Chemicals and LKB). Since such equipment was not available to the author, an alternate approach

utilizing an all nonmetal isotachophoretic analyzer was mapped out (see section on Isotachophoresis).

Survey of Pl-MeU by LC -

To this point there has been very little discussion about the matter of the stability of the dimer platinum 1-methyluracil in aqueous solution. Information can be shed on its stability in aqueous solution by examining its solutions under different conditions as a function of time by LC(IPRPLC). One feature of its solutions, although not reproducibly so, is their tendency to gradually acquire a violet or purple color, a manifestation of the polymerization and oxidation of Pl-MeU to a platinum blue. While this was true for aqueous preparations containing an electrolyte, this may not be true for strictly aqueous preparations. Also, fully-electrolyzed Pl-MeU, yellow after electrolysis, was sometimes observed to turn a greenish- or reddish-brown, although in most cases it simply reverted back to a partial green, the color characteristic of the mixed-valence state. While tan (or dark red) polymeric platinum preparations have been noted to exhibit some of the intriguing properties of the blues, including mixed-valency(21), the green "blues" seem to exhibit no extraordinary properties(21,35), possibly because of a longer Pt-Pt distance.

As illustrations of the time-behavior of aqueous solutions of Pl-MeU, a series of chromatograms is shown in Figure 57. Not every effect observed is readily explained.

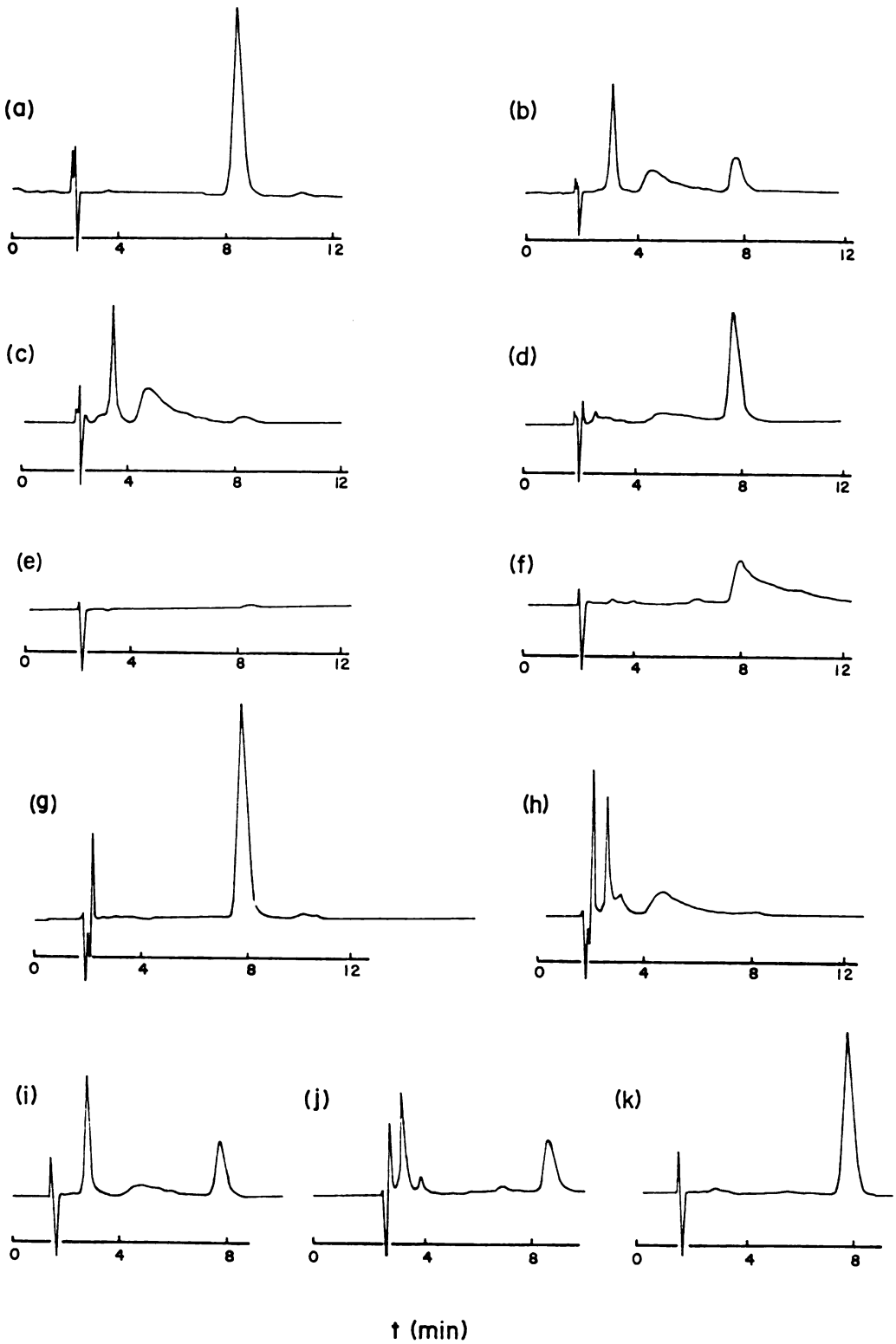

Figure 57. Chromatograms illustrating the time-behavior of Pl-MeU.

Figure 57a is the chromatogram of undecomposed Pl-MeU (2 day old preparation), b the chromatogram after 12 days, and c after 17, at which time decomposition was virtually complete; none of these solutions was colored. The extent of decomposition is seen to be proportional to time. By contrast, a more than 1-1/2 month old, partially-electrolyzed solution of Pl-MeU revealed very little decomposition, as shown in d. What little decomposition was evident, may have arisen from unelectrolyzed P(II,II)1-MeU. This attests to the high stability, by comparison, accorded the mixed-valence state. A stark contrast is presented in e, which shows the absence of any peak for a fully-electrolyzed Pl-MeU which had stood for one month after electrolysis. This effect was reproducible except in one case (example to follow). The aged solutions (some as old as 4 months) varied in color from a brownish-red to purple. Apparently, the same decomposition pathway available to the divalent $[P(II,II)1\text{-MeU}]^{2+}$ is not taken by tetravalent $[P(III,III)1\text{-MeU}]^{4+}$. A younger (17 day old), fully-electrolyzed Pl-MeU yielded the chromatogram in f. The peak at the t_R of Pl-MeU may have resulted from a partial reversion to the mixed-valent state; the long tail probably reflects the early stages of the decomposition of the fully-electrolyzed material.

It was noted in the Experimental section that dissolution of $[P(II,III)1\text{-MeU}](ClO_4)_3$ in DMSO turned the solution pink, while this did not occur for $[P(II,II)1\text{-MeU}](NO_3)_2$. Figure 57g, which shows a chromatogram of freshly-prepared $[P(II,II)1\text{-MeU}](NO_3)_2$ in DMSO, and h, the chromatogram of an analogous 15 day old preparation, together demonstrate the same behavior as in aqueous solution. The fact that

a peak is present at the expected retention time some 2-1/2 months after sequential oxidative and reductive electrolysis (i) may speak to the less than complete reversibility of the system - i.e., some $[P(II,III)1\text{-MeU}]^{3+}$ remained after reduction, although the possibility of some air oxidation to the mixed-valent state cannot be ruled out. Figure 57j is the chromatogram of a solution of P1-MeU that had turned violet after more than three months of standing. If there were no decomposition, the peak height shown in k would have been obtained. Later it will be shown that the color is attributable to a blues-like polymeric distribution. Under the LC conditions employed here, the polymeric platinum blue is retained on the column.

As to the nature of possible decomposition products exclusive of the formation of polymeric components, reference can be made to the work of Woollins and Rosenberg(80). Reasonable decomposition products of P1-MeU, $[(NH_3)_2Pt(1\text{-MeU})_2Pt(NH_3)_2]^{2+}$, which have been identified include $Pt(NH_3)_2(OH)(1\text{-MeU})$, $Pt(NH_3)_2(1\text{-MeU})_2$, and, in saline, $Pt(NH_3)_2Cl(1\text{-MeU})$. The latter two are akin to two of the "whites" identified as decomposition products of platinum thymine blue(147): $Pt(NH_3)_2(TH)_2$ and $Pt(NH_3)_2Cl(TH)$. In forming the first and third of these, 1-MeU would also be liberated. Unaccountably, 1-methyluracil was not detected (even at λ =254 nm) under the LC conditions of analysis used here, although it was detected by Woollins and Rosenberg using a pH 3.0 HNO_3 eluent on Partisil ODS-3. Unfortunately, not all of these possible decomposition products were available as standards to the author. However, this was not a major shortcoming in that, since no controlled decomposition studies were

undertaken, the chromatograms of Figure 57 and the accompanying descriptions are only meant to be illustrative.

LC of Pl-MeUB -

Method Devlopment. As mentioned, the higher molecular weight, polymeric platinum 1-methyluracil blue does not elute under the LC conditions of the previous section. One of the goals of the LC portion of this work was to be able to estimate, however crudely, the molecular weight distribution of Pl-MeUB. This could, in principle, be done through the application of an appropriate equation (vide infra), together with certain assumptions, under isocratic conditions of eluent flow. As it turned out, it proved extremely difficult to find conditions of constant mobile phase composition which yielded an acceptable chromatogram. There seemed to be a very fine line, which on one side led to early elution (near the solvent front) of the lighter components of the polymeric blue followed by a massive tail as the heavier components eluted. On the other side of the line, all components were retained on the column. As an example, when using an eluent consisting of 0.01M sodium hexanesulfonate and 0.003M TBA^+ in 50% MeOH-in-H_2O at pH 3.0, Pl-MeU eluted within a few minutes, whereas no blue component had eluted even after an hour's elapsed time. On the other hand, with the same eluent except for 0.01M sodium pentanesulfonate replacing the hexanesulfonate, the polymeric components began to elute within a few minutes, but displayed a horrendously long tail. Switching back to the hexanesulfonate, but increasing the MeOH concentration, elution again began early,

followed by a long tail.

Apparently, the range of molecular weights is too great to allow successful elution under isocratic conditions. This is a manifestation of what chromatographers refer to as the general elution problem (166). It was precisely to combat this problem that temperature programming was devised in gas chromatography and gradient elution in liquid chromatography. Consequently, chromatograms to be shown were generated under conditions of gradient elution.

As is well known, gradient elution requires the utmost attention to the purity of all solvents and reagents. Impurities present in either $TBA^{+}NO_3^{-}$ or in the sulfonic acid or in both required that the A solvent (containing 10% MeOH, B contained 80% MeOH) first be cleaned up by passage through a C_{18} column. For the present analysis, there was a danger in too-rapid a gradient. In going from 10% MeOH to 80% MeOH and from 0.01M $C_4H_9SO_3Na$ to 0.01M $C_2H_5SO_3H$ in the space of 20 minutes, a kind of displacement or frontal chromatography resulted, which led to the compression of the oligomers comprising Pl-MeUB into a tight band; hence, no useful information was obtained. Furthermore, it was almost impossible to reproduce retention times under such conditions of a double gradient.

Characterization of Pl-MeUB. A satisfactory analysis was achieved using the following solvent system:

A - 50% MeOH in H_2O

0.01M $HepSO_3Na$

0.002M TBA^{+3}

pH 3.0 w HNO_3

B - 80% MeOH in H_2O

0.008M $EthaneSO_3H$

0.003M TBA^{+}

Program conditions: 100% A for 20 min, $\xrightarrow{\text{linear}}$ 100% B in 30 min.

A few representative chromatograms are presented in Figure 58.

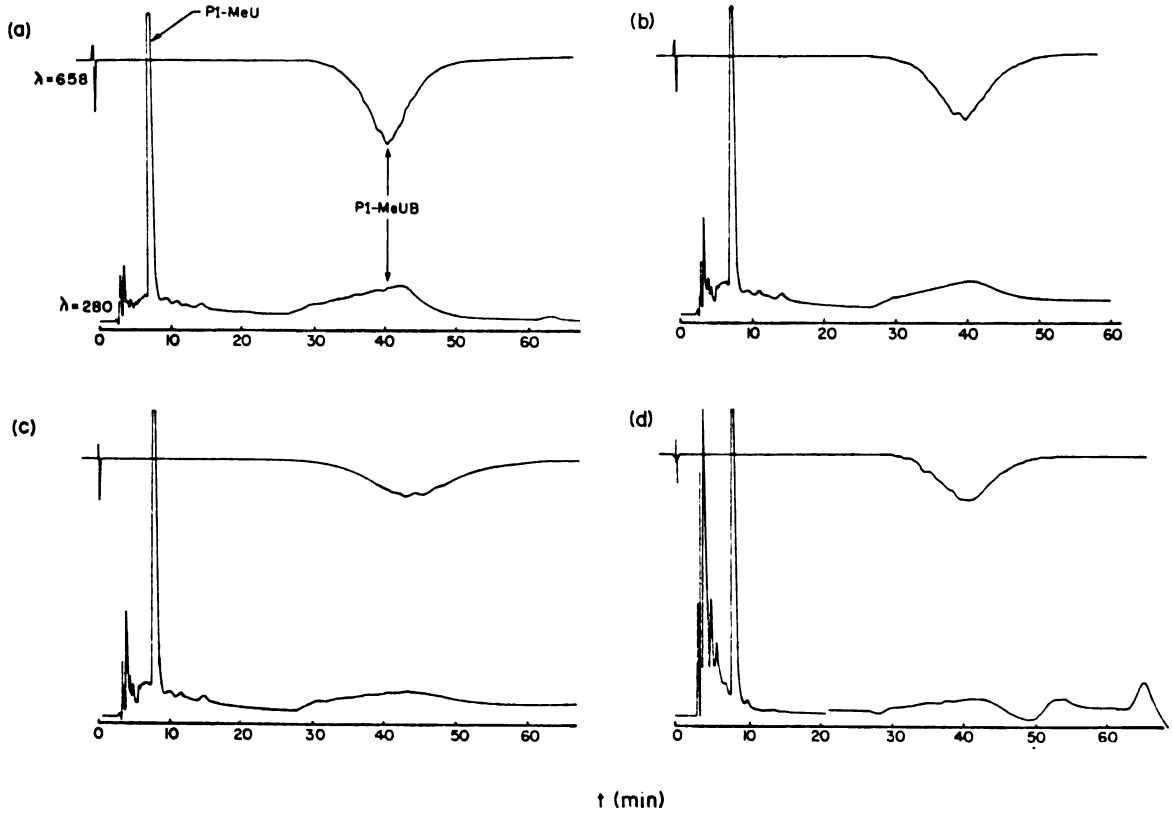

Figure 58. Chromatograms of platinum 1-methyluracil blue (Pl-MeUB).

Figure 58a is a dual detector presentation of a freshly-prepared, aqueous solution of Pl-MeUB. The large peak at 7.5 min is due to Pl-MeU. Note that this peak rides atop an envelope, thus exemplifying the complexity of the composition of relatively low molecular weight

species. The nature of the blue's envelope is, perhaps, best gleaned from the λ =658 trace, since the higher wavelength is less subject to interferences than is λ =280. Since the gradient continues through the envelope out to 50 min, the breadth of the envelope is due to the complexity of the blue, and not to band spreading or to poor chromatography. Straightforward interpretation concludes that the band consists of a broad distribution of totally unresolved oligomeric components. The apparent complexity as deduced from the shape of the envelope suggests a continuous distribution. Probably also lending complexity to the profile are the various bonding permutations (there are two available exocyclic oxygens, a single heterocyclic nitrogen) possible along the length of a given oligomeric chain.

Unlike the situation for the dimer precursor Pl-MeU, on-column reduction either doesn't occur at all, or is less effective in the polymer. This finding is consistent with the shape of the reductive electrolysis curve for this system (Figure 35), which suggested that complete reduction proceeds extremely slowly. We also know from cyclic voltammetry that Pt(III) in the polymer is more difficult to reduce than is Pt(III) in P(II,III)l-MeU or in P(III,III)l-MeU. The question of on-column reducibility was further tested by making multiple injections of the platinum blue while pure A was being pumped, then continuing to pump eluent A overnight (under which conditions the oligomers do not elute), and then finally introducing the gradient. The fact that a response was obtained at λ =658 as well as at λ =280 after the gradient was passed, indicated that the

species still possessed color. To conclude further from this that not all (and perhaps none) of the Pt(III) had been reduced to Pt(II), assumes that an all-Pt(II) system would not absorb at 658. This is not an unreasonable assumption since the evidence accumulated on platinum blues indicates that the color is due to mixed-valency. It is relevant to recall that the exhaustively reduced polymer possesses a brownish tint.

Related to this is the question of the retention characteristics of fully-electrolyzed Pl-MeUB, assumed here to consist exclusively of Pt(III). P(all III)l-MeUB appears to be very stable judging from the honey color which remained unchanged over more than six months of observation. If all platinum sites participate in the ion-pairing process, then we would expect the retention time to increase relative to the unelectrolyzed material. It turns out that the retention characteristics of the broad band were unchanged (chromatogram not shown). To attribute this to reduction to the mixed-valence state of unelectrolyzed polymer would be highly speculative (and very probably wrong, vide supra), since the response at λ =658 was depressed relative to that of unelectrolyzed blue. (We would predict the opposite.) Because of the number of charges to be neutralized over the length of a polymer chain, it is unlikely that all sites are acting in an ion-pair mode. While the ion-pairing mechanism may accurately depict the operative process for the dimer, the retention mechanism for the polymeric species is very likely more complex. However, the notion that ion-pairing is not operative at all for this system can be dispelled by comparing the chromatograms in Figures 58b

and c: in b the A eluent was as on page 286, while B consisted of 0.008M $ButSO_3Na$ and 0.003M TBA^+ in 80% $MeOH/H_2O$ at pH 3.0; in c, 0.008M $HexSO_3Na$ was substituted for the $ButSO_3Na$.

The sometime tendency of a colorless solution of freshly-prepared Pl-MeU to turn violet or purple with time has been noted; no such change occurred in the solid phase. Examination of the chromatogram in Figure 58d shows that the color derives from a blues-like mixture formed on standing. Since run d was not repeated, it is not known if the undulating appearance of the λ = 280 record after 40 min was aberrant or representative. Interestingly, Lippert et al. made a similar observation (50): slight warming (to 40°C) of a 4 mM aqueous solution (containing 0.04M $NaNO_3$) of the head-to-head platinum(II) 1-methylthymine dimer in an open flask over a period of 9 days led to a color change from pale yellow (same as Pl-MeU) via green and purple to blue.

A careful time study by LC noting changes in the absorbance of the 280 envelope or a change in the oligomeric pattern was not made on aqueous solutions of Pl-MeUB. However, in this vein, it was noted earlier that aqueous solutions of the polymeric material sometimes lost their color. (Similar behavior was noted for platinum uracil blue (7) and platinum α-pyridone blue (18); in the latter case, decomposition was attributed (speculatively) to degradation of the oligomer into smaller units.) Of impurities present, only the peak at the retention time of the dimer (~7.5 min) was identified with any certainty. Woollins and Rosenberg also identified $Pt(NH_3)_2(OH)$(1-MeU) and $Pt(NH_3)_2$(1-MeU)$_2$ (and $Pt(NH_3)_2Cl$(1-MeU) in

saline solution) as impurities and hydrolysis products, with the former being both the major impurity and the primary hydrolysis product (80). They report that the loss of blue color is concurrent with the appearance of $Pt(NH_3)_2(OH)(1\text{-MeU})$ without, apparently, the intermediate formation of $[(NH_3)_2Pt(1\text{-MeU})_2Pt(NH_3)_2]^{2+}$. This, they speculate, may argue against double bridging such as is found in the tetramer platinum α-pyridone blue. This would be consistent with the singly-bridging structural representation made throughout this dissertation.

They further suggest that the loss of color is almost certainly accompanied by reduction of platinum. (They erroneously assumed an average Pt oxidation state of 2.25.) This question could be studied directly by electrochemistry by, say, differential pulse polarography or RDV at Pt, or indirectly by LC-EC in the reductive mode. Careful study of the hydrolysis with identification of all hydrolysis products would allow enlightened (hopefully) speculation as to the bridging character of the polymer, similar to the speculations Woollins and Rosenberg based on calf serum and DNA experiments (80). While the color faded from some aqueous preparations of Pl-MeUB, this was by no means universally true. Some preparations turned brown or honey colored with time, indicative of an oxidative process, as was also observed for Pl-MeU. Obviously, the variability in behavior of the blue and precursor requires carefully-controlled experiments for meaningful study. The two other blues in the author's possession - platinum benzoate blue and platinum phthalate blue - could not be run using the developed LC conditions since neither was soluble in the mobile phase.

A Method for the Estimation of the Molecular Weight Range of Platinum 1-Methyluracil Blue -

Estimation of the molecular weight range of platinum blues is an important part of the characterization of these species. By gel electrophoresis the molecular weight distribution of platinum thymine blue was estimated to range from 3,000 to 1,000 or less with a maximum around 2,000 amu (5). By sedimentation analysis (ultracentrifugation), an upper limit of 5,000 amu was estimated for the molecular weight of bis(cyclopropylamine)platinum 1-methylthymine blue (19). A polymer consisting of roughly 20 units seems to be a currently accepted vlaue for the blues(18). There is no way to make an accurate estimate of the molecular weight range of Pl-MeUB based on the chromatograms of Figure 58, although at the risk of contradiction within the same sentence, to postulate 20 units does not appear to be unreasonable. In an earlier section, an estimate of 30 units was made based solely on electrochemical data, but there is considerable uncertainty attached to this figure (pp. 134-138). A treatment follows which, <u>in principle</u>, should allow a molecular weight estimate from IPRPLC measurements. The method relies on a quantitative description of the ion-pairing LC technique (151). As a forewarning, though, the analysis is simplistic in that it assumes a single mechanism to be operative - i.e., ion-pairing - without complication from other modes such as adsorption, ion-exchange, size exclusion, or solubility of unpaired ions in the stationary phase.

Let us develop the treatment for ion-pairing with reference to

$[(NH_3)_2Pt(1\text{-}MeU)_2Pt(NH_3)_2]^{2+}$. We can represent the ion-pairing process as

$$R^{n+}_{aq} + nC^-_{aq} \rightleftarrows (RC_n)_{aq} \rightleftarrows (RC_n)_{org}$$

where R^{n+} =

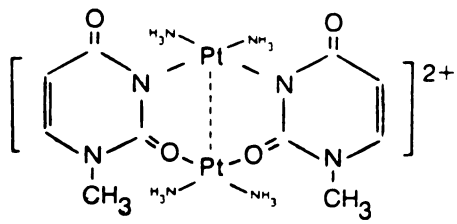

will be of immediate interest, but recognizing that the treatment is a general one; C is an alkylsulfonate counter ion. An overall ion-pair equilibrium constant can be written:

$$K_{ip} = \frac{[(RC_n)_{org}]}{[R^{n+}_{aq}][C^-_{aq}]^n}$$

The ratio of solute in the two phases is given by

$$\frac{[(RC_n)_{org}]}{[R^{n+}_{aq}]} = K_{ip}\,[C^-_{aq}]^n$$

The retention of solute in LC is given by

$$t_R = (L/\mu)(1 + k')$$

where L = the length of the column,

μ = the linear velocity of the eluent,

k' = the capacity factor, the number of moles of solute in the stationary phase divided by the number of moles in the mobile phase; i. e.,

$$k' = \frac{[(RC_n)_{org}]V_s}{[R^{n+}_{aq}]V_m}$$

where V_s = the volume of the stationary phase

and V_m = the volume of the mobile phase.

Then $$t_R = (L/\mu)(1 + \frac{[(RC_n)_{org}]V_s}{[R^{n+}_{aq}]V_m})$$

$$= (L/\mu)(1 + (V_s/V_m)K_{ip}[C^-_{aq}]^n)$$

or, since V_s/V_m is a constant,

$$t_R = (L/\mu)(1 + K[C^-_{aq}]^n) \qquad (293.1)$$

The retention time is seen to be dependent on both the ion-pair formation constant and on the concentration of the ion-pairing anion (at least up to a point). Hence, for each oligomeric species we can write

$$t_R(n_1) = (L/\mu)(1 + K_{n_1}[C^-_{aq}]^{n_1})$$

$$t_R(n_2) = (L/\mu)(1 + K_{n_2}[C^-_{aq}]^{n_2})$$

etc.

These equations can be used to determine n as follows. For the known dimeric system we have $t_R = L/\mu + (L/\mu)K[C^-_{aq}]^2$. Rearranging and taking the logarithm of each side,

$$\ln(t_R - L/\mu) = \ln[(L/\mu)K] + 2\ln[C^-_{aq}] \qquad (294.1)$$

Plotting $\ln(t_R - L/\mu)$ vs $\ln[C^-_{aq}]$, the slope should be 2 if the equation is obeyed. If we assume that the charge per dimeric unit in the polymer is also 2 (and it is very close to 2), then by the same approach, we can calculate n for the center of the chromatographic band as well as at each edge to get the range of n. In actuality, since data previously discussed suggest that approximately 1 Pt atom in 12 or more is in the +3 oxidation state, the value obtained for n will have to be multiplied by a factor $\geq$ 11/12. Obviously, the premise here is that all charged sites participate in the ion-pairing process. The implausibility of this assumption was indicated in the previous section with regard to the retention time of P(all III)1-MeUB. The reader is reminded that the use of eq. 293.1 assumes isocratic elution.

A plot of $\ln(t_R - L/\mu)$ vs $\ln[C^-_{aq}]$ (octylsulfonate), over the range 4 mM to 14 mM, was linear, as shown in Figure 59a; however, the slope is not 2.0, but is, rather, 1.1. Over the range 1 mM to 5 mM, the plot shown in b was obtained, for which a slope of 1.6 was calculated. Note that the last two points in plot b fall below the line, in agreement with a. Also, the first point (corresponding to 1 mM) is well below the line, almost suggesting the possibility that

points in this region might yield a line of slope equal to 2. However, the concentrations of counter ion (pairing agent) in this region fall below those considered effective in IPRPLC (167). Why the slopes are different over these two concentration ranges in the observed order is not certain. In any case, since the agreement between the experimental (n = 1.6) and expected (n = 2.0) values was not better for a single dimeric unit, it would be folly to attempt to apply this procedure over many units, where the uncertainty would be multiplied.

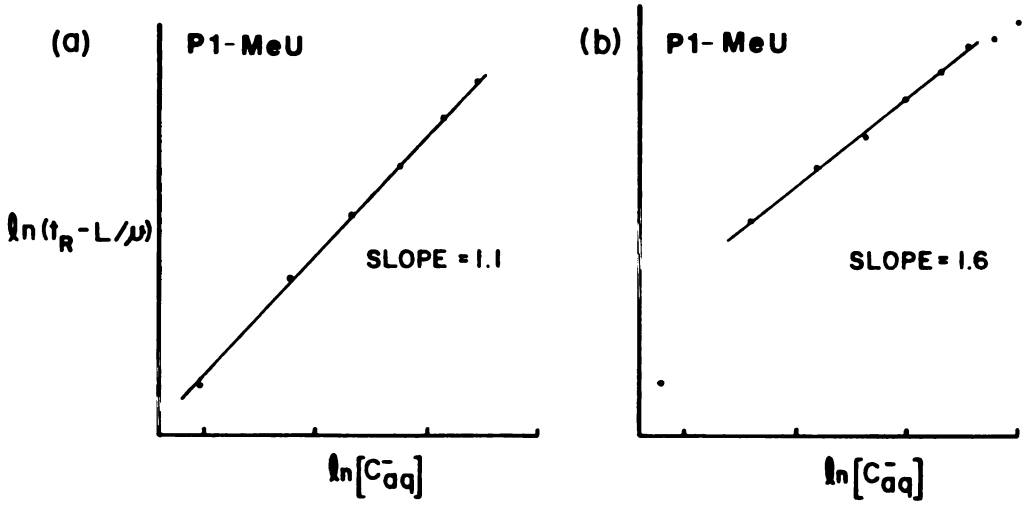

Figure 59. Plots of $\ln(t_R - L/\mu)$ vs $\ln[C^-_{aq}]$ for $[C^-]$ over the range a) 4-14 mM and b) 1-5 mM.

It is of interest to test the fit of eq. 294.1 to data published in the literature. O'Laughlin and Hanson applied IPRPLC to the separation of 1,10-phenanthroline complexes of several metals including iron (163). Data were taken from Table II in their publication, which covers a concentration range of 10^{-4}M to 10^{-2}M for the heptanesulfonate pairing ion, and eq. 294.1 applied. The

theoretical n for $[Fe(phen)_3]^{2+}$ is 2; the calculated, based on their data, is 0.18, an order of magnitude below the theoretical. Based on the observations made above regarding concentration of the counter ion, perhaps it is an unfair test to try to apply the equation over two orders of magnitude. Additionally, perhaps a mixed-separation mechanism was at work there, just as here.

Before leaving this section, it is appropriate to mention that a direct technique, one used in conjunction with column chromatography (usually size-exclusion), exists for the determination of molecular weights in polymers: A computerized detection scheme based on low angle laser light scattering (LALLS) allows the calculation of molecular weights without reference to standards of known molecular weight (15, 168). Unfortunately, this detection scheme cannot be used when the analyte either absorbs or fluoresces significantly upon irradiation by the incident laser beam. As the wavelenth of the incident helium-neon laser used in the commercial apparatus (Chromatix, Inc.) is 6330 Å, and since Pl-MeUB exhibits a broad absorption band that peaks at 6600 Å, LALLS would not be helpful in the present case.

Size-Exclusion Chromatography -

The most straightforward way of determining molecular weights of polymeric materials, both synthetic and naturally-occurring, is by gel permeation (or filtration) chromatography, today more generally lumped under the heading size-exclusion chromatography. A Waters Protein I-60 column was used in an attempt to obtain a fractionation

on the basis of size. This column contains a functionalized packing with pore size distribution adequate to the separation of native globular proteins ranging in molecular weight from 1,000-20,000 or of random coiled protein over the range 600-8,000 (169). Platinum 1-methyluracil blue almost certainly falls within these limits. A typical mobile phase employed consisted of 0.025M $TBA^{+}NO_3^{-}$ in 50:50 $MeOH/H_2O$ adjusted to pH 3.0 with HNO_3.

In size-exclusion chromatography, compounds of a given molecular configuration or of similar shape, elute in the inverse order of their size. Regardless of the conditions employed here, though, the compounds of interest could not be made to elute in any order except in the order of <u>increasing</u> molecular weight. Obviously, size-exclusion was overwhelmed by (an)other mode(s). There is no point in belaboring the issue, but experimentation suggested that a combination of adsorption and reversed phase interactions may have been operative, and that these charged compounds simply are unsuited for a separation based on size-exclusion; this was true even when ion-pairs were first formed. While, apparently, the size-exclusion separation of metal ions can be accounted for in terms of the size of the hydrated ion, the size separation of metal complexes seems to have been restricted to neutral, covalently-bonded complexes, exclusive of salts (153).

Isotachophoresis[1] (170, 171)

Goals -

The original intent of using isotachophoresis (ITP) in this work was to obtain an estimate of the molecular weight range of the polymeric Pl-MeUB. In order to accomplish this, certain assumptions of perhaps questionable validity regarding the relationship between size and mobility would have to be made. This is somewhat akin to the assumptions made earlier when using the Einstein-Stokes equation to estimate the average molecular weight of Pl-MeUB (p. 134). However, after LC examination of Pl-MeUB showed it to be a highly complex mixture of unresolved components, the probability of acquiring additional useful molecular weight information by ITP was deemed to be too low to justify the expenditure of time that would be required. An alternative use for ITP was found, though, and that was to follow the oxidative electrolysis of Pl-MeU in support of either 1) $[P(II,II)1\text{-MeU}]^{2+} \xrightarrow{-e^-} [P(II,III)1\text{-MeU}]^{3+} \xrightarrow{-e^-} [P(III,III)1\text{-MeU}]^{4+}$ or 2) $[P(II,II)1\text{-MeU}]^{2+} \xrightarrow{-2e^-} [P(II,IV)1\text{-MeU}]^{4+}$. The problem encountered in attempting to make this distinction by LC has been previously discussed. For the reader who is unfamiliar with isotachophoresis, a short introduction follows.

---

1. Since there is no literature on isotachophoresis applied to blues or related compounds, no discussion was given of this technique in the Literature Review; consequently, it is introduced at this point.

Introduction -

Isotachophoresis(ITP) is an electrophoretic separation technique that separates ions on the basis of their differing mobilities. As such it is related to the better-known zone electrophoresis. However, in ITP a stabilizing gel is not required as it is in electrophoresis; ITP is a free-flowing technique. Another difference is that, while in electrophoresis diffusion causes bands to broaden as in conventional chromatography, in ITP the zones are contiguous and sharp at their borders (vide infra).

As the name isotachophoresis implies, the equilibrium (steady state) condition of ITP requires that, under the application of a constant electric field, all zones migrate (phoresis, short for electrophoresis, meaning to carry) at the same (iso) velocity (tacho). In the idealized case, sharp boundaries demarcate ions (zones) of differing mobility. Within a zone, the concentration of a separand (ionic solute) is constant, so that the length of a zone is in direct proportion to the concentration of the solute ion. Unlike most differential migration methods in which dispersion via diffusion prevents a sharp demarcation between bands or zones, in ITP the combined effects of a constant electric field within a given zone and an abrupt change in the magnitude of that field at the boundary between zones (vide infra), serve to counter intermixing of ions between zones. Hence, distinct, contiguous zones are maintained once the steady state has been achieved. Before elaborating on the technique, the previous statement should be tempered with the

observation that in actuality the boundary is less abrupt than implied here.

Several conditions must obtain in order to satisfy the steady-state requirements of isotachophoresis: A discontinuous electrolyte system is used in which sample ions of intermediate mobility are introduced between a leading electrolyte of highest mobility and a terminating electrolyte of lowest mobility. (It is very similar to the moving boundary method for the determination of transference numbers, familiar to electrochemists.) A counter ion common to all zones provides the required electroneutrality. When power (the electric field) is first applied to the system, sample ions migrate differentially in accordance with their differing mobilities. As the ions begin to separate into their contiguous zones, the magnitude of the field within each zone (ill-defined at this point) reflects the conductance (or resistance) and in turn the mobility of the ions in each zone. This process continues until equilibrium is attained throughout the system. At this point the electric field is constant, and different, in each zone and its magnitude inversely proportional to ion mobility. Under this steady-state condition, each zone, including the leading and terminating zones, moves at the same velocity; this is the moving boundary principle of ITP. The partial differential equations describing the dynamics of the isotachophoretic separation have been solved by Vacik and Fidler (172).

As stated in the preceding paragraph, in order to achieve and

maintain the sharp boundaries attendant to the steady state, the separands must be flanked by leading and terminating ions of higher and lower mobility, respectively; in addition, there is the requirement of a common counter ion. Experience is the best guide as to what ions to try in the leading and terminating zones, although tables of suggested ions have been compiled for many applications (170). The sharp boundary between zones is maintainable because there is no background electrolyte to support conductance from zone to zone (as there is in zone electrophoresis), and therefore all zones migrate with the same velocity.

The mathematical expression fundamental to isotachophoresisis is due originally to Kohlrausch (173), although in 1897 he most certainly did not derive the equation in relation to isotachophoresis, as the technique as we know it today is only about a dozen years old:

$$\frac{C_B}{C_A} = \frac{U_B(U_A + U_C)}{U_A(U_B + U_C)} \cdot \frac{Q_A}{Q_B}$$

This equation expresses the condition that exists at a boundary. C_A and C_B are the concentrations of ions A and B in leading and trailing zones (for any two contiguous zones), respectively, U_A and U_B are their respective mobilities, and U_C is the mobility of the counter ion. Q_A and Q_B are the charges on A and B. Their inclusion extends the theoretical treatment to ions of differing valency. The mobilities U may be determined using the equation $v = U \cdot E$, where v is

velocity and E is the electrical field strength.

The Kohlrausch equation assumes an abrupt boundary between zones. Refinements to the Kohlrausch expression take into account the boundary-comprising effects of diffusion, electroosmosis, radial and axial temperature gradients, gravity effects, and pH (for protolytic species) (174). Protolytic or not, the pH should be kept in the range ~4-10.5 (depends somewhat on the leading electrolyte concentration) to prevent a too-large fraction of the current from being carried by the highly mobile hydrogen and hydrolxyl ions. Again for the reader who is not familiar with isotachophoresis, a brief description of apparatus and brief mention of the range of applicability of ITP is included in the next two sections.

Isotachophoretic Apparatus -

Analytical isotachophoresis is usually conducted in open, coiled capillaries of lengths up to 1 m, either glass or (usually) teflon. The separating apparatus is an all nonmetallic system, an important consideration for many kinds of samples, including Pl-MeU as we saw in the LC section of this dissertation. Modern analytical isotachophoresis is known as capillary isotachophoresis. Universal detection may be by either conductimetry or thermal gradient, although only the latter has been commercialized. A change in detector signal appears at each zone boundary. The output is typically in integral form. Where applicable, UV/Vis detection can also be used; this is also commercially available. Power supplies

capable of delivering up to 30 kV @ 300 μA are used in isotachophoresis. The amount of current passed affects both the time of analysis and resolution.

Applications -

The range of applicability of isotachophoresis extends from the separation of metal ions through charged organics to the separation of large biomolecules, although not all in the same run. It is relevant to the current investigation to mention that the systematic application of theory is less straightforward for large, less-well characterized molecules because mobility data are often lacking. ITP is notable for its many applications to trace determinations of drugs and metabolites in physiological fluids with minimum sample workup.

Applicability to Pl-MeU and Pl-MeUB -

Analytical (capillary) isotachophoresis is characterized by its speed, resolution, sensitivity, and also for its concentrating effect on dilute samples (175). The first two of these are relevant to the study at hand. Its speed and the lack of sample manipulation required make it particularly attractive to unstable chemical species.

The failed attempt due to on-column reduction to distinguish between the two alternative oxidative pathways 1) $[P(II,II)1\text{-}MeU]^{2+} \xrightarrow{-e^-} [P(II,III)1\text{-}MeU]^{3+} \xrightarrow{-e^-} [P(III,III)\text{-}1\text{-}MeU]^{4+}$ and 2) $[P(II,II)1\text{-}MeU]^{2+} \xrightarrow{-2e^-} [P(II,IV)1\text{-}MeU]^{4+}$ by liquid chromatography was detailed earlier. As was mentioned there, the

electrolysis of Pl-MeU may be, alternatively, monitored by ITP, which in commercial form utilizes a (nonmetal) teflon separating tube. In the former case (1)), three zones, corresponding to the di-, tri-, and tetravalent species, are to be expected, whereas in the latter, two zones, corresponding to the di- and tetravalent species would obtain.

The argument has been made throughout this thesis in behalf of the $Pt(II)\text{-}Pt(II) \xrightarrow{-e^-} Pt(II)\text{-}Pt(III) \xrightarrow{-e^-} Pt(III)\text{-}Pt(III)$ sequence. ITP allows ready prediction of the order of elution of these three species. This is because the intrinsic mobilities (i.e., the mobility independent of charge, not to be confused with conductance) can be presumed to be identical for these three species since their molecular composition is identical. Then, under the influence of the electric field, the (III,III) species, having the highest charge, will elute first and the (II,II) last. Hence, by using isotachophoresis to follow the electrolysis of P(II,II)l-MeU, evidence either supportive of or contradictive to the presumed formation of the P(II,III)l-MeU and P(III,III)l-MeU species may be obtained.

A second area of possible application, as previously mentioned, is to the blue. A previous, attempted analysis of Pl-MeUB by zone electrophoresis reportedly led to its decomposition (176). ITP, which should be an inherently "gentler" technique than electrophoresis, provides an alternative to electrophoresis to study the oligomeric distribution of blues. By making certain assumptions, not unlike was

done earlier when the Einstein-Stokes equation was invoked in conjunction with electrochemical measurements to make an estimate of the average molecular weight of Pl-MeUB, an estimate of molecular weight based on ITP measurements could also be made: Having determined the mean mobility of the blue, $\bar{U}$, from ITP measurement, then D, the diffusion coefficient, may be calculated from $D = \bar{U}_{abs}kT$, an equation due to Eistein. M, the molecular weight, can then be obtained, as before, from the Einstein-Stokes eq: $D = (2.96 \times 10^{-7}/\eta)(d/M)^{1/3}$. The particular problem that the continuously-distributed Pl-MeUB (vide supra) would be expected to pose to the use of ITP, is that the requirement of sharp zones between ions will not be easily met. Hence, $\bar{U}$, as well as the range of U, ΔU ($=U_{max} - U_{min}$) (from which the range of M may be obtained), may be difficult to ascertain. Although initially plans were made to examine the polymer by ITP, as previously mentioned, those plans were later abandoned in light of the bleaker prognosis for ITP which evolved.

Results[1] -

Isotachophoretic conditions were worked out for the migration of $[Pl\text{-}MeU]^{n+}$ where n = 2, 3, or 4 (see Experimental section). The intermediate (n=3) and final (n=4) electrolysis products of Pl-MeU used in working out the conditions of ITP analysis had been isolated

---

1. The work was performed by Dr. S. W. Barr of the Analytical Laboratories, The Dow Chemical Co., Midland, MI.

some months prior to commencing the isotachophoretic work. The fact that they had discolored and obviously decomposed over those few months, made them unsuited for use in addressing the question of the mechanistic pathway posed in the previous section. Unfortunately, a joint electrolysis/ITP experiment akin to the earlier-described electrolysis/LC experiment was not performed.

CONCLUSIONS AND RECOMMENDATIONS

A platinum pyrimidine blue - platinum 1-methyluracil blue (Pl-MeUB) - and its comparatively simple relative (parent) - the dimeric platinum 1-methyluracil - have been characterized as to their chemical properties via examination by electrochemistry, redox titrimetry, liquid chromatography (LC), and several techniques in conjunction with controlled-potential coulometry (CPC): visible/near infrared spectroscopy, electron paramagnetic resonance spectroscopy, and nuclear magnetic resonance spectroscopy.

The polymeric blue was shown to be weakly paramagnetic. Both the blue's paramagnetism and that of the dimer's electrolysis intermediate were attributed to the III valence state. The paramagnetism was accounted for in terms of molecular orbital theory. Indirect confirmation of the +3 state was sought by a joint CPC/LC experiment and later by CPC/isotachophoresis (ITP). X-ray photoelectron spectroscopy (XPS), although not done, could furnish complementary evidence for the existence of a III valence in the solid state. The emerging picture from this and previous work is that tervalent platinum is integrally associated with the chemical properties of the platinum blues.

A characteristic feature of blues is their intense color.

Application of the Hush model treatment to Pl-MeUB and to the Pl-MeU electrolysis intermediate indicated extensive delocalization of (the) unpaired electron(s), although the treatment of the former was hampered somewhat by imprecise molecular weight information. The extensive delocalization, in turn, implies significant Pt-Pt overlap. Somewhat disconcerting is the fact that the calculated thermal rate constants for the intervalence electron transfer are inordinately low relative to other known complexes.

Cyclic voltammetry and redox titrimetry also supported the existence of the III valence state for platinum in the dimer, and by inference, in the blue. By comparison, unbridged complexes and compounds containing saturated ligands were shown not to stabilize the tervalent state. A satisfying explanation for this behavior was not advanced; this is an area of potential study for the theoretician. Oxidation to tetravalent platinum, a common and long-recognized oxidation state of platinum, was not achieved in these compounds using Ce(IV) as the oxidant.

The cyclic voltammetric (CV) profiles as a function of scan rate proved interesting, particularly for Pl-MeU. Adsorption or precipitation on the electrode was invoked, in part, to account for the observed behavior. Precipitation on the electrode was also demonstrated by rotating disk voltammetry and controlled-potential coulometry, particularly for Pl-MeUB. While Pl-MeU exhibited first-order behavior during oxidative electrolysis (by CPC), Pl-MeUB proved much more troublesome. This was thought to be due secondarily

to adsorption, but primarily to sluggish kinetics - i.e., the last electrons removed from Pl-MeUB are removed with great difficulty; the latter may be related to the former.

As an alternative to CPC in conventional cells, thin-layer CPC could, possibly, make more definitive the determination of n, ameliorating the drawn-out electrolysis curves obtained using conventional CPC; this was discussed briefly in the earlier text. Drawing on coulometric studies made of biological molecules, the use of a suitable mediator-titrant to accelerate electron transfer might also prove useful to a determination of n for the polymeric Pl-MeUB. Another approach is to chemically modify the electrode to accelerate the electron transfer process (178). As a general statement - meaningful application of electrochemical techniques to Pl-MeUB in this study was limited by a lack of knowledge of n (and also M, which in turn yields C).

The attempted use of LC to estimate a molecular weight range for Pl-MeUB was not entirely successful, although a crude estimate based solely on electrochemical measurements was made. Mass spectroscopic examination of Pl-MeUB by fast atom bombardment for the purpose of elucidating molecular weight also proved unsuccessful. The use of ^{252}Cf plasma desorption might prove successful, although use of this technique is limited by the few instruments in existence. The primary use of LC in this work was a qualitative one: Variously prepared and aged aqueous solutions of Pl-MeU and Pl-MeUB were run, thereby furnishing information about the stability of these

preparations. A careful, controlled study beyond that conducted here would lend additional, useful information.

The accurate determination of molecular weights would provide an enormously valuable contribution toward a better understanding of platinum blues. As an adjunct to this, chromatographic characterization of a blues mixture would shed new light on the composition of these materials. Having obtained in this work only a broad envelope for Pl-MeUB by LC due to the complexity of the oligomeric material, it is clear that only the highest efficiency chromatographic system has a chance of unraveling the nature of Pl-MeUB and other blues. The blues could serve as excellent trial compounds for capillary LC as this emerging technique continues to be developed.

In retrospect, the method for molecular weight estimation developed (proposed) in this thesis, one based on ion-pair LC, was perhaps a bit naive in that it was contingent on a pure mechanism being operative. Although certain assumptions would also be inherent to an attempt at molecular weight determination by isotachophoresis - viz., relating the mobility of the oligomeric chains to the mobility of the dimer - the mechanism in ITP is a <u>pure</u> one (migration) since neither a support nor a stationary phase is used in this technique. Therefore, capillary ITP could prove elucidative in this regard.

An alternate approach to molecular weight determination may be provided by electrical field flow fractionation (EFFF), a technique originally due to Giddings (ref. 177 provides an overview of FFF).

Using EFFF, the diffusion coefficient may be gotten from $\lambda = D/(\mu Ew)$, where λ is the retention parameter, w is the channel width, μ is the electrophoretic mobility, E is the electrical field strength, and D is the diffusion coefficient. The ability to change E throughout a run (a programmed E run), makes EFFF quite versatile, and increases the resolution of the method. As before, having determined D, M may then be calculated from the Einstein-Stokes equation. One other technique - LALLS (low angle laser light scattering) - could yet prove usable if a longer-wavelength laser (an infrared laser) were used as the incident beam (although the scattering intensity would be decreased).

Ever since the first synthesis of platinum blues, the so-far elusive goal has been to obtain crystalline material suitable for X-ray analysis. Wider availability of extended X-ray absorption fine structure spectroscopy (EXAFS) would help in future structural characterizations. A number of comparatively simple, largely binuclear compounds similar to the dimeric Pl-MeU have been structurally characterized by X-ray crystallography and were discussed in the body of this thesis. The (II,III) electrolysis intermediate formed in this study was not suitable for X-ray analysis (neither was the (II,II) starting compound). Since, to our knowledge, a binuclear Pt(II)Pt(III) compound has not been previously reported in the literature, it would be of interest to obtain a crystalline material, if possible.

It had been one of the goals of this project to study the

formation of $[P(II,III)1\text{-}MeU]^{3+}$ under different conditions of electrolysis. This was to be done in conjunction with periodic examination of the electrolyte by LC to assess purity of the mixed-valence compound. However, because of the on-column reduction problem alluded to in the LC section, this was not done. Even without this study though, we recognize the difficulty in forming $[P(II,III)1\text{-}MeU]^{3+}$ to the exclusion of $[P(III,III)1\text{-}MeU]^{4+}$. While accurate $E^{o'}$s corresponding to the two half-reactions were not obtained in this study, inspection of the CV's suggests that they may be quite close. Hence, the reason that we are able to generate and isolate the $[P(II,III)1\text{-}MeU]^{3+}$ intermediate at all, may be that the thermodynamics of the situation can be circumvented ("cheated") by the slow kinetics associated with the second electron transfer. It might be of interest to perform the electrolysis at low temperatures, perhaps in an organic solvent with a lower freezing point than that of water, and note the dependence of $\{[P(II,III)\text{-}1\text{-}MeU]^{3+}\}/\{[P(III,III)1\text{-}MeU]^{4+}\}$ on temperature.

With regard to the determination of $E^{o'}$s for quasi-reversible and/or highly irreversible systems, such as those we have been concerned with here - in recent years spectroelectrochemistry, particularly thin-layer spectroelectrochemistry, has been successfully applied to the study of these less tractable systems (e.g., 107, 179). In one type of spectroelectrochemical experiment involving transmission measurements, the ratio of oxidized to reduced forms may be determined spectroscopically at several different

potentials. This is most readily done when separate wavelengths are available which are characteristic of the oxidized and reduced forms. However, in the event that no single characteristic peak is available for each form, as is the case here, then several wavelengths may be monitored, either simultaneously, or in rapid succession, and the ratios of oxidized to reduced forms calculated through the use (usually) of a microcomputer. For a highly irreversible system, a mediator-titrant may be required. Appropriate plotting of the data then yields the E^{o}. In general, the application of thin-layer spectroelectrochemistry, utilizing either optically transparent or minigrid electrodes, could prove extremely valuable to an electrochemical study of the colored platinum blues and related compounds.

Scant attention was paid in this thesis to the carboxylate blues - platinum benzoate blue and platinum phthalate blue - blues whose properties, based on brief CV and titrimetric experiments, were shown to be different from those of the more conventional pyrimidine blue, Pl-MeUB. This difference is typified in the considerably higher average oxidation state of Pt determined for PBzB vis-a-vis Pl-MeUB. Essentially the whole gamut of techniques used in this study could be applied to the investigation of these interesting and unusual compounds, although because of solubility differences, certain difficulties might be encountered.

It is apparent, that for a thorough understanding of the blues and related compounds, a number of different disciplines or

REFERENCES

techniques need to be brought to bear in any investigation. Hence, although a study of the blues is perhaps most appropriately within the purview of the inorganic or bioinorganic chemist, such a study can also have appeal to the analytical chemist. Interpretation of data beyond the level often required of the analytical chemist can serve as a stimulating and expansive experience. However, for the "hard-core" analytical chemist who wishes to devise methods for the determination of blues and related compounds, challenging opportunities will no doubt present themselves if the blues are brought to clinical trial, as sensitive methods will be required for their determination in physiological fluids.

REFERENCES

1. Rosenberg, B. Interdiscipl. Sci. Rev., 3, 1, 1978.

2. Davidson, J. P., Faber, P. J., Fischer, R. G., Jr., Mansy, S., Peresie, H. J., Rosenberg, B., and VanCamp, L. Cancer Chemoth. Rep. Part 1, 59, 287, 1975.

3. Kurnakow, N. J. Prakt. Chem., 51, 234, 1895.

4. Hofmann, K. A. and Bugge, G. Berichte, 41, 312, 1908.

5. Lippert, B. J. Clin. Hematol. Oncol., 7, 26, 1977.

6. Blake, C. C. F., Oatley, S. J., and Williams, R. J. P. J. Chem. Soc. Chem. Comm., 1043, 1976.

7. Lippard, S. J. Acc. Chem. Res., 11, 211, 1978.

8. Connors, T. A. and Roberts, J. J., eds. Platinum Coordination Complexes in Chemotherapy, Springer, 1974.

9. Cleare, M. J. Coord. Chem. Rev., 12, 349, 1974.

10. Zipp, A. P. and Zipp, G. S. J. Chem. Educ., 54, 739, 1977.

11. Speer, R. J., Ridgway, H., Hall, L. M., Stewart, D. P., Howe, K. E., Lieberman, D. Z., Newman, A. D., and Hill, J. M. Cancer Chemother. Rep. Part 1, 59, 629, 1975.

12. Barton, J. K. and Lippard, S. J. Ann. N. Y. Acad. Sci., 313, 686, 1978.

13. Cotton, F. A. and Wilkinson, G. Advanced Inorganic Chemistry, Fourth ed., Chpt. 22, John Wiley & Sons, 1980.

14. Goldberg, R. N. and Hepler, L. G. Chem. Rev., 68, 229, 1968.

15. Ouano, A. C. and Kaye, W. J. Polym. Sci., Part A-1, 12, 1151, 1974.

16. Gillard, R. D. and Wilkinson, G. J. Chem. Soc., 2835, 1964.

17. Flynn, C. M., Jr., Viswanathan, T. S., and Martin, R. B. Inorg. Nucl. Chem., 39, 437, 1977.

18. Barton, J. K., Caravana, C., and Lippard, S. J. J. Am. Chem. Soc., 101, 7269, 1979.

19. Thompson, A. J., Roos, I. A. G., and Graham, R. D. J. Clin. Hematol. Oncol., 7, 242, 1977.

20. Teo, B.-K., Kijima, K., and Bau, R. J. Am. Chem. Soc., 100, 621, 1978.

21. Matsumoto, K. and Fuwa, K. J. Am. Chem. Soc., 104, 897, 1982.

22. Ettorre, R. Inorg. Chim. Acta, 46, L27, 1980.

23. Zaplatynski, P., Neubacher, H., and Lohmann, W. Z. Naturforsch., 34b, 1466, 1979.

24. Chang, C. A., Marcotte, R. B., and Patterson, H. H. Inorg. Chem., 20, 1632, 1981.

25. Brown, D. B., Robin, M. B., and Burbank, R. D. J. Am. Chem. Soc., 90, 5621, 1968.

26. Brown, D. B., Burbank, R. D., and Robin, M. B. J. Am. Chem. Soc., 91, 2895, 1969.

27. Barton, J. K., Rabinowitz, H. N., Szalda, D. J., and Lippard, S. J. J. Am. Chem. Soc., 99, 2827, 1977.

28. Herrmann, M. S., Cardin, A. D., and Behnke, W. D. Biochem. Pharmacol., 27, 1571, 1978.

29. Harrison, R. and McAuliffe, C. A. J. Clin. Hematol. Oncol., 7, 258, 1977.

30. Laurent, J.-P., Lepage, P., Castan, P., and Arrizabalaga, P. Inorg. Chim. Acta, 67, 31, 1982.

31. Neubacher, H., Zaplatynski, P., Haase, A., and Lohmann, W. Z. Naturforsch., 34b, 1015, 1979.

32. Melius, P. and Friedman, M. E. Inorg. Perspect. Biol. Med., 1, 1, 1977.

33. Arrizabalaga, P., Castan, P., and Laurent, J.-P. Z. Naturforsch., 35b, 1508, 1980.

34. Arrizabalaga, P., Castan, P., Laurent, J.-P., and Charlson, A. J. Inorg. Chim. Acta, 66, L9, 1982.

35. Brown, D., ed. Mixed-Valence Compounds, D. Reidel Publishing Co., 1980.

36. Robin, M. B. and Day, P. Adv. Inorg. Chem. Radiochem., 10, 247, 1967.

37. Drago, R. S. Physical Methods in Chemistry, Chapt. 15, W. B. Saunders Company, 1977.

38. Brown, D. B. and Wrobleski, J. T. Application of the Mössbauer Effect to the Study of Mixed-Valence Compounds, pp. 243-270, from Mixed-Valence Compounds, ed., Brown, D. B., D. Reidel Publishing Co., 1980.

39. Day, P. Introduction to Mixed-Valence Chemistry, p. 13, from Mixed-Valence Compounds, ed., Brown, D. B., D. Reidel Publishing Co., 1980.

40. Macfarlane, R. D. and Torgerson, D. F. Science, 191, 920, 1976.

41. Hollis, L. S. and Lippard, S. J. J. Am. Chem. Soc., 103, 6761, 1981.

42. Laurent, M. P., Tewksbury, J. C., Krogh-Jespersen, M.-B., and Patterson, H. Inorg. Chem., 19, 1656, 1980.

43. Barton, J. K., Best, S. A., Lippard, S. J., and Walton, R. A. J. Am. Chem. Soc., 100, 3785, 1978.

44. Laurent, M. P., Biscoe, J., and Patterson, H. H. J. Am. Chem. Soc., 102, 6575, 1980.

45. Lerner, E. I. Ph.D. Dissertation, Columbia Univ., New York, N.Y., 1976.

46. Lippard, S. J. Science, 218, 1075, 1982.

47. Barton, J. K., Szalda, D. J., Rabinowitz, H. N., Waszezak, J. V., and Lippard, S. J. J. Am. Chem. Soc., 101, 1434, 1979.

48. Hollis, L. S. and Lippard, S. J. J. Am. Chem. Soc., 103, 1230, 1981.

49. Lock, C. J. L., Peresie, H. J., Rosenberg, B., and Turner, G. J. Am. Chem. Soc., 100, 3371, 1978.

50. Lippert, B., Neugebauer, D., and Schubert, U. Inorg. Chim. Acta, 46(B1), L11, 1980.

51. Lippert, B. and Neugebauer, D. Inorg. Chim. Acta, 46(B1), 171, 1980.

52. Koningsberger, D.C. and Prins, R. Trends in Anal. Chem., 1, 16, 1981.

53. Hitchcock, A. P., Lock, C. J. L., and Pratt, W. M. C. Inorg. Chim. Acta, 66, L45, 1982.

54. Che, C.-M., Schaefer, W. P., Gray, H. B., Dickson, M. K., Stein, P. B., and Roundhill, D. M. J. Am. Chem. Soc., 104, 4253, 1982.

55. Lippert, B. Inorg. Chem., 20, 4326, 1981.

56. Seul, M., Neubacher, H., and Lohmann, W. Z. Naturforsch., 36b, 272, 1981.

57. Seul, M., Neubacher, H., and Lohmann, W. Z. Naturforsch., 36b, 651, 1981.

58. Neubacher, H., Seul, M., and Lohmann, W. Z. Naturforsch., 37c, 553, 1982.

59. Krigas, T. and Rogers, M. T. J. Chem. Phys., 55, 3035, 1971.

60. Amano, C. and Fujiwara, S. Bull. Chem. Soc. Jpn., 50, 1437, 1977.

61. Swartz, W. E., Jr. Anal. Chem., 45, 789A, 1973.

62. Hendrickson, D. N. Photoelectron Spectroscopy, Chpt. 16, from Physical Methods in Chemistry, Drago, R. S., W. B. Saunders Co., 1977.

63. Cox, P. A., Edgell, R. G., and Orchard, A. F. Photoelectron Spectroscopy of Mixed-Valence Compounds, pp. 475-502, in Mixed-Valence Compounds, ed., Brown, D., D. Reidel Publishing Co., 1980.

64. Matienzo, C. J. Diss. Abstr. Int. B, 34(12), 5890, 1974.

65. Riggs, W. M. Anal. Chem., 44, 830, 1972.

66. Burness, J. H. Inorg. Chim. Acta, 44, L49, 1980.

67. Hollis, L. S. and Lippard, S. J. Inorg. Chem., 21, 2116, 1982.

68. Muravieskaya, G. S., Kukina, G. A., Orlova, V. S., Evstefera, O. N., and Porai-Koshits, M. A. Dokl. Akad. Nauk. SSSR, 226, 596, 1976.

69. Schagen, J. D., Overbeck, A. R., Schenk, H. Inorg. Chem., 17, 1938, 1978.

70. Cotton, F. A., Falvello, L. R., and Han, S. Inorg. Chem., 21, 1709, 1982.

71. Steele, B. R. and Vrieze, K. Transition Met. Chem. (Weinheim, Ger.), 2, 169, 1977.

72. Faggiani, R., Lippert, B., Lock, C. J. L., and Rosenberg, B. J. Am. Chem. Soc., 99, 777, 1977.

73. Lippert, B. and Neugebauer, D. Inorg. Chem., 21, 451, 1982.

74. Faggiani, R., Lock, C. J. L., Pollock, R. J., Rosenberg, B., and Turner, G. Inorg. Chem., 20, 804, 1981.

75. Faggiani, R., Lippert, B., Lock, C. J. L., and Speranzini, R. A. J. Am. Chem. Soc., 103, 1111, 1981.

76. Lippert, B., Lock, C. J. L., and Speranzini, R. A. Inorg. Chem., 20, 335, 1981.

77. Faggiani, R., Lippert, B., Lock, C. J. L., and Pfab, R. Inorg. Chem., 20, 2381, 1981.

78. Britten, J. F., Lippert, B., Lock, C. J. L., and Pilon, P. Inorg. Chem., 21, 1936, 1982.

79. Faggiani, R., Lippert, B., and Lock, C. J. L. Inorg. Chem., 21, 3210, 1982.

80. Woollins, J. D. and Rosenberg, B. J. Inorg. Biochem., 19, 41, 1983.

81. Private communication with Dr. D. L. Ward, resident X-ray crystallographer, Dept. of Chemistry, Michigan State University.

82. Barber, M., Bordoli, R. S., Elliott, G. J., Sedgwick, R. D., and Tyler, A. N. Anal. Chem., 54, 645A, 1982.

83. Sawyer, D. T. and Roberts, J. L., Jr. Method 1, p. 40 in Experimental Electrochemistry for Chemists, John Wiley & Sons, Inc., 1974.

84. Cavalieri, L. F. and Lowy, B. A. Arch. Biochem. and Biophys., 35, 83, 1952.

85. Hamer, D., Waldron, D. M., and Woodhouse, D. L. Arch. Biochem. and Biophys., 47, 272, 1953.

86. Smith, D. L. and Elving, P. J. J. Am. Chem. Soc., 84, 2741, 1962.

87. Polcyn, D. S. and Shain, I. Anal. Chem., 38, 370, 1966.

88. Bard, A. J. and Faulkner, L. R. Electrochemical Methods. Fundamentals and Applications, p. 435, John Wiley & Sons, 1980.

89. Flanagan, J. B., Margel, S., Bard, A. J., and Anson, F. C. J. Am. Chem. Soc., 100, 4248, 1978.

90. Smith, T. W., Kuder, J. E., and Wychick, D. J. Polym. Sci., 14, 2433, 1976.

91. Bauer, W., Gonias, S. L., Kam, S. K., Wu, K. C., and Lippard, S. J. Biochem., 17, 1060, 1978.

92. Bauer, N. and Lewin, S. Z. Determination of Density, pp. 176, from Techniques of Organic Chemistry, Vol. I - Part I, Physical Methods of Organic Chemistry, 3rd ed., Weissberger, A., ed., Interscience Publishers, Inc., 1959.

93. Bard, A. J. and Santhanam, K. S. V. Application of Controlled-Potential Coulometry to the Study of Electrode Reactions, pp. 215-315, from Electroanalytical Chemistry, Vol. 4, ed., Bard, A. J., Marcel Dekker, Inc., 1970.

94. Harrar, J. E. Techniques, Apparatus, and Analytical Applications of Controlled-Potential Coulometry, pp. 1-167, from Electroanalytical Chemistry, Vol. 8, ed., Bard, A. J., Marcel Dekker, Inc., 1975.

95. Meites, L. Controlled-Potential Electrolysis, Chpt. IX, pp. 645-712, in Physical Methods of Chemistry, Part IIA, Electrochemical Methods, Weissberger, A. and Rossiter, B. W., eds., Techniques of Chemistry, Vol. I, Wiley-Interscience, 1971.

96. Reichnitz, G. A. Controlled-Potential Analysis, Vol. 13 of International Series of Monographs on Anal. Chem., The MacMillan Co., 1963.

97. MacNevin, M. W. and Baker, B. B. Anal. Chem., 24, 986, 1952.

98. Hanamura, S. Talanta, 2, 278, 1959.

99. Hanamura, S. Talanta, 9, 901, 1962.

100. Meites, L. Anal. Chem., 27, 1116, 1955.

101. Meites, L. Anal. Chem., 31, 1285, 1959.

102. Gelb, R. I. and Meites, L. J. Phys. Chem., 68, 630, 1964.

103. Karp, S. and Meites, L. J. Electroanal. Chem., 17, 253, 1968.

104. Untereker, D. F. and Bruckenstein, S. Anal. Chem., 44, 1009, 1972.

105. Meites, L. Pure Appl. Chem., 18, 35, 1969.

106. Stephens, F. B., Jakob, F., Rigdon, L. P., and Harrar, J. E. Anal. Chem., 42, 764, 1970.

107. Heineman, W. R., Meckstroth, M., Norris, B. J., and Su, C.-H. J. Electroanal. Chem., 104, 577, 1979.

108. Szentrimay, R., Yeh, P., and Kuwana, T. Evaluation of Mediator-Titrants for the Indirect Coulometric Titration of Biocomponents, in Electrochemical Studies of Biological Systems, ed., Sawyer, D. T., ACS Symposium Series, Vol. 38, 1977.

109. Hubbard, A. T. and Anson, F. C. The Theory and Practice of Electrochemistry with Thin Layer Cells, pp. 179-80, in Electroanalytical Chemistry, Vol. 4, ed., Bard, A. J., Marcel Dekker, Inc., 1970.

110. Hawkridge, F. M. and Bacon, K. Anal. Biochem., 78, 76, 1977.

111. Durliat, H. and Comtat, M. Anal. Chem., 54, 856, 1982.

112. Conway, A. C., Goyal, R. N., and Dryhurst, G. J. Electroanal. Chem., 123, 243, 1981.

113. Skoog, D. A. and West, D. M. Fundamentals of Analytical Chemistry, Third ed., pp. 346-7, Saunders, 1976.

114. Private communication with Dr. J. D. Woollins.

115. Allen, G. C. and Hush, N. S. Prog. Inorg. Chem., 8, 357, 1967.

116. Skoog, D. A. and West, D. M. Fundamentals of Analytical Chemistry, Third ed., Chpt. 15, Saunders, 1976.

117. Hush, N. S. Progr. Inorg. Chem., 8, 391, 1967.

118. Hush, N. S. Electrochim. Acta, 13, 1005, 1968.

119. Hush, N. S. Electron Delocalization, Structure and Dynamics in Mixed-Valence Systems, from Mixed-Valence Compounds, ed., Brown, D. B., D. Reidel Publishing Co., 1980.

120. Cowan, D. O., LeVanda, C., Park, J., and Kaufman, F. Acc. Chem. Res., 6, 1, 1973.

121. Wudl, F., Wobschall, D., and Hufnagel, E. J. J. Am. Chem. Soc., 94, 672, 1972.

122. Beattie, J. K., Hush, N. S., and Taylor, P. R. Inorg. Chem., 15, 992, 1976.

123. Powers, M. J. and Meyer, T. J. J. Am. Chem. Soc., 102, 1289, 1980.

124. Powers, M. J. and Meyer, T. J. J. Am. Chem. Soc., 100, 4393, 1978.

125. Creutz, C. and Taube, H. J. Am. Chem. Soc., 95, 1086, 1973.

126. Wong, K. Y., Schatz, P. N., and Piepho, S. B. J. Am. Chem. Soc., 101, 2793, 1979.

127. Piepho, S. B., Krausz, E. R., and Schatz, P. N. J. Am. Chem. Soc., 100, 2996, 1978.

128. Drago, R. S. Chpts. 9, 10, & 13 from Physical Methods in Chemistry, W. B. Saunders Co., 1977.

129. McGarvey, B. R. Electron Spin Resonance of Transition-Metal Complexes, pp. 89-201, from Transition Metal Chemistry, Vol. 3, ed., Carlin, R. L., Marcel Dekker, Inc., 1966.

130. Kastening, B. Joint Application of Electrochemical and ESR Techniques, Chpt. 6, pp. 421-494, from Electroanalytical Chemistry, Vol. 10, ed., Nürnberg, H. W., Advances in Analytical Chemistry and Instrumentation, ed., Reilly, C. N., John Wiley & Sons, 1974.

131. McKinney, T. M. Electron Spin Resonance and Electrochemistry, pp. 97-278, from Electroanalytical Chemistry, Vol. 10, ed., Bard, A. J., Marcel Dekker, Inc., 1977.

132. Tabner, B. J. Electron Spin Resonance (e.s.r.) Spectroscopy, Chpt. 4, p. 219, in Spectroscopy, eds., Straughan, B. P. and Walker, S., Chapman and Hall, 1976.

133. Amano, C. and Fujiwara, S. Bull. Chem. Soc. Jpn., 46, 1379, 1973.

134. Ballhausen, C. J. Introduction to Ligand Field Theory, McGraw-Hill Book Co. Inc., 1962.

135. Mehran, F. and Scott, B. A. Phy. Rev. Lett., 31, 99, 1973.

136. Mehran, F. and Scott, B. A. Phy. Rev. Lett., 31, 1347, 1973.

137. Assour, J. M. J. Chem. Phys., 43, 2477, 1965.

138. Drago, R. S. Chpt. 9, p. 324, Physical Methods in Chemistry,

W. B. Saunders Co., 1977.

139. Deduced from hydration energies - Cotton, F. A. and Wilkinson, G. Advanced Inorganic Chemistry, Second ed., Chpt. 2, John Wiley & Sons, Inc., 1966 - and from apparent (so-called thermochemical) radii of polyatomic anions - Huheey, J. E. Inorganic Chemistry, Second ed., Chpt. 3, Harper & Row, Published, Inc., 1978.

140. Drago, R. S. Chpt. 9, pp. 348-49, Physical Methods in Chemistry, W. B. Saunders Co., 1977.

141. Drago, R. S. Chpt. 12, Nuclear Magnetic Resonance Spectra of Paramagnetic Transition Metal Ion Complexes, from Physical Methods in Chemistry, W. B. Saunders Co., 1977.

142. Drago, R. S. Chpt. 9, p. 348, Physical Methods in Chemistry, W. B. Saunders Co., 1977.

143. Cooper, J. W. Chpt. 3, p. 60, Spectroscopic Techniques for Organic Chemists, John Wiley & Sons, 1980.

144. Snyder, L. R. and Kirkland, J. J. Introduction to Modern Liquid Chromatography, 2nd ed., John Wiley & Sons, Inc., 1979.

145. Hamilton, R. J. and Sewell, P. A. Introduction to High Performance Liquid Chromatography, Chapman and Hall, 1977.

146. Schwedt, G. Chromatograhic Methods in Inorganic Analysis, Dr. Alfred Hüthig Verlag Heidelberg, 1981.

147. Woollins, J. D. and Rosenberg, B. Inorg. Chem., 21, 1280, 1982.

148. Horvath, C., Melander, W., Molnar, I., and Molnar, P. Anal. Chem., 49, 2295, 1977.

149. Kissinger, P. T. Anal. Chem., 49, 883, 1977.

150. Bidlingmeyer, B. A., Deming, S. N., Price, W. P., Jr., Sachok, B., and Petrusek, M. J. Chromatogr., 186, 419, 1979.

151. Gloor, R. and Johnson, E. L. J. Chromatogr. Sci., 15, 413, 1977.

152. Bidlingmeyer, B. A. J. Chromatogr. Sci., 18, 525, 1980.

153. Yoza, N. J. Chromatogr., 86, 325, Chromatogr. Rev., 1973.

154. Pfab, R., Jandik, P., and Lippert, B. Inorg. Chim. Acta, 66, 193, 1982.

155. Enos, C. T., Geoffroy, G. L., and Risby, T. H. J. Chromatogr.

Sci., 15, 83, 1977.

156. Haworth, D. T. and Liu, T. J. Chromatogr. Sci., 14, 519, 1976.

157. Gast, C. H. and Kraak, J. C. J. Liq. Chromatogr., 4, 765, 1981.

158. Borch, R. F., Markovitz, J. H., and Pleasants, M. E. Anal. Lett., 12(B8), 917, 1979.

159. Bannister, S. J., Sternson, L. A., and Repta, A. J. J. Chromatogr., 173, 333, 1979.

160. Bushee, D., Krull, I. S., Savage, R. N., and Smith, S. B., Jr. J. Liq. Chromatogr., 5, 463, 1982.

161. Valenty, S. J. and Behnken, P. E. Anal. Chem., 50, 834, 1978.

162. O'Laughlin, J. W. Anal. Chem., 54, 178, 1982.

163. O'Laughlin, J. W. and Hanson, R. S. Anal. Chem., 52, 2263, 1980.

164. Johansson, I. M., Wahlund, K.-G., and Schill, G. J. Chromatogr., 149, 281, 1978.

165. Wahlund, K.-G. and Sokolowski, A. J. Chromatogr., 151, 299, 1978.

166. Snyder, L. R. and Kirkland, J. J. Introduction to Modern Liquid Chromatography, Second ed., p. 663, John Wiley & Sons, Inc., 1979.

167. Snyder, L. R. and Kirkland, J. J. Chpt. 11, Introduction to Modern Liquid Chromatography, Second ed., John Wiley & Sons, Inc., 1979.

168. Jordan, R. C. J. Liq. Chromatogr., 3, 439, 1980.

169. Product brochure, manual no. CU 20052, Waters Associates, Inc., 1980.

170. Everaerts, F. M., Beckers, J. L., and Verheggen, P. E. M. Isotachophoresis, Theory, Instrumentation and Applications, J. Chromatogr. Library, Vol. 6, Elsevier, 1976.

171. Hjalmarsson, S.-G. and Baldesten, A. CRC Crit. Rev. Anal. Chem., 11, 261, 1981.

172. Vacik, J. and Fidler, V. Dynamics of the Isotachophoretic Separation, pp. 19-24, from Analytical Chemistry Symposium Series - Vol. 6, Analytical Isotachophoresis, Elsevier, 1981.

173. Kohlrausch, F. Ann. Physik., 62, 209, 1897.

174. Bier, M. and Allgyer, T. T. Isotachophoresis, pp. 443-469, in Electrokinetic Separation Methods, eds., Righetti, P. G., VanOss, C. J., and Vanderhoff, J. W., Elsevier/North Holland Biomedical Press, 1979.

175. Mikkers, F. and Everaerts, F. Theoretical and Practical Aspects of Isotachophoresis, pp. 1-17, from Analytical Chemistry Symposium Series - Vol. 6, Analytical Isotachophoresis, Elsevier, 1981.

176. Private communication with Dr. J. D. Woollins.

177. Giddings, J. C., Fisher, S. R., and Myers, M. N. Am. Lab., 10(5), 15, 1978.

178. Ryan, M. D. and Wilson, G. S. Anal. Chem., 54, 20R, 1982.

179. Heineman, W. R. Anal. Chem., 50, 390A, 1978.

180. Bard, A. J. and Faulkner, L. R. Electrochemical Methods. Fundamentals and Applications, pp. 213-231, John Wiley & Sons, Inc., 1980.

181. Sawyer, D. T. and Roberts, J. L., Jr. Experimental Electrochemistry for Chemists, pp. 337-343, John Wiley & Sons, 1974.

APPENDICES

APPENDIX A

APPLICABLE EQUATIONS FOR SINGLE-SWEEP AND CYCLIC VOLTAMMETRY AT A PLANAR ELECTRODE (180, 181)

Single-Sweep Voltammetry

For an electrochemically-reversible system (written for Ox → Red) -

$$(1)\quad i_p = 0.4463nFAC_o^* \left(\frac{nF}{RT}\right)^{1/2} v^{1/2} D_o^{1/2} \qquad \text{or}$$

$$(2)\quad i_p = (2.69\times10^5)n^{3/2} A D_o^{1/2} v^{1/2} C_o^* \qquad @25^oC$$

where i_p = the peak current in amperes,

n = the number of electrons transferred,

F = the Faraday (= 9.64846×10^4 C/equiv),

C_o^* = the concentration of Ox in mol/cm^3,

R = the molar gas constant (=8.31441 J mol^{-1} K^{-1}),

T = the temperature in K,

v = the sweep rate in V/s

and D_o = the diffusion coefficient of Ox in cm^2/s.

$$(3)\quad E_{p/2} = E_{1/2} + 1.09\frac{RT}{nF} = E_{1/2} + 28.0/n \qquad @\ 25^oC$$

where $E_{p/2}$ = the half-peak potential in mV (= the potential at 1/2 i_p) and $E_{1/2}$ = the polarographic half-wave potential. A diagnostic for a nernstian (reversible) wave is

$$(4)\quad |E_p - E_{p/2}| = 2.2\frac{RT}{nF} = 56.5/n \text{ mV } @25^oC$$

where E_p = the potential corresponding to i_p. This implies that E_p is independent of the scan rate. Also, $i_p/v^{1/2}$ is independent of scan rate in a nernstian system.

For an electrochemically-irreversible system (written for Ox → Red) -

$$(5)\quad i_p = (2.99\times10^5)n(\alpha n_a)^{1/2} A C_o^* D_o^{1/2} v^{1/2}$$

where α = the electrochemical transfer coefficient and n_a = the number of electrons involved in the rate-determining step (as distinguished from the overall number of electrons transferred.

$$(6)\quad |E_p - E_{p/2}| = \frac{1.857\ RT}{\alpha n_a F} = \frac{47.7}{\alpha n_a}\ mV \qquad @\ 25^oC$$

For an electrochemically-quasireversible system - the wave shape is a complex function of v, k^o, α, and E_λ, where k^o = the standard (intrinsic) heterogeneous rate constant and E_λ = the switching potential for cyclic voltammetry.

Cyclic Voltammetry (Reversal Techniques)

For a reversible system, $i_{pa}/i_{pc} = 1$. The ratio is independent of the scan rate v (for $E_\lambda > 35/n$ mV past E_p) and of the magnitude of the diffusion coefficients. $i_{pa}/i_{pc} \neq 1$ is indicative of a kinetic problem or of other complications in the electrode process. ΔE_p ($=E_{pa}-E_{pc}$) is diagnostic of a nernstian reaction: ΔE_p is a slight function of E_λ, but is always close to 2.3RT/nF or 59/n mV @ 25°C. For repeated cycling at steady state in a nernstian system, ΔE_p =

58/n mV @ 25°C.

APPENDIX B

THE LEVICH EQUATION IN ROTATING DISK VOLTAMMETRY

The Levich equation is an expression of the totally mass transfer limited condition which obtains at the RDE in RDV (written for Ox → Red):

$$i_\ell = 0.620nFAD_o^{2/3}\omega^{1/2}\nu^{-1/6}C_o^*$$

where i_ℓ = the limiting current in amperes,

n = the number of electrons transferred,

F = the Faraday (=9.64846x10^4 C/equiv),

D_o = the diffusion coefficient in cm^2/s,

ω = the angular velocity (=2πf where f is the rotational frequency in rps) in s^{-1},

ν = the kinematic viscosity (=η/d where η is the viscosity and d is the density) in cm^2/s,

and C_o^* = the concentration in mol/cm^3.

APPENDIX C

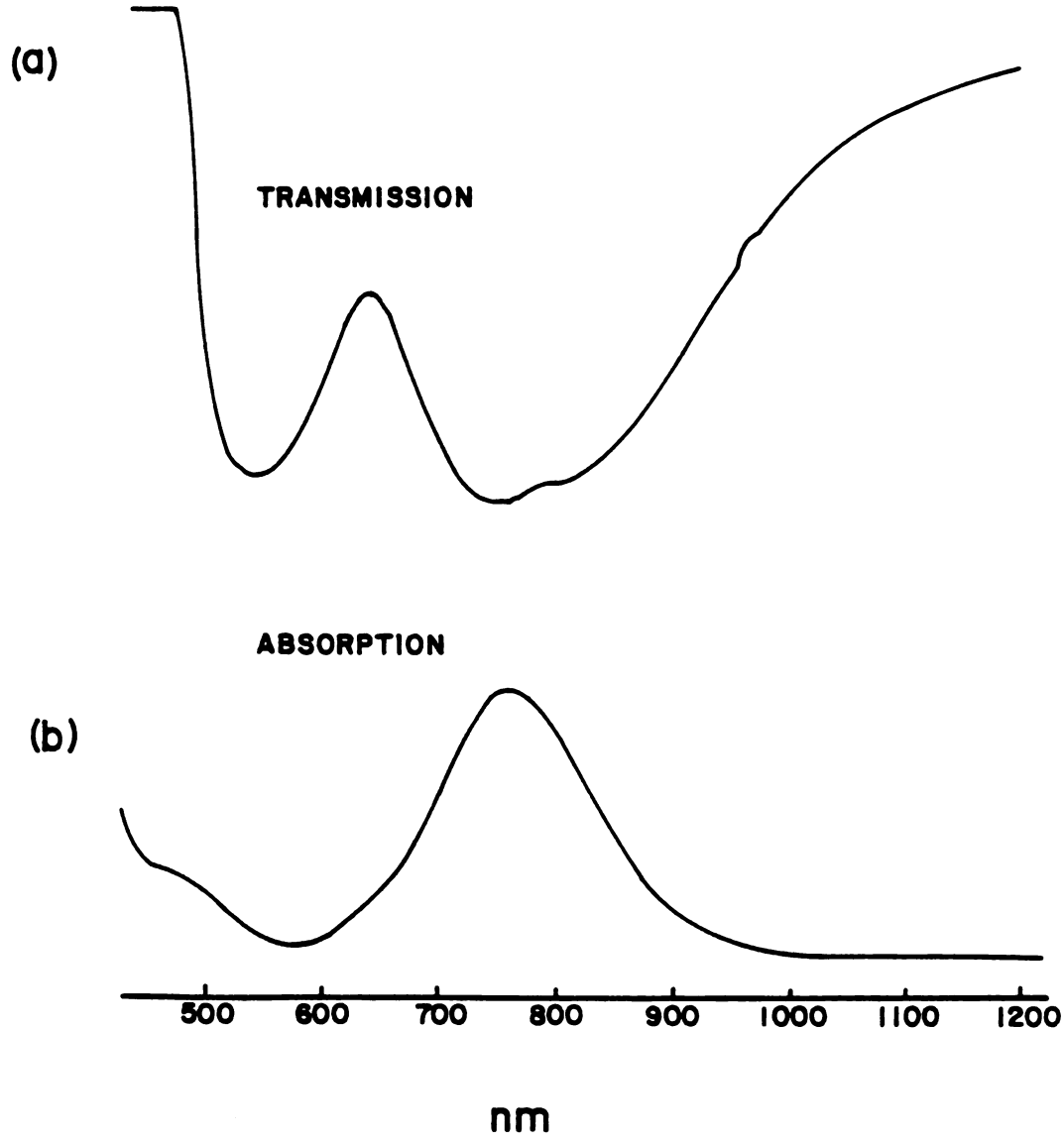

Figure C1. a) Transmission spectrum of [P(II,III)-1-MeU]$(ClO_4)_3$ as the KBr pellet; b) absorbance spectrum of [P(II,III)1-MeU]$(NO_3)_3$ in solution.